AD-TR-83-86

FINAL REPORT

TRANSMITTED THRUST ON A LARGE DUAL RAIL ROCKET SLED SYSTEM

TEST TRACK DIVISION
6585TH TEST GROUP
HOLLOMAN AIR FORCE BASE, NEW MEXICO

NOVEMBER 1983

APPROVED FOR PUBLIC RELEASE
DISTRIBUTION UNLIMITED

ARMAMENT DIVISION
AIR FORCE SYSTEMS COMMAND • UNITED STATES AIR FORCE

EGLIN AIR FORCE BASE, FLORIDA

REVIEWED AND APPROVED.

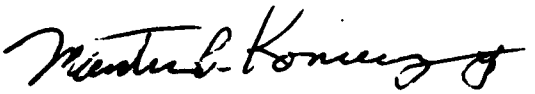

MARTIN P. KONIECZNY, Lt Col, USAF
Director, Test Track Division
6585th Test Group (AFSC)

UNCLASSIFIED

SECURITY CLASSIFICATION OF THIS PAGE (When Data Entered)

REPORT DOCUMENTATION PAGE		READ INSTRUCTIONS BEFORE COMPLETING FORM
1. REPORT NUMBER AD-TR-83-86	2. GOVT ACCESSION NO. AD-A137 151	3. RECIPIENT'S CATALOG NUMBER
4. TITLE (and Subtitle) Transmitted Thrust on a Large Dual Rail Rocket Sled System		5. TYPE OF REPORT & PERIOD COVERED Technical Report (TR), Feb 81 - Nov 83 6. PERFORMING ORG. REPORT NUMBER
7. AUTHOR(s) Dr Larry C. Mixon		8. CONTRACT OR GRANT NUMBER(s)
9. PERFORMING ORGANIZATION NAME AND ADDRESS 6585 Test Group (AFSC) Test Track Division Holloman AFB, New Mexico 88330		10. PROGRAM ELEMENT, PROJECT, TASK AREA & WORK UNIT NUMBERS JON: TKSI1000
11. CONTROLLING OFFICE NAME AND ADDRESS 6585 Test Group (AFSC) (TK) Holloman AFB, New Mexico 88330		12. REPORT DATE November 1983 13. NUMBER OF PAGES
14. MONITORING AGENCY NAME & ADDRESS(if different from Controlling Office) Same as Item #11		15. SECURITY CLASS. (of this report) UNCLASSIFIED 15a. DECLASSIFICATION/DOWNGRADING SCHEDULE

16. DISTRIBUTION STATEMENT (of this Report)

Approved for Public Release; Distribution Unlimited.

17. DISTRIBUTION STATEMENT (of the abstract entered in Block 20, if different from Report)

Same as Item #16

18. SUPPLEMENTARY NOTES

19. KEY WORDS (Continue on reverse side if necessary and identify by block number)

Rocket Sled	Fourier Analysis	Regression Analysis
Test Track	Power Spectral Density	Quasi-Steady State Forces
Thrust	Forcing Function	Oscillatory Forces
Transmitted Thrust	Model Analysis	Acceleration

20. ABSTRACT (Continue on reverse side if necessary and identify by block number) A measurements program was conducted as part of the Tether Qualification Program. A large dual-rail sled system consisted of a pusher sled with two Sergeant rocket motors and two Improved Honest John (IHJ) rocket motors and a guidance system forebody. In the tether configuration, the two Sergeant motors are ignited, launch minus 10 seconds and excess fuel burned off. The two IHJ motors are ignited later in the test profile to provide a step in the acceleration profile which assists in the identification and separation of guidance system errors. The prime instrumentation consisted of an instrumented bolt (force transducer) that connected the

DD FORM 1 JAN 73 1473 EDITION OF 1 NOV 65 IS OBSOLETE

UNCLASSIFIED

SECURITY CLASSIFICATION OF THIS PAGE (When Data Entered)

pusher sled to the forebody sled. Other instrumentation was added to the guidance forebody ~~later in the program~~ for correlation studies. Extremely good quality and consistent data was obtained on all instrumentation systems.

Correlation studies were conducted whereby the theoretical quasi-steady state (Q.S.S.) transmitted thrust was compared to measured data and it was established that 35% of the total system drag was attributed to the pusher in the wake of the forebody. Several different approaches were made to correlate the oscillatory transmitted thrust to system parameters. The most acceptable approach was to express the peak oscillatory forces as an amplification factor times the predictable Q.S.S. transmitted thrust. In addition, a modal analysis was conducted, and it was established that the first 4-5 pusher pitch plane modes of vibrations must be included in a complete two-system dynamic mathematical model.

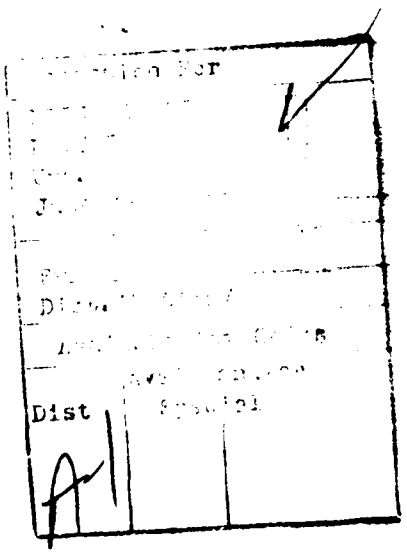

TABLE OF CONTENTS

LIST OF FIGURES

LIST OF FIGURES (CONT'D)

LIST OF TABLES

1. INTRODUCTION

1.1 Objective

The objective of this study is to document the results of a transmitted thrust measurements program conducted in conjunction with a Test Track in-house development program titled "Tether Sled Qualification." The secondary objective is to compare tether measurements with previously reported transmitted thrust measurements and established design criteria, and recommend a new design criteria that is safe but not overly conservative.

1.2 Background

1.2.1 Tether Sled Qualification Program. The Tether Sled Qualification Program was established to provide an alternative and back-up to the liquid engine/guidance forebody configuration that has been used to test missile inertial guidance systems for the past twenty-three (23) years. The older configuration uses a pusher sled whose propulsion system consists of modified Bomark missile liquid propellant engines. The three Bomark A chambers will produce approximately 35,000 pounds of thrust each for a total available thrust of 105,000 pounds for approximately seven (7) seconds. The propellants are red-fuming nitric acid (IRFNA) as oxydizer and unsymmetrical di-methyl-hydrazine (UDMH) as fuel. The forebody sled which carries the guidance system is a standard design with slipper beams and an aluminum honeycomb main structure. The design includes an appropriate aerodynamic shape and fairings to control or balance quasi-steady state lift forces. Figure 1 shows a photograph of the sled system at launch.

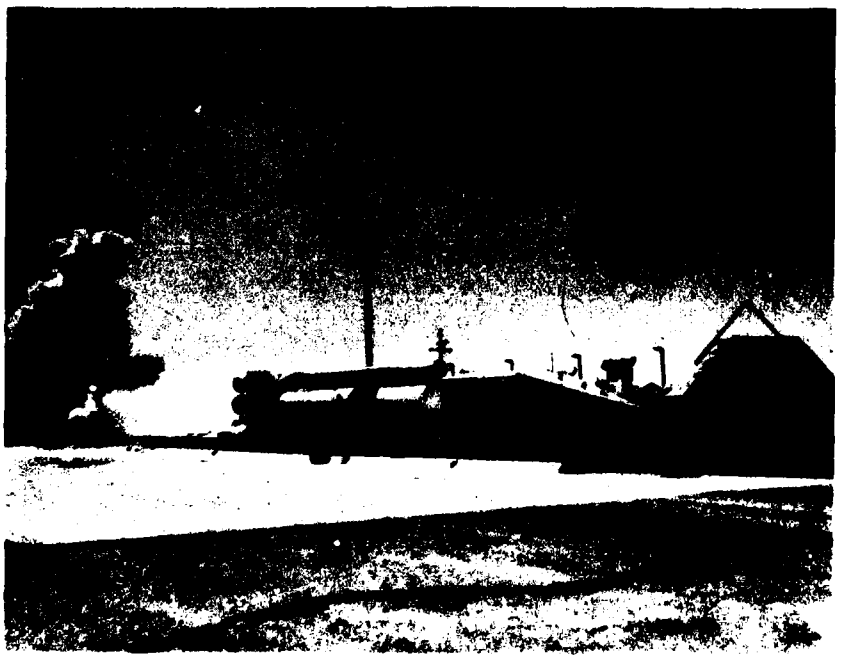

Figure 1. Liquid Engine/Guidance Forebody.

The sled trajectory is planned to promote the growth of guidance system error terms to permit a comprehensive evaluation and subsequent correction of error sources. A typical trajectory is to accelerate at 6 g's for four (4) seconds using three (3) chambers. At a velocity of 660 feet per second, one chamber is shut down and the guidance system is subjected to 2.1 to 3.8 g's for 5.3 seconds, reaching a peak velocity of approximately 1250 feet per second (Mach 1.12). The system is then allowed to decelerate due to air drag and friction and at a velocity of 675 feet per second enters into water braking. The maximum braking acceleration is a negative 6 g's. Typical velocity and acceleration profiles are shown in Figure 2.

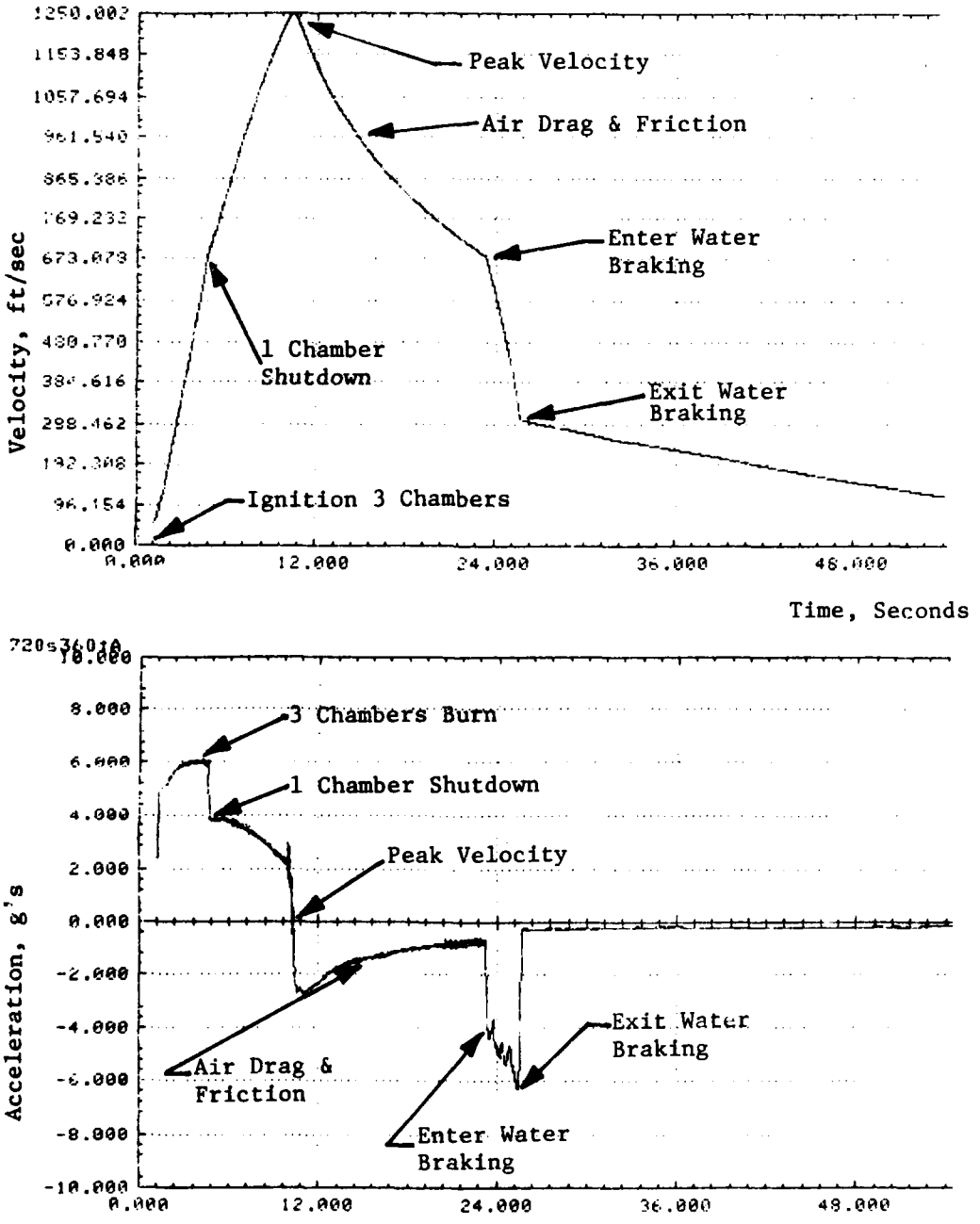

Figure 2. Typical Guidance Test Velocity & Acceleration Profiles.

While this sled system has proven invaluable in testing guidance systems for such systems as Minuteman I and II, and Peacekeeper, future systems require even longer acceleration times which translates to higher velocities. In addition, the logistics and resources required to maintain and operate this one-of-a-kind liquid system has proven to be expensive in terms of spare parts, rocket fuels and human resources. The Bomark liquid propellant system is the only liquid rocket used on the Holloman High Speed Test Track. All other Test Track users such as escape systems, impact fuze, rain erosion, aerodynamic simulation, etc., use solid propellant rocket motors.

Previous attempts to use other rocket motors for testing inertial guidance systems have been less than successful because a number of rocket motors were required to reproduce the required acceleration profile. For example, a sled was modified to use nine (9) small rocket motors, and firing of the motors was sequenced to result in the required acceleration profile. As the motors ignited, transients were introduced into the down-track acceleration profile which made separation of guidance system errors difficult.

The tether concept uses only two each Sergeant (Sgt) solid propellant rocket motors and two each Improved Honest John (IHJ) rocket motors. A photograph of this pusher and a typical guidance forebody is shown in Figure 3.

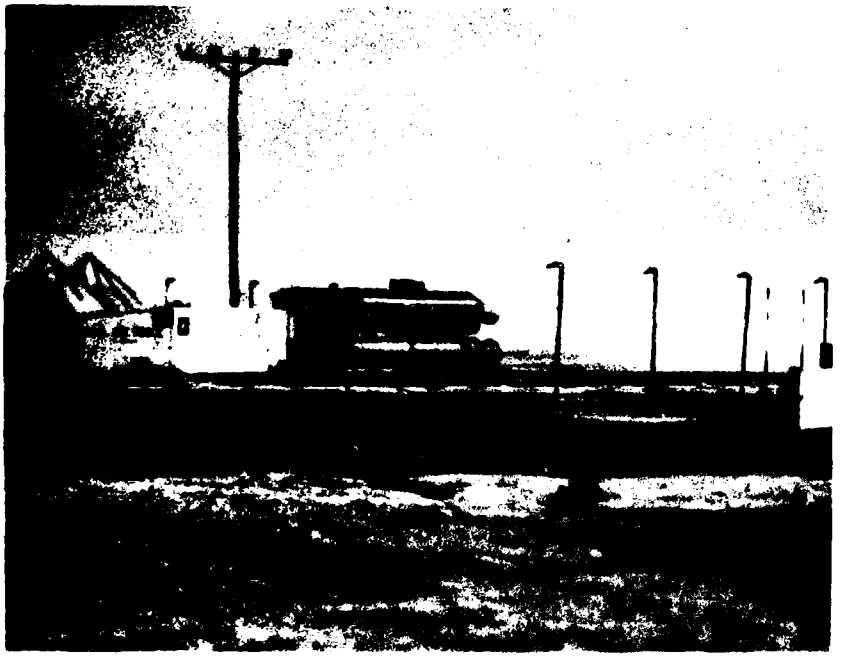

Figure 3. Tether Pusher/Guidance Forebody

The ignition and burnout onset rates for the Sergeant rocket motors are well behaved (no rapid onset or rapid burnout). The need for tethering results because the burn time for the Sergeant motors is approximately 36 seconds. If a portion of the fuel was not burned off prior to system release, an excessive high velocity would be obtained and extremely high braking forces would be required to recover the system on the rails. Essentially, the pusher sled is constrained to the rail heads, the two Sergeant motors are ignited, and after approximately 10 seconds, an explosive device is used to sever the link holding the pusher. (See Figure 4).

Figure 4. Tether Release Mechanism.

The two Sergeant rocket motors continue to burn and reach a velocity of 200 feet per second in two seconds at which time the two IHJ motors are ignited. The sled train is accelerated to 1400 feet per second at 5.2 seconds from launch. The two IHJ motors burn out and the two Sergeant motors continue to burn. The two Sergeant motors slowly accelerate the sled system to a peak velocity of approximately 1500 feet per second (1460 to 1550 fps depending on temperature). After peak velocity, the sled system is allowed to coast with air drag and friction serving as retarding forces. At approximately 32 seconds into the mission, the sleds enter water braking at a velocity of 850 feet per second and the system is recovered. This profile provides the required steps in acceleration without the unacceptable transients associated with numerous solid rocket motors. Figure 5 shows a typical "tether" velocity and acceleration profiles with the indicated levels.

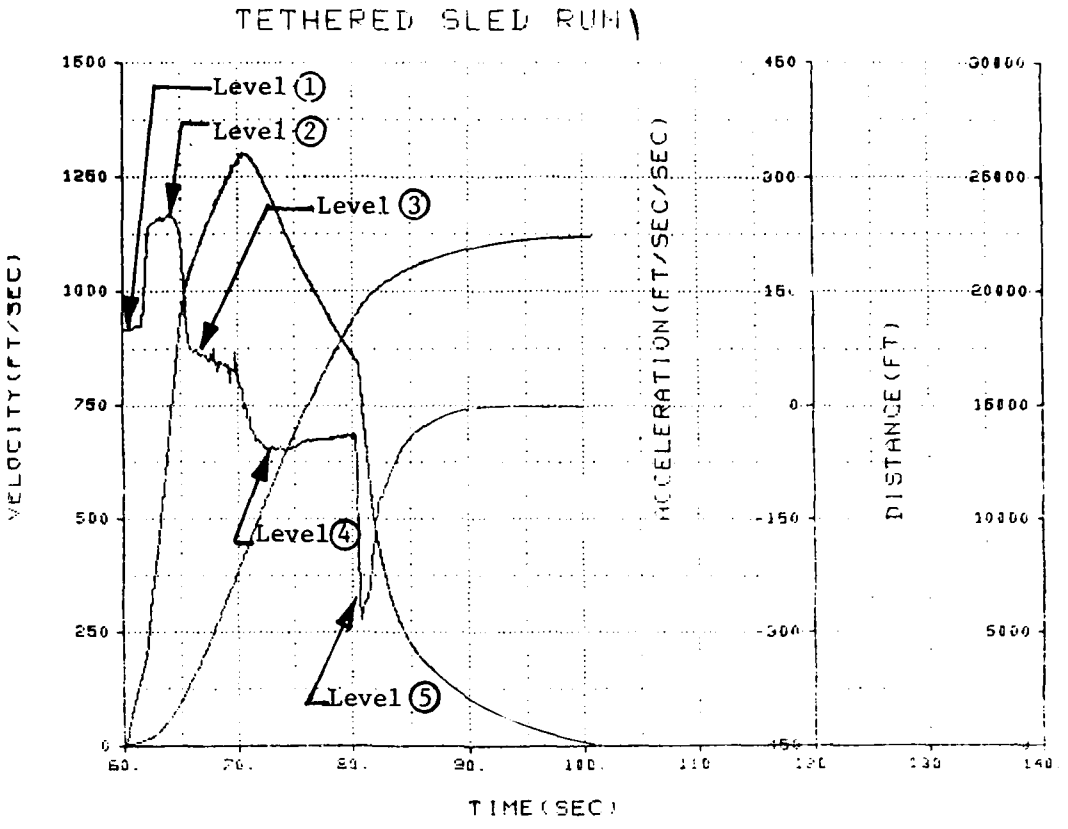

Level 1	Two each Sergeants burn	3.2 g's
Level 2	Two each Sergeants burn plus two each Improved Honest Johns	7.9 g's
Level 3	Two each Sergeants continued burn	2.3 to 1.4 g's
Level 4	Air Drag plus friction	-1.9 to -1.2 g's
Level 5	Water-braking	-8.4 g's

Figure 5. Typical Tether Test Profiles.

1.2.2 Tether Measurements Program. Late into the Tether Sled Qualification Program, the transmitted thrust between the pusher sled and the guidance forebody sled was specified as a required measurement. The two sleds are connected by two clevices and a 15½-inch long 1½-inch diameter instrumented bolt. See photographs in Figures 6 and 7.

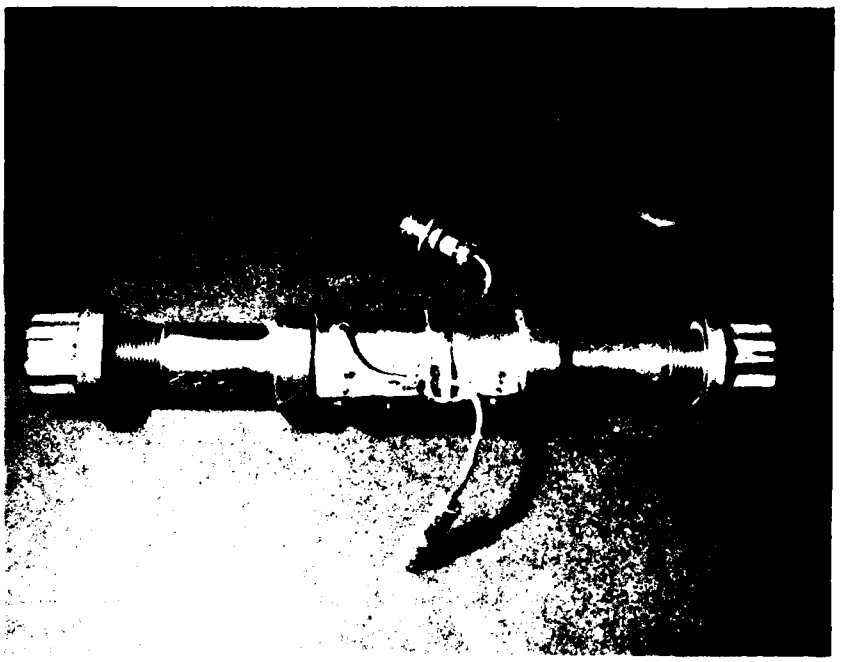

Figure 6. Instrumented Bolt.

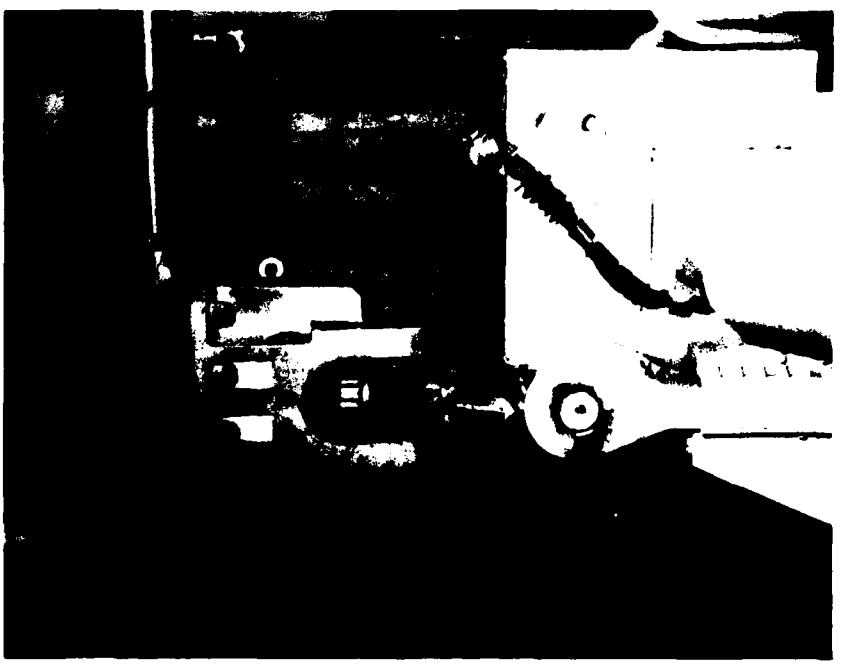

Figure 7. Instrumented Bolt Mounted.

This bolt was originally instrumented by the University of New Mexico, and development is documented in Reference 1. The intent was to use the instrumented bolt on a large sample of dual rail sled systems and over a period of time document quasi-steady state as well as oscillatory transmitted thrust data.

The bolt is instrumented with strain gages arranged to provide additive tensile/compressive outputs and cancel outputs due to bending strains. The bolt is calibrated in a tensile test machine and loads referenced to resistance placed across one leg of the wheatstone bridge.

Late in the measurements program, strain gages were also added to the forebody sled slipper beams to identify interaction between the transmitted thrust measurements and forebody pitch plane forces.

2. DATA PROCESSING

2.1 Transmitted Thrust. The transmitted thrust data was first received in an analog format on oscillograph records. Data was checked for calibration levels, telemetry dropouts, noise, time delays, event timing and numerous amplitude levels hand reduced to engineering units for subsequent comparison to digitized data. Three (3) of four (4) separate test data were found to be of excellent quality, i.e., 18Y-F9C, 18Y-F10C, and 18Y-F11C. One test transmitted thrust data 18Y-F8C indicated significantly higher loads than the three other tests. Subsequent investigation into the data processing procedure showed that the reference calibration level was not added immediately prior to the test, but dubbed onto the tape at a later date. Consequently, 18Y-F8C transmitted thrust data is considered invalid and not included in this analysis.

Transmitted thrust data was then digitized, time delays corrected and formatted with proper scale factors and record speeds. Copies of the expanded records for 18Y-F9C, 18Y-F10C and 18Y-F11C are given in Appendix A. A comparison of the three records shows excellent agreement and repeatability.

2.2 Transmitted Thrust Residuals. One of the correlation techniques planned for the transmitted thrust data was to describe the peak thrust as an amplification factor times the quasi-steady state thrust. The quasi-steady state thrust can be estimated using a computer code and is made up of thrust as a function of time, weight loss as a function of time, air drag as a function of velocity, time varying inertia and friction as a function of weight. If the quasi-steady state forces are rapidly changing, the separation of the two signals (quasi-steady state and oscillatory transmitted thrust) is difficult if not impossible. Examples of three such conditions are shown in Figure 8.

Since an unbiased oscillatory force was of interest, the two signals needed to be separated. The data was in a digital format and the slower time varying quasi-steady state forces could be subtract from the oscillatory signal. Since the data was so consistent from run to run, it was only necessary to separate the residuals on one test. Test 18Y-F9C was selected for more indepth processing. Results are shown in Appendix B and a small one-second sample is shown in Figure 9.

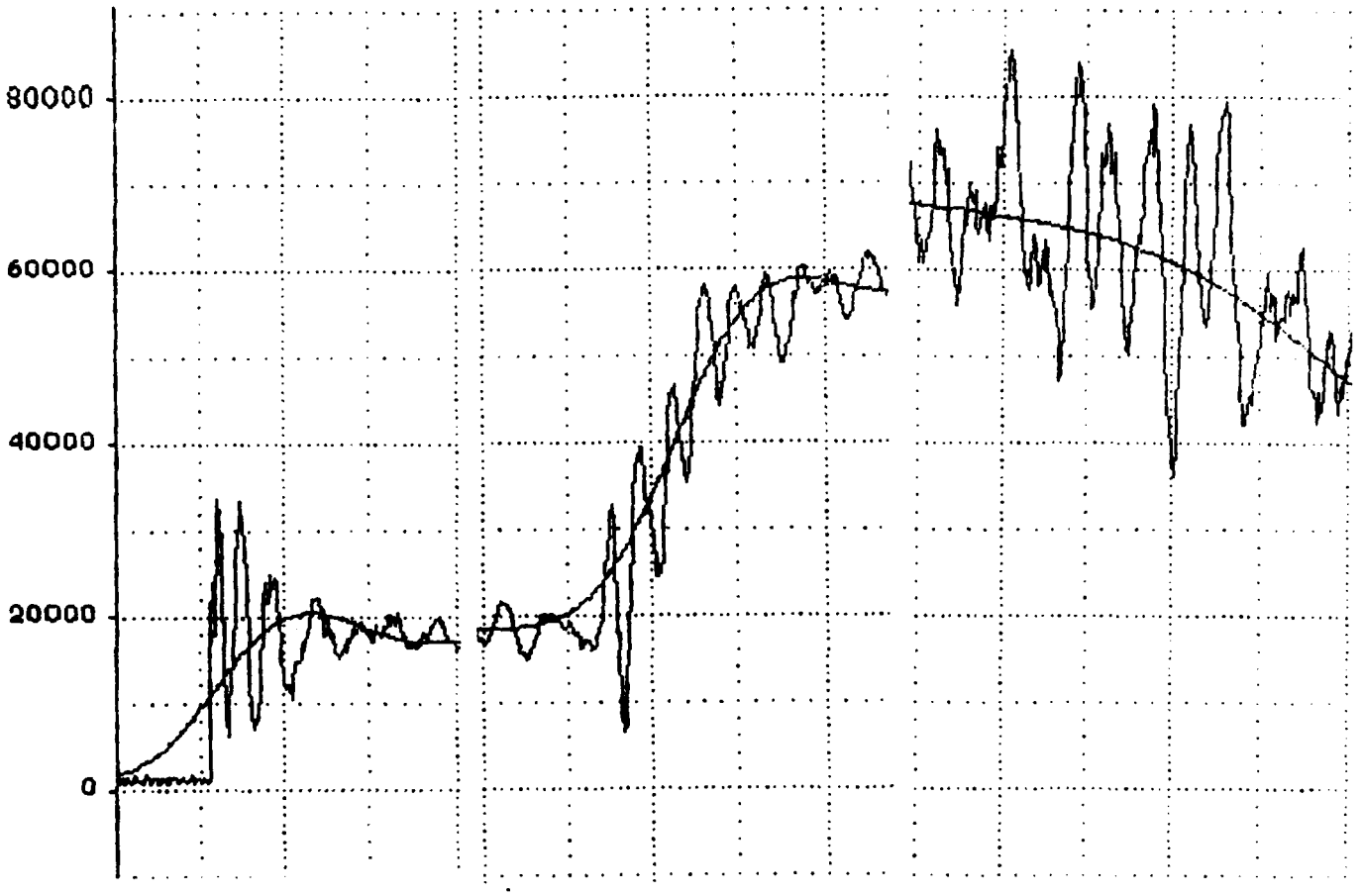

(a) Tether Release (b) Improved Honest John Ignition (c) Improved Honest John Burnout

Figure 8. Rapid Changing Quasi-Steady State Forces.

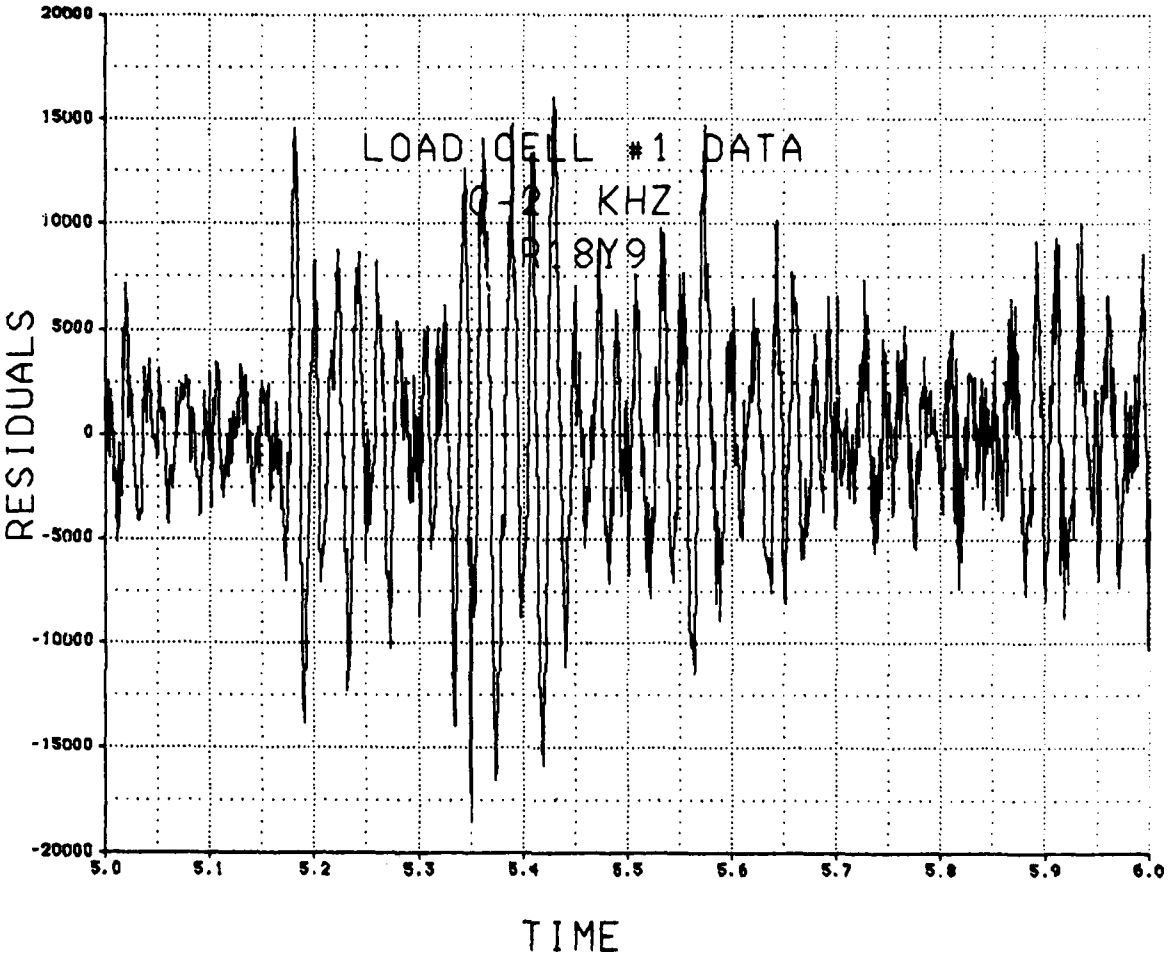

Figure 9. Example of Residuals Extraction

2.3 Trajectory Data. Since two of the variables that effect transmitted thrust are velocity and acceleration, accurate measurement of these parameters is required to perform a complete analyses. Velocity is measured using the space-time system on the Holloman High Speed Test Track. Complete background on this system is given in References 2 and 3. Results for test 18Y-F8C, 18Y-F9C, 18Y-F10C, and 18Y-F11C are shown in Figure 10.

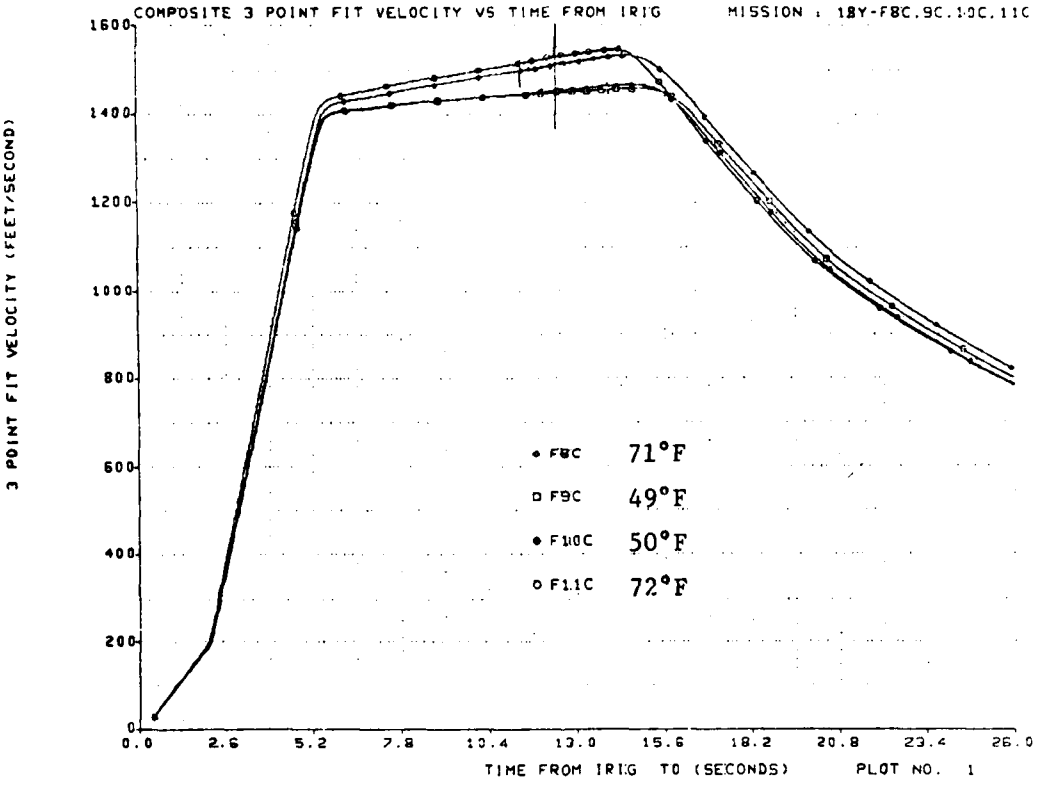

Figure 10. Velocity versus Time.

Again, the data was extremely consistent and repeatable from one test to the next. Test 18Y-F8C is included since the velocity data was of good quality even though the transmitted thrust was of unacceptable quality as previously discussed. The velocity profiles can be grouped in two categories: 18Y-F8C and 18Y-F11C versus 18Y-F9C and 18Y-F10C. Review of the temperature during the tests explains the two separate categories. Test 18Y-F8C and 18Y-F11C were tested at temperatures of 70°F and 72°F respectively; hence, enhancement of the rocket motor performance with maximum velocities of approximately 1550 feet per second. The 18Y-F9C and 18Y-F10C tests were conducted at 49°F and 50°F respectively, and reached lower maximum velocities of approximately 1460 feet per second. Also, note the less time to reach maximum velocity for the higher temperature tests.

The other trajectory parameter required for analysis is acceleration. One method to measure acceleration is to differentiate the velocity versus time data. Another method is to directly measure acceleration using an on-board accelerometer. This measurement was made on Test 18Y-F11C and is shown in Figure 11.

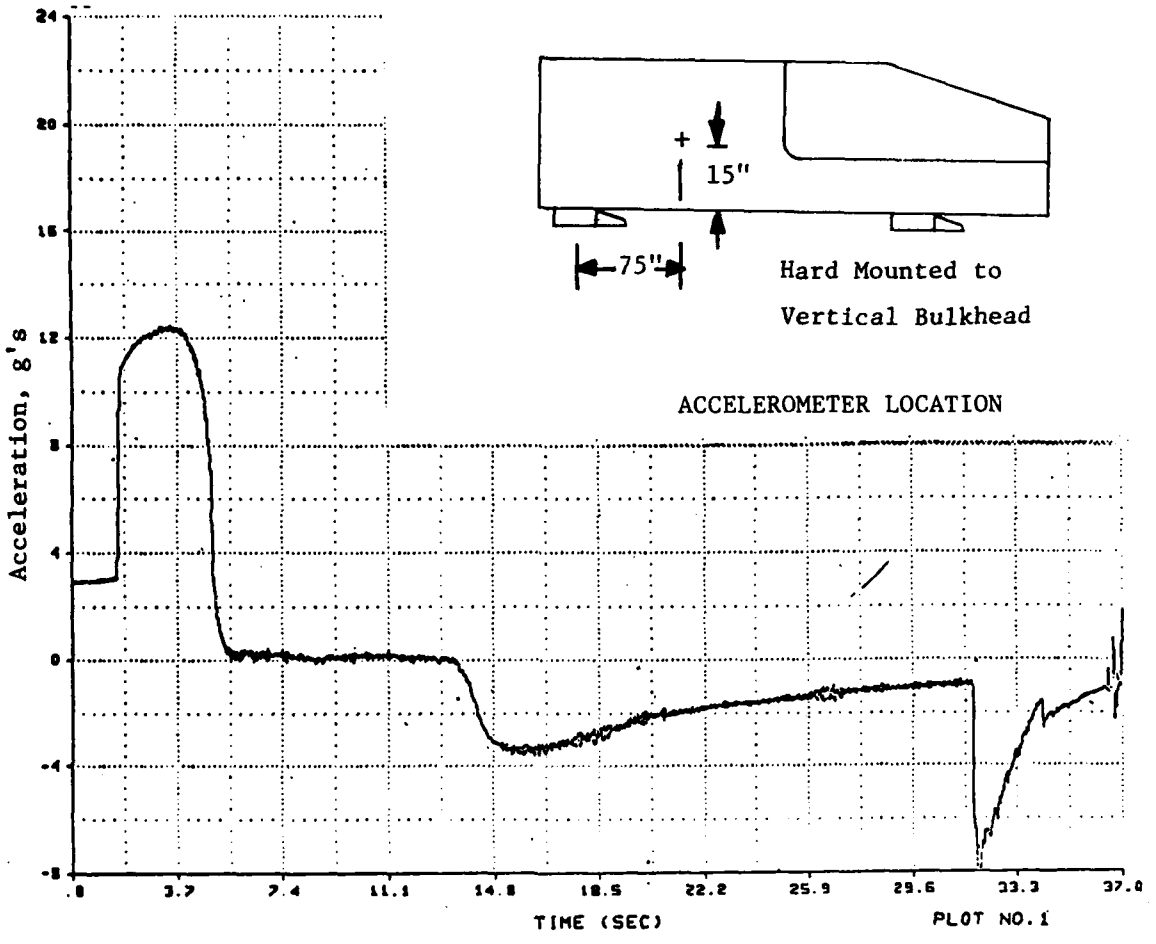

Figure 11. Plot of Accelerometer Data

2.4 Slipper Beam Forces. Late in the Transmitted Thrust Measurements Program, it was established that the interaction of the transmitted thrust and slipper beam forces could be of importance. Consequently, on test 18Y-F11C strain gages were applied to the forebody slipper beams. The instrumentation technique is described in detail in Reference 4. In this previous study, this instrumentation scheme was used to correlate wind tunnel lift force predictions on forebody sleds with measured test track data. A simplified schematic is shown in the following figure.

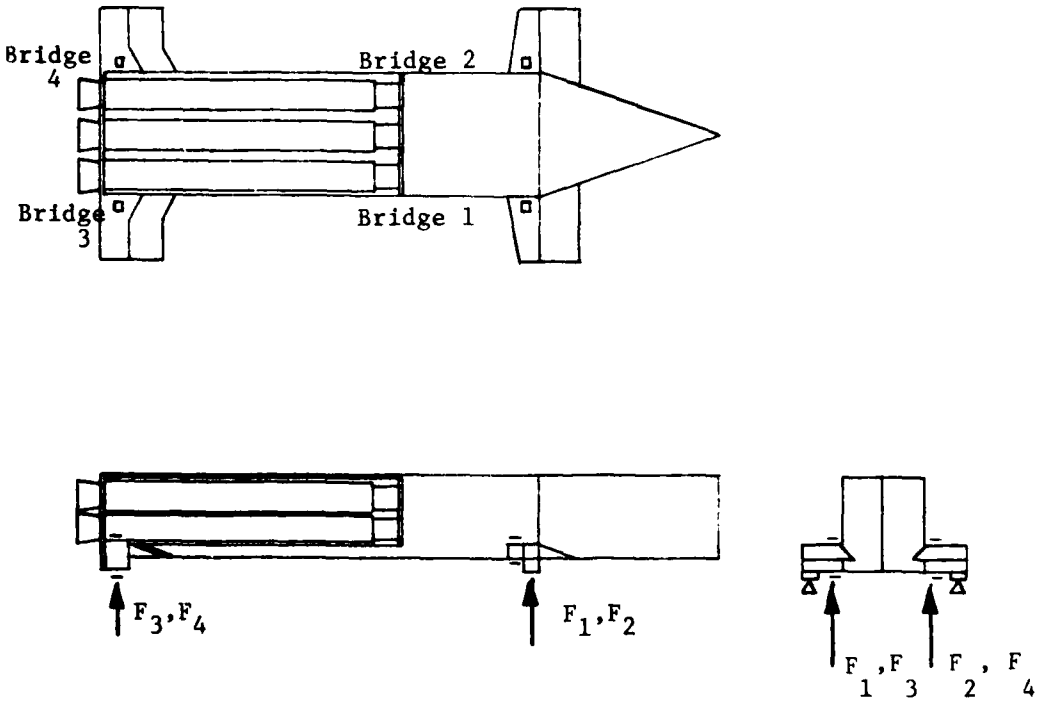

Figure 12. Strain Gage Location Diagram

Essentially, strain gages are bonded on the top and bottom surfaces of the slipper beams and arranged in a Wheatstone Bridge to provide additive outputs for beading strains and null outputs for tensile/compressive strains. Next, a hydraulic jack and load cell are placed beneath the sled and near the gages. In this manner, the strain gage circuits can be calibrated in terms of force; hence, force transducers. Typical results are shown in Figure 13.

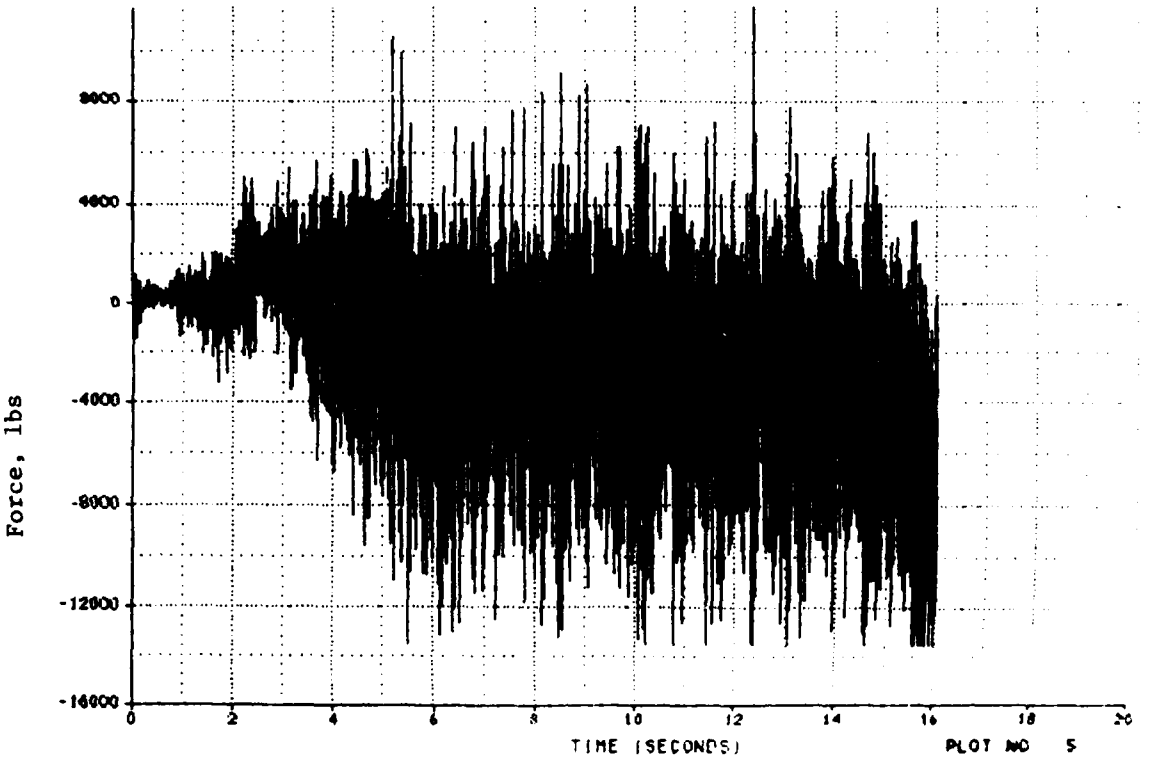

Front Slipper Beam

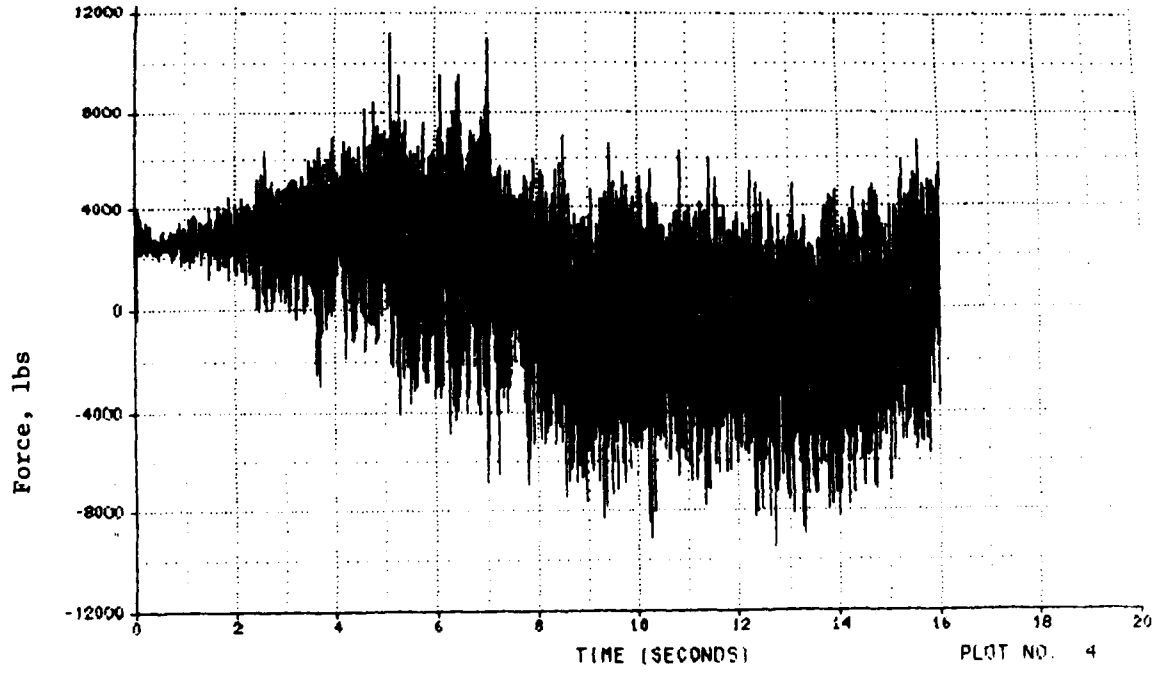

Aft Slipper Beam

Figure 13. Slipper Beam Forces versus Time.

As shown in this figure, some coupling is evident, especially on the aft beam. Note, aft beam forces at tether release.

2.5 Power Spectral Density Analyses. Since the oscillatory component of the transmitted thrust and the slipper beam forces are associated with the structural response of the sled structures, Power Spectral Density (PSD) Analyses was of interest. Sample data were processed through a Discrete Finite Transform (DFT) computer code at the Guidance Test Division (GD). One (1) second time slices were first weighted by multiplication by a Hanning function to reduce leakage effects. The data was smoothed using a 10-pass smoothing. Typical results for transmitted thrust for test 18Y-F10C is given in Figure 14. The time increment for the plot was 4.0 to 5.0 seconds.

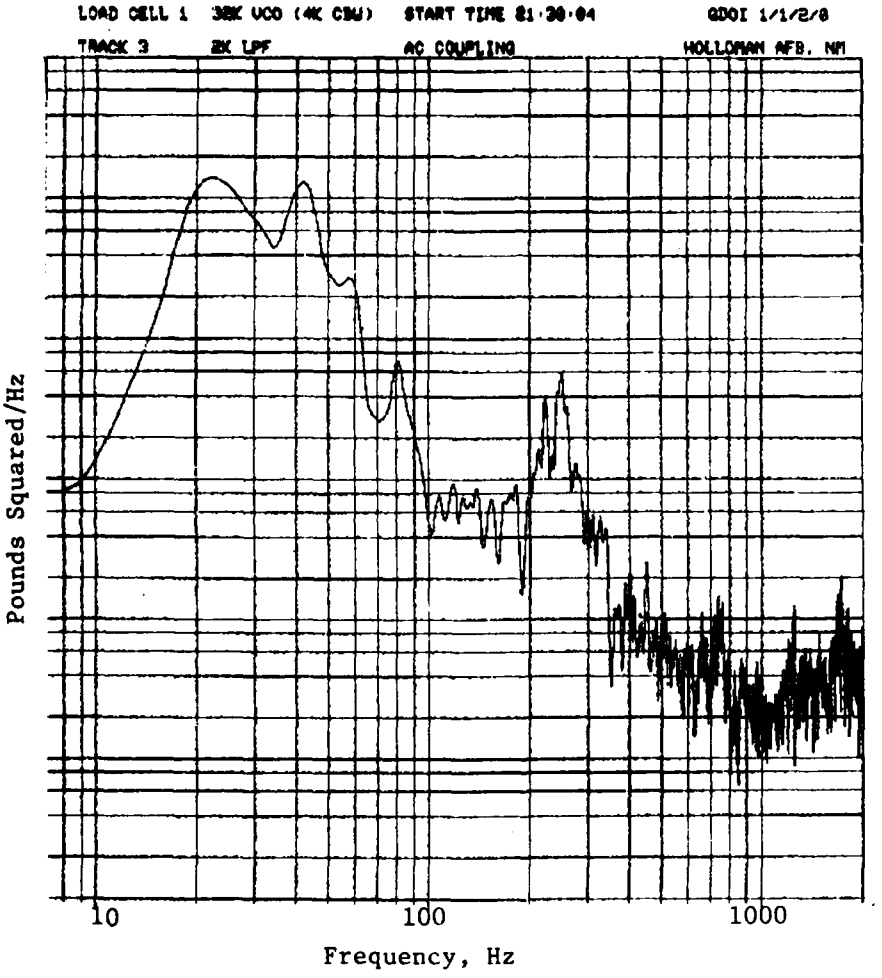

Figure 14. Transmitted Thrust PSD

The interpretation of this and similar PSD analyses will be discussed later in this report.

2.6 Test for Normality. Specified samples of transmitted thrust were also run through a CHi Square Goodness-of-fit computer program to check for normality. These one second samples were selected during high load periods such as 5 to 6 seconds and 6 to 7 seconds after tether release. Typical results are shown in Figure 15.

Figure 15. Histogram-CHi Square Goodness-of-Fit.

As noted on the figure, the computed CHi-square was 11.55 and the CHi-square value from tables was 5.99 for the specified degrees of freedom. Hence, the data is non-normal. This information coupled with the previously described Power Spectral Density (PSD) analyses and by tracking the envelope of the peak values provides sufficient information to classify the transmitted thrust oscillations. First, the histogram shown in Figure 15 is definitely not the bell shape associated with normality, but appears to approach a U shape associated with a sine function. Secondly, the PSD contains nearly all the power at 23 Hz and 43 Hz. See Figure 14. The last data source is shown in Figure 16.

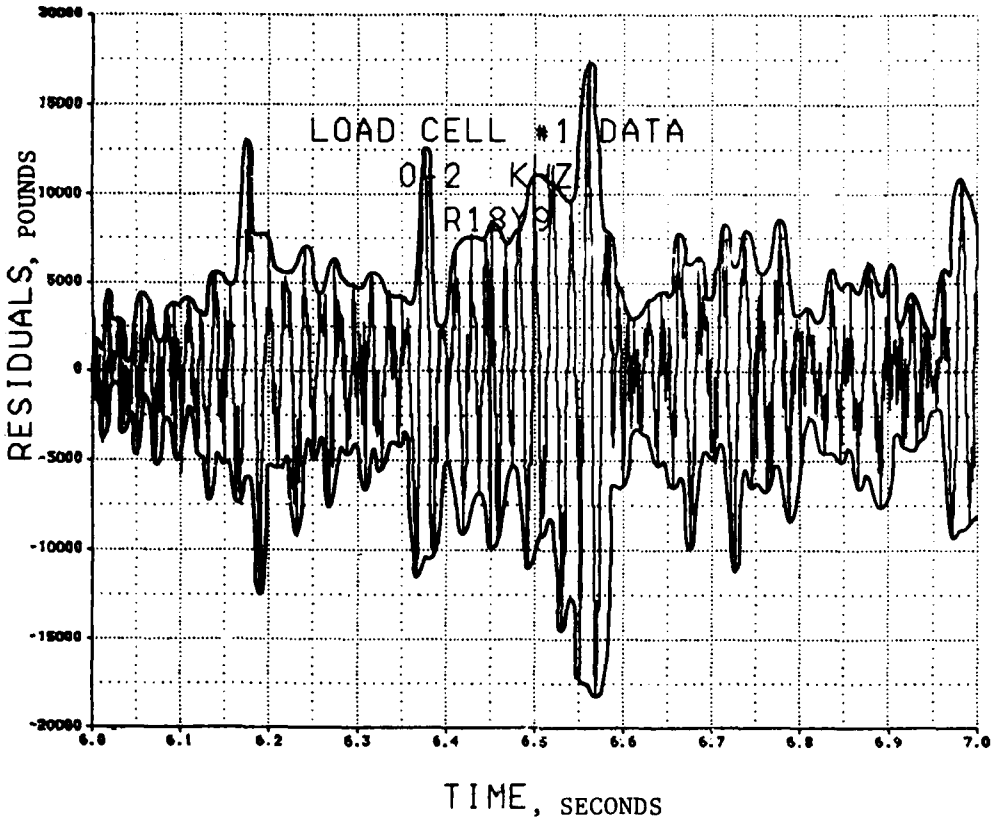

Figure 16. Envelope or Peak Residuals.

For one second of residuals (6.0 - 7.0 seconds - test 18Y-F9C), the peaks were connected to form an envelope of the peak oscillations. As shown in this figure, the residuals appear to be a 43 Hz signal modulated with a 23 Hz signal. The conclusion being that the primary longitudinal frequency is 43 Hz associated with the two large sled masses and some yet to be specified stiffness. The 23 Hz modulating signal can be a longitudinal frequency or possibly a coupling of the pusher or forebody vertical bounce frequency. This subject will be discussed later in the correlation paragraph.

3. CORRELATION

3.1 Quasi-Steady State Forces. Computer codes have previously been developed to predict the quasi-steady state transmitted thrust force. Reference the following Figure 17.

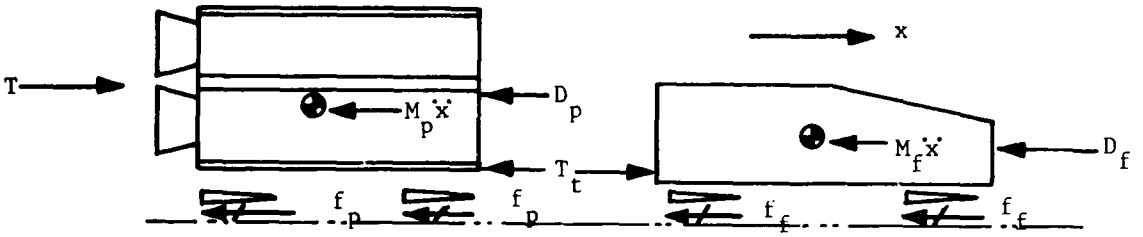

Figure 17. Quasi-Steady State Forces

The following differential equation is solved for the overall trajectory using a digital code.

$$[M_p + M_f]\ddot{x} + \frac{1}{2}\rho[C_{dp}A_p + C_{df}A_f]\dot{x} + f_p + f_f = T_{(t)}$$

Where:

M_p - Mass of pusher (function of time)

M_f - Mass of forebody (constant for this example)

$\ddot{x}$ - Longitudinal acceleration (function of time)

ρ - Density of air (constant)

$C_{dp}A_p$ - Coefficient of drag and frontal area of pusher in presence of the forebody (function of velocity)

$D_{df}A_f$ - Coefficient of drag and frontal area of forebody (function of velocity)

$\dot{x}$ - Longitudinal velocity (function of time)

f_p - Friction of pusher (function of velocity)

f_f - Friction of forebody (function of velocity)

T - Thrust of pusher (function of time)

If the force of interest is the transmitted thrust, then the forces can be summed about the pusher or forebody, e.g.,

$$T_t = T - M_p\ddot{x} - \frac{1}{2}\rho C_{dp}A_p - f_p$$

Where:

T_t - transmitted thrust (function of time)

The input parameters are derived from a number of sources:

Mass Pusher [Mp] - Sled structure and loaded rocket motors are weighed.

Propellant weights are extracted from applicable documents associated with each rocket motor type.

Mass Forebody [Mf] - Sled structure and payload weighed.

Overall Drag

Coefficients [$C_{dp}A_p + C_{df}A_f$] - The overall drag coefficients are derived by analyzing the coast portion of the trajectory after the thrust phase is complete and mass is constant.

Pusher Drag

Coefficient [$C_{dp}A_p$] - Usually assumed a percentage of the overall drag, e.g., 25%.

Friction [$f_p + f_f$] - Derived from earlier studies. Coefficient of friction varies from 0.30 breakaway friction to 0.11 at higher velocities.

Thrust [T] - Reference documents and static test stand data are used to derive thrust. Thrust shape is dependent on the age of the propellant and temperature, but overall impulse has been found to be constant.

Four separate measured trajectories were available for analysis as shown in Figure 18.

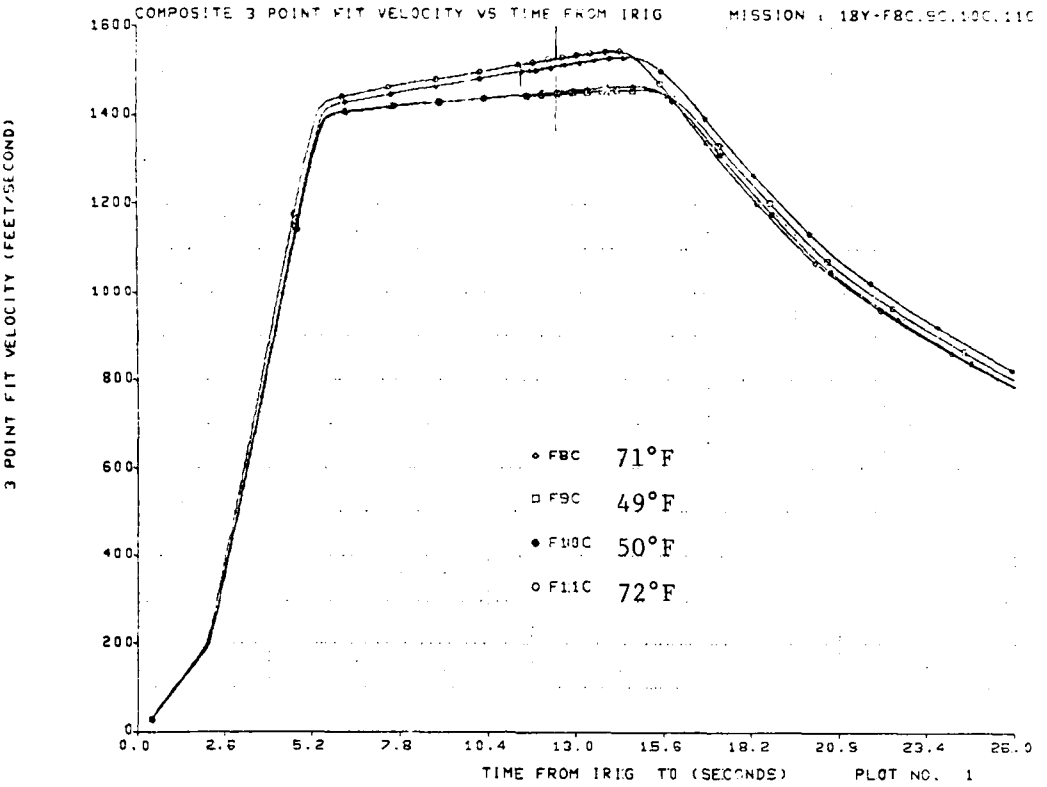

Figure 18. Velocity versus Time.

As shown in this figure, the data was extremely consistent and fell into two groupings, i.e., 49°F - 50°F and 71°F - 72°F. Due to this consistency, it was only necessary to analyze one sled test, i.e., 18Y-11C.

First, the overall trajectory was solved for the particular sled train in question. The overall sled train drag coefficients were derived from the coast portion of the trajectory, and then the thrust versus time curve was iterated until satisfactory correlation was obtained. Impulse was held constant. Results are shown in Figures 19 and 20.

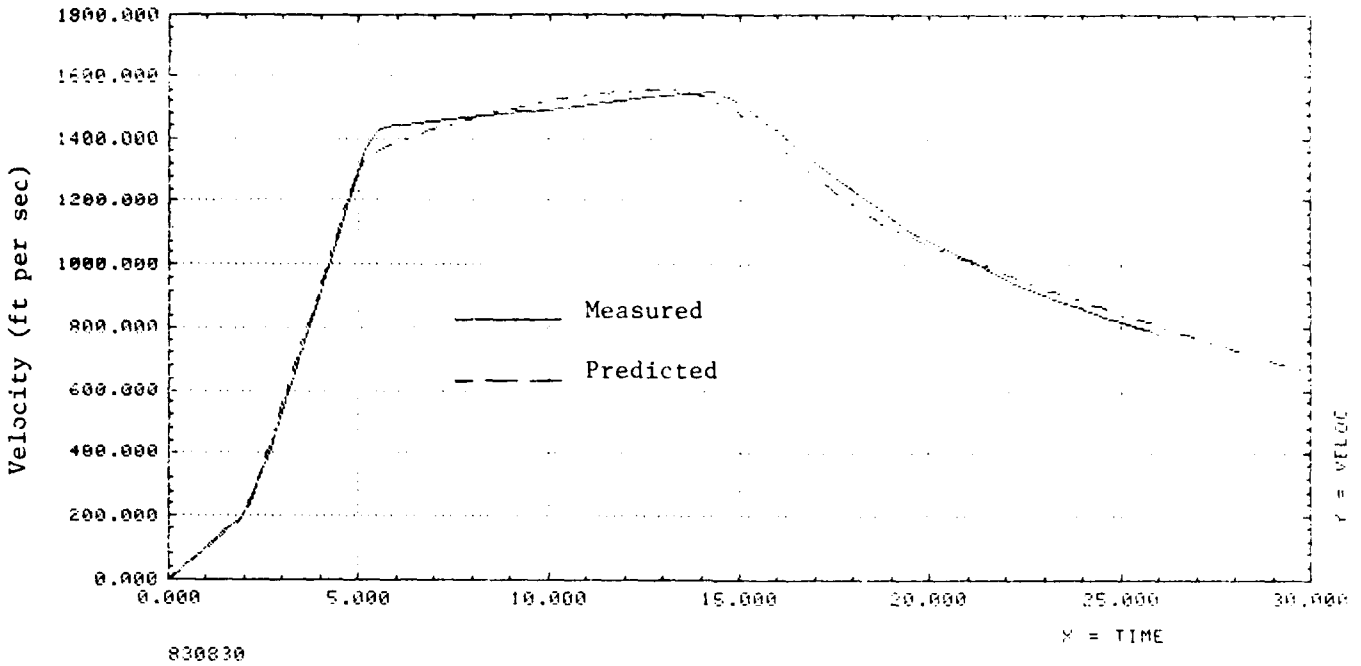

Figure 19. Velocity versus Time.

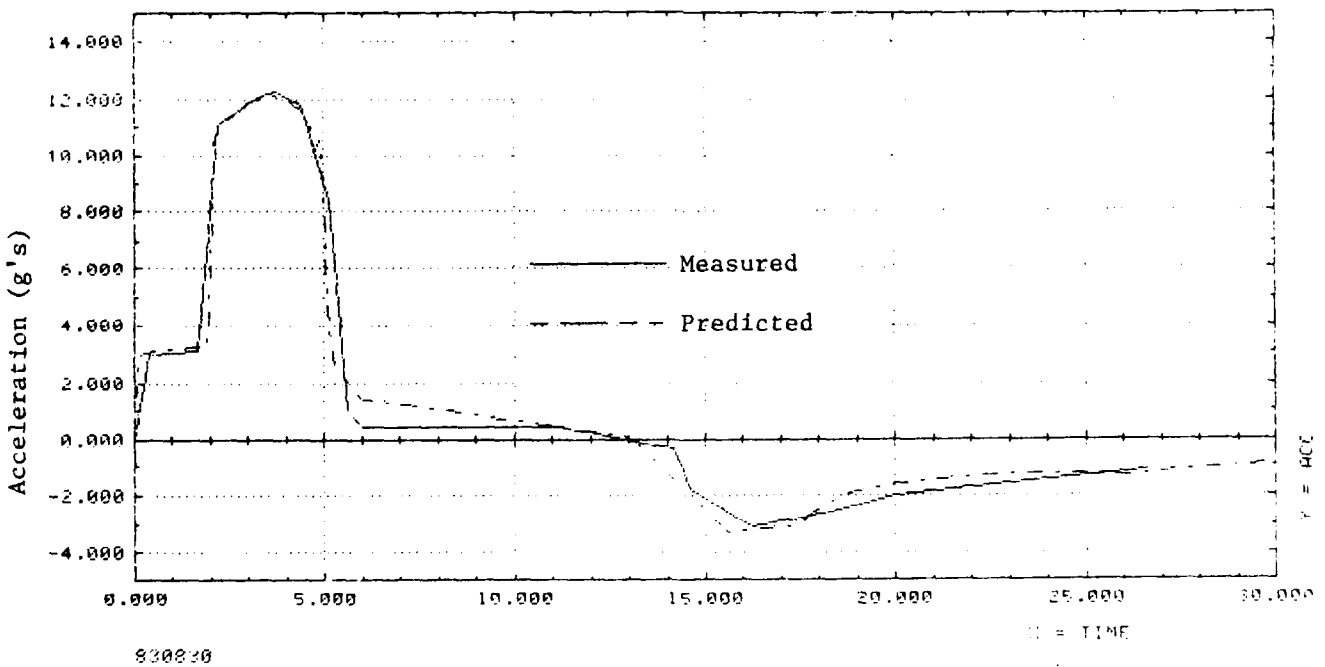

Figure 20. Acceleration versus Time.

As shown by these figures, both the velocity and acceleration were correlated to a satisfactory level of acceptance. The measured acceleration was obtained from two sources, an on-board accelerometer and by taking the derivative of the velocity versus time function. Again, these two data sources were found to agree.

A sensitivity test was conducted to study the transmitted thrust. Different percentages of the overall drag was allocated to the pusher in accordance with the following table.

TABLE 1. ALLOCATION OF TOTAL SYSTEM DRAG

% DRAG PUSHER	% DRAG FOREBODY
75	25
50	50
40	60
35	65
25	75

The predicted transmitted thrust was then compared to measured value as a function of time. Results are as follows (see Figures 21, 22, 23, 24 and 25).

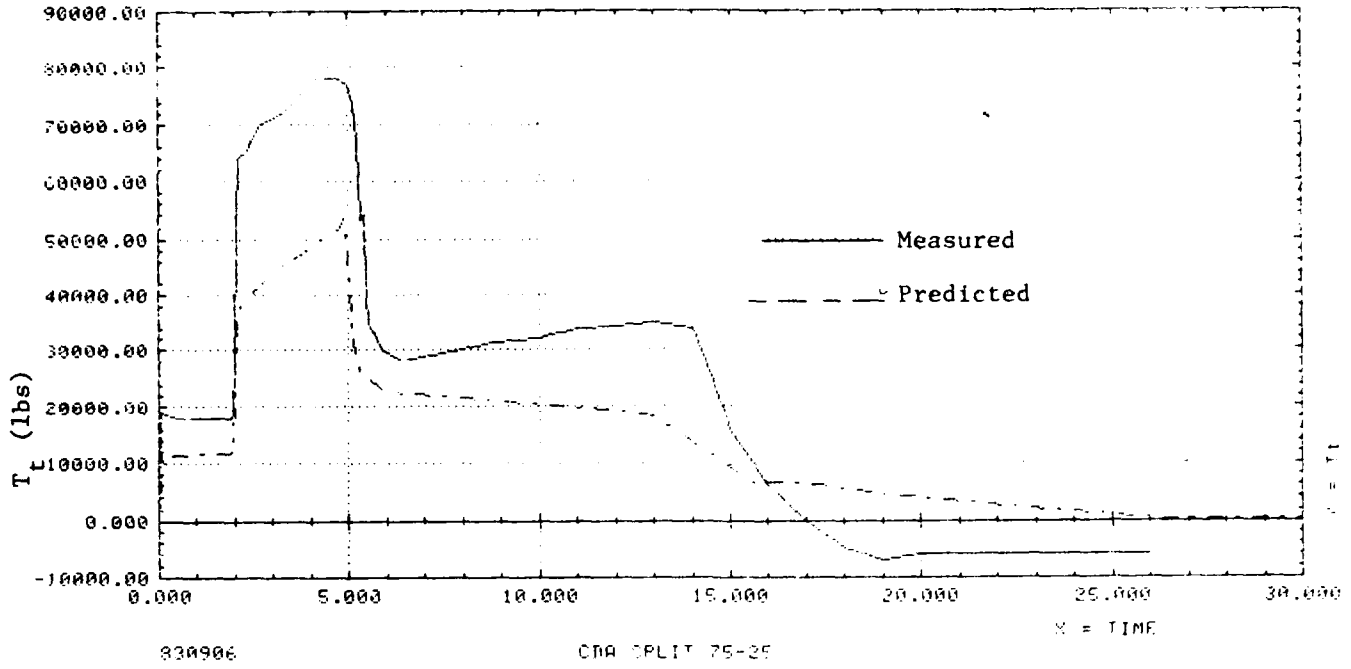

Figure 21. CDA Split 75% Pusher.

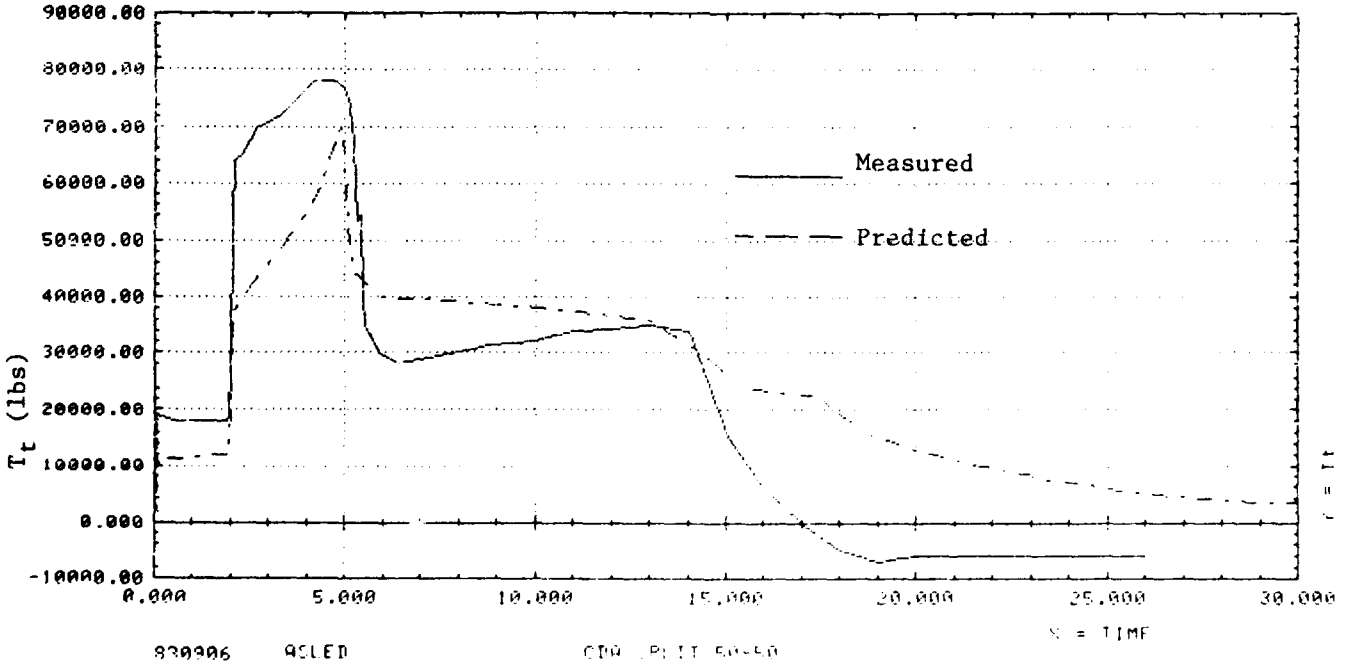

Figure 22. CDA Split 50% Pusher.

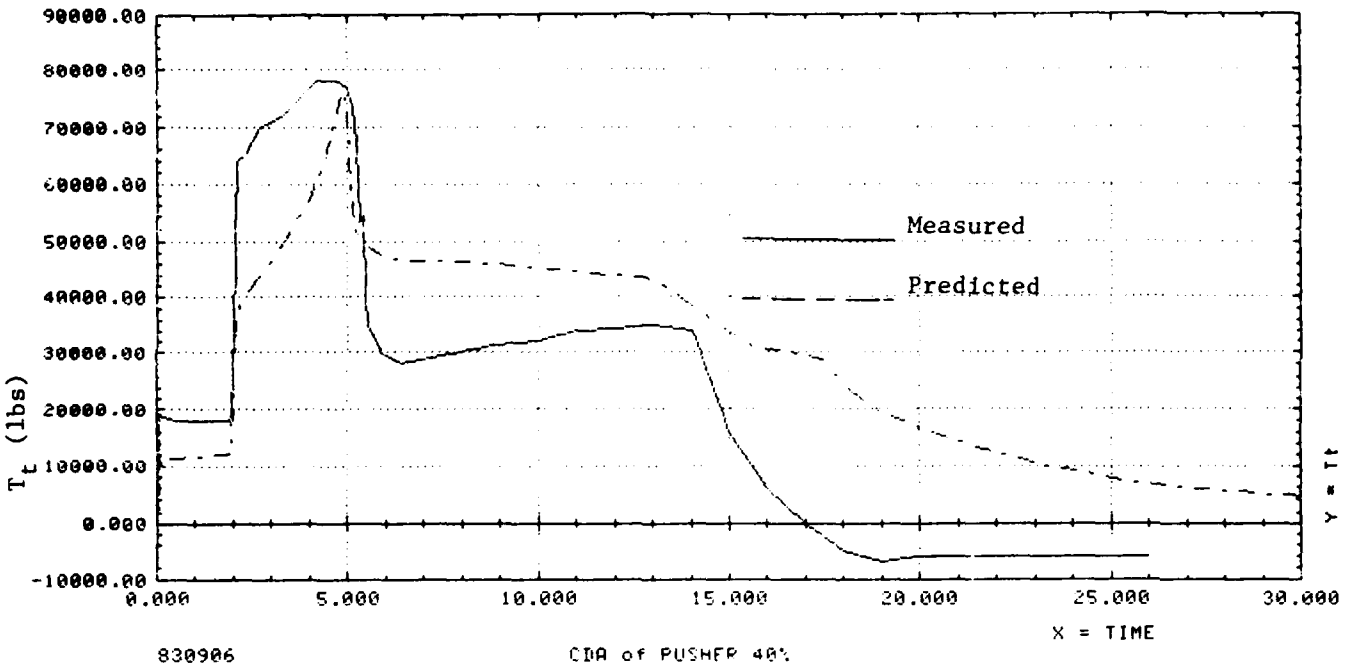

Figure 23. CDA Split 40% Pusher.

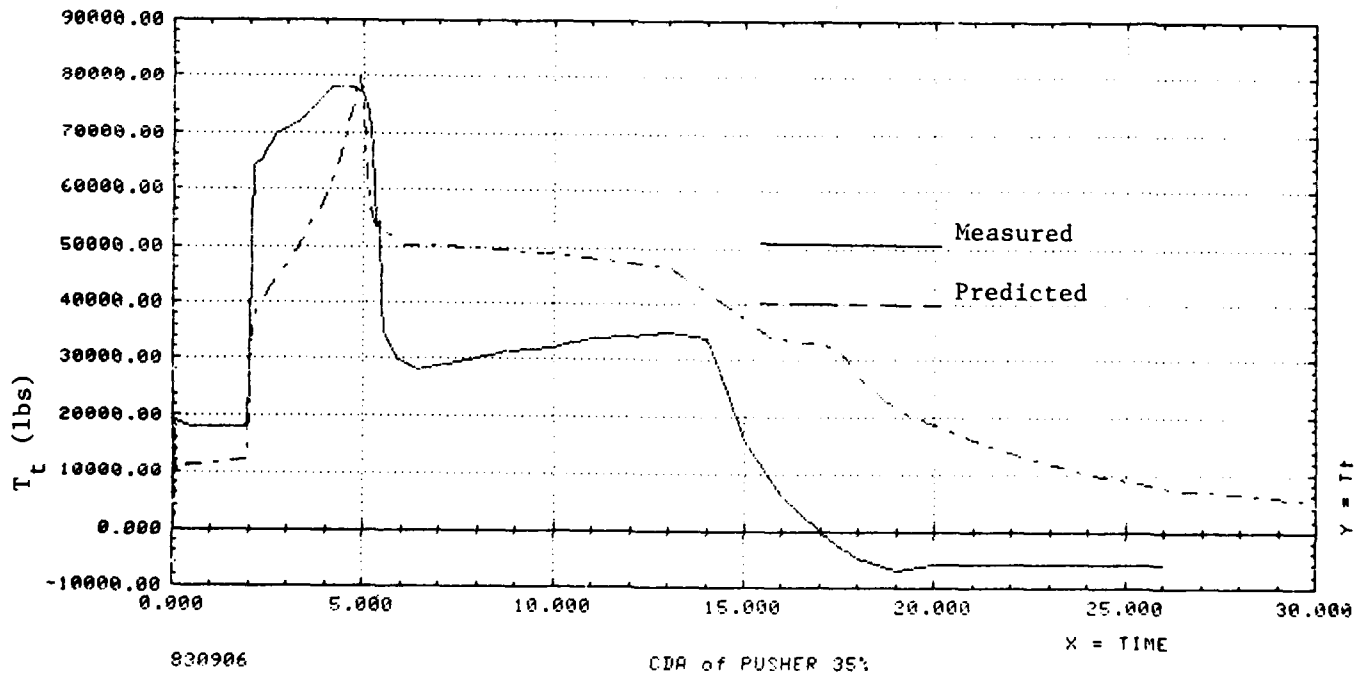

Figure 24. CDA Split 35% Pusher.

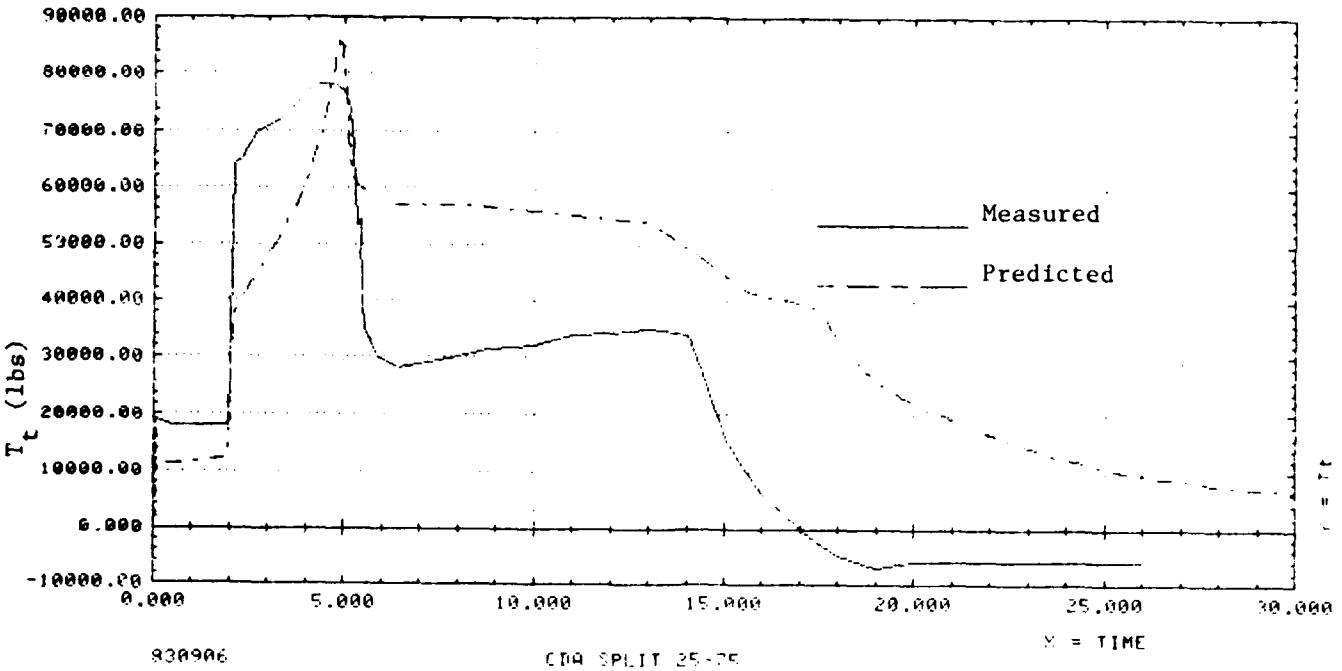

Figure 25. CDA Split 25% Pusher.

Although correlation was not obtained throughout the trajectory, an allocation of 35% of the overall drag to the pusher provided the best overall correlation and best agreement of peak transmitted thrust. Some thought was given to varying the percentage as a function of velocity, but for this particular trajectory, little was to be gained since the velocity did not vary significantly from 5.0 to 15.0 seconds.

3.2 Oscillatory Forces. Historically, the peak oscillatory forces have been expressed as a factor times the quasi-steady state transmitted thrust force which can be calculated as described in paragraph 3.1. A goal of this study was to establish a more indepth analysis procedure by finding parameter(s) proportional to the oscillatory transmitted thrust.

3.2.1 Velocity. First, the envelope of the peak oscillatory force was investigated as a function of the trajectory profile. The peak force envelope as a function of time is shown in Figure 26. Superimposed on the bar diagram is the velocity profile. Comparison of the plots verifies that

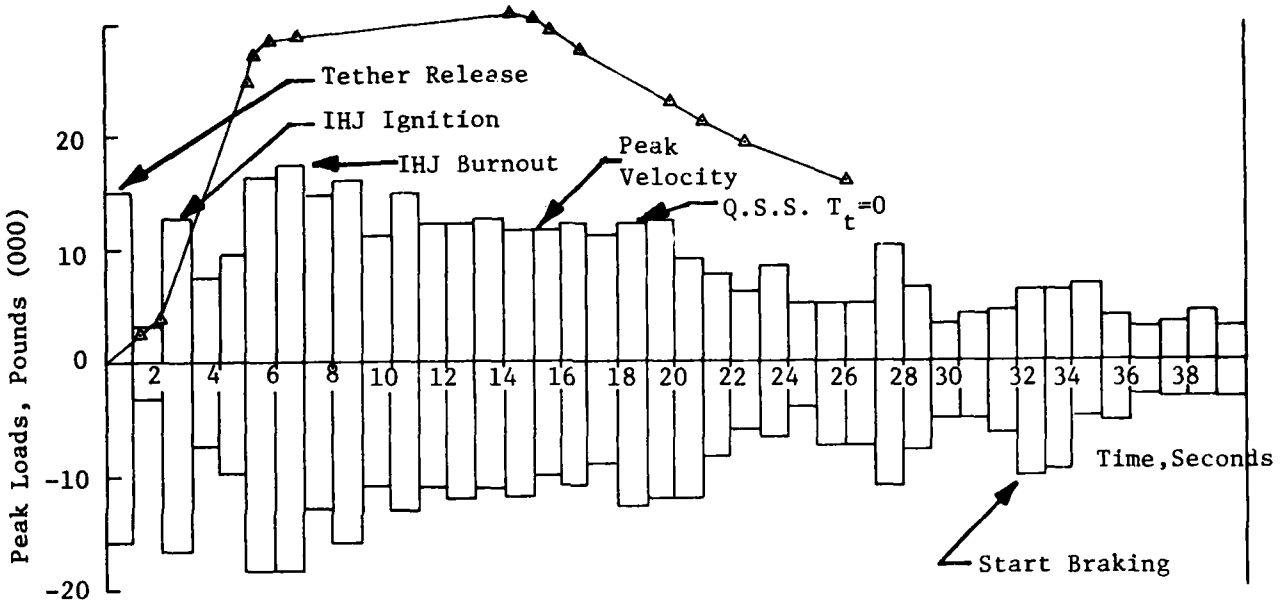

Figure 26. Oscillatory Peak T_t Envelope & Velocity Versus Time.

the oscillatory transmitted thrust is not a function of velocity. The peak oscillatory forces, ±18,000 pounds, occur at the burnout of the Improved Honest John rocket motors between 6 and 7 seconds. Peak velocity does not occur until approximately 15 seconds into the run and the peak oscillatory forces have settled down to approximately ±12,000 pounds. The peak forces appear to be a function of "events" and not a trajectory parameter.

3.2.2 Acceleration. The same type of plot was constructed with acceleration. Figure 27 shows the peak oscillatory envelope with acceleration superimposed. Again, the lack of correlation is obvious.

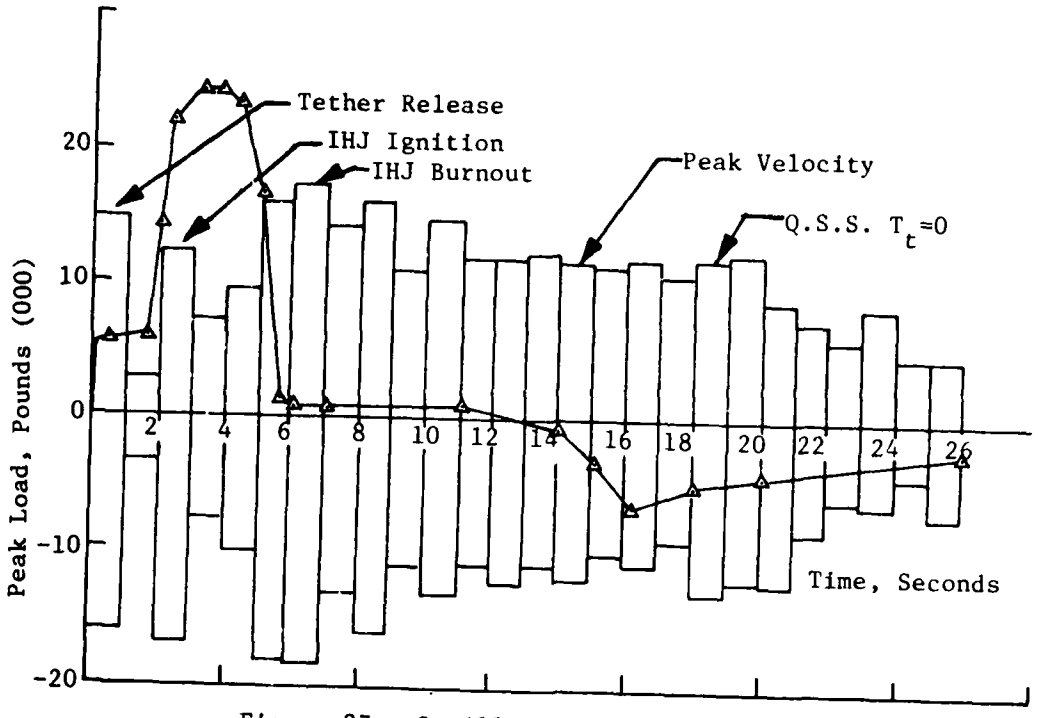

Figure 27. Oscillatory Peak T_t Envelope & Acceleration Versus Time.

3.2.3 Jerk. A third parameter was theorized as a potential correlation function. This parameter is sometimes referred to as "jerk" or the derivative of acceleration. The trajectory profile was modified to calculate this term. The absolute value of the derivative of acceleration |A dot| , is shown in Figure 28, as a function of time.

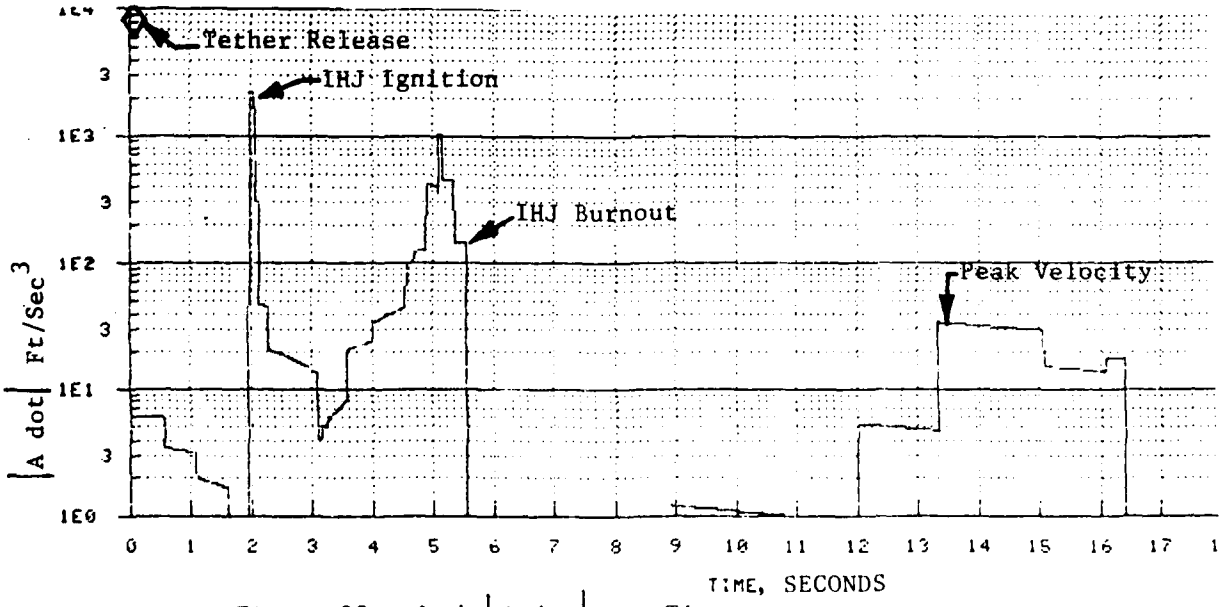

Figure 28 Jerk |A dot| vs Time.

This data was then replotted as peak oscillatory force as a function of |A dot| as shown in Figure 29. Obviously, no correlation can be established from this approach.

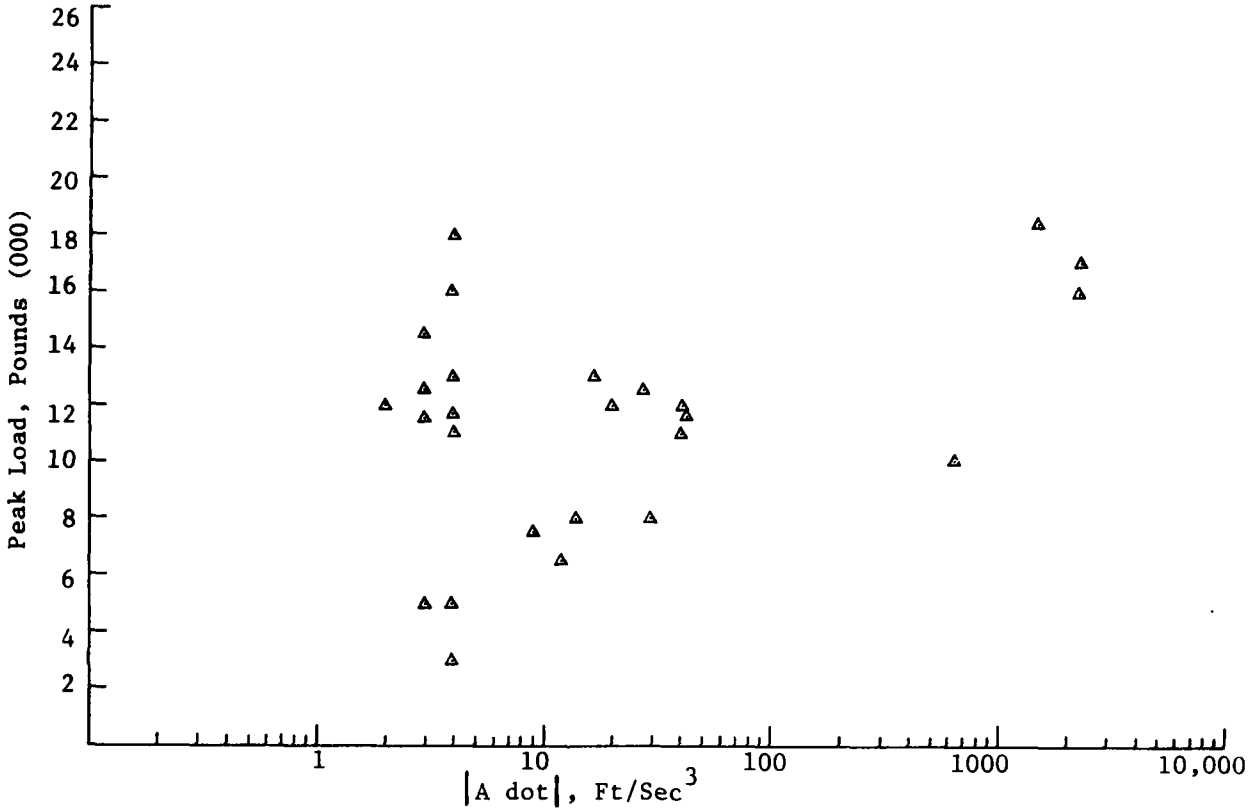

Figure 29. Peak Load versus |A dot|

3.2.4 Rocket Motor Burnout. As previously mentioned the peak oscillatory force occurred at the burnout of the Improved Honest John (IHJ) rocket motors. The question could be asked why equal or higher peak forces are not experienced at the burnout of the Sergeant rocket motors. Since burnout occurs at a higher velocity and presumably a greater amount of energy is present. First, the thrust of a Sergeant just before burnout is approximately 50,000 pounds, while the prior to burnout thrust of an Improved Honest John (IHJ) is approximately 120,000 pounds. Consequently, higher relative values are present with the IHJ rocket motor. Second and probably more significant is the time it takes for the two motors to terminate. In Figure 30, the burnout characteristics of the two motors are examined.

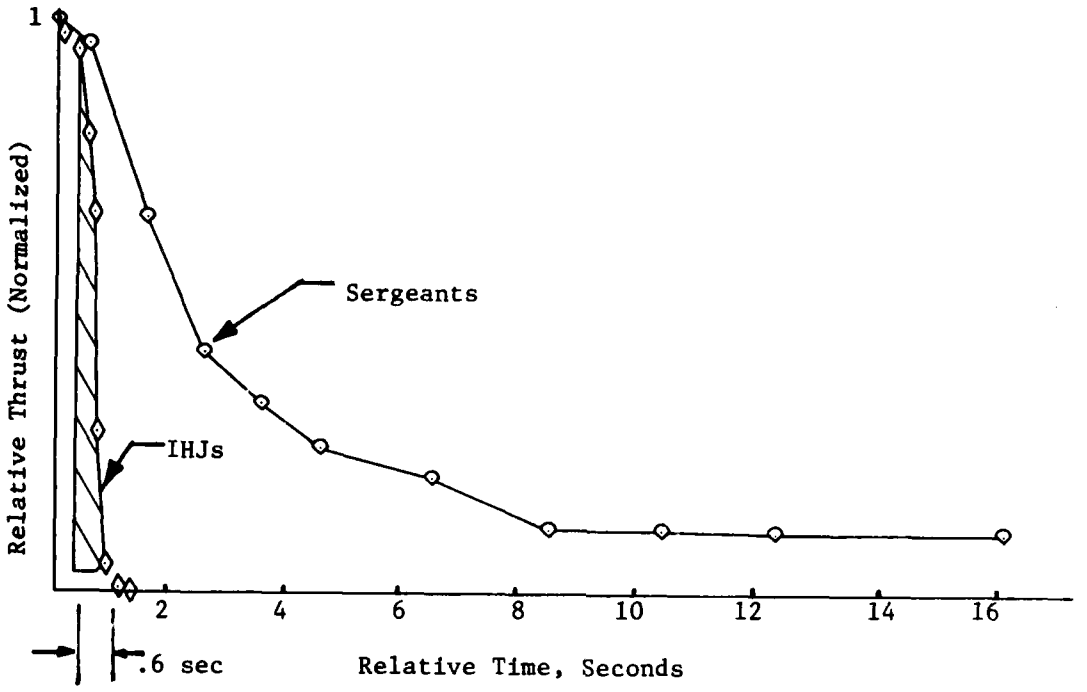

Figure 30. Comparison of Sergeant & IHJ Termination Times.

The thrust level for the two rocket motors has been normalized for comparison purposes. As shown, the termination of the IHJ motor is considerably more abrupt. While the IHJ 0.6 second period is long compared to periods associated with the structure, other phenomena associated with rocket motor shutdown dynamics may induce the relative high peak forces. For example, lateral dynamics are introduced into the structures as well as longitudinal dynamics.

3.2.5 Amplification Factor. As previously discussed, a goal of this study was to identify new parameter(s) other than quasi-steady state transmitted thrust to relate to oscillatory transmitted thrust. This goal was not achieved. It appears that the use of an amplification factor is still the most appropriate method to describe the dynamic forces. The original dynamic factor used in rocket sled design was 2.0 based on the response of a simple oscillator to a step input without damping. Based on data similar to that presented in this report, this factor was recently reduced to 1.5.

In this study the highest amplification factor occurs at tether release. As previously shown in the peak oscillator force envelopes, tether release did not experience the maximum peak force but the maximum amplification factor. See Figure 31.

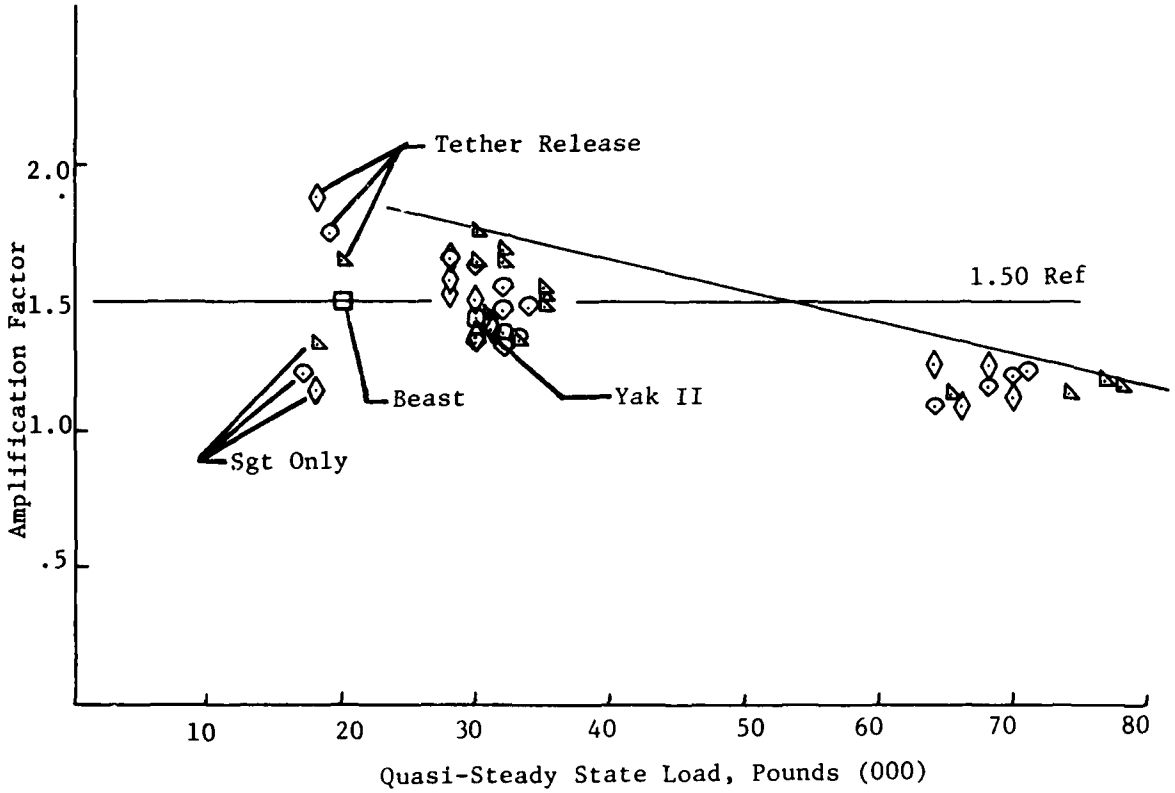

Figure 31. Amplification Factor vs Quasi-Steady State Load

The amplification factor at tether release varied from 1.65 to 1.89. This factor is the highest ever measure during this and similar studies of transmitted thrust. However, factors as high as 2.0 have been measured at on-set of water braking. The high amplification factor at tether release is due to the near instantaneous release of the sled system which approximates a step input relative to the natural frequencies of the sled structures.

The next interesting phenomenon is the very low amplification factors, 1.17 to 1.33, measured during the Sergeant burn prior to the ignition of the Improved Honest John rocket motors. The vibration is extremely quiet. No explanation is offered.

The remaining data as shown in Figure 31 is clustered around to quasi-steady state (Q.S.S.) levels, i.e., 28 - 33,000 pounds at 64 - 78,000 pounds. The maximum amplification factor was 1.75 for the low level of Q.S.S. levels and 1.25 for the higher Q.S.S. levels. A factor of 1.5 still appears appropriate.

3.3 Modal Correlation. Some knowledge of the mechanism of transmission of the oscillatory dynamic transmitted thrust can be gained by study of the sled system modes of vibration. Power Spectral Density (PSD) plots of the transmitted thrust force are shown in Figures 32, 33 and 34.

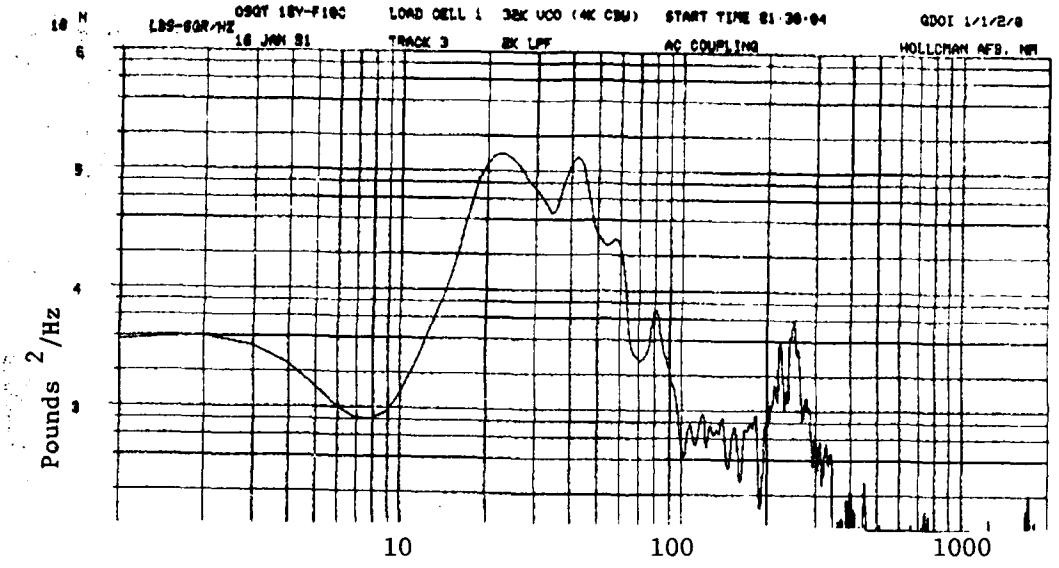

Figure 32. PSD Time Interval 4-5 Seconds.

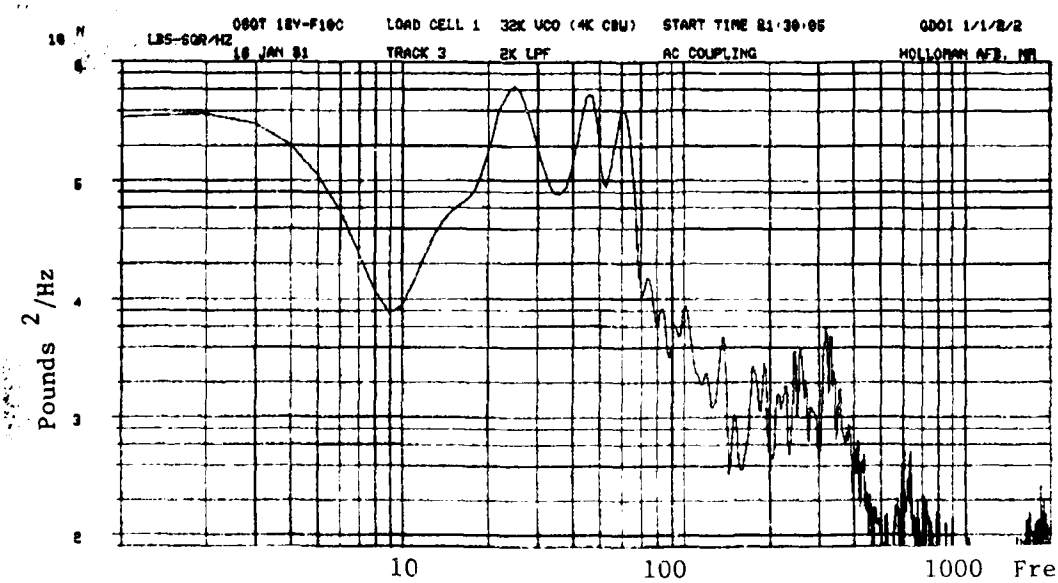

Figure 33. PSD Time Interval 5-6 Seconds.

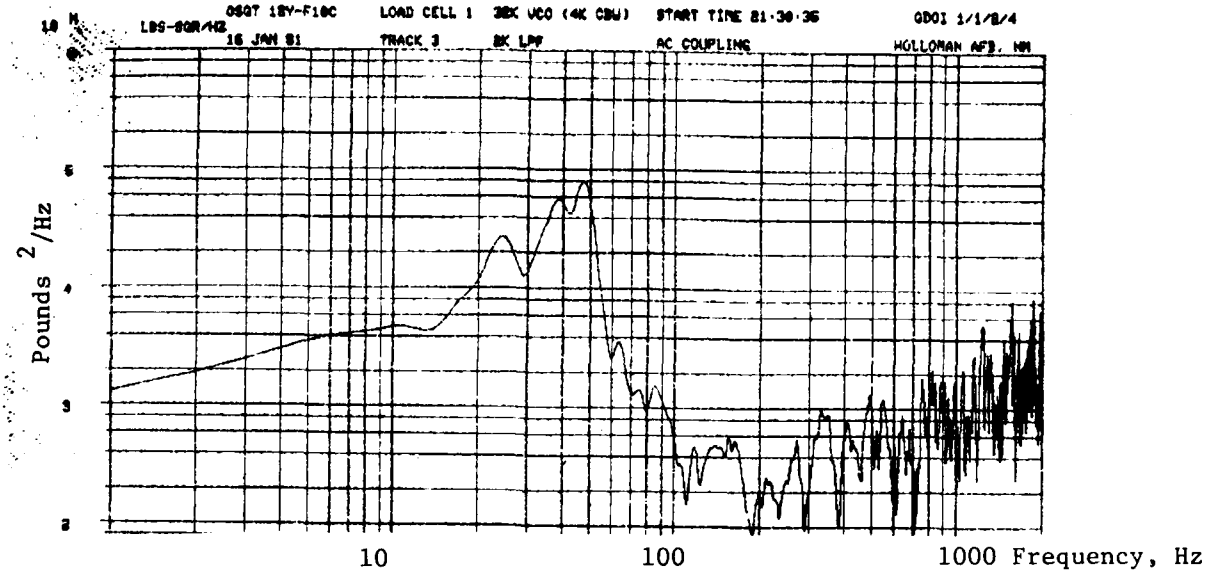

Figure 34. PSD Time Interval 35-36 Seconds.

These PSD's were computed for the following time intervals:

FIGURE	TIME INTERVAL	EVENT
32	4-5 seconds	Peak Q.S.S. transmitted thrust
33	5-6 seconds	I.H.J. Burnout
34	35-36 seconds	Water Braking

The primary strain energy is located at 23 Hz, 36 - 38 Hz, 42-47 Hz, and 61-63 Hz. Initially, it was theorized that the mechanism of vibration was the two sleds acting as two rigid masses connected by flexible clevises and instrumented bolt. Using stiffnesses measured in the laboratory for the clevises, calculated stiffness for the simple instrumented bolt, and calculated masses as a function of trajectory, a basic frequency of 76 to 79 Hz was calculated. Obviously, these values do not agree with the measured data, and the mechanism of vibration is not as theorized. In order to identify what structural elements were contributing to the lower measured modes of vibration, a shake test was conducted on the complete sled train.

A B335 Ling Electronics exciter with a 17,500 pound capacity was connected via a stiff fixture to the aft of the Tether pusher. The exciter was configured to shake in the longitudinal or down track direction. The instrumented bolt was used to couple the tether pusher to the Guidance forebody and a mixture of graphite and oil was placed between the eight slippers and the rail heads to reduce down-track friction.

The initial test was designed to identify which vehicle (pusher or forebody) or what combination was contributing to the measured vibration. By exciting the sled train with 0.26 g's RMS with a relative flat PSD spectrum from 10 Hz to 100 Hz, it was obvious that the modes of vibration of interest were associated primarily with the pusher sled and not the forebody. From this point on, the investigation was centered around the pusher sled.

A 10 Hz to 100 Hz sine sweep was conducted with the system configured as previously described. A reference accelerometer was mounted at the base plate which holds the tether clevis and was oriented in the vertical direction. A plot of this sine sweep is shown in Figure 35.

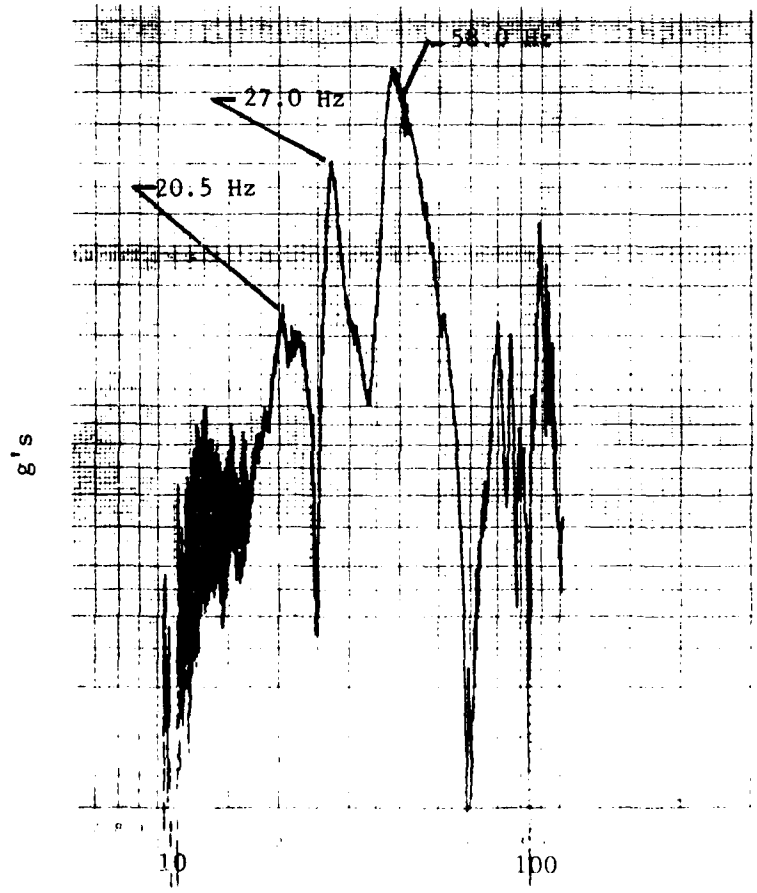

Figure 35. Sine Sweep Vertical Accelerometer.

As shown in this figure, resonances are evident at approximately 20.5, 27.0 and 38.0 Hz. This sine sweep was conducted with an input of 0.3 g's 0-peak amplitude. The excitation frequency was then focused at exact frequencies and the mode shape measured by positioning accelerometer along the sled structure while dwelling at a specified resonance frequency. The accelerometers were located as follows:

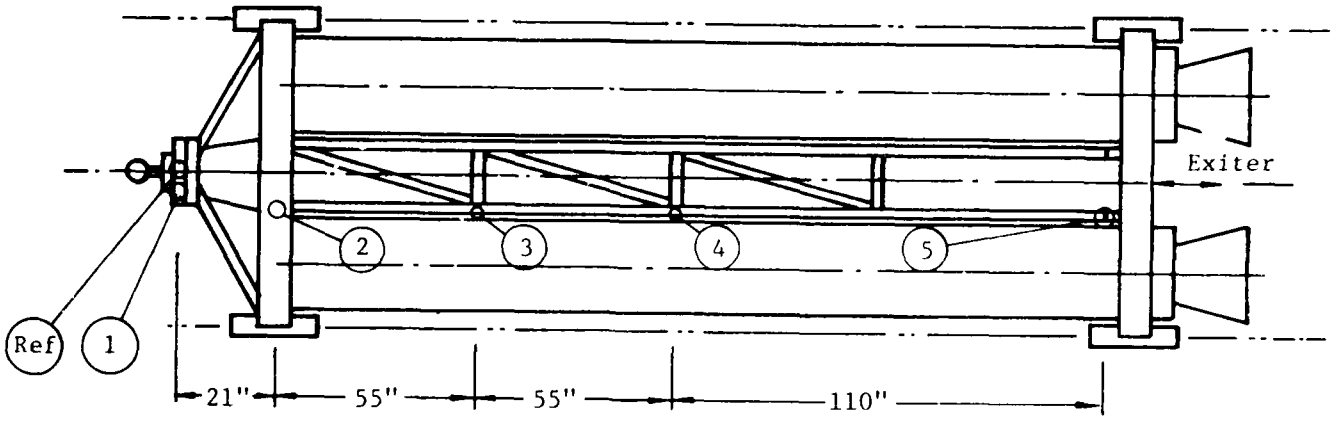

Figure 36. Schematic of Accelerometer Locations (Top View)

The following table summarizes results for the first three resonances.

TABLE 2. NORMALIZED MODES, VERTICAL

Accelerometer	f_o = 20.7 Hz			f_o = 25.3 Hz			f_1 = 36.5 Hz		
	Volts	Φ	Norm	Volts	Φ	Norm	Volts	Φ	Norm
Ref	.098	0°	1.00	.22	0°	1.00	.36	0°	1.00
1	.095	0°	1.00	.22	0°	1.00	.36	0°	1.00
2	.074	0°	.76	.15	0°	.68	.30	0°	.83
3	.022	0°	.22	.08	0°	.36	.024	70°	.02
4	.006	0°	.06	.04	0°	.15	.26	180	-.72
5	.002	0°	.02	.12	180°	-.54	.38	180	-1.06

Plots of these normalized modes of vibration are given in the next figure.

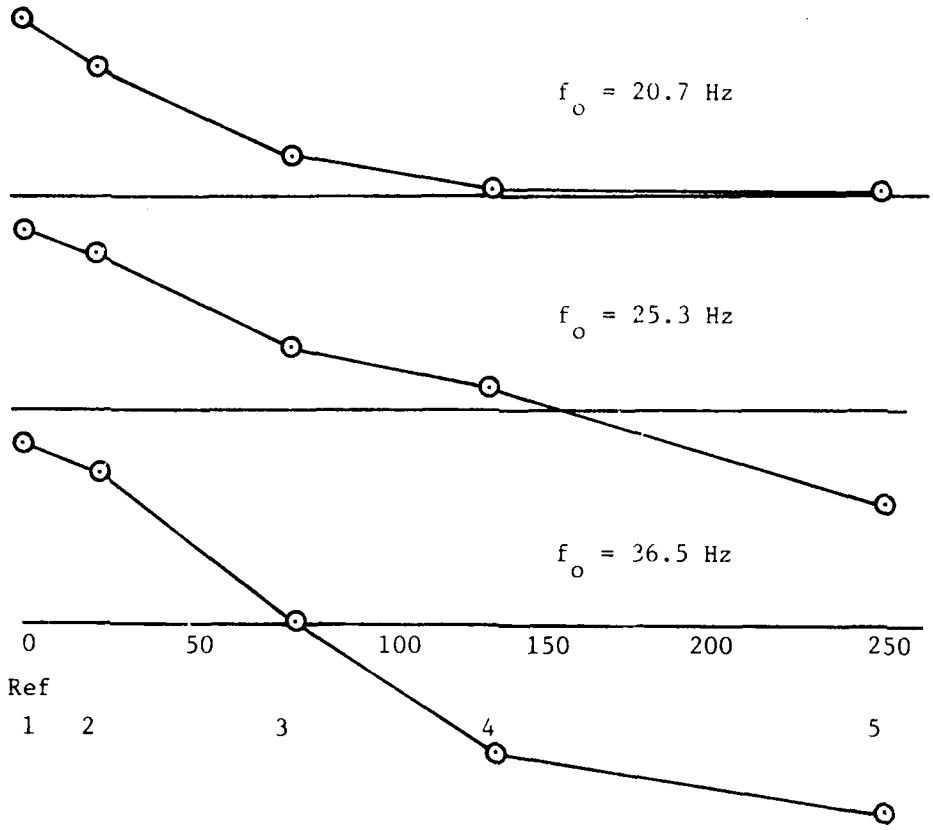

Figure 37. Normalized Modes.

The same procedure was followed for the longitudinal (down track) direction. The only difference being the accelerometers were oriented in the longitudinal direction.

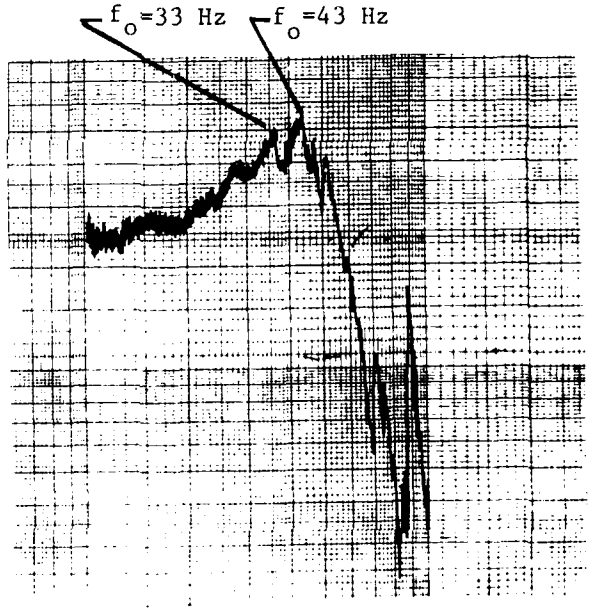

Figure 38. Sine Sweep Longitudinal Accelerometer.

The two lowest resonances are approximately 33 Hz and 43 Hz. Again, the exciter was tuned until the exact resonances were obtained and the modes measured. Results are summarized in the following table.

TABLE 3. NORMALIZED MODES, LONGITUDINAL

f_o = 34.7 Hz				f_o = 42.5 Hz		
Accelerometer	Volts	Φ	Norm	Volts	Φ	Norm
Ref	.28	0°	.73	.26	0°	1.00
1	.28	0°	.73	.26	0°	1.00
2	.39	0°	1.00	.22	0°	.85
3	.38	0°	.97	.18	0°	.69
4	.38	0°	.97	.22	0°	.85
5	.37	0°	.95	.20	0°	.77

The modes are rather difficult to plot since the motion is in the longitudinal direction; consequently, visual presentation of the modes is not provided.

4. DISCUSSION

The dynamic forces measured with the instrumented bolt were centered around the following frequencies, 23, 36-38, 42-47, and 61-63 Hz with the first three modes containing the majority of the strain energy. Mode shapes were measured at 20.7 and 25.3 Hz in the vertical direction which accounts for the sled test 23 Hz measurement. Considering the relative magnitude of forces, i.e., shake test versus sled test and the resolution of the PSD, it is entirely feasible that the 20.7 Hz and 25.3 Hz modes combine in the high dynamic sled test at 23 Hz. The 36.5 Hz measured mode appears to be pitch plane rocking mode which correlates to the track measured frequency of 36-38 Hz. The first measured longitudinal mode of 34.7 Hz appears to be a rigid body longitudinal mode of vibration whereby the sled acts as a rigid body suspended on flexible slipper beams. Evidently, the oil and graphite did not sufficiently free the ends of the pusher slipper beams. The measured 42.5 longitudinal modes correlates with the measured 42-47 Hz strain measured during the sled tests. Time was not taken to attempt to identify the higher less significant 61-63 Hz mode apparent in the Test Track data.

In conclusion, the modes of vibration observed during the sled test were identified in the laboratory test and were found to be associated with the pitch plane pusher modes of vibration. Any mathematical model of the sled train must include the first four to five pusher modes of vibration.

5. CONCLUSIONS

The Tether Sled Qualification Program provided the opportunity to study the transmitted thrust on a large dual rail rocket sled system at minimal extra expense. A strain-gauged instrumented bolt (force transducer) was inserted between the pusher sled and the guidance forebody which produced excellent quality data of the quasi-steady state forces and the superimposed oscillatory transmitted thrust. Additional instrumentation was applied on one sled test in terms of strain-gauges on the guidance forebody slipper beams and a down-track accelerometer. These data assisted in correlation studies and to identify the interaction of the transmitted thrust and forebody response.

The data was checked for quality control, digitized and engineering units applied. In addition, the transmitted thrust was separated into the quasi-steady state force and residuals which represented the unbiased oscillatory forces. Also, Power Spectral Density (PSD) analysis was performed on one second interval to identify the modes of vibration. Normally tests were conducted on the data. Additional data was obtained from shake tests in terms of acceleration plots. All these data sources proved the basis for correlation studies.

The first correlation study was conducted on the quasi-steady state (Q.S.S.) forces. A computer code was used to predict the Q.S.S. force, velocity, acceleration, and transmitted thrust. Results were then compared with measured velocity and acceleration and input parameters were varied until adequate correlation of the trajectory was obtained. Then, a sensitivity test was conducted where varying percentages of the total system drag was applied to the pusher sled. The best correlation of transmitted thrust was obtained when 32% of the total system drag was allocated to the pusher.

One of the objectives of this study was to identify new parameters for correlation to oscillatory transmitted thrust. This objective was not satisfied. First, no correlation was found between the oscillatory transmitted thrust and the trajectory parameters, i.e., velocity and acceleration. Then a computer code was modified to predict jerk or the derivative of acceleration. Again, lack of correlation was obtained. The peak oscillatory forces were a function of events such as onset of the Improved Honest John rocket motor and more especially burnout of the same rocket motor. After failure to establish a new technique to predict peak oscillatory transmitted thrust, the approach was to revert back to expressing the peak forces as an amplification factor times the predictable quasi-steady state (Q.S.S.) transmitted thrust. A plot of amplification factor versus Q.S.S. force is provided which shows an amplification factor of 1.75 for the low Q.S.S. forces (28,000 - 35,000 pounds), and 1.25 for the higher Q.S.S. forces (65,000 - 80,000 pounds). The result was consistent with previous measurement of transmitted thrust and lends credibility to the now used factor of 1.5.

The last phase of the correlation study was to identify what modes of sled vibration contributed to oscillatory dynamic thrust. PSDs were used to identify the transmitted thrust mode of vibration, and the strain energy was centered around four predominant modes, i.e., 23, 36-38, 42-47, and 58-63 Hz. The rocket sleds were then taken to an environmental laboratory and random and sine tests conducted. Initial vibration surveys showed the three lowest frequencies to be associated with the pusher and not the guidance forebody. Dwell tests were conducted and the mode shapes measured. Excellent correlation was obtained for the three more important lower modes. The higher 58-63 Hz mode was not identified. This modal analysis was important because it is now established that at least four to five pusher modes of vibration must be included in future mathematical models of the coupled sled system.

REFERENCES

1. BAKER, W.E., "Force Measurement on Rocket Sleds," January 1967, Air Force Missile Development Center, MDC-TR-66-119, AD 647038, Holloman AFB, New Mexico.

2. "The Holloman Track Facilities and Capabilities," 1974, Armament Division, Air Force Special Weapons Center, 6585th Test Group, Test Track Division, Holloman AFB, New Mexico.

3. SCHWINGE, H.T., "Effectiveness and Limitations of Moving Polynominal Arc Smoothing of Position-Time Data from the Holloman Track," February 1962, MDC-TDR-62-2, Deputy for Development and Test, Air Force Missile Development Center, Test Track Division, Holloman AFB, New Mexico.

4. KRUPOVAGE, D.J., Mixon, L.C., and Pokorny, O.T., "Wind Tunnel and Full-Scale Forces on Rocket Sleds," January 1967, MDC-TR-67-12, Air Force Missile Development Center, Holloman AFB, New Mexico.

5. KRUPOVAGE, D.J., Mixon, L.C., and Pokorny, O.T., "Wind-Tunnel and Full-Scale Forces on Rocket Sleds," October 1967, Vol 4, No. 10, Journal of Spacecraft and Rockets, American Institute of Aeronautics and Astronautics.

APPENDIX A

18Y-F9C, 18Y-F10C, 18Y-F11C RESIDUALS

18Y-F9C

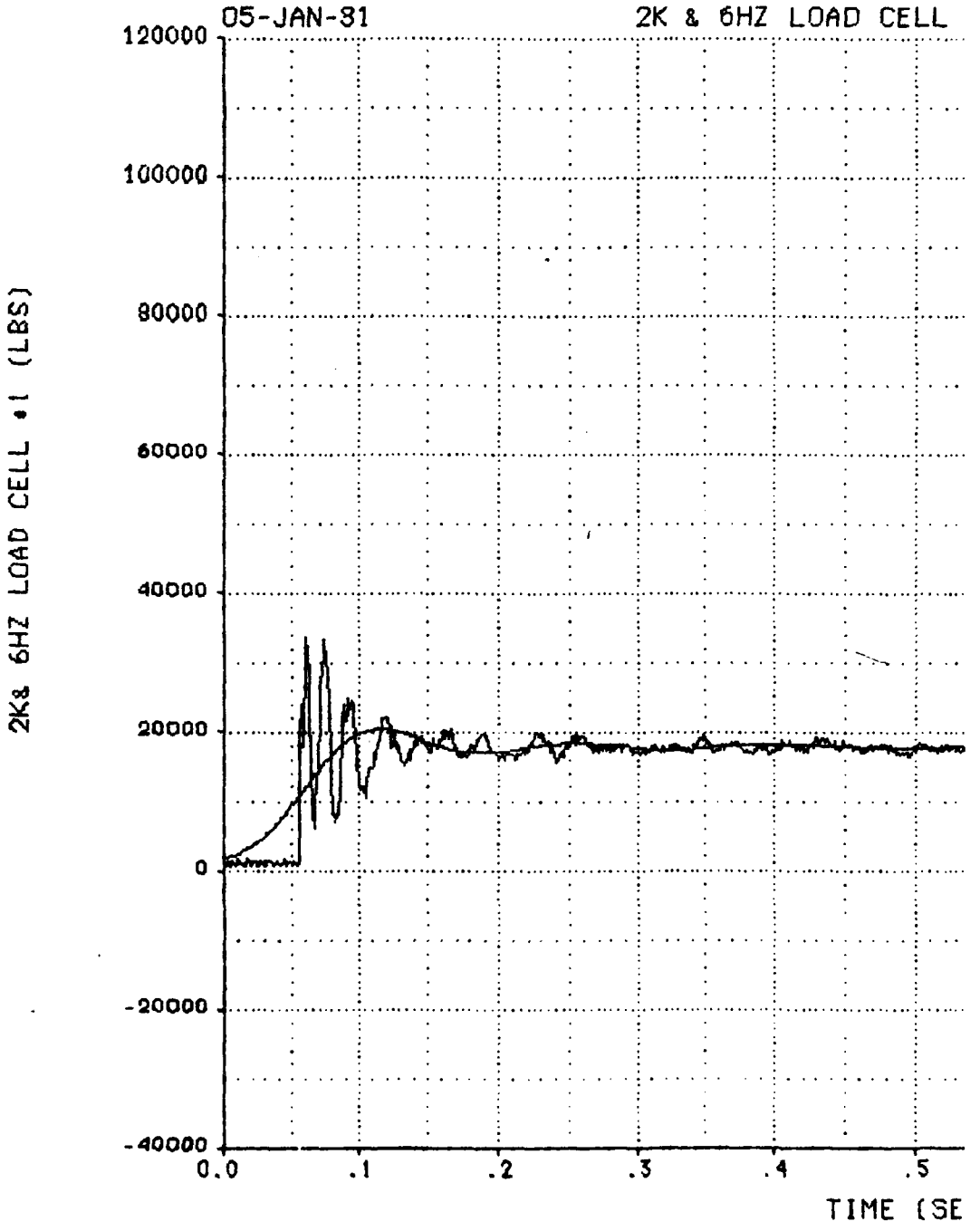
05-JAN-81
2K & 6HZ LOAD CELL
120000
100000
80000
60000
40000
20000
0
-20000
-40000
0.0
.1
.2
.3
.4
.5
TIME (SE
2K& 6HZ LOAD CELL #1 (LBS)

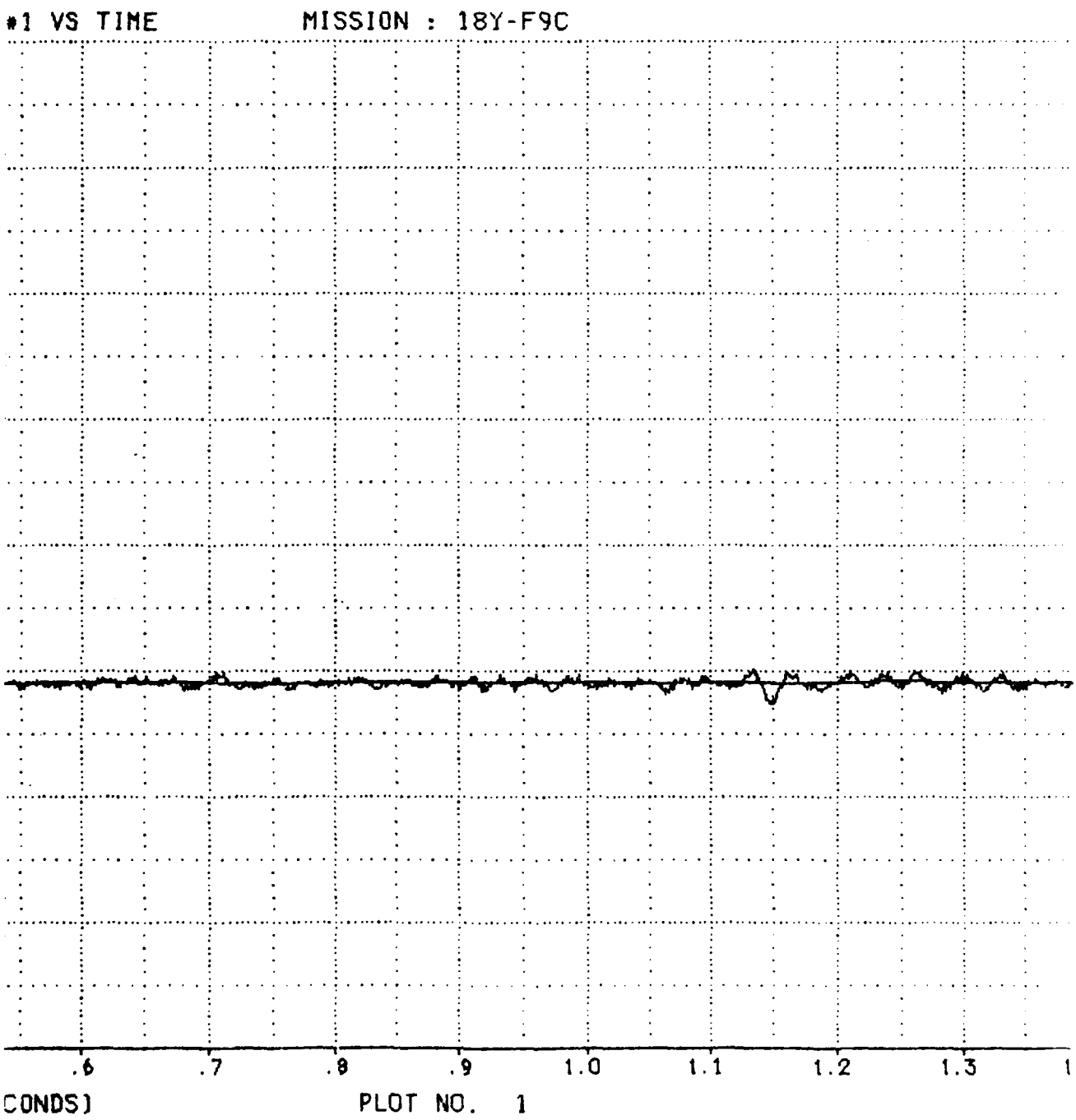
#1 VS TIME
MISSION : 18Y-F9C
.6
.7
.8
.9
1.0
1.1
1.2
1.3
CONDS)
PLOT NO. 1

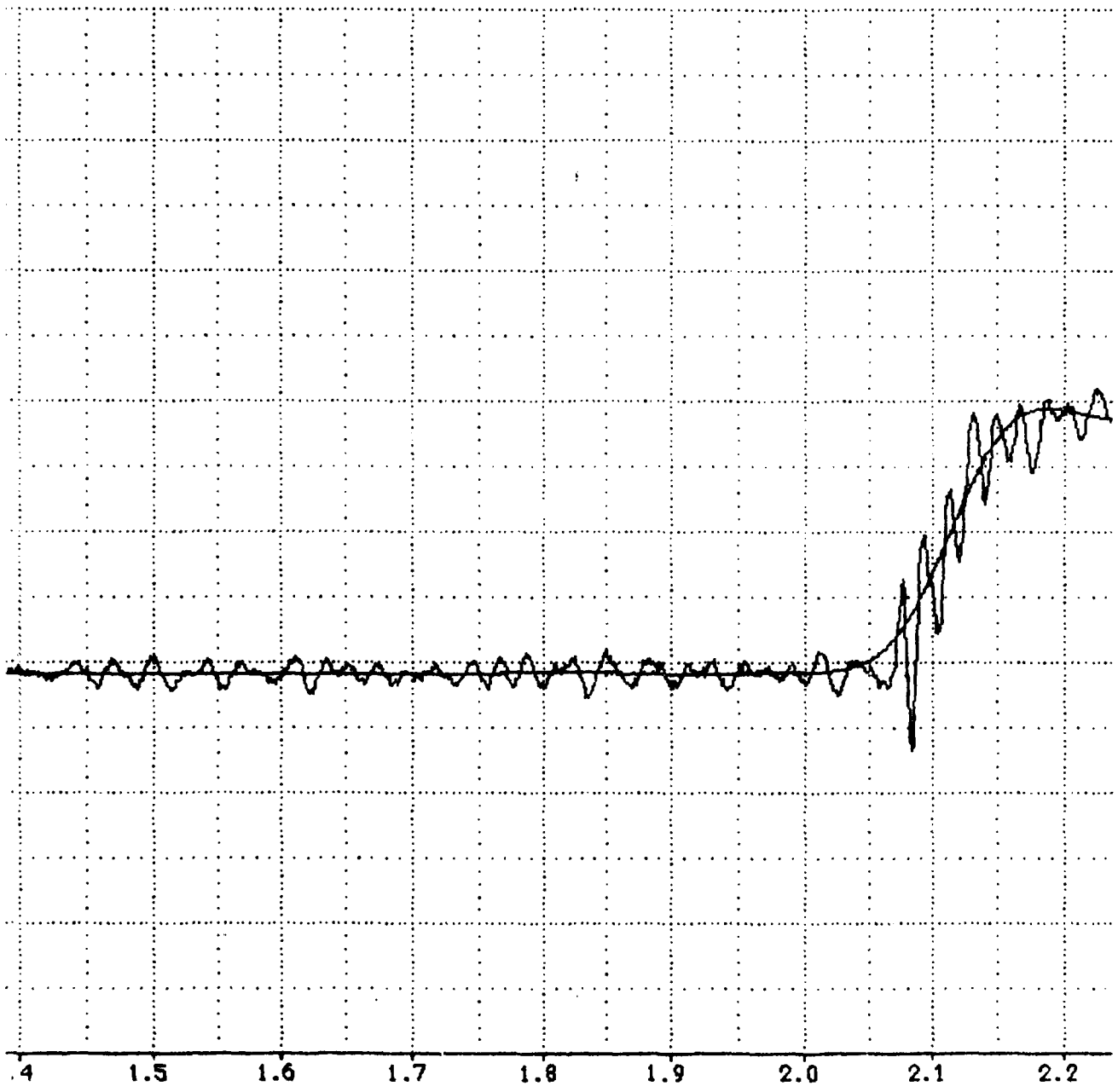
.4
1.5
1.6
1.7
1.8
1.9
2.0
2.1
2.2

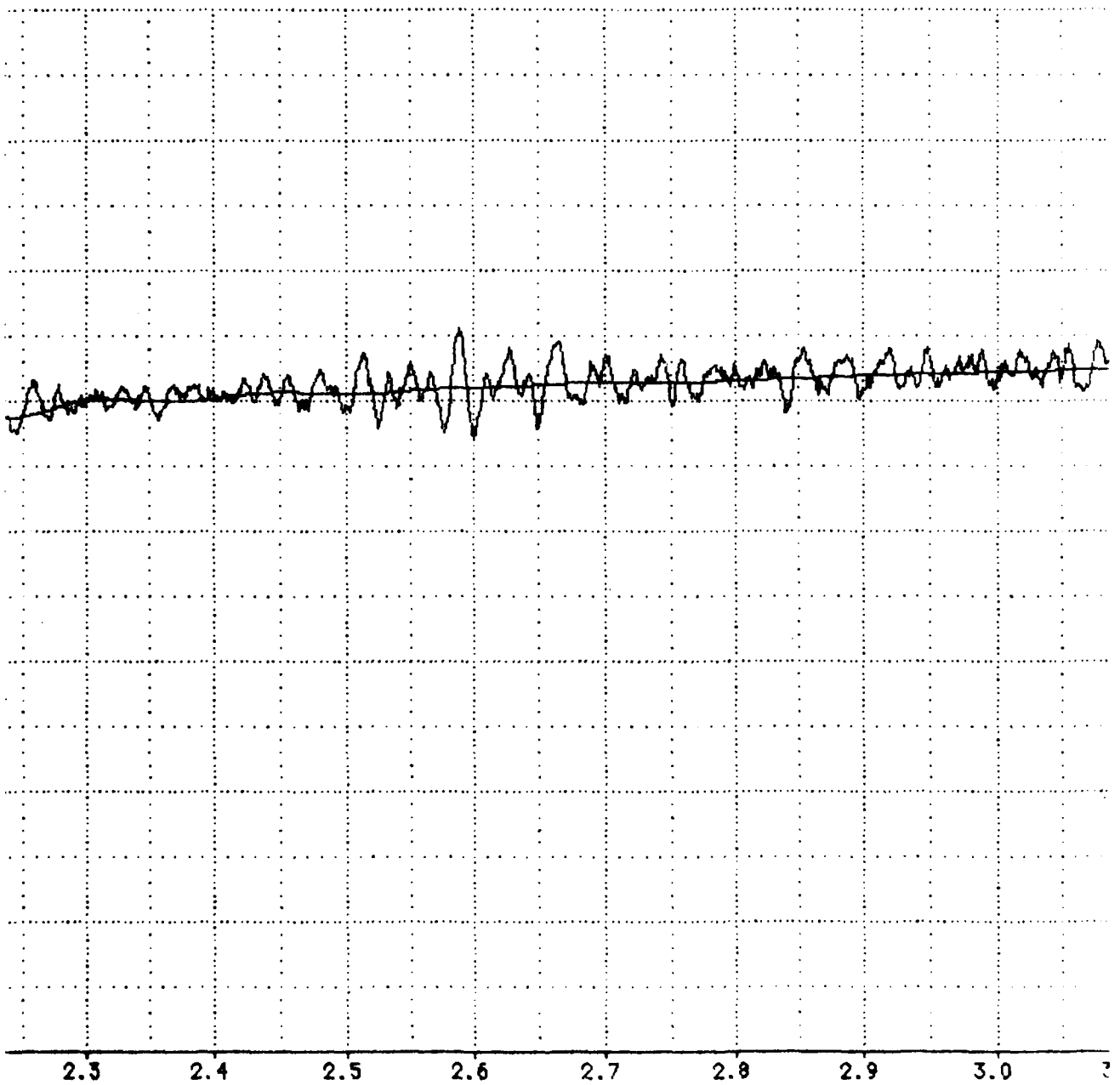
2.3
2.4
2.5
2.6
2.7
2.8
2.9
3.0

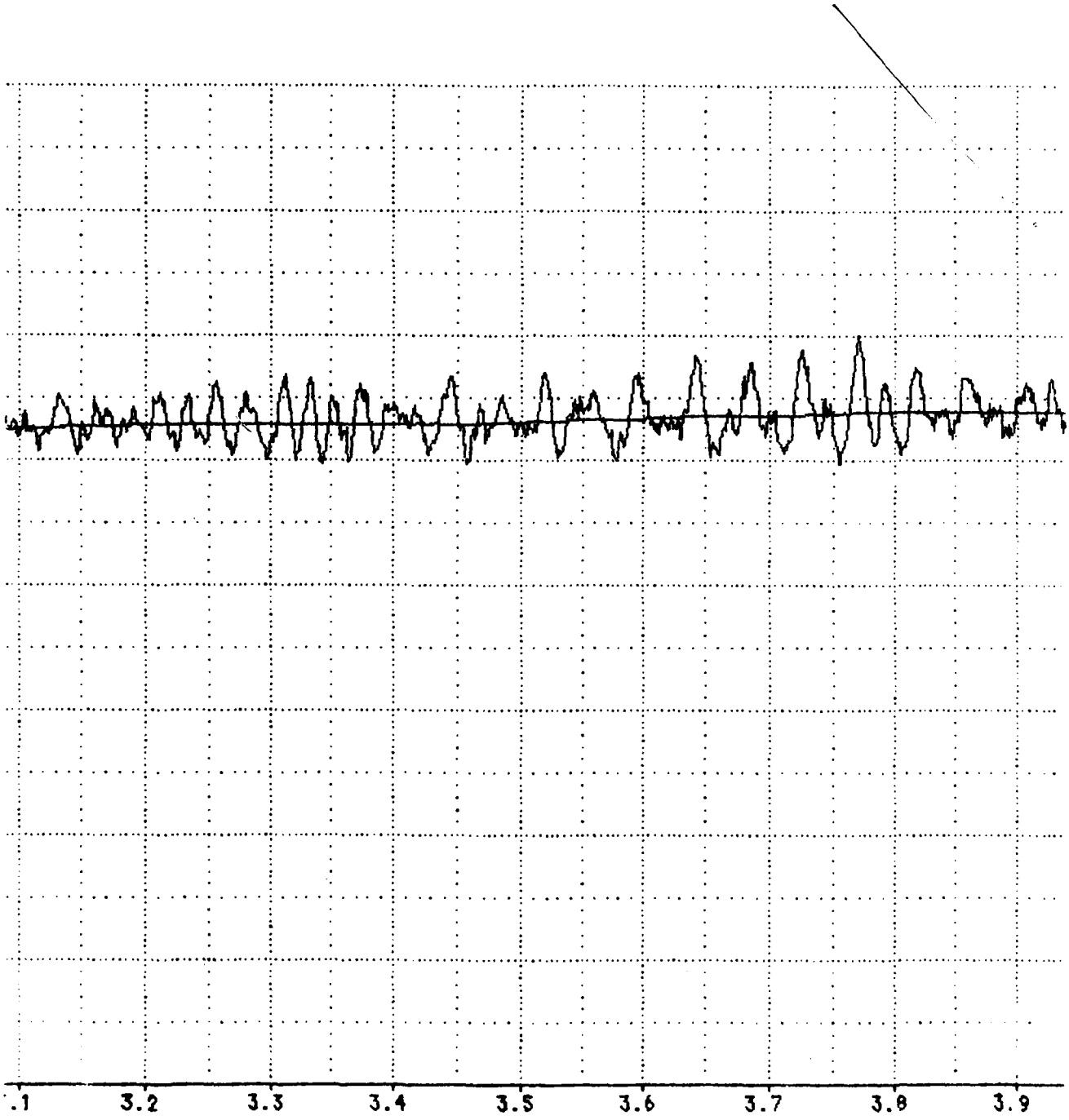
.1
3.2
3.3
3.4
3.5
3.6
3.7
3.8
3.9

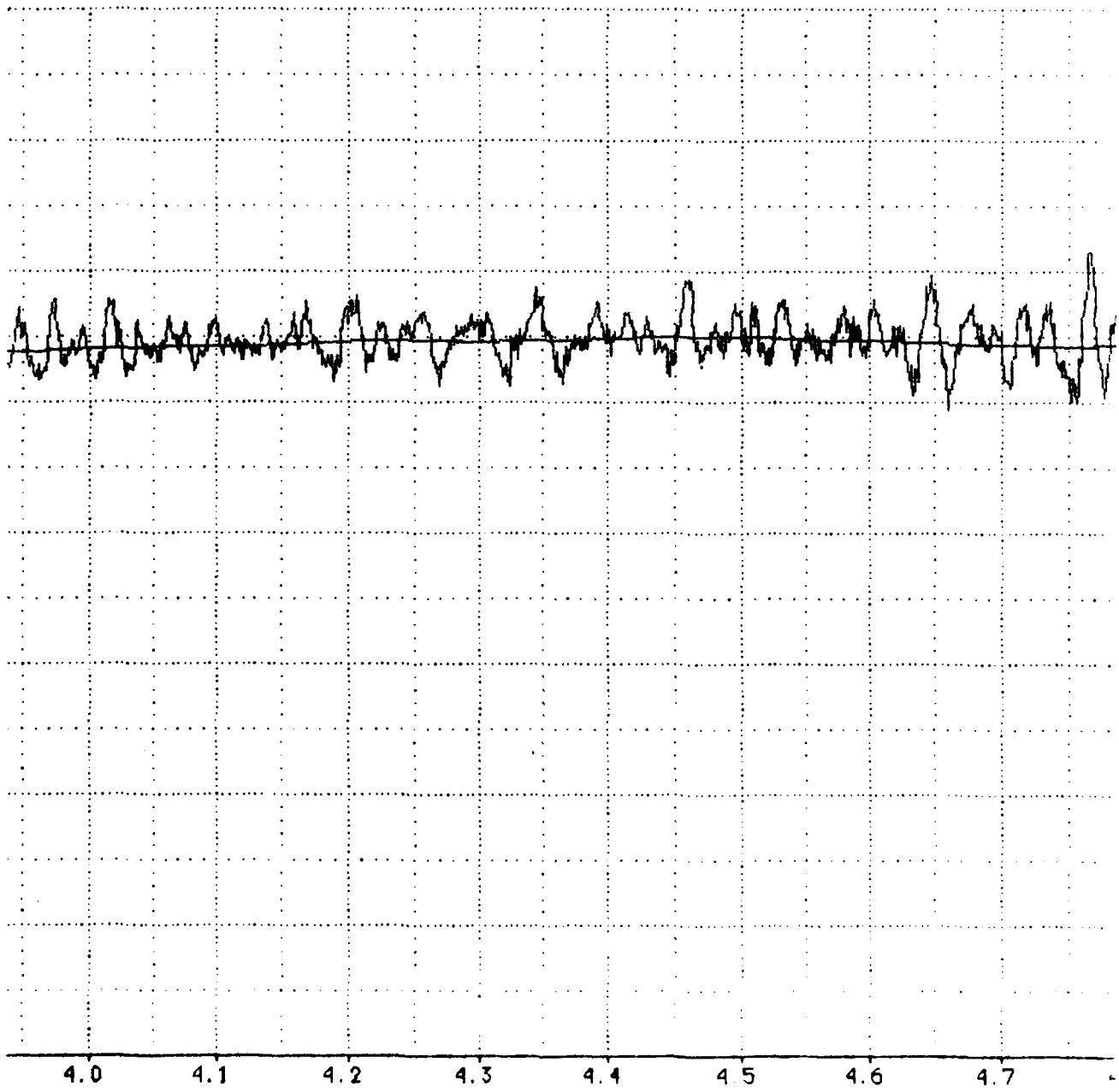
4.0
4.1
4.2
4.3
4.4
4.5
4.6
4.7

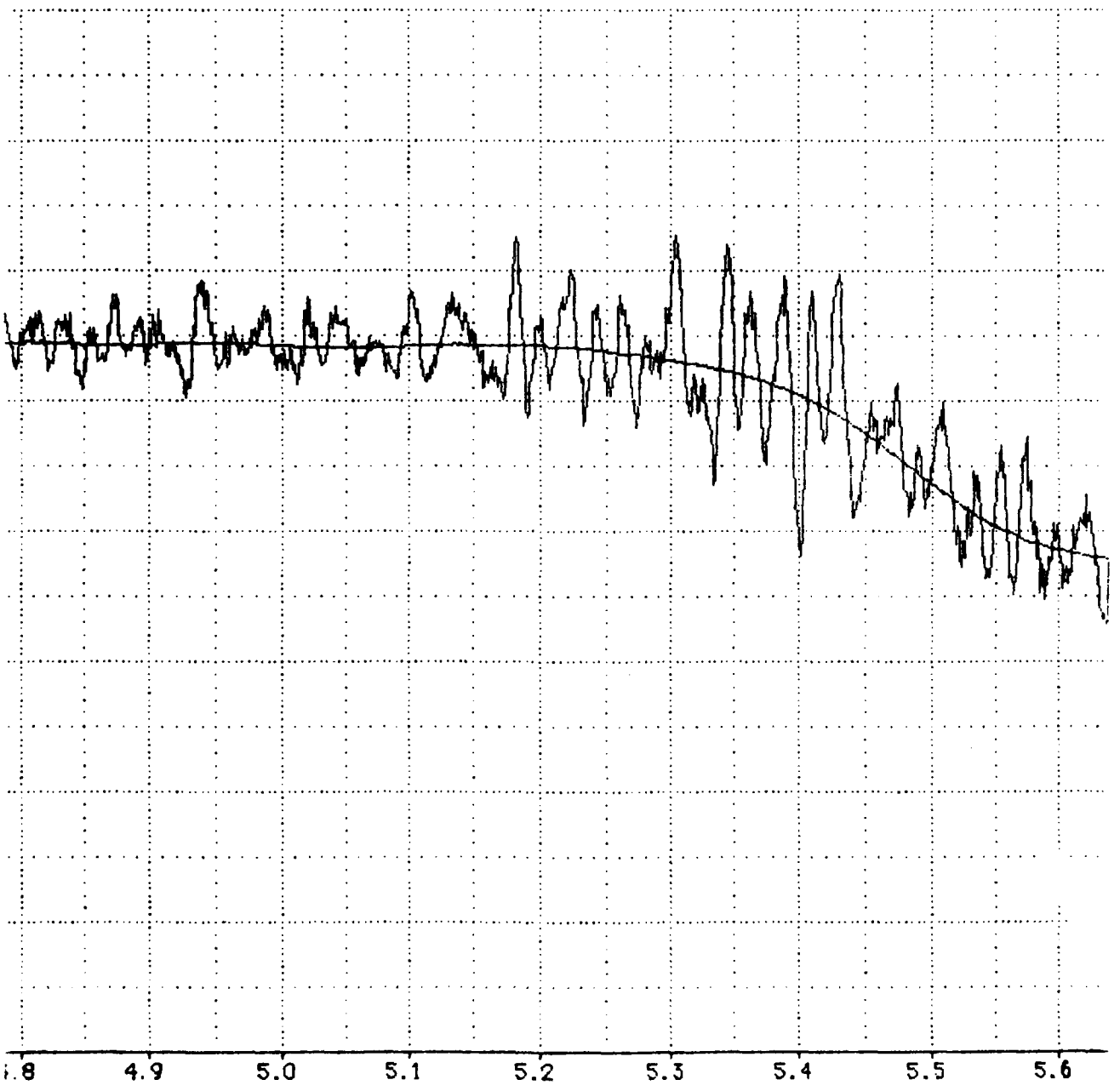
.8
4.9
5.0
5.1
5.2
5.3
5.4
5.5
5.6

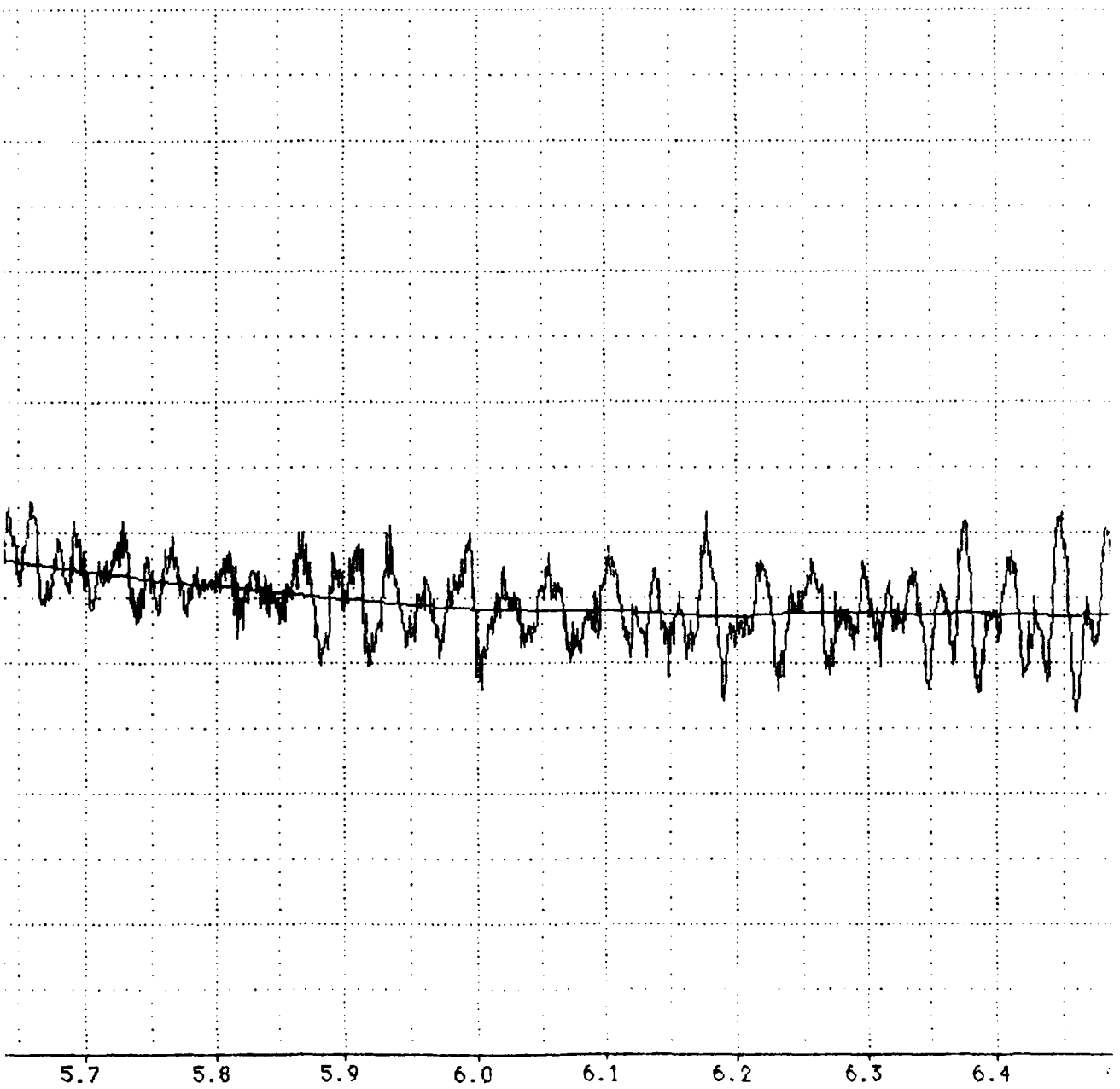
5.7
5.8
5.9
6.0
6.1
6.2
6.3
6.4

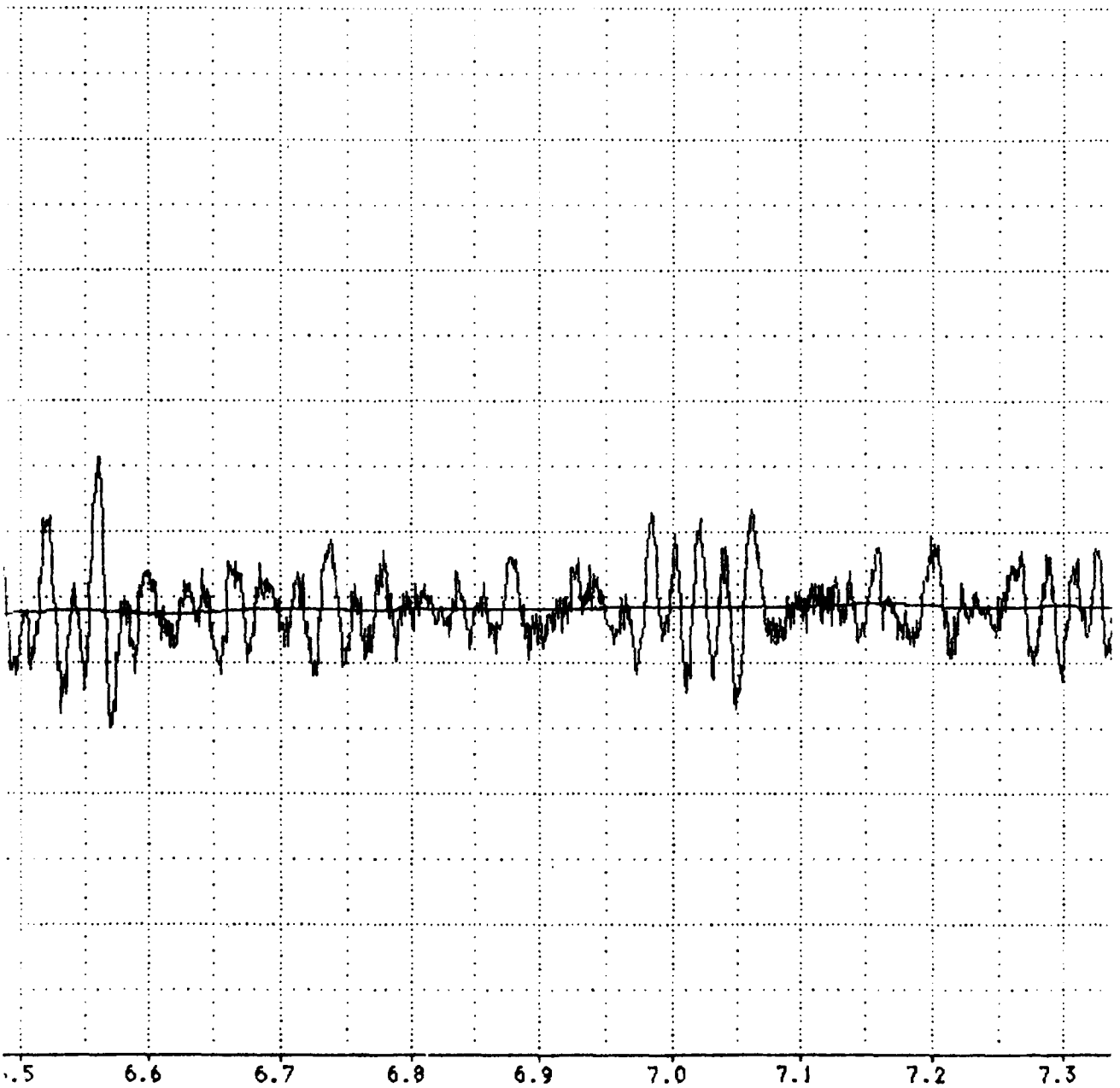
.5
6.6
6.7
6.8
6.9
7.0
7.1
7.2
7.3

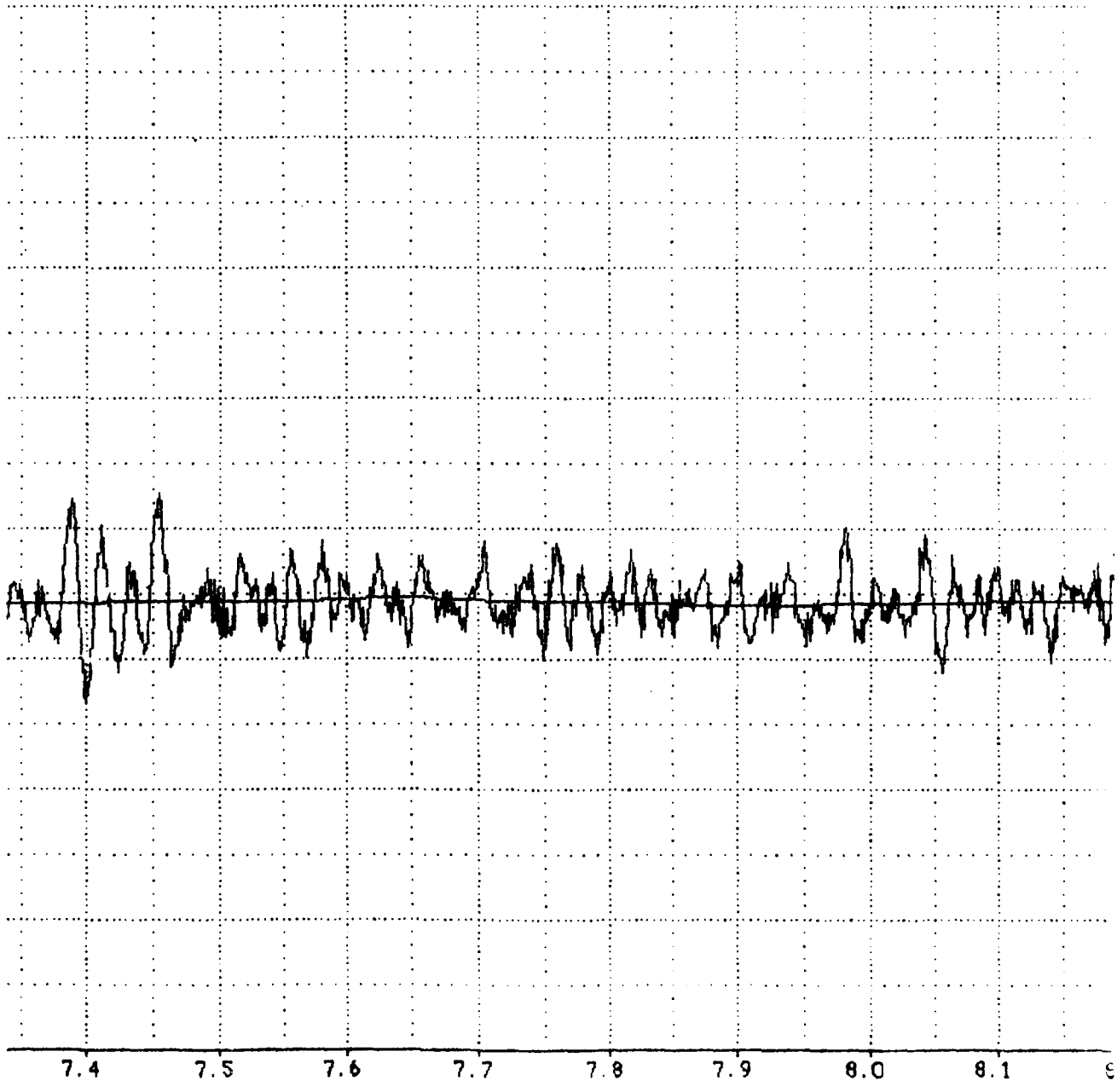
7.4
7.5
7.6
7.7
7.8
7.9
8.0
8.1

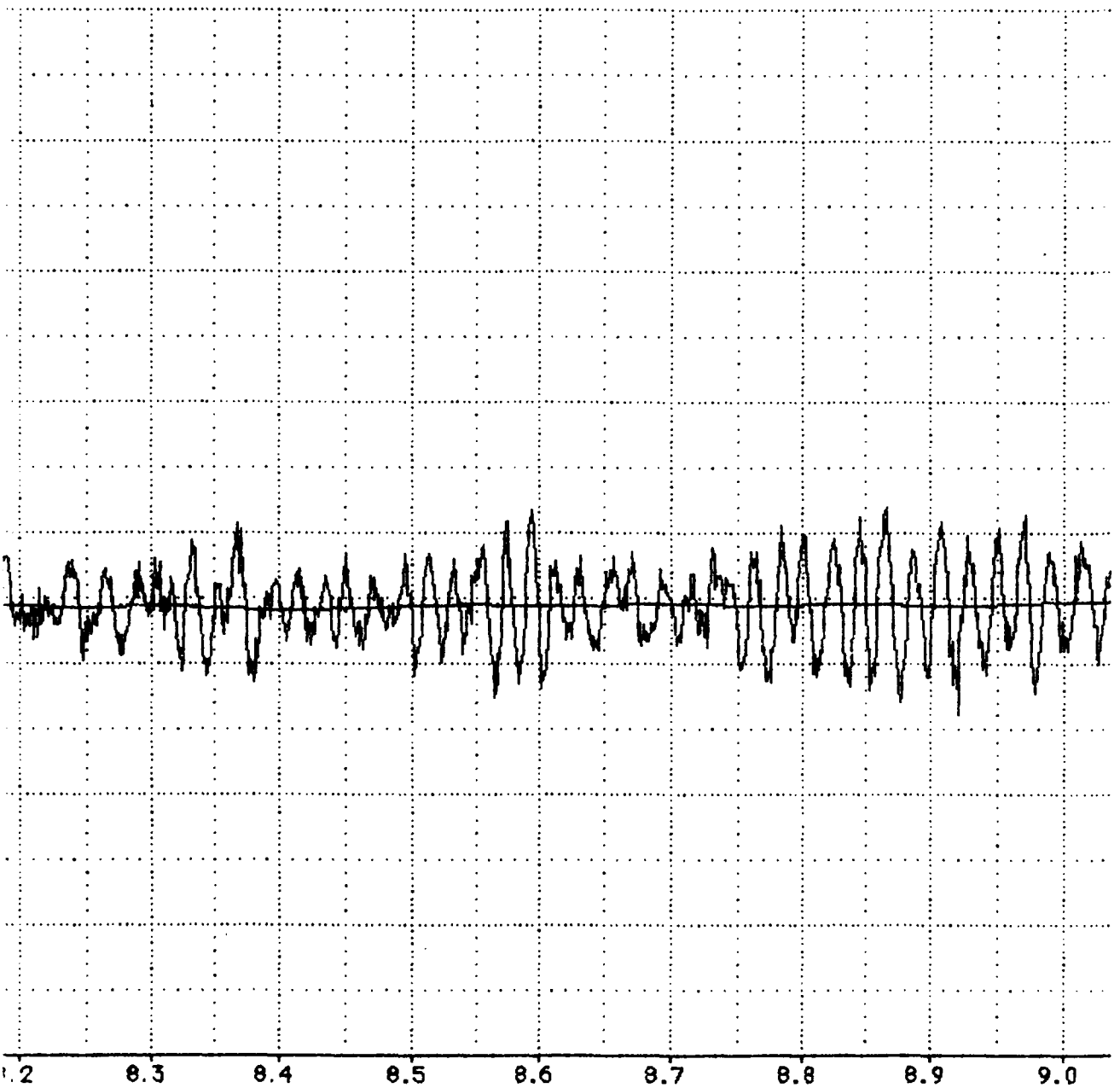
.2
8.3
8.4
8.5
8.6
8.7
8.8
8.9
9.0

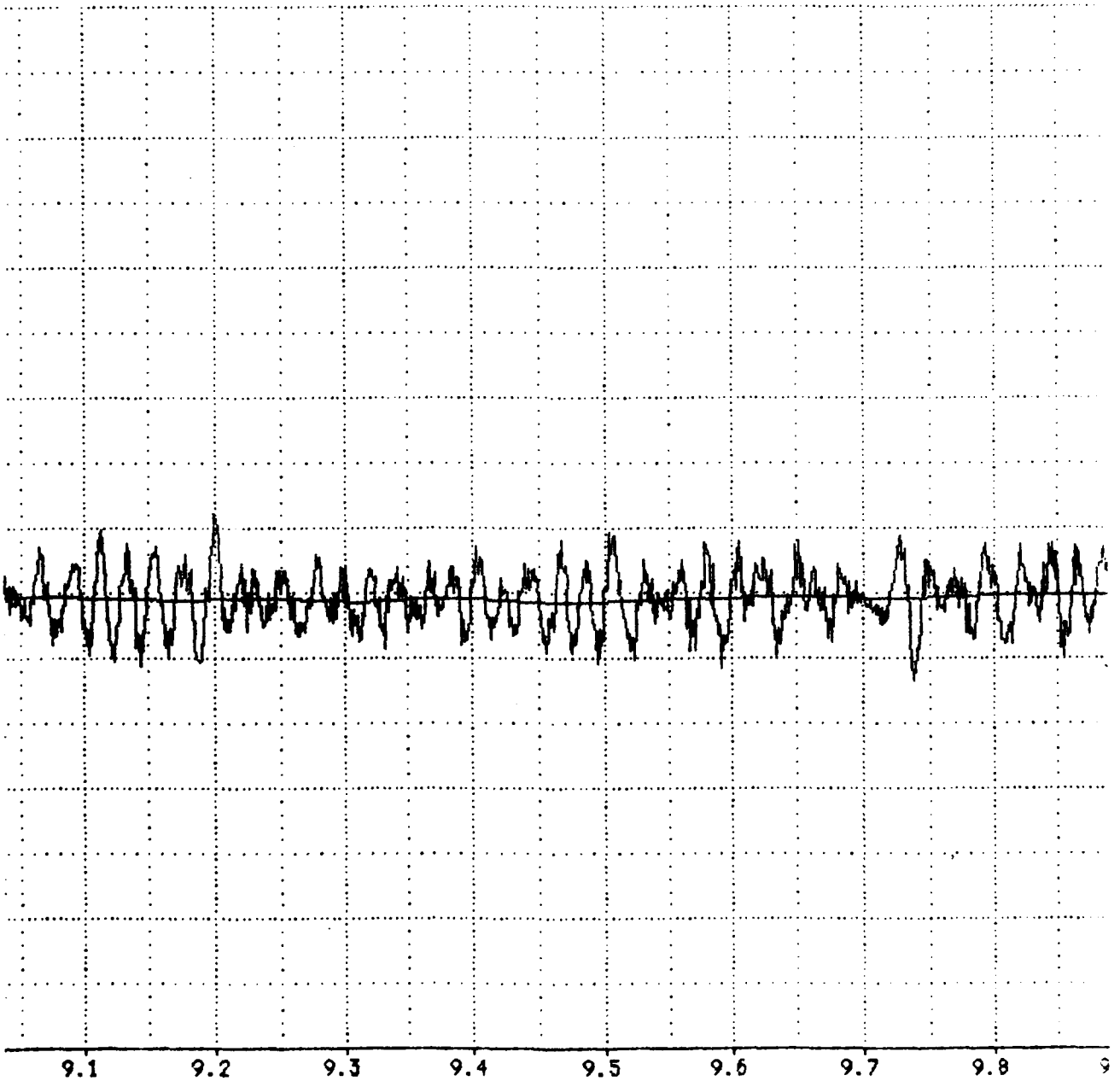
9.1
9.2
9.3
9.4
9.5
9.6
9.7
9.8

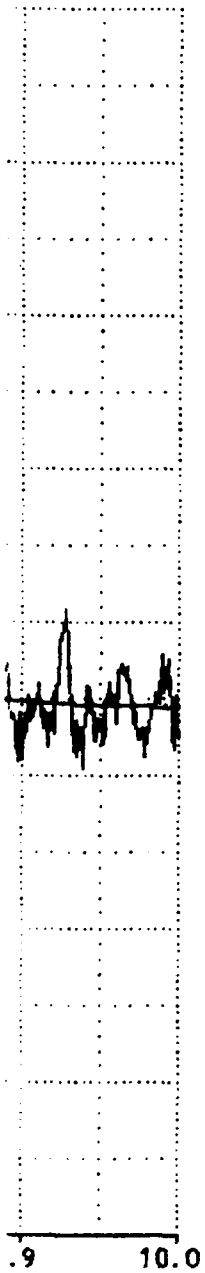
.9
10.0

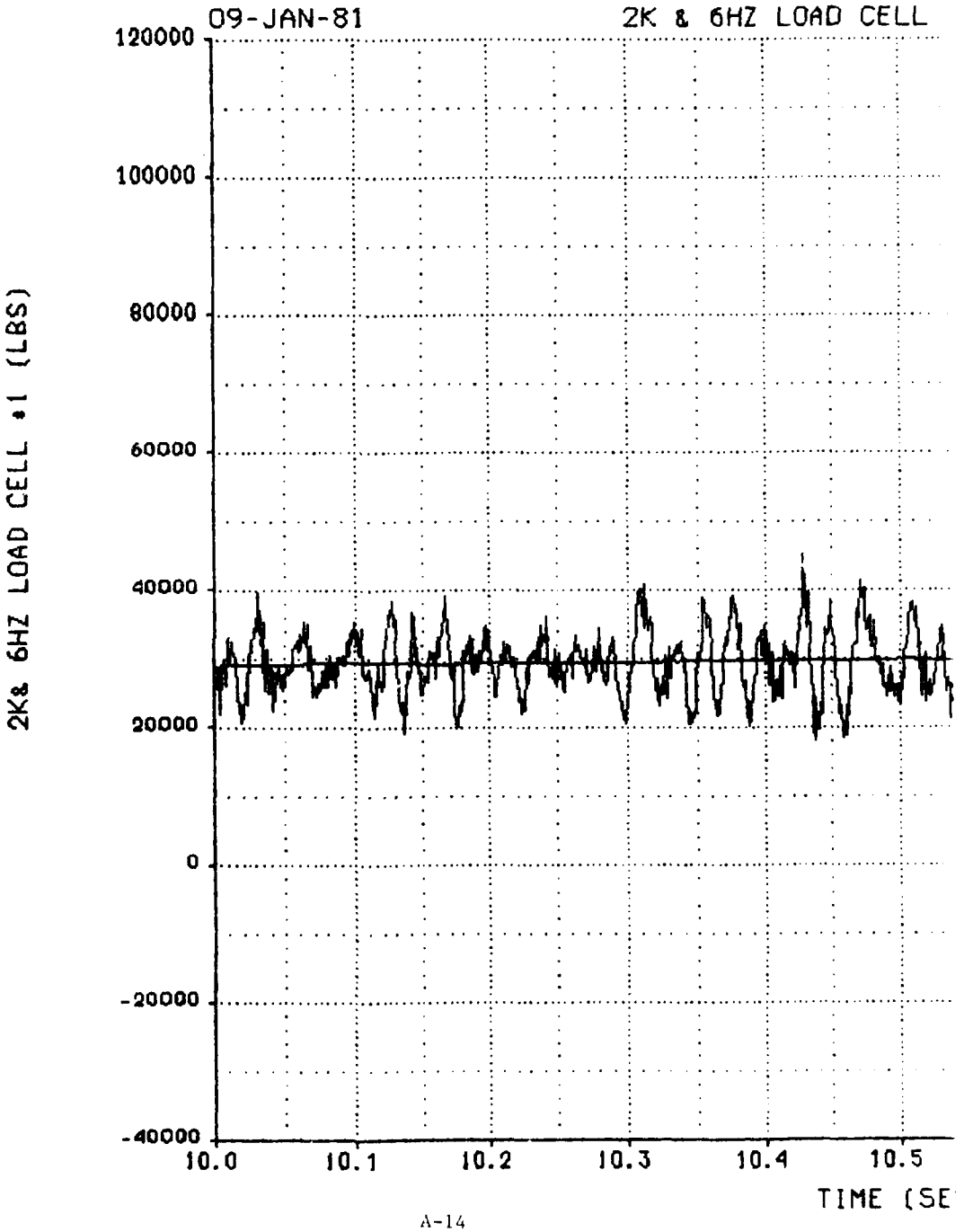
09-JAN-81
2K & 6HZ LOAD CELL
120000
100000
80000
60000
40000
20000
0
-20000
-40000
2K& 6HZ LOAD CELL #1 (LBS)
10.0
10.1
10.2
10.3
10.4
10.5
TIME (SE

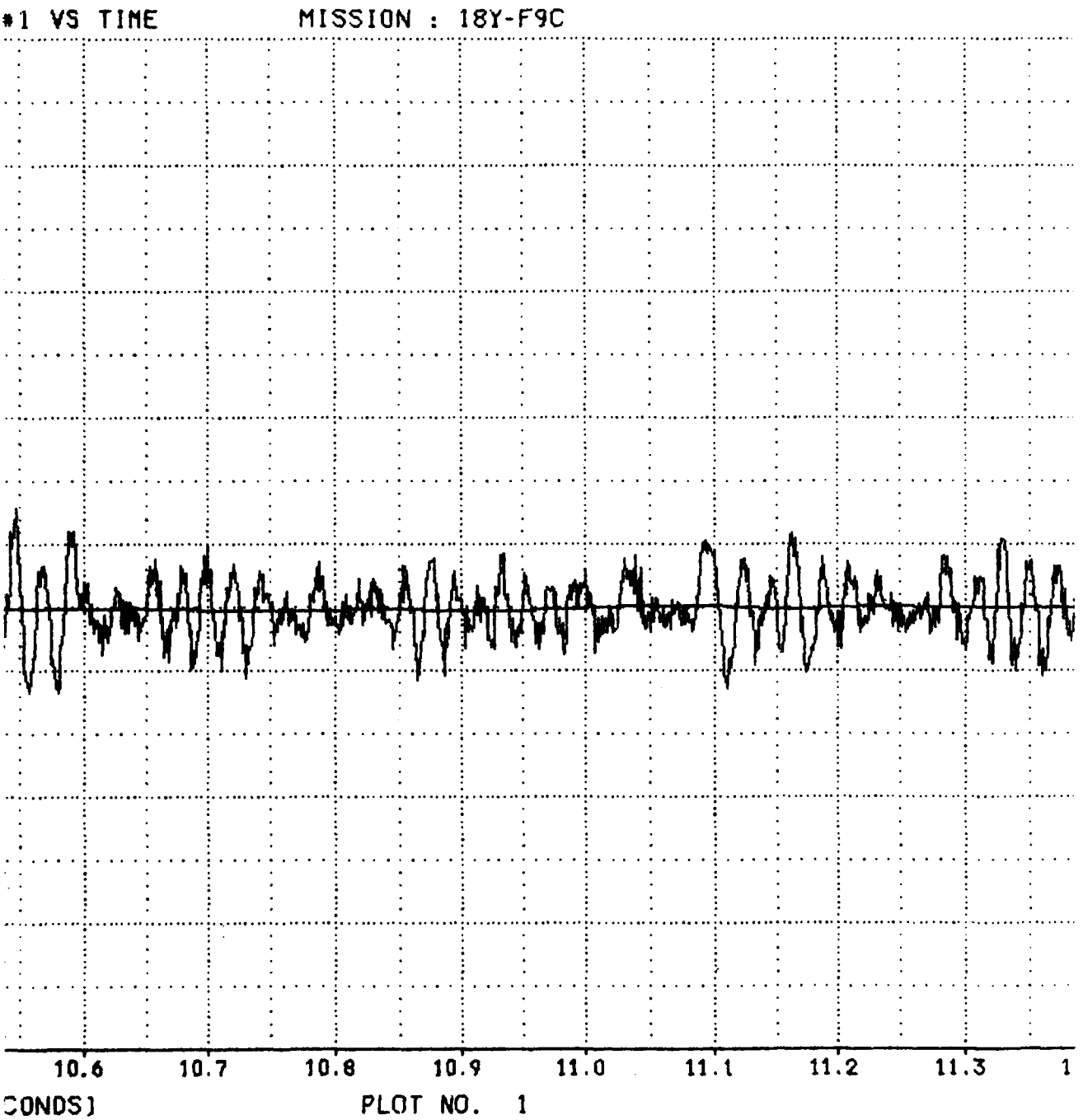
#1 VS TIME
MISSION : 18Y-F9C
10.6
10.7
10.8
10.9
11.0
11.1
11.2
11.3
1
CONDS]
PLOT NO. 1

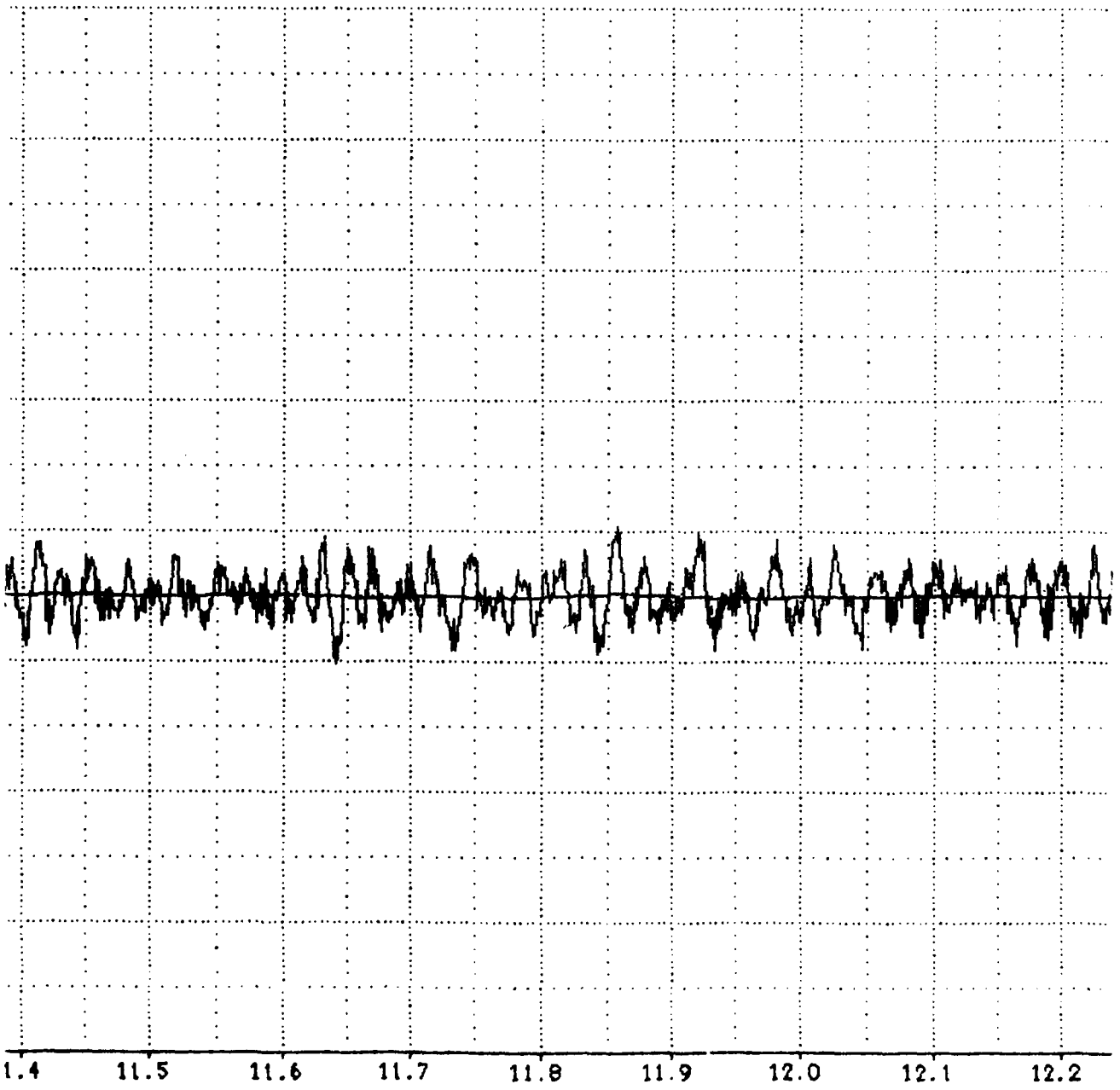
1.4
11.5
11.6
11.7
11.8
11.9
12.0
12.1
12.2

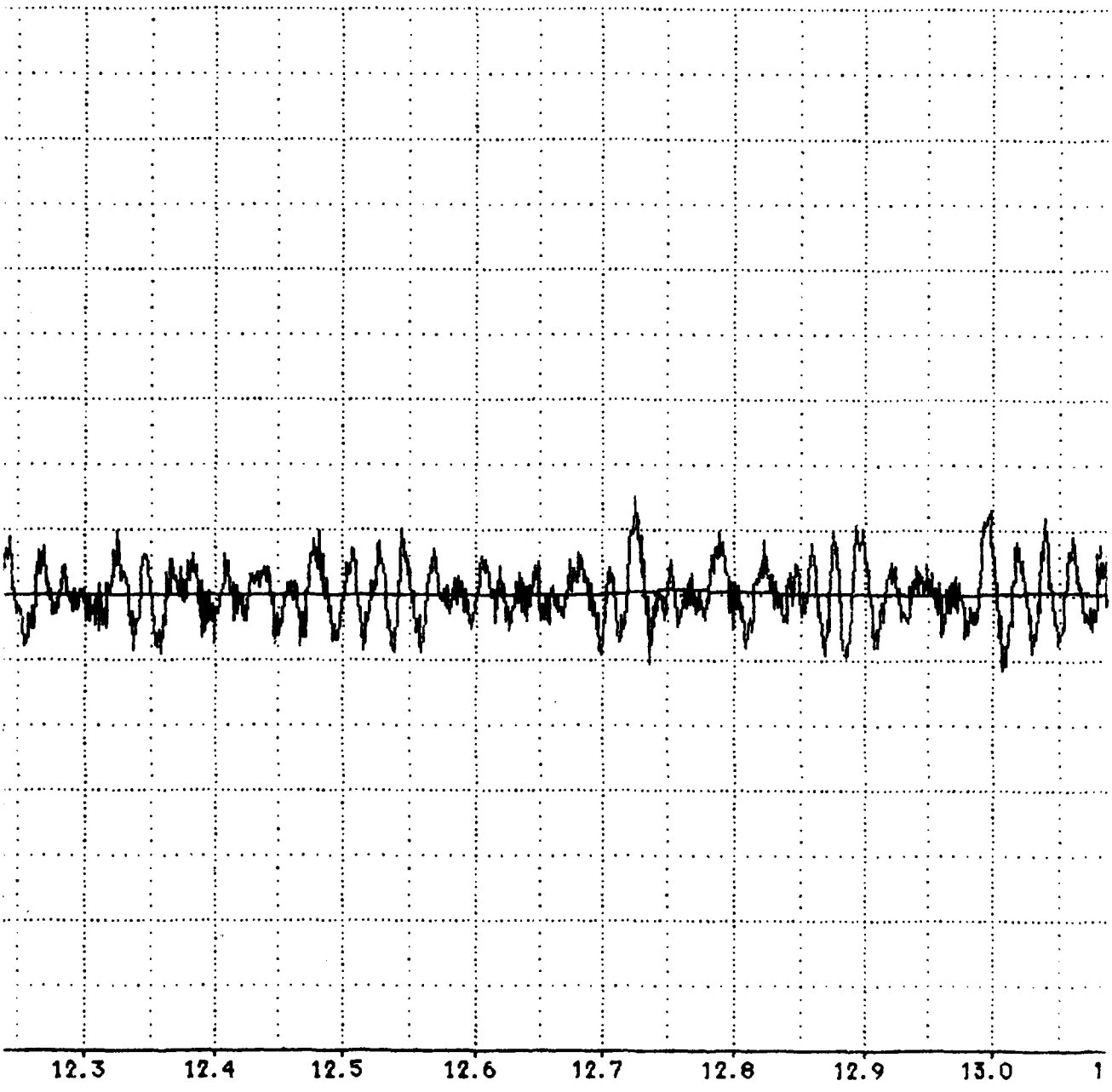
12.3
12.4
12.5
12.6
12.7
12.8
12.9
13.0
1

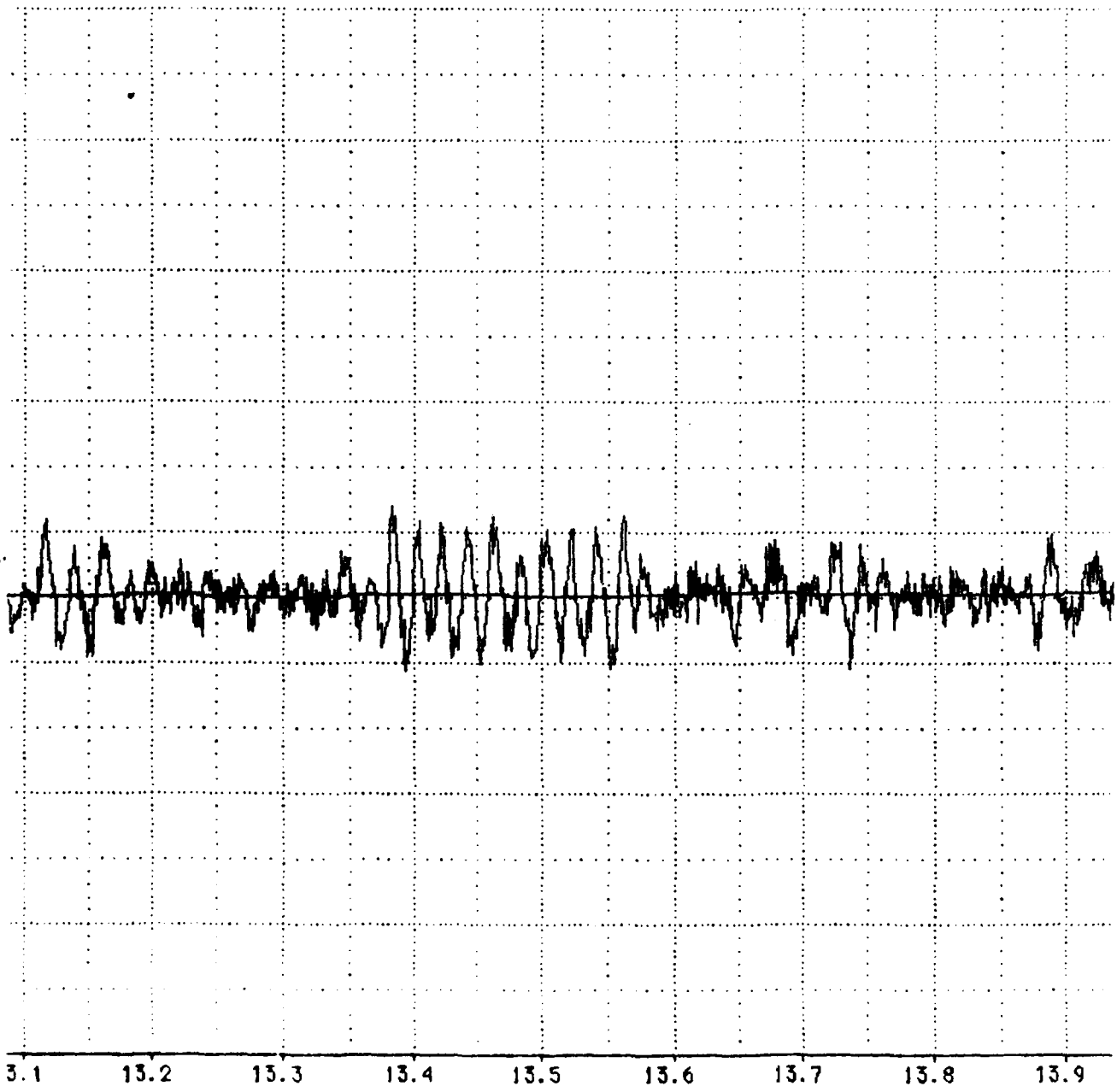
13.1
13.2
13.3
13.4
13.5
13.6
13.7
13.8
13.9

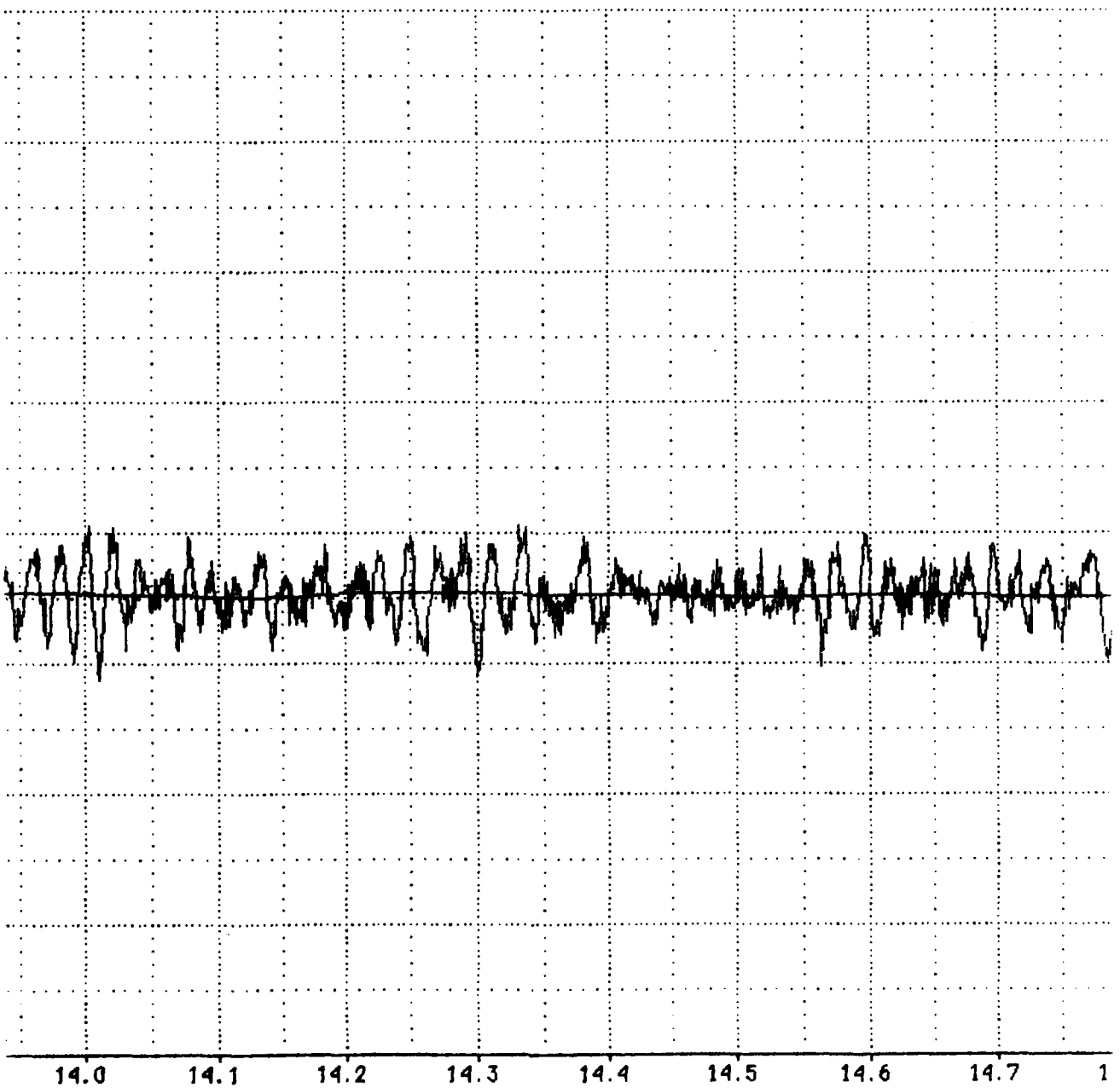
14.0
14.1
14.2
14.3
14.4
14.5
14.6
14.7
1

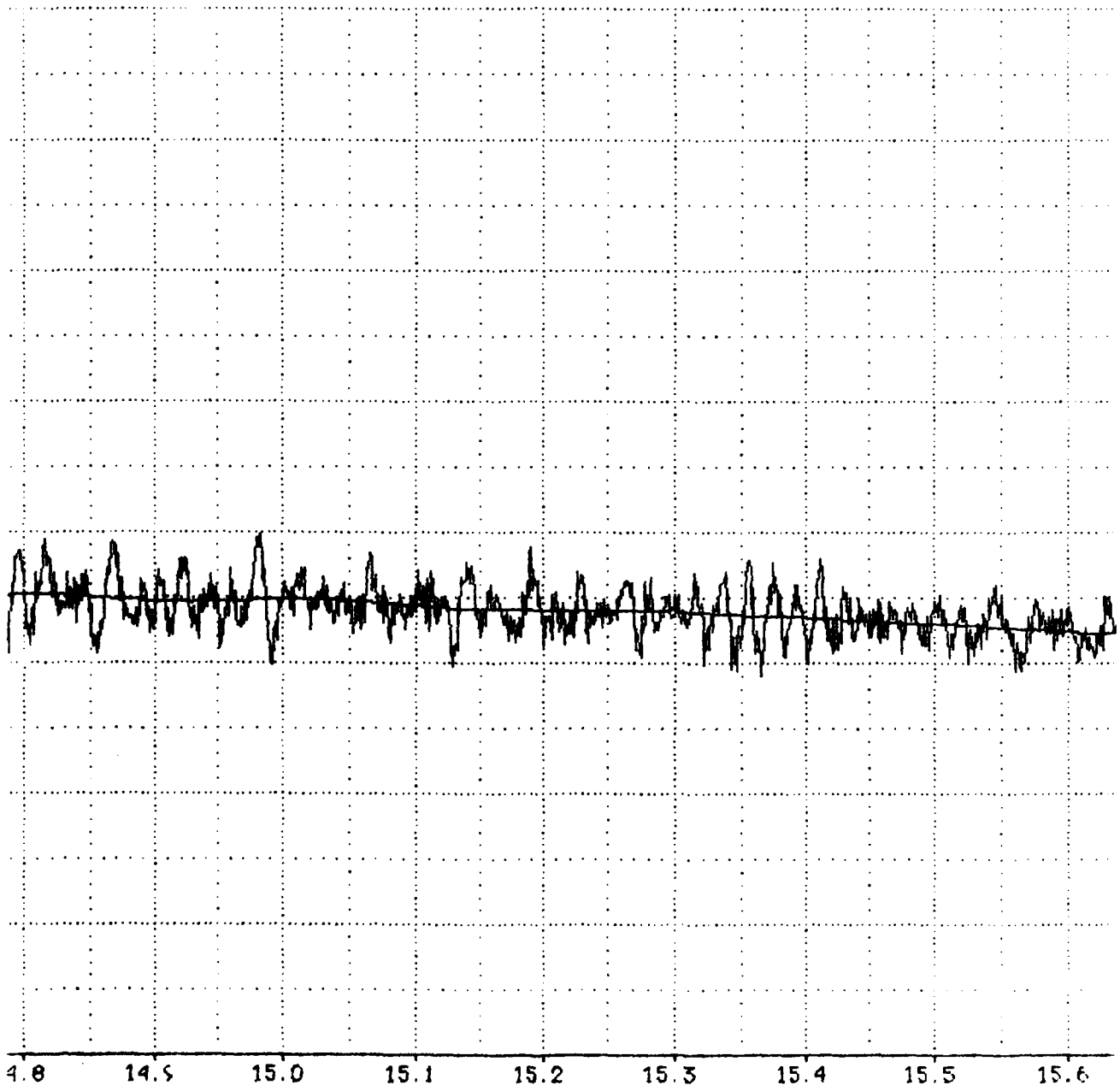
14.8
14.9
15.0
15.1
15.2
15.3
15.4
15.5
15.6

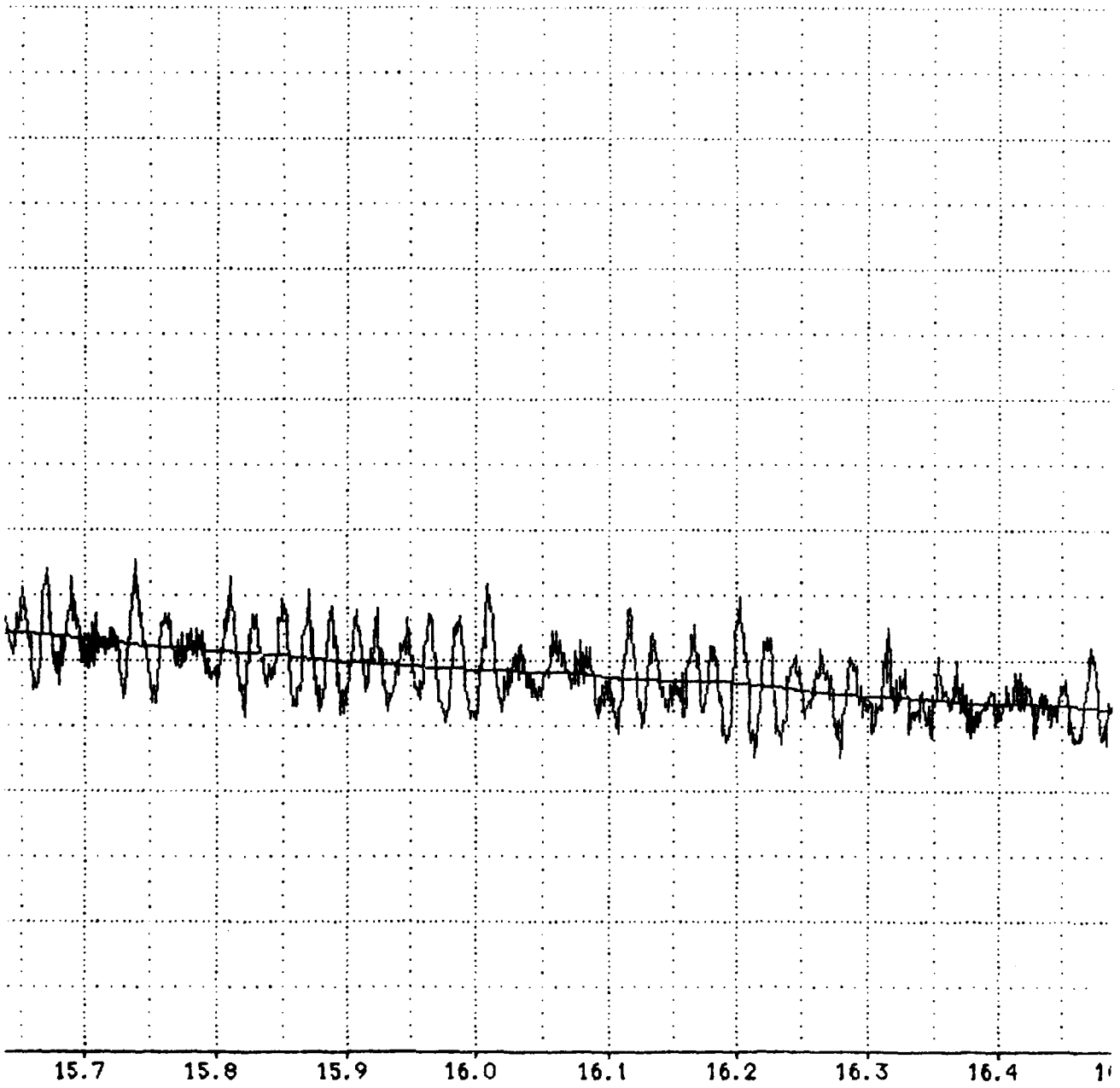
15.7
15.8
15.9
16.0
16.1
16.2
16.3
16.4

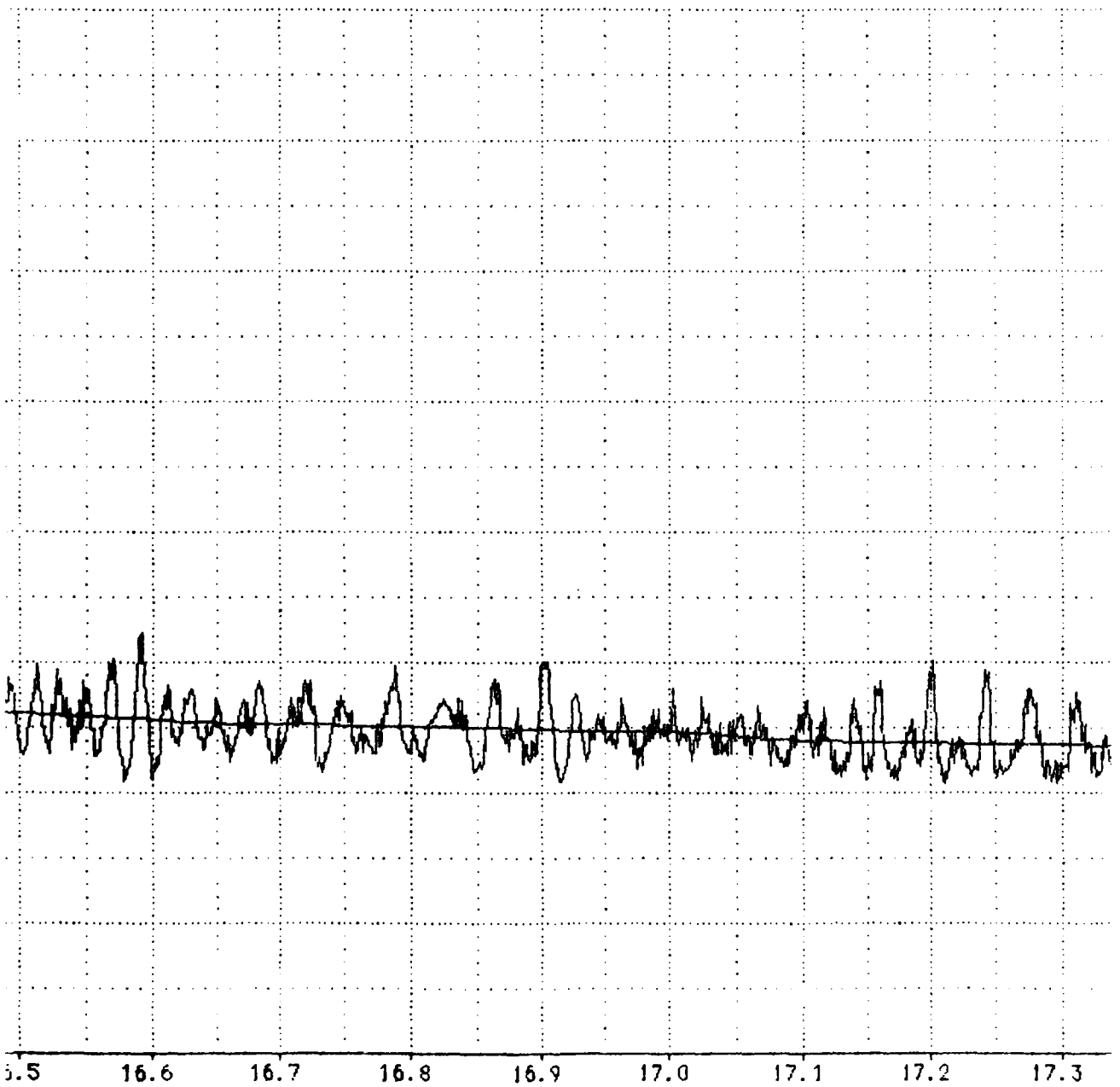
5.5
16.6
16.7
16.8
16.9
17.0
17.1
17.2
17.3

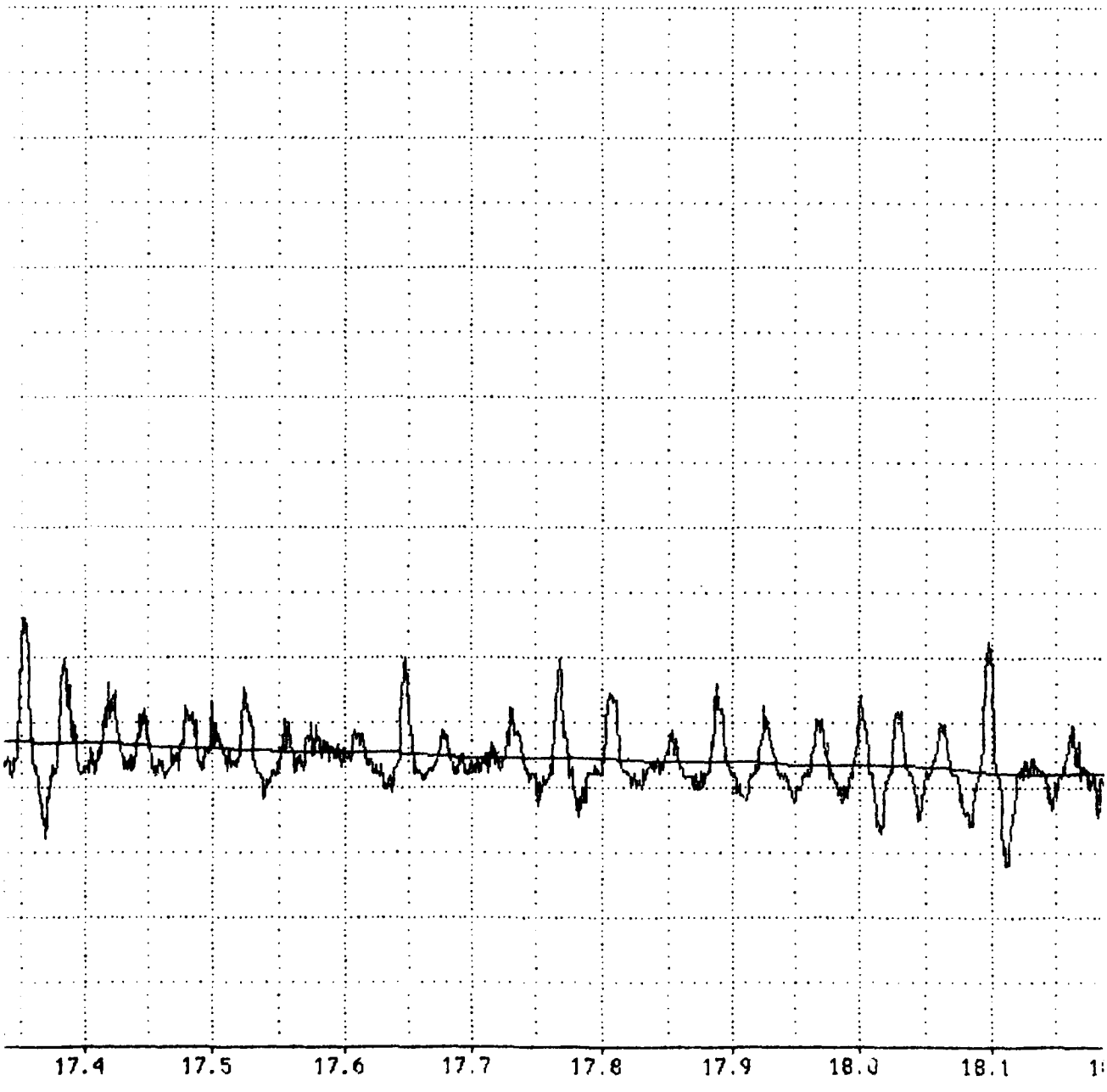
17.4
17.5
17.6
17.7
17.8
17.9
18.0
18.1

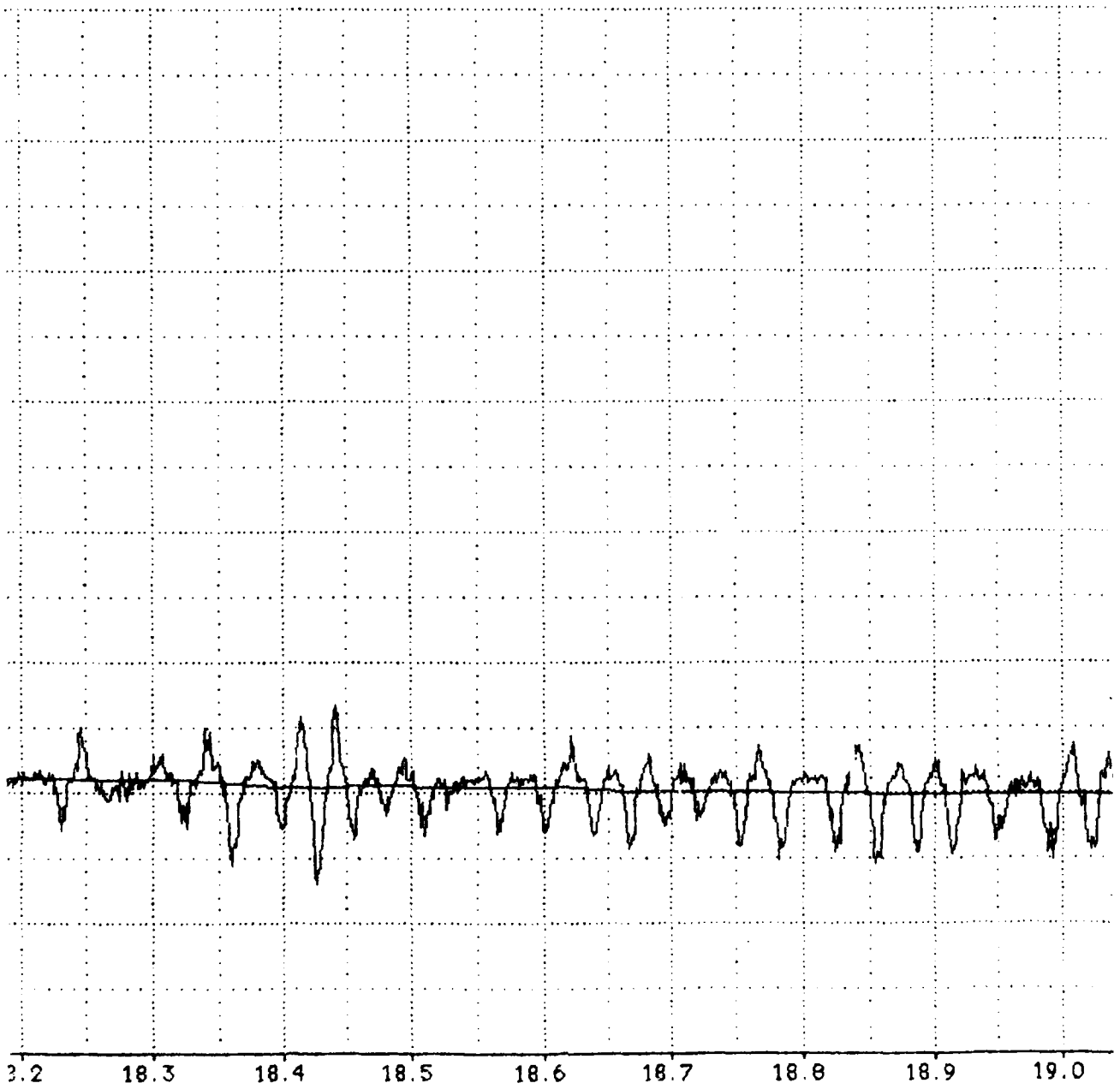
3.2
18.3
18.4
18.5
18.6
18.7
18.8
18.9
19.0

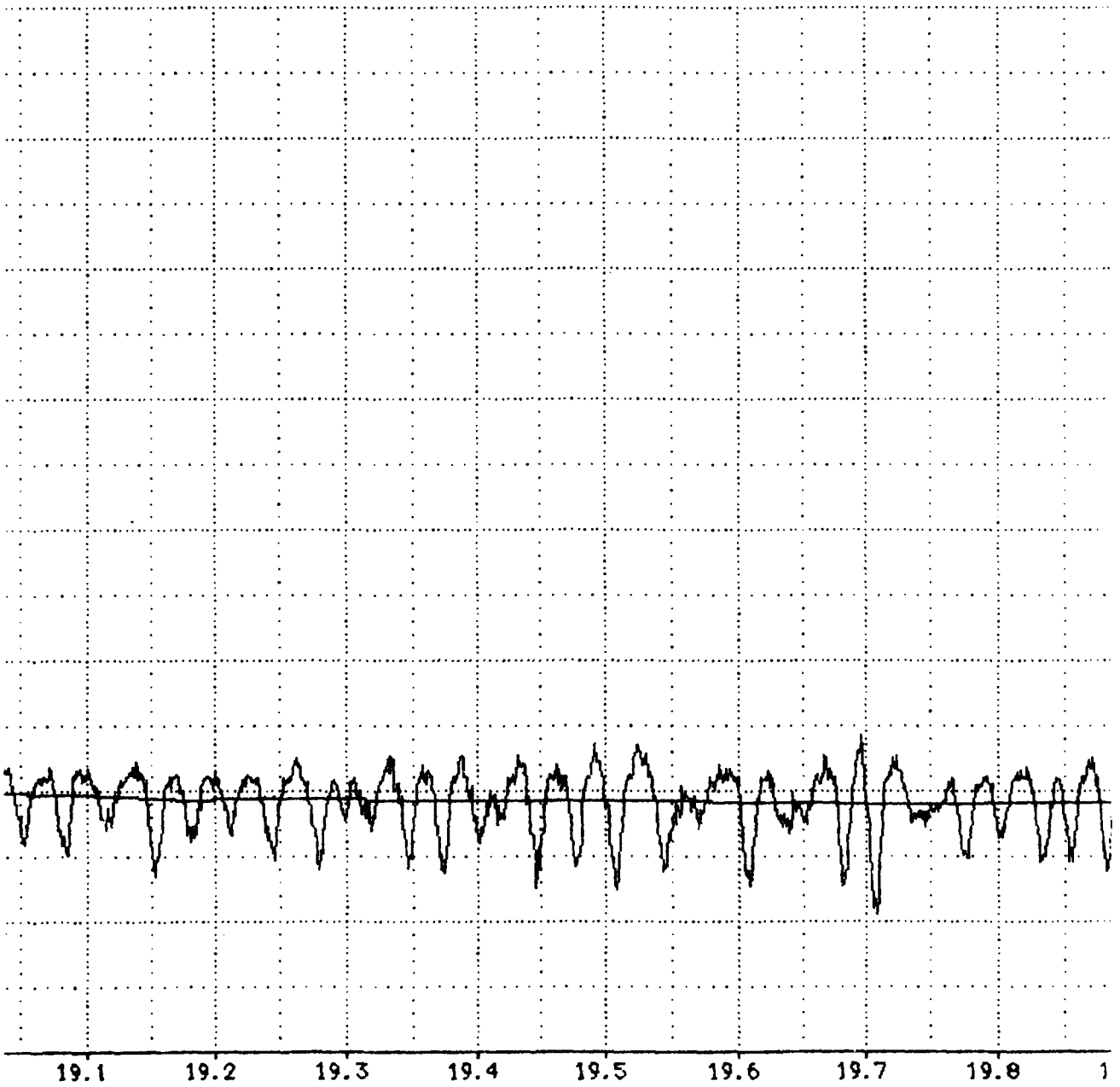
19.1
19.2
19.3
19.4
19.5
19.6
19.7
19.8

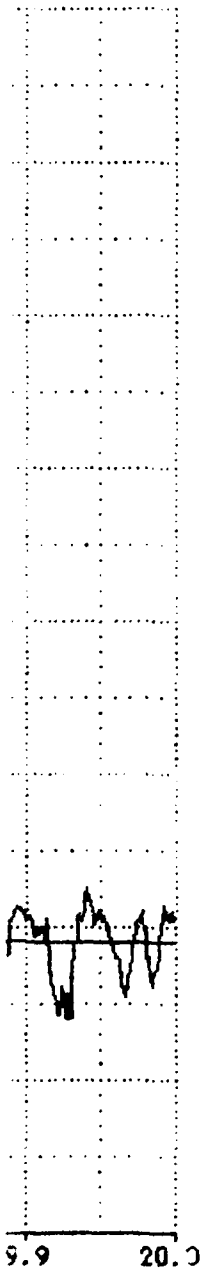
9.9
20.0

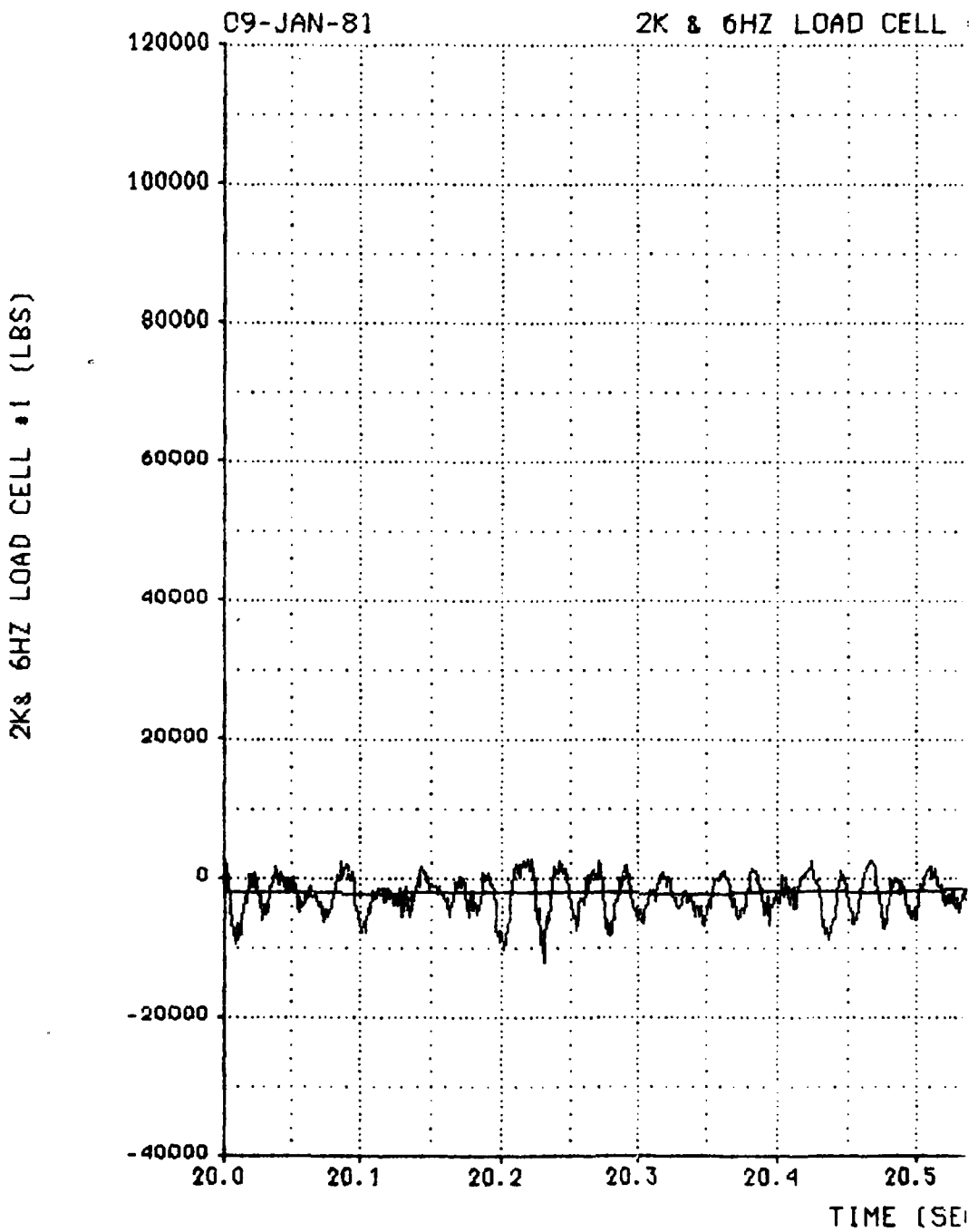
09-JAN-81
2K & 6HZ LOAD CELL
120000
100000
80000
60000
40000
20000
0
-20000
-40000
2Ks 6HZ LOAD CELL #1 (LBS)
20.0
20.1
20.2
20.3
20.4
20.5
TIME (SE

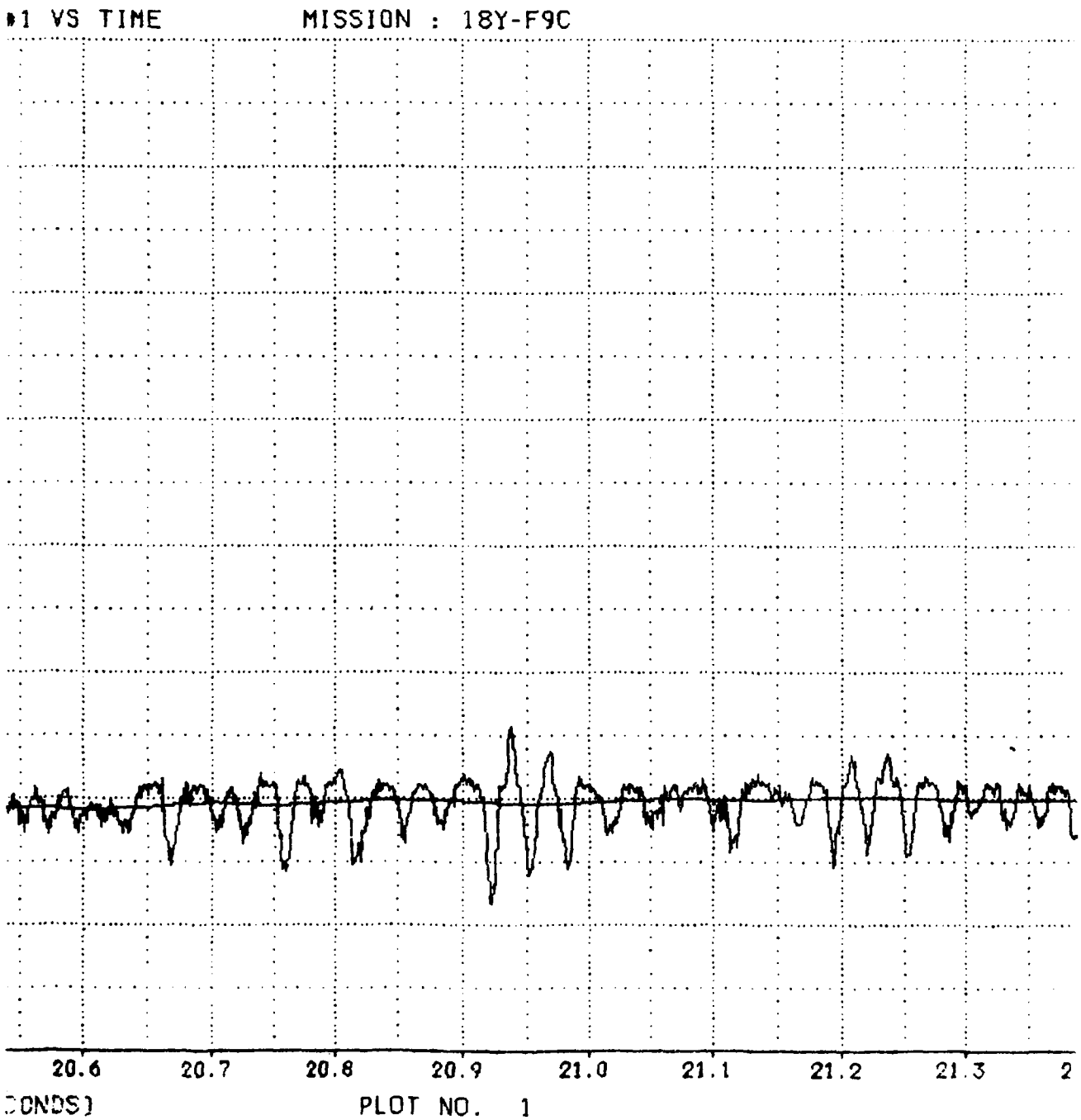
▮1 VS TIME
MISSION : 18Y-F9C
20.6
20.7
20.8
20.9
21.0
21.1
21.2
21.3
2
CONDS)
PLOT NO. 1

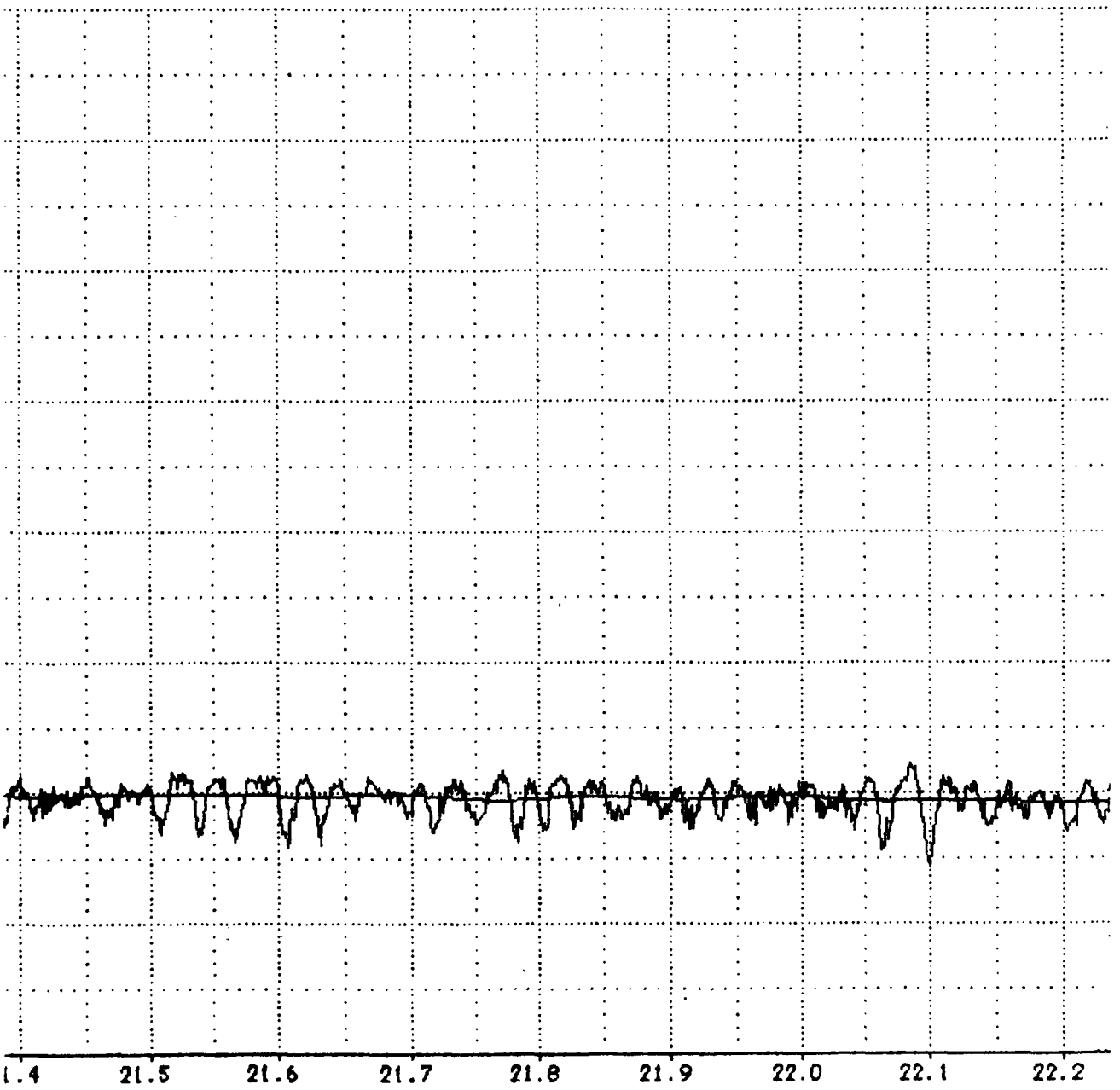
1.4
21.5
21.6
21.7
21.8
21.9
22.0
22.1
22.2

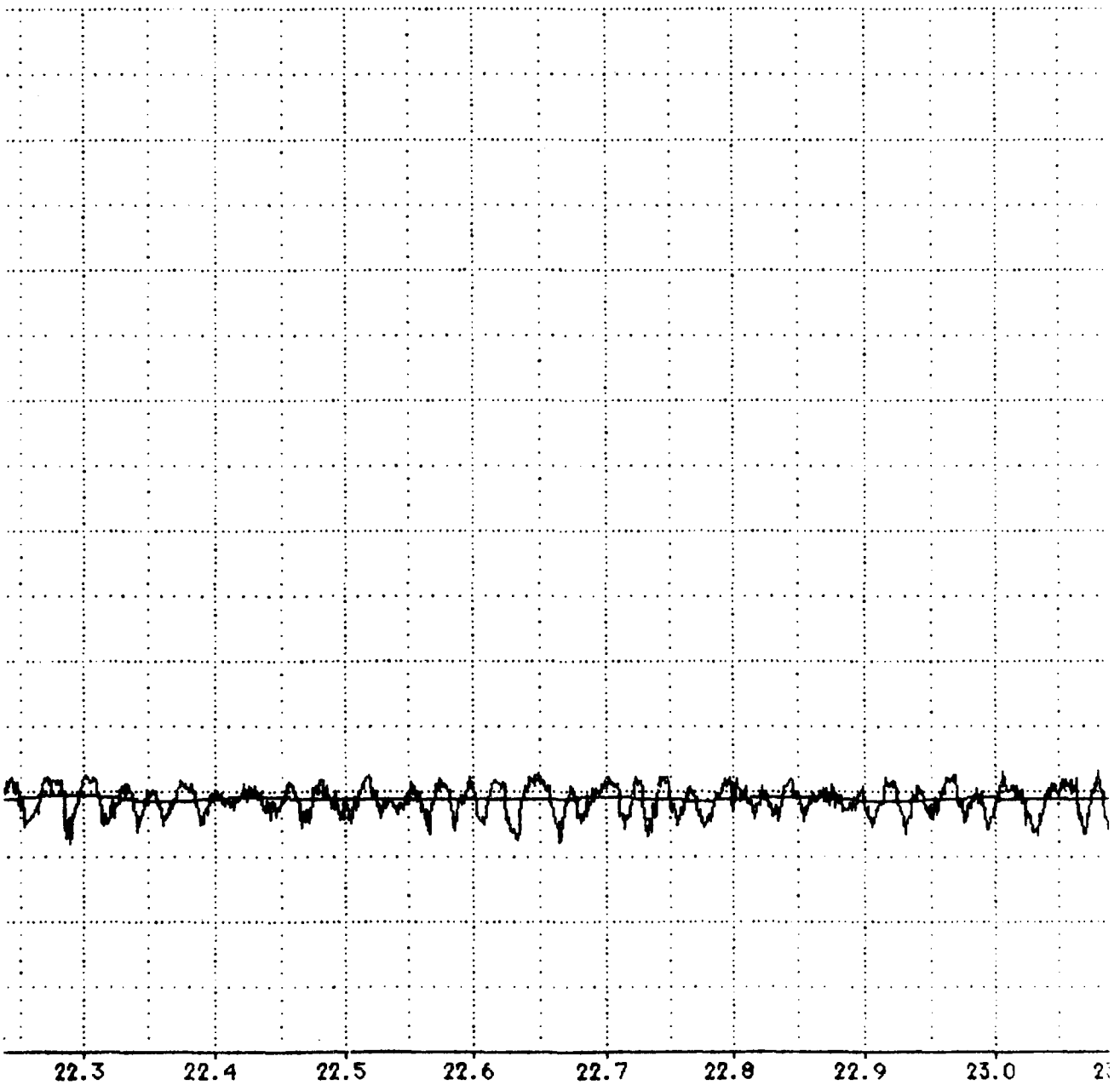
22.3
22.4
22.5
22.6
22.7
22.8
22.9
23.0

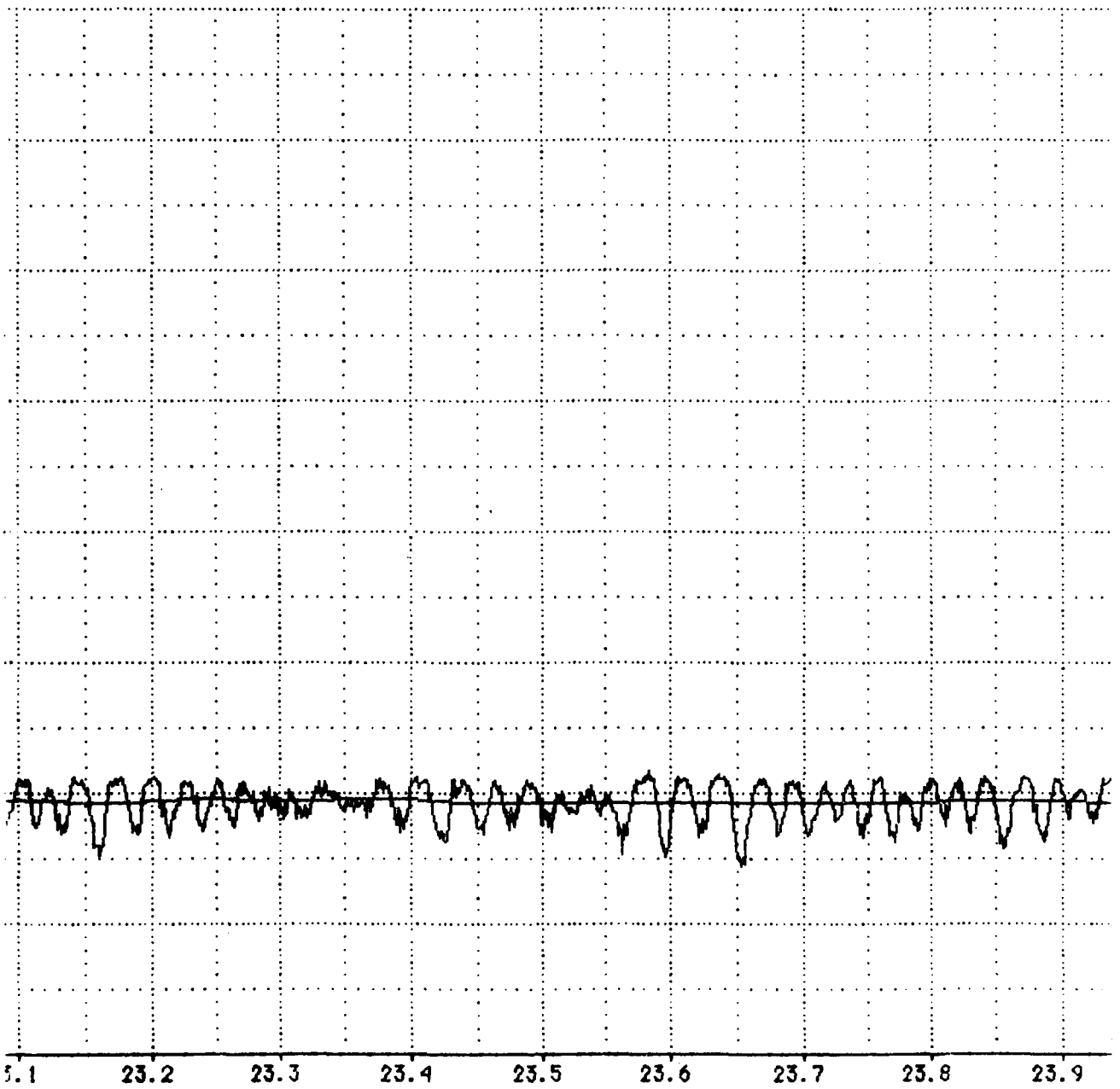
5.1
23.2
23.3
23.4
23.5
23.6
23.7
23.8
23.9

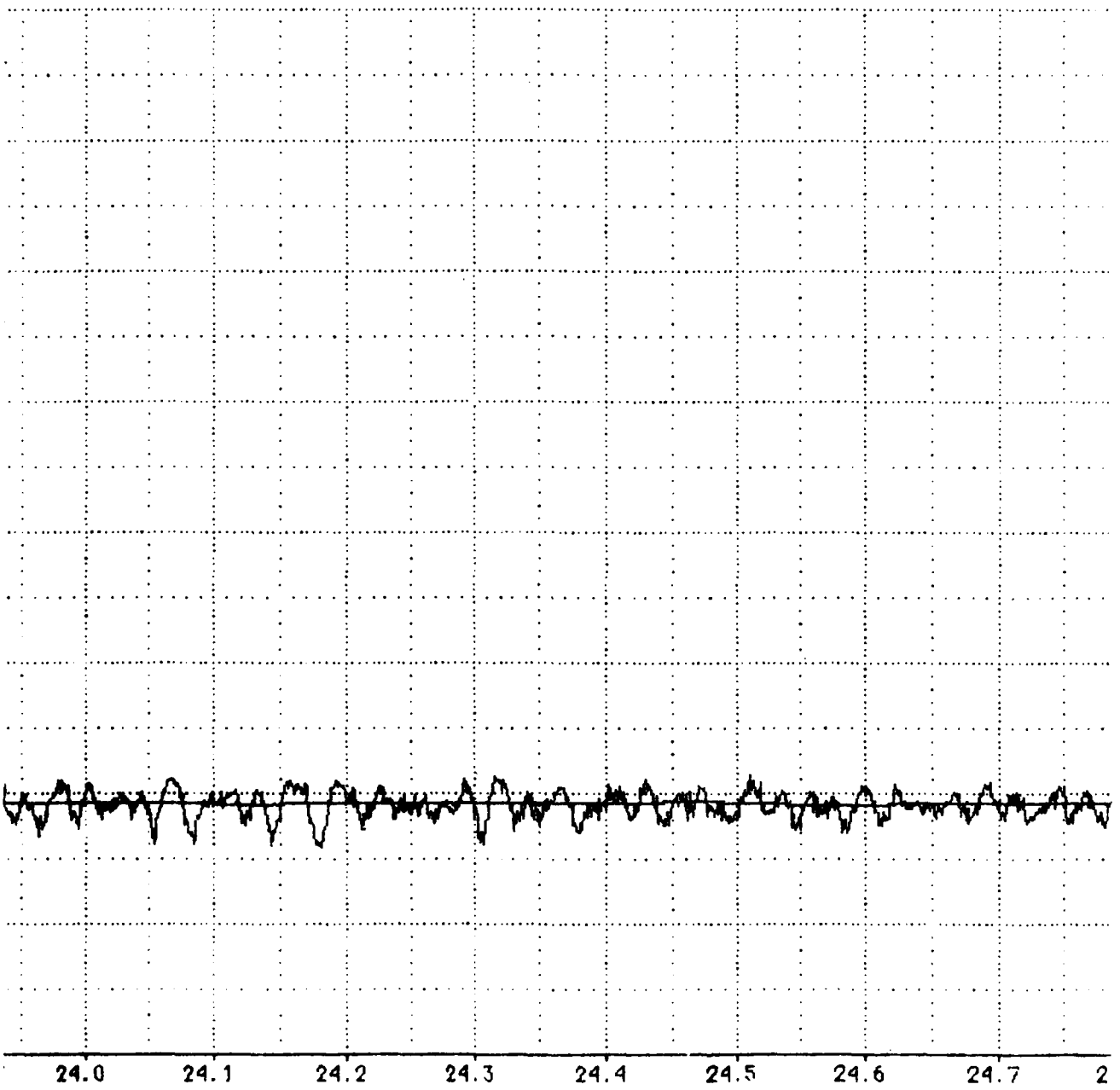
24.0
24.1
24.2
24.3
24.4
24.5
24.6
24.7
2

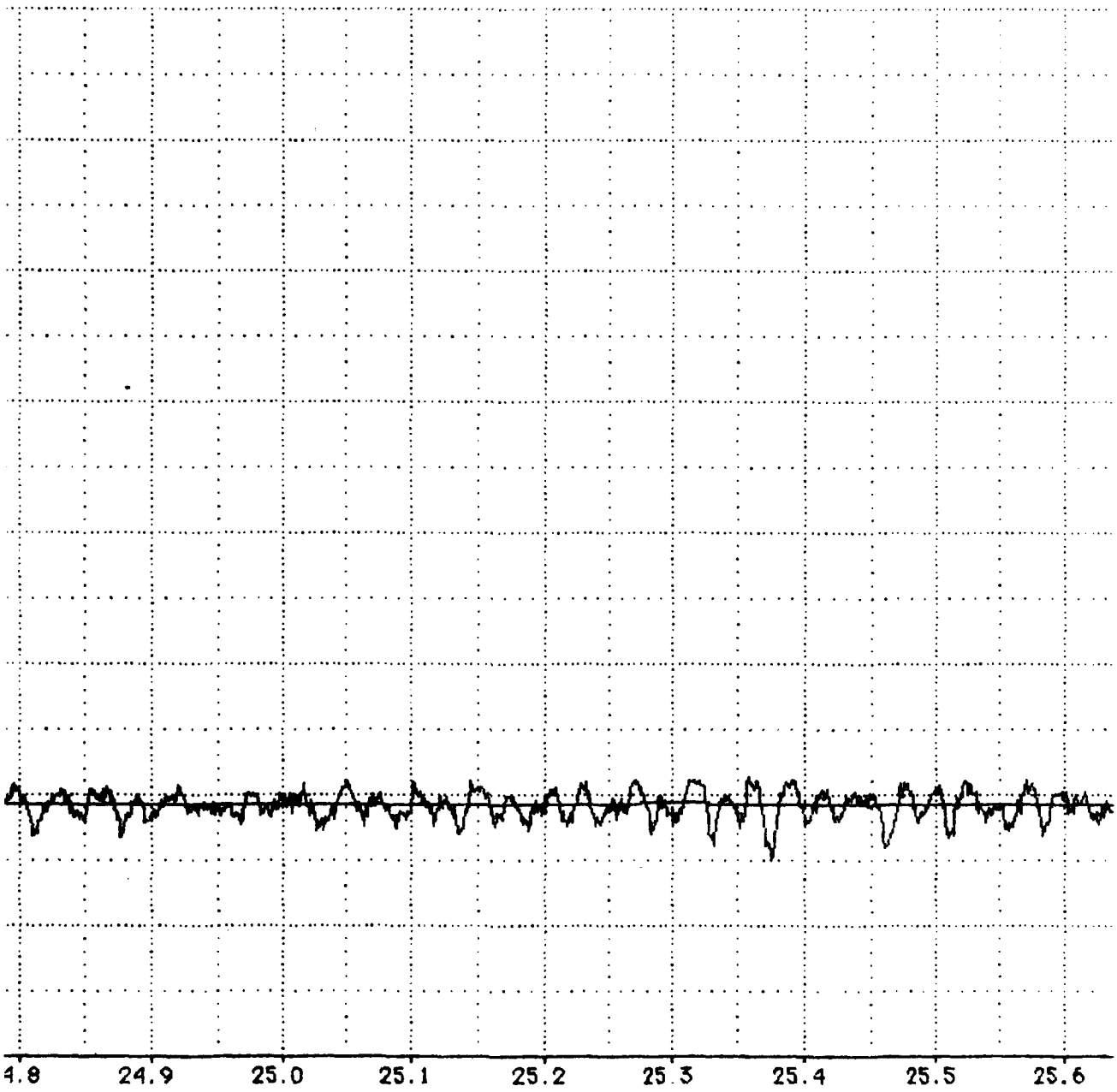
4.8
24.9
25.0
25.1
25.2
25.3
25.4
25.5
25.6

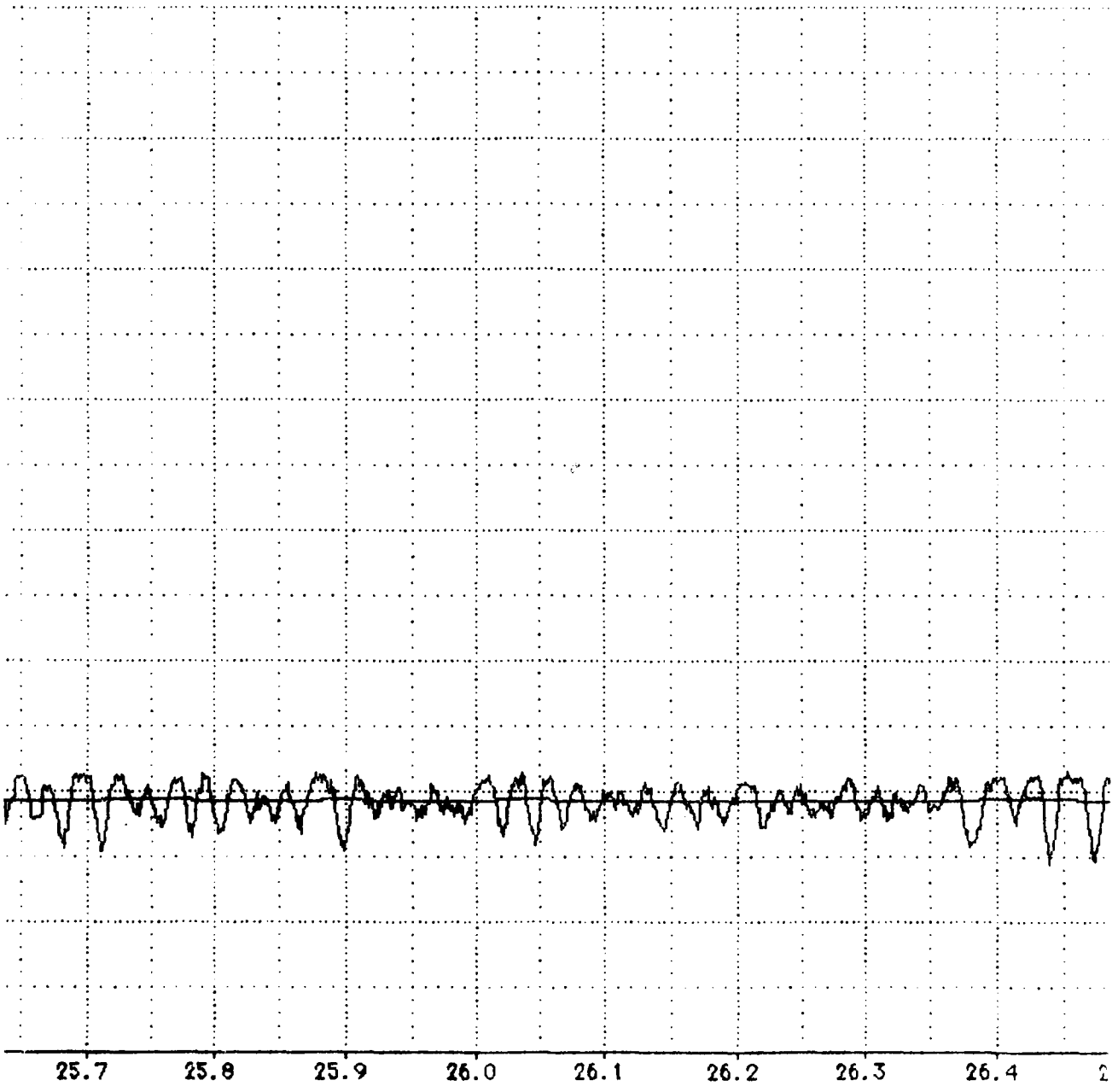
25.7
25.8
25.9
26.0
26.1
26.2
26.3
26.4

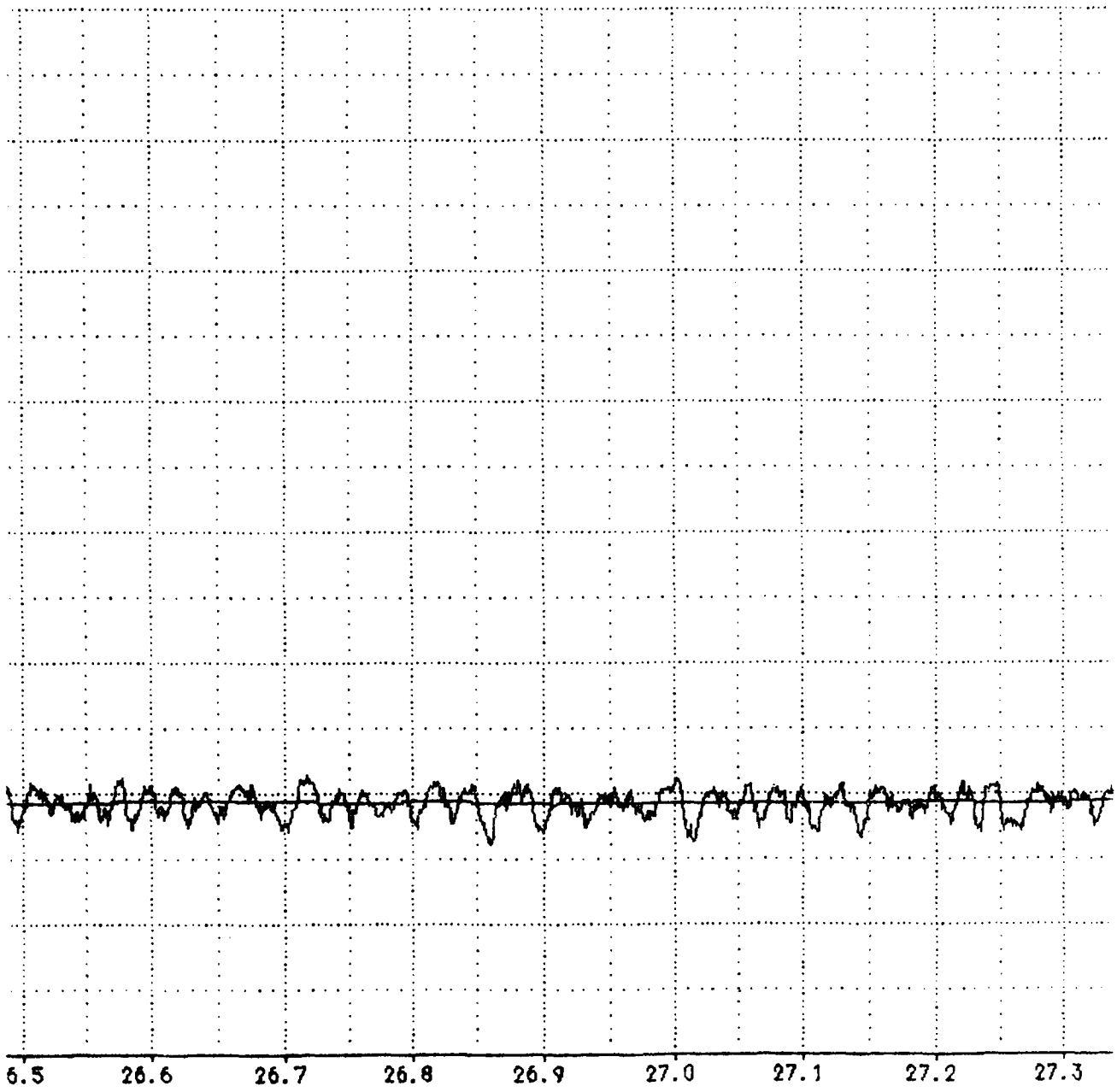
6.5
26.6
26.7
26.8
26.9
27.0
27.1
27.2
27.3

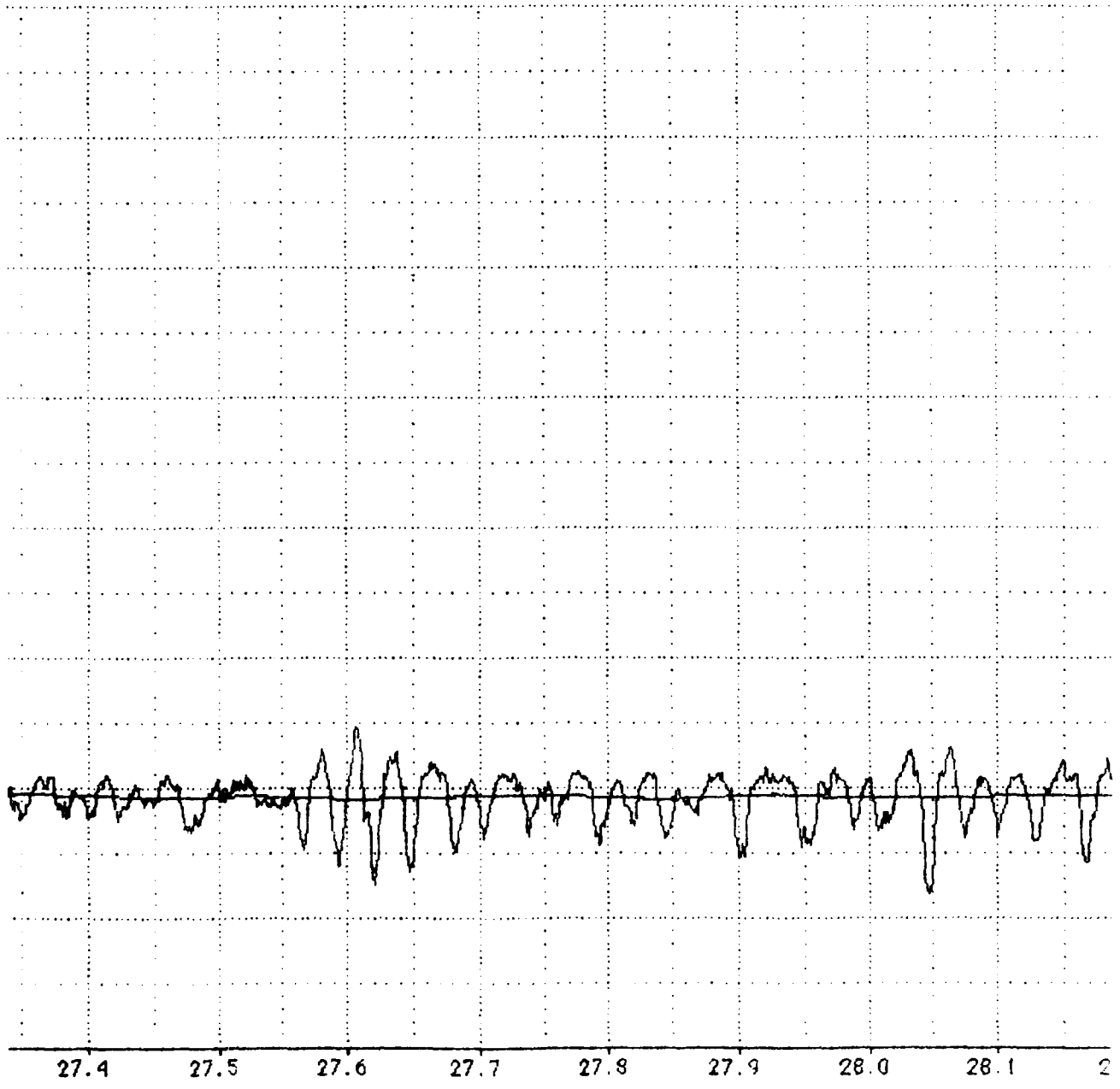
27.4
27.5
27.6
27.7
27.8
27.9
28.0
28.1
2

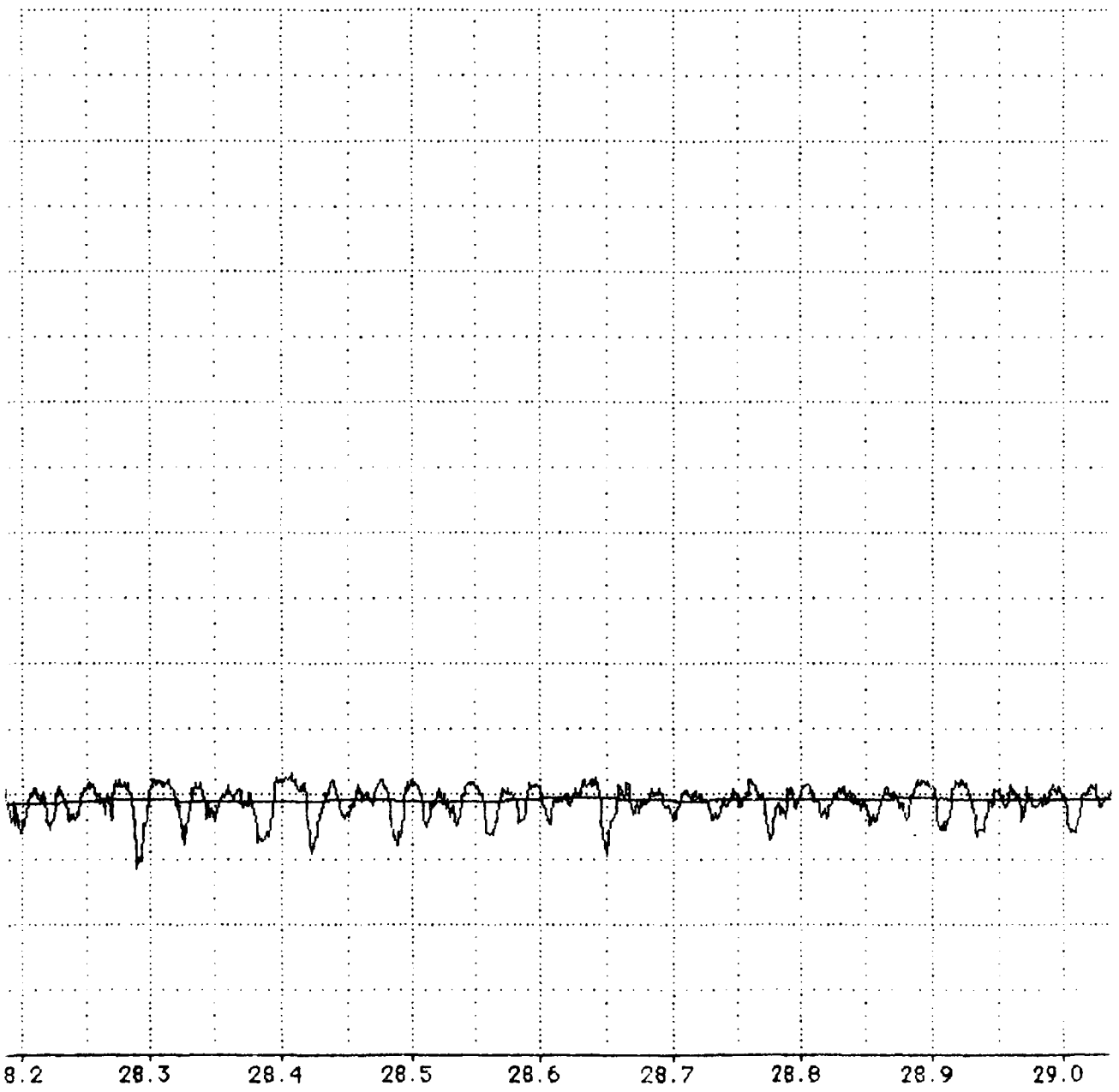
8.2
28.3
28.4
28.5
28.6
28.7
28.8
28.9
29.0

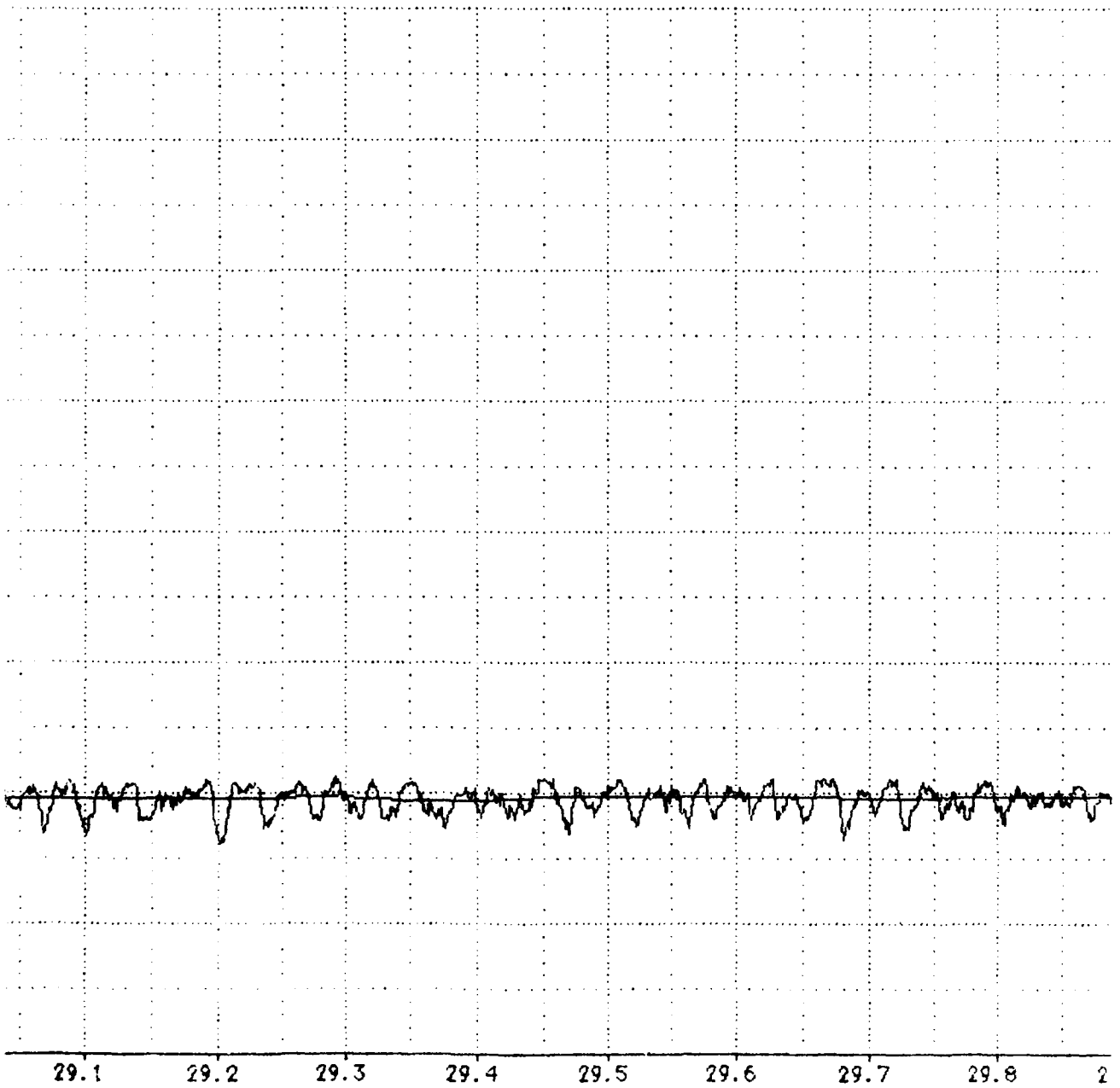
29.1
29.2
29.3
29.4
29.5
29.6
29.7
29.8
2

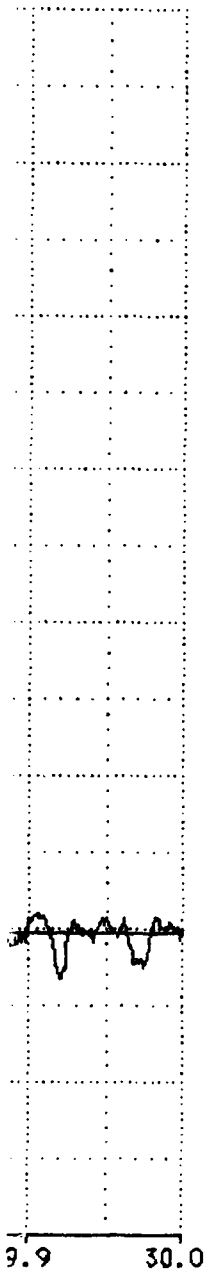
9.9
30.0

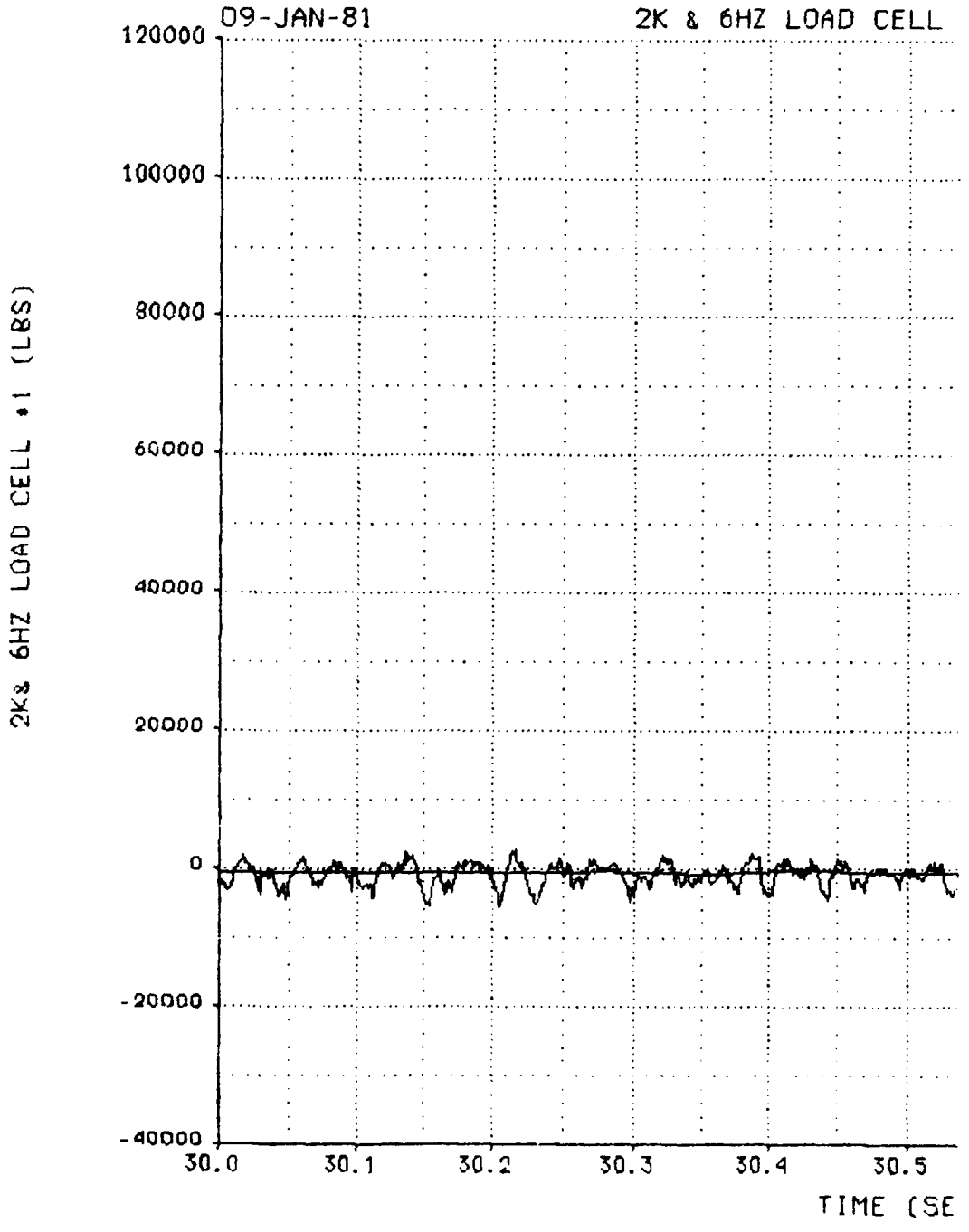
09-JAN-81
2K & 6HZ LOAD CELL
120000
100000
80000
60000
40000
20000
0
-20000
-40000
2K& 6HZ LOAD CELL #1 (LBS)
30.0
30.1
30.2
30.3
30.4
30.5
TIME (SE

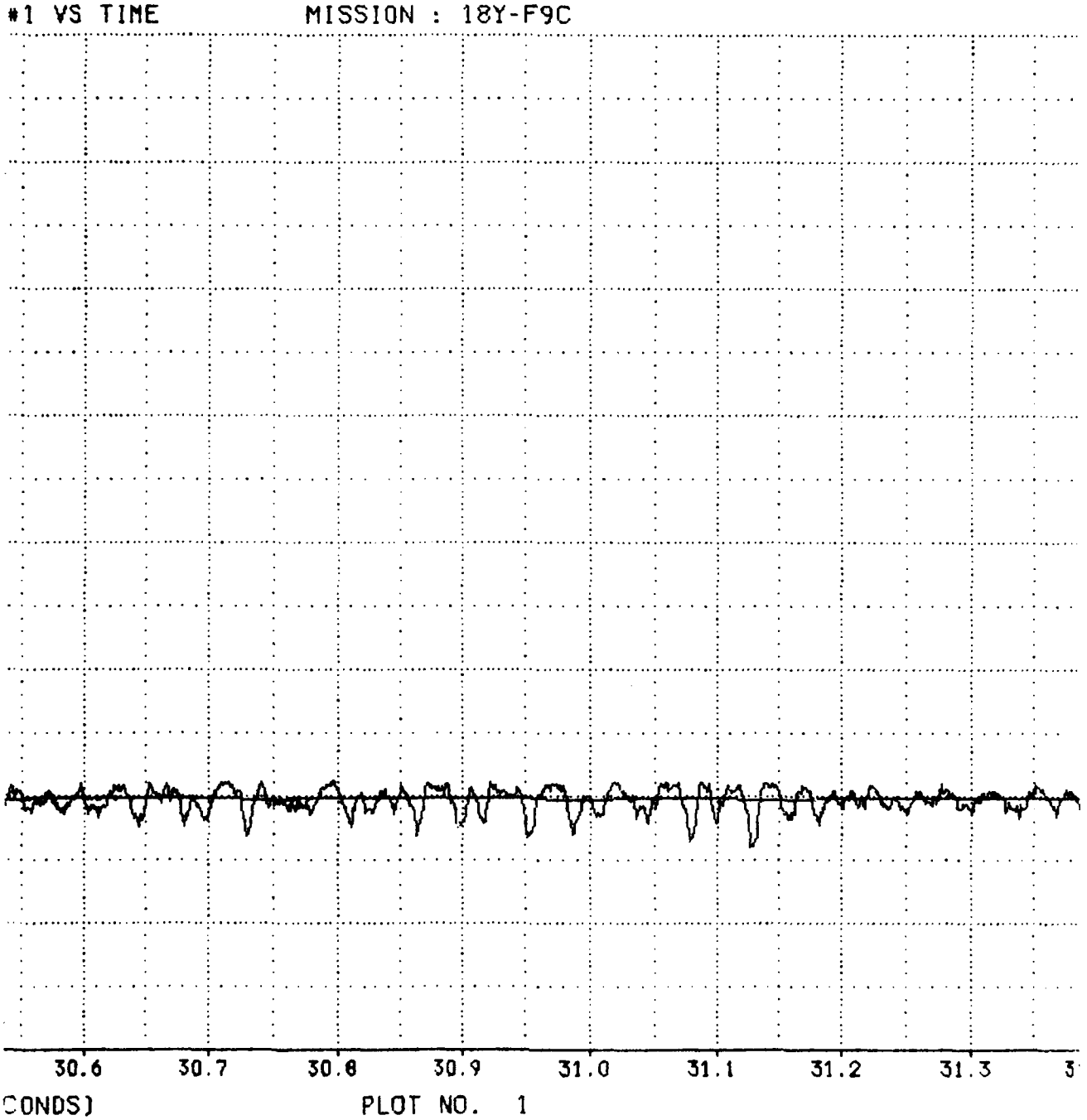
#1 VS TIME
MISSION : 18Y-F9C
30.6
30.7
30.8
30.9
31.0
31.1
31.2
31.3
CONDS)
PLOT NO. 1

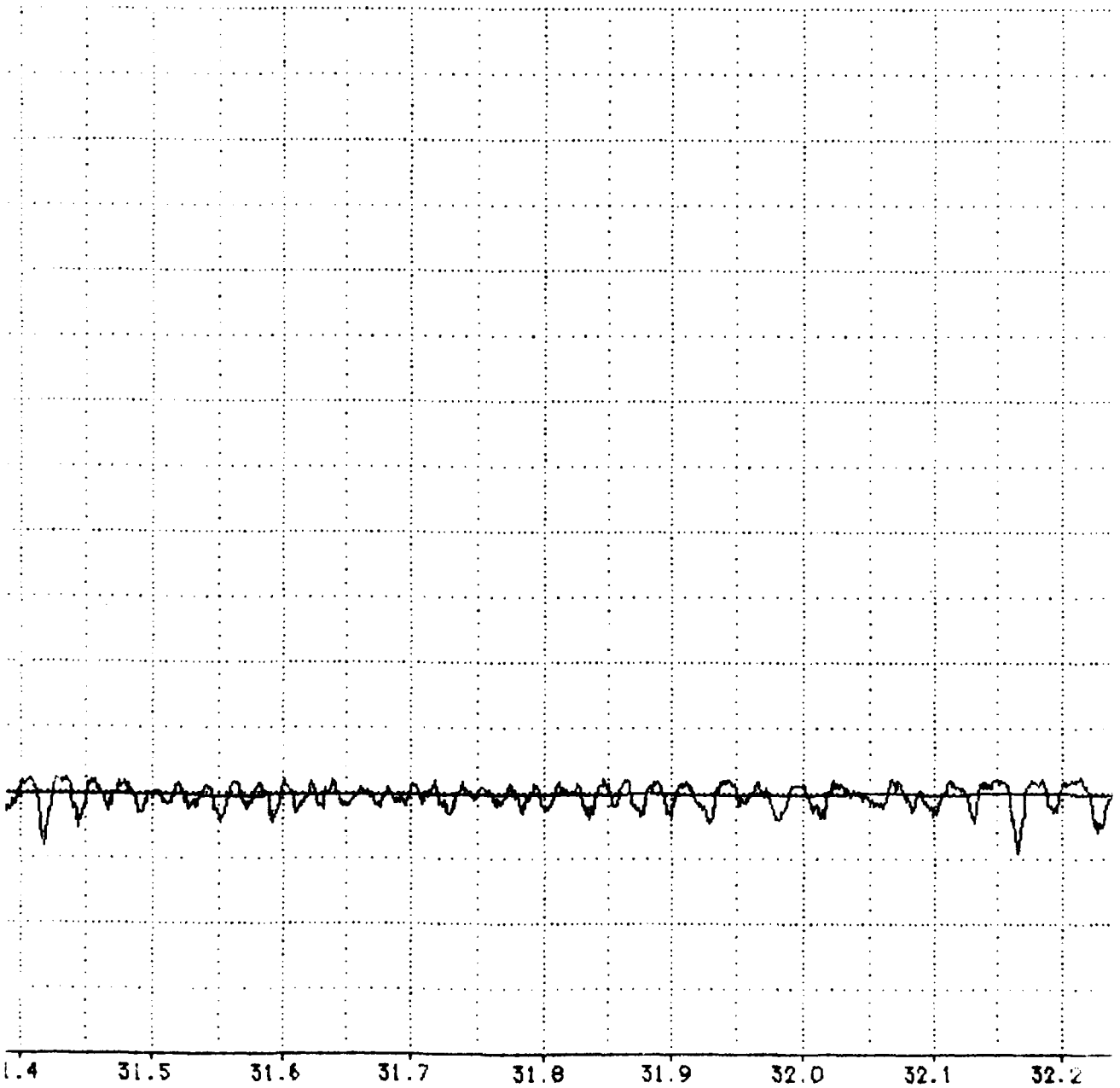
1.4
31.5
31.6
31.7
31.8
31.9
32.0
32.1
32.2

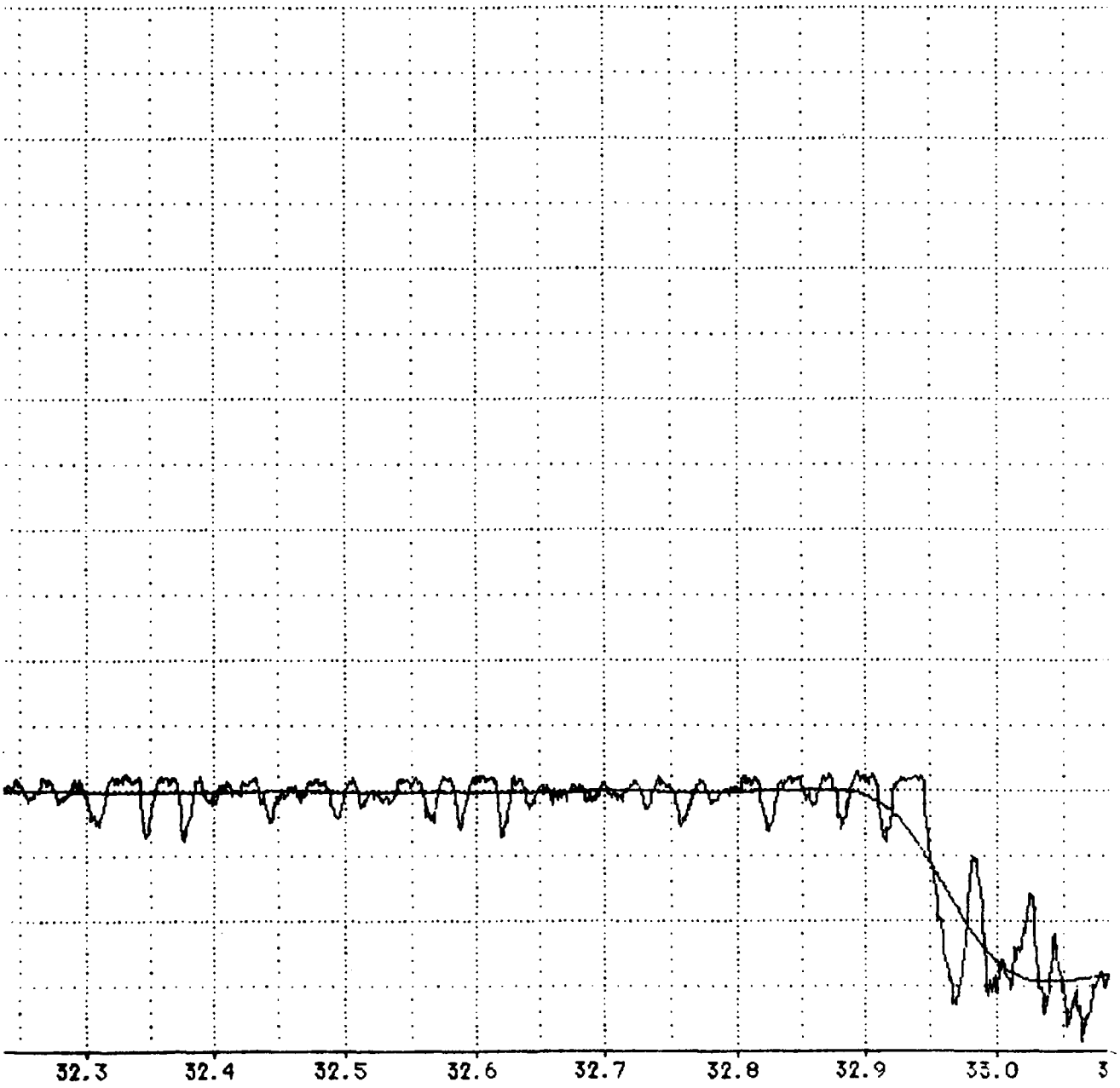
32.3
32.4
32.5
32.6
32.7
32.8
32.9
33.0

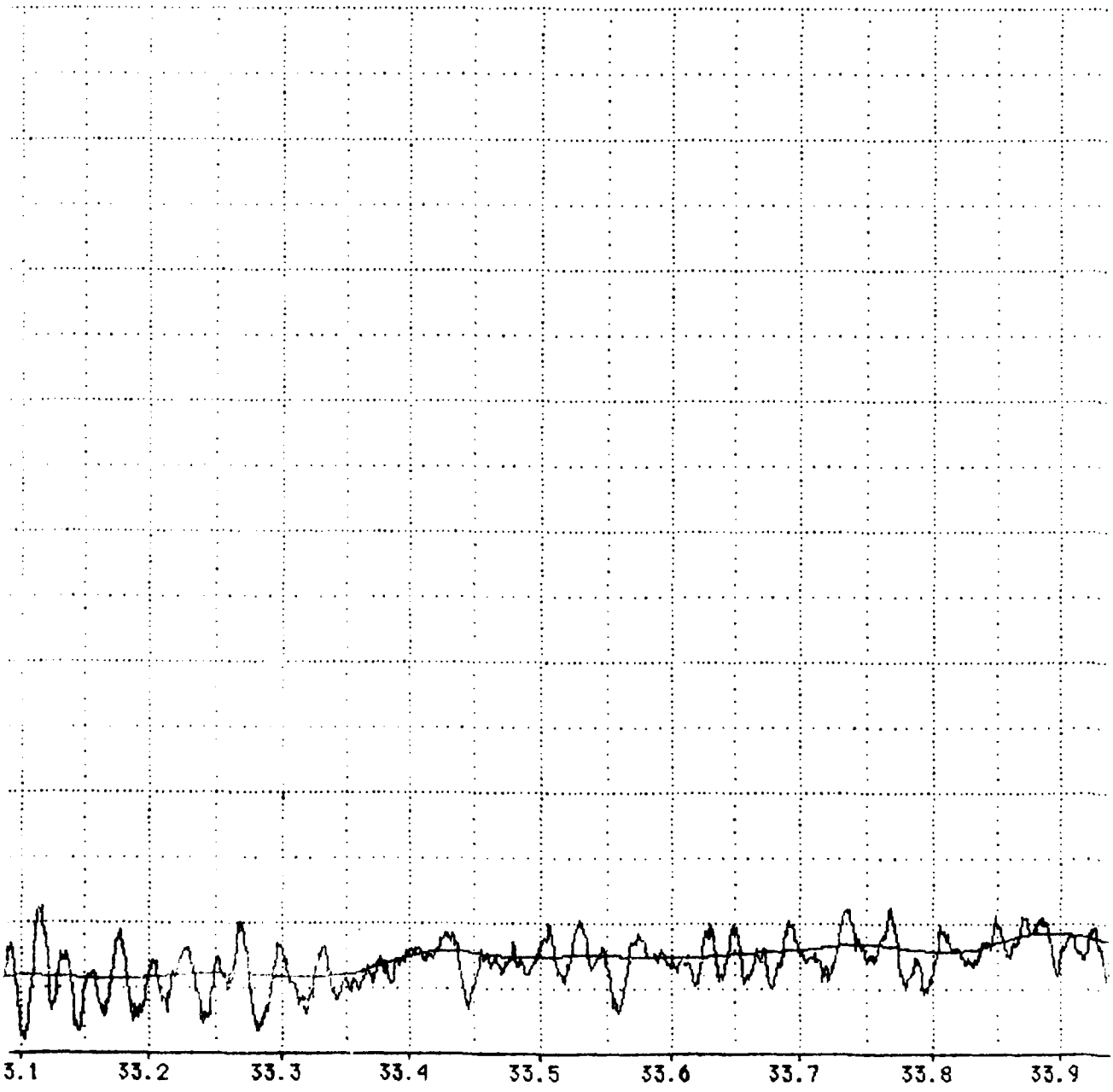
3.1
33.2
33.3
33.4
33.5
33.6
33.7
33.8
33.9

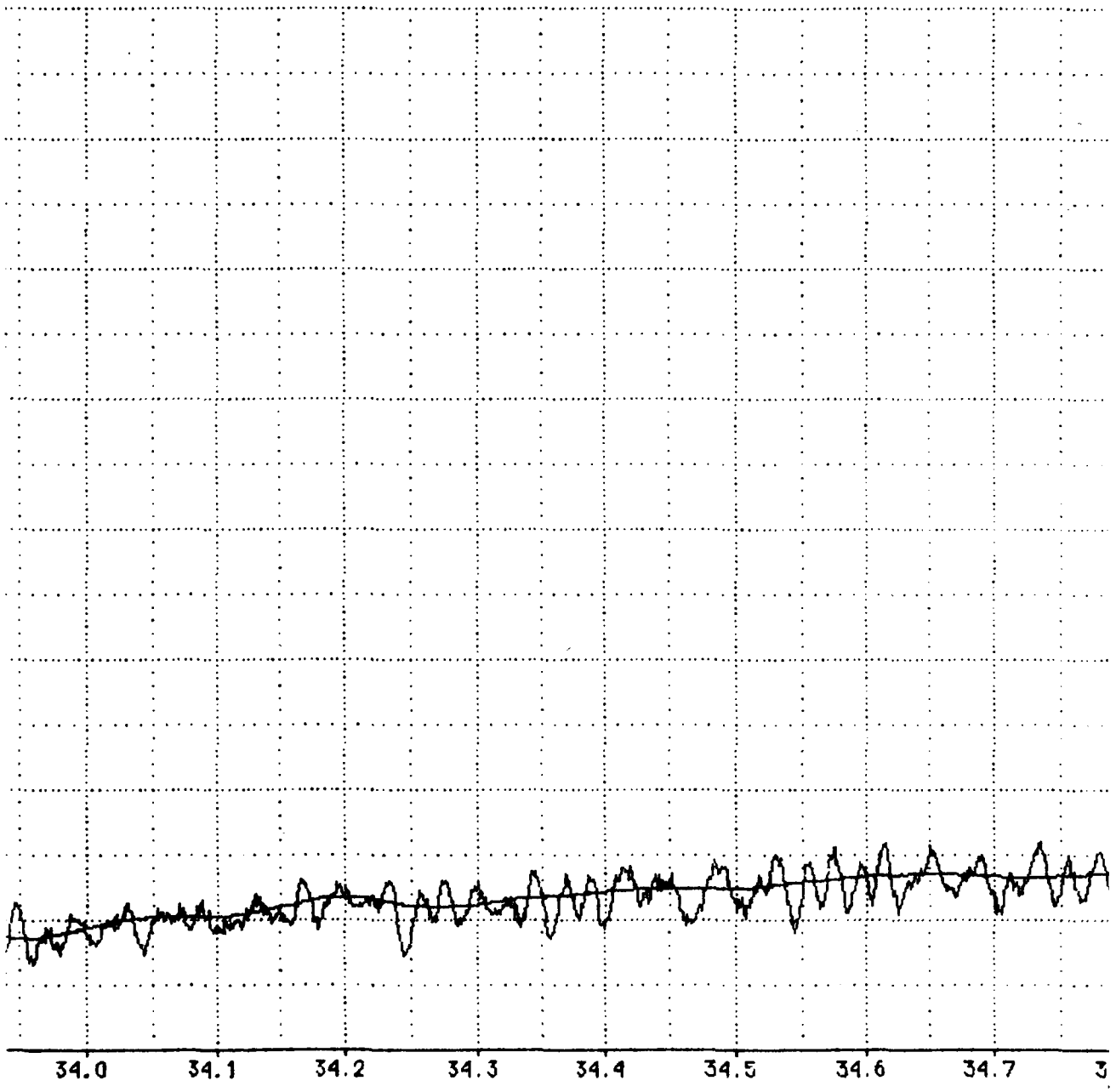
34.0
34.1
34.2
34.3
34.4
34.5
34.6
34.7
3

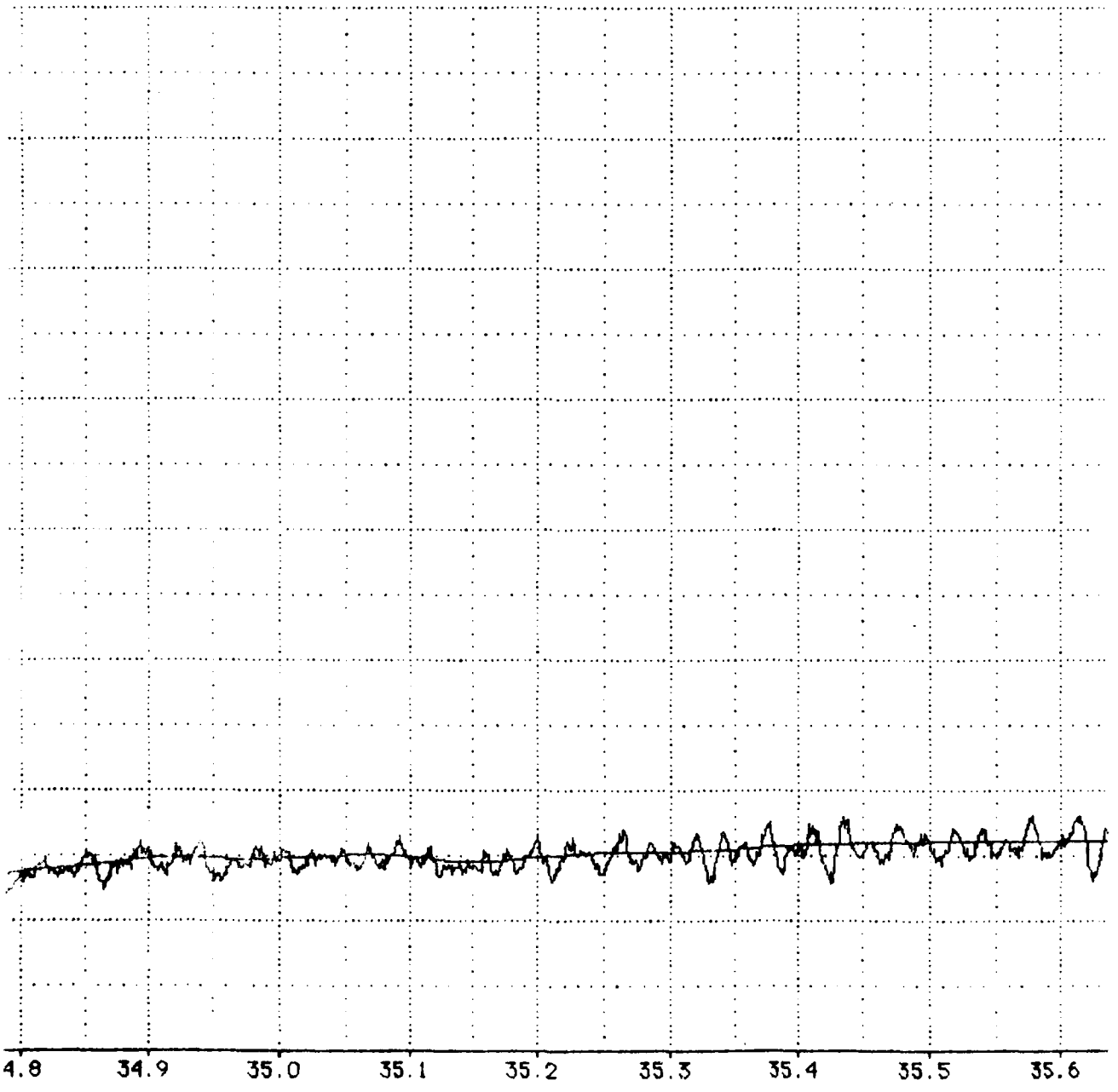
4.8
34.9
35.0
35.1
35.2
35.3
35.4
35.5
35.6

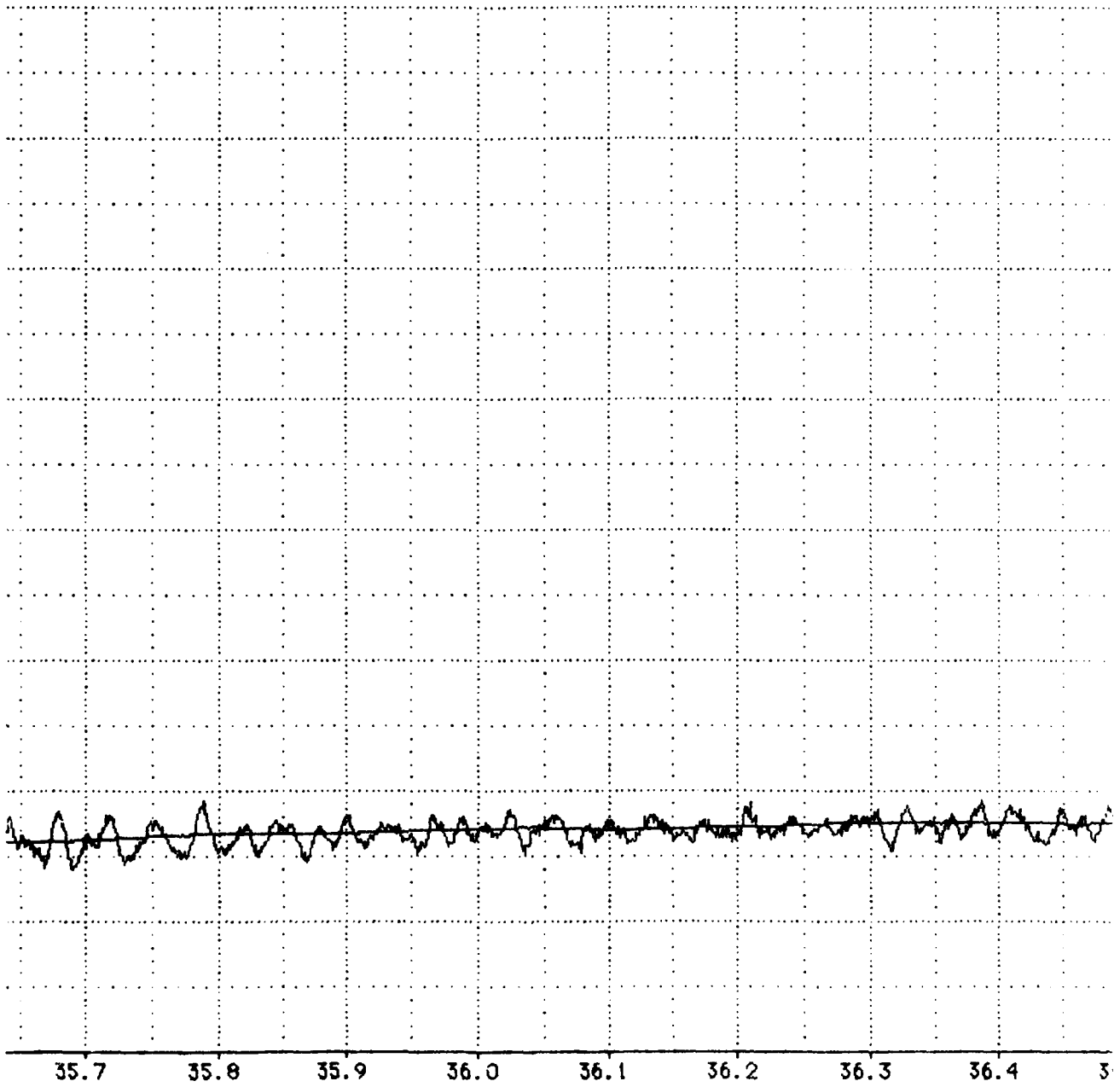
35.7
35.8
35.9
36.0
36.1
36.2
36.3
36.4

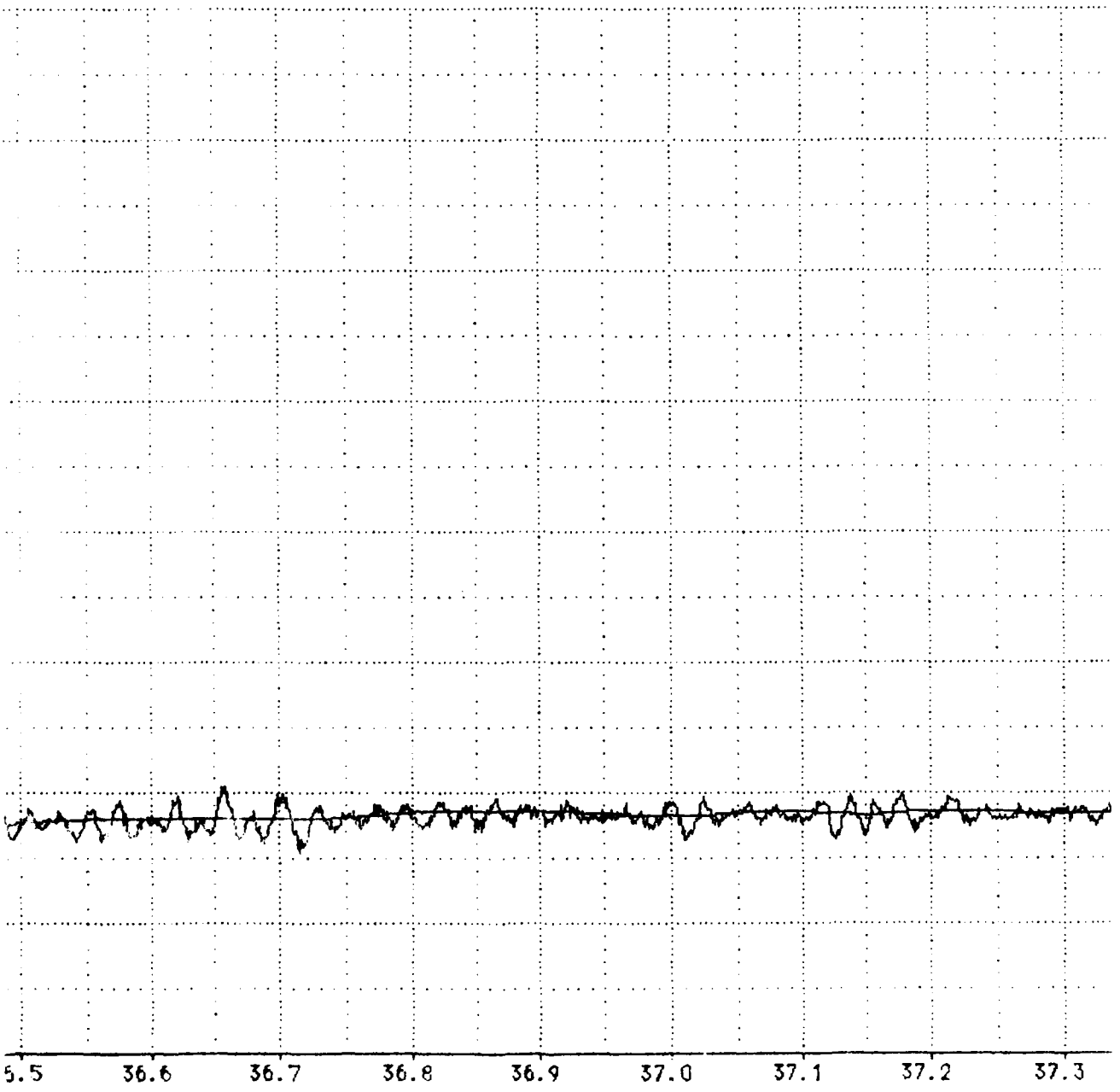
5.5
36.6
36.7
36.8
36.9
37.0
37.1
37.2
37.3

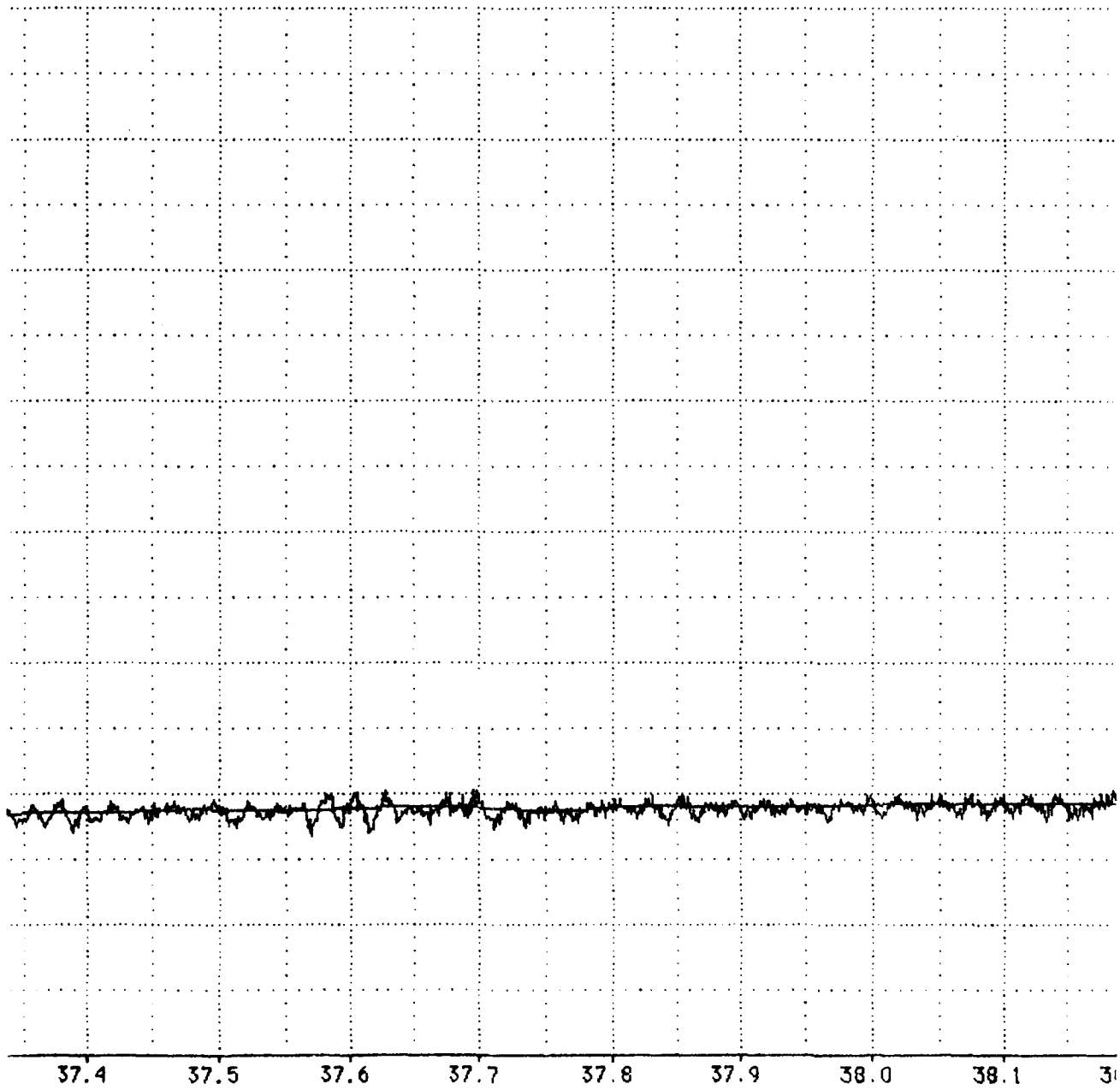
37.4
37.5
37.6
37.7
37.8
37.9
38.0
38.1

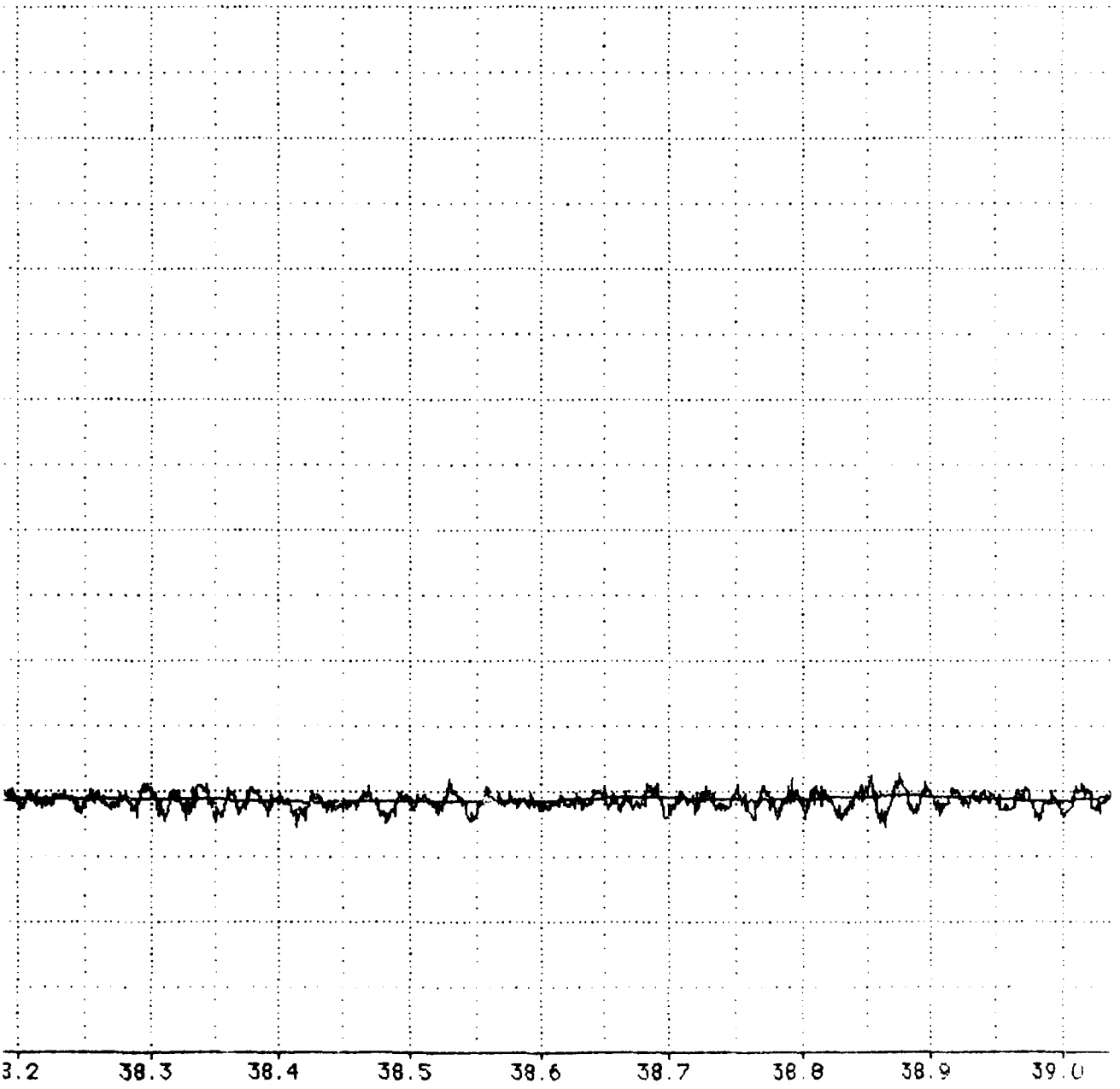
3.2
38.3
38.4
38.5
38.6
38.7
38.8
38.9
39.0

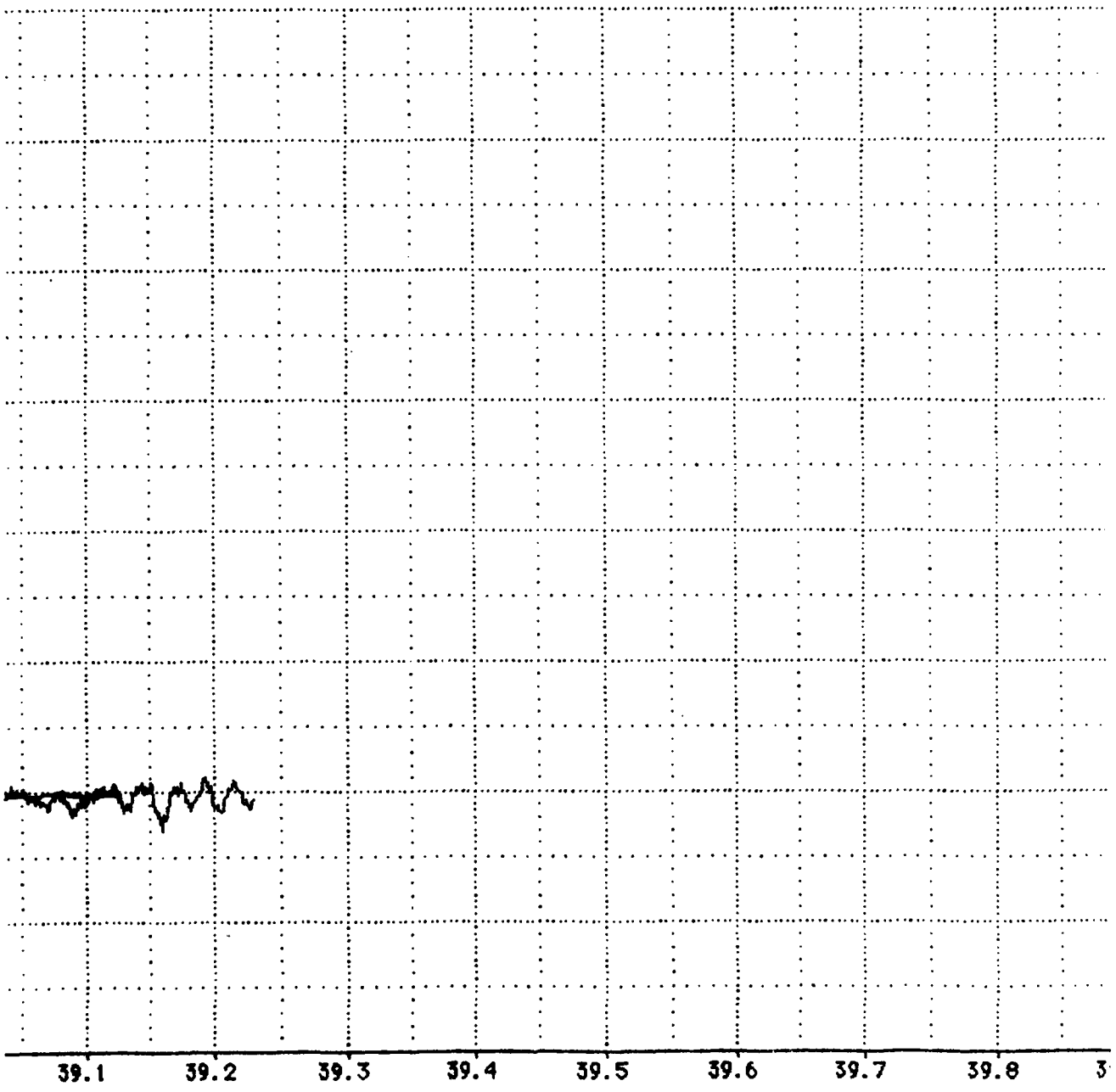
39.1
39.2
39.3
39.4
39.5
39.6
39.7
39.8

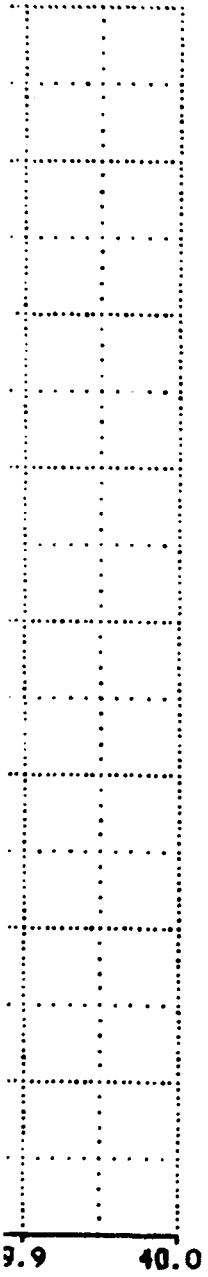
9.9
40.0

18Y-F10C

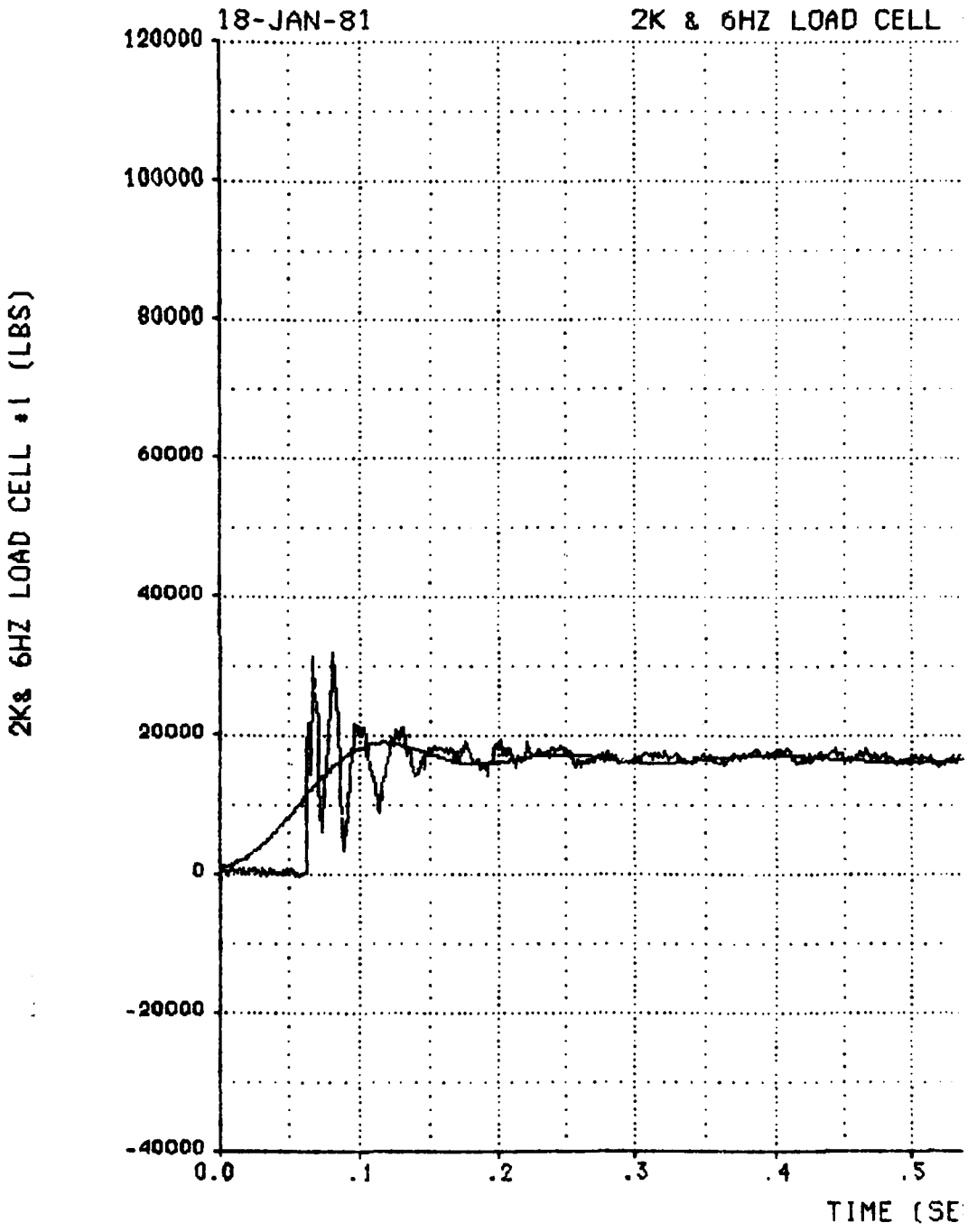
18-JAN-81
2K & 6HZ LOAD CELL
120000
100000
80000
60000
40000
20000
0
-20000
-40000
2K& 6HZ LOAD CELL #1 (LBS)
0.0
.1
.2
.3
.4
.5
TIME (SE

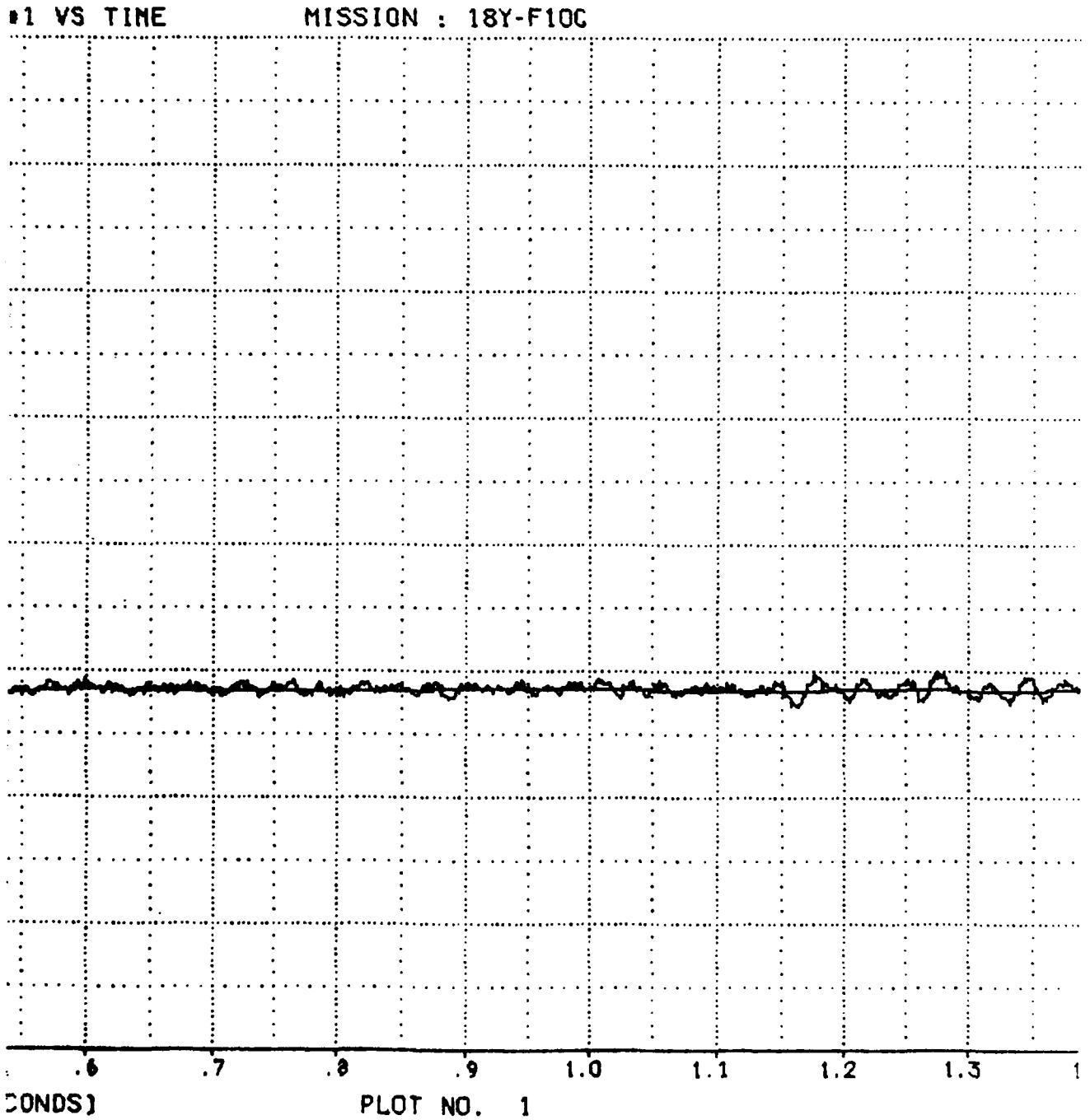
#1 VS TIME
MISSION : 18Y-F10C
.6
.7
.8
.9
1.0
1.1
1.2
1.3
CONDS)
PLOT NO. 1

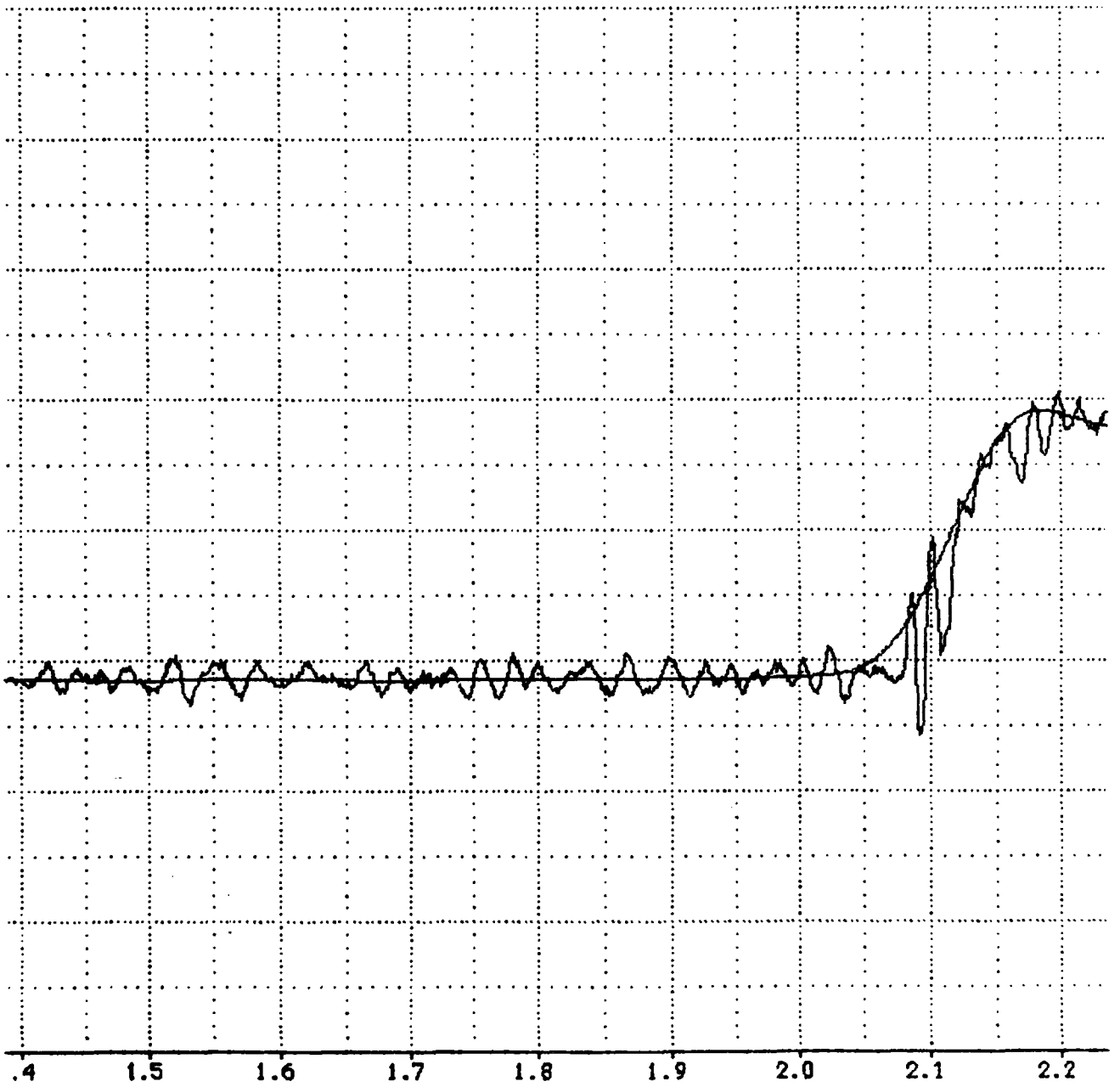
.4
1.5
1.6
1.7
1.8
1.9
2.0
2.1
2.2

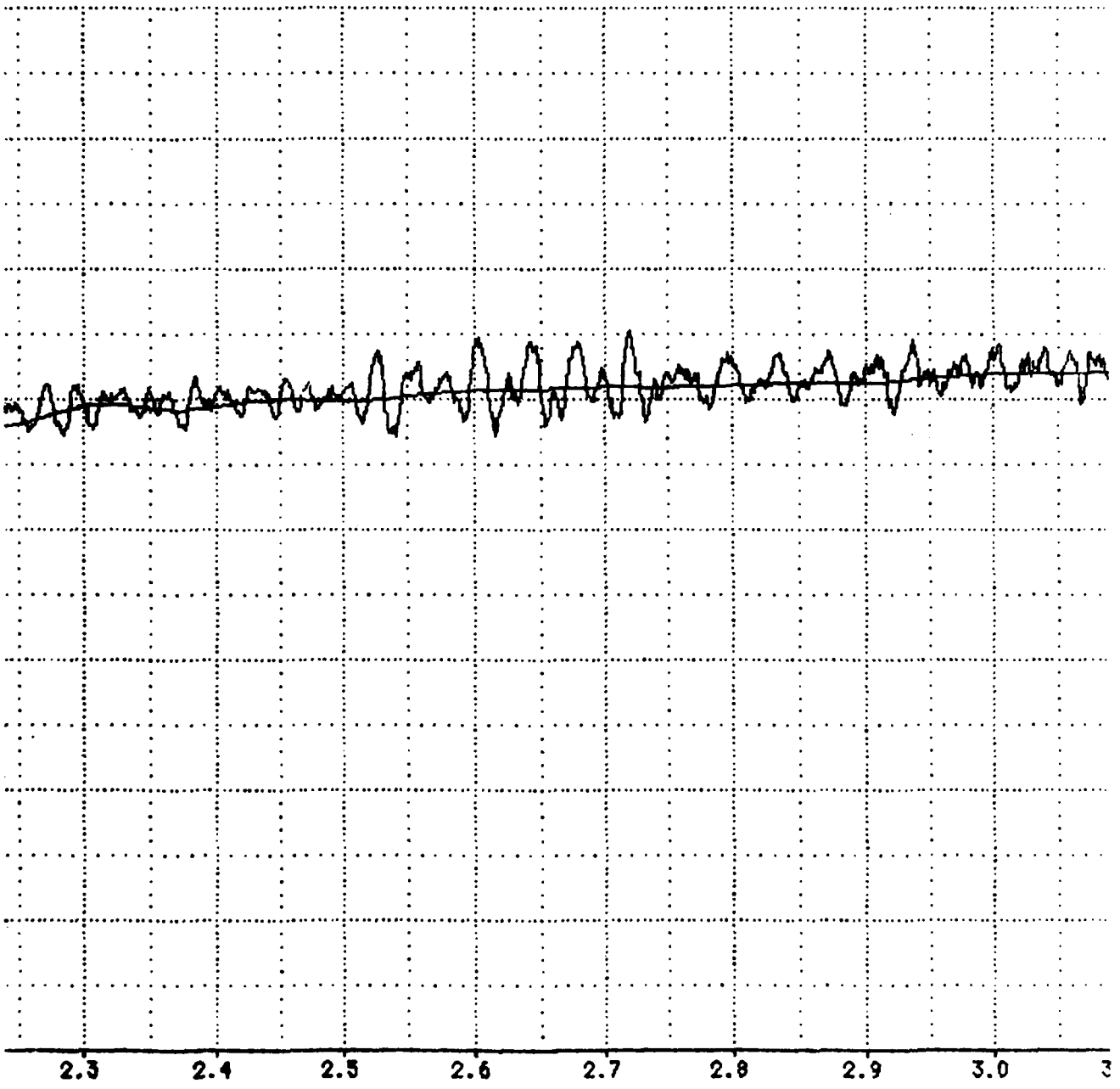
2.3
2.4
2.5
2.6
2.7
2.8
2.9
3.0
3

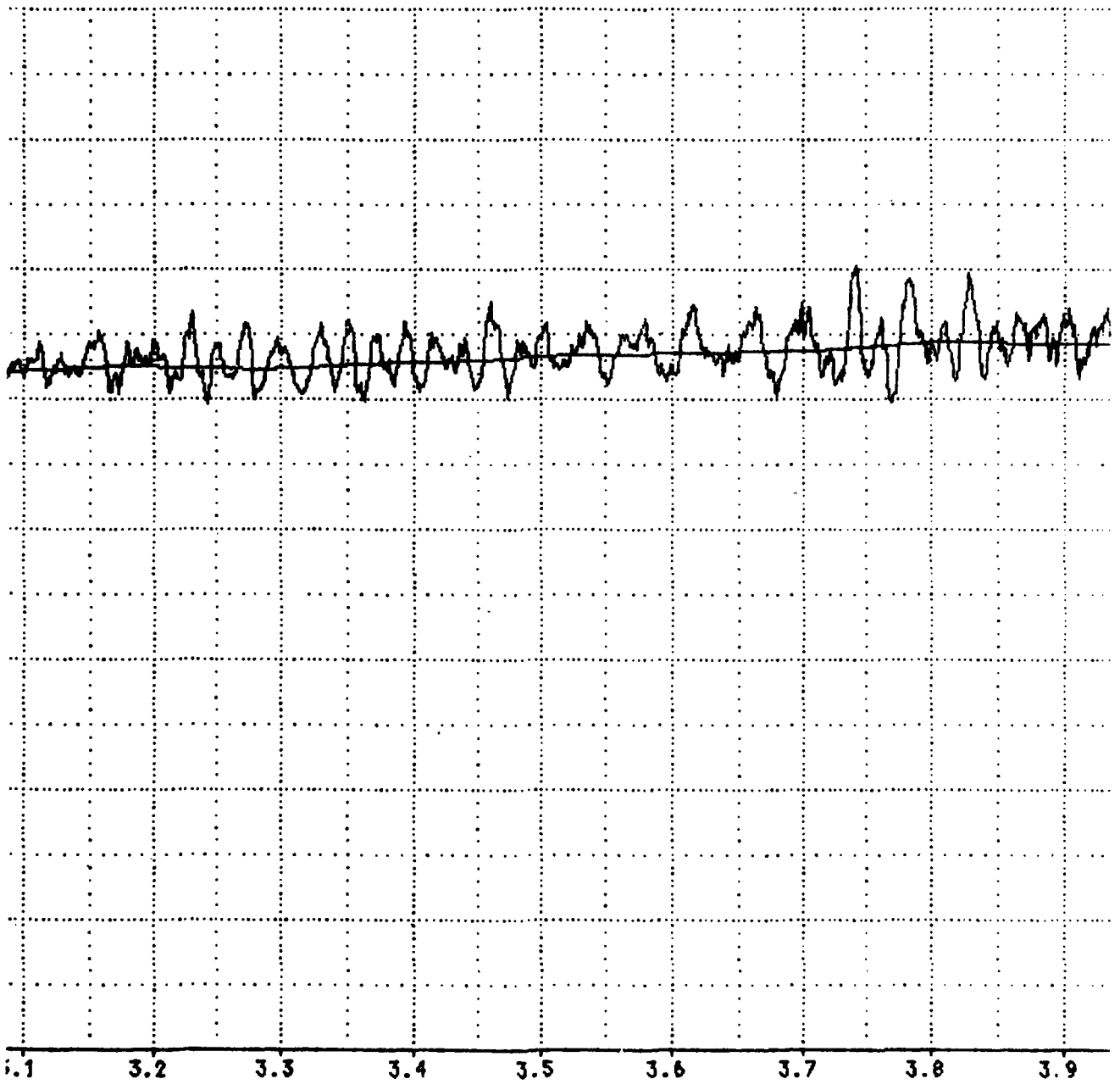
3.1
3.2
3.3
3.4
3.5
3.6
3.7
3.8
3.9

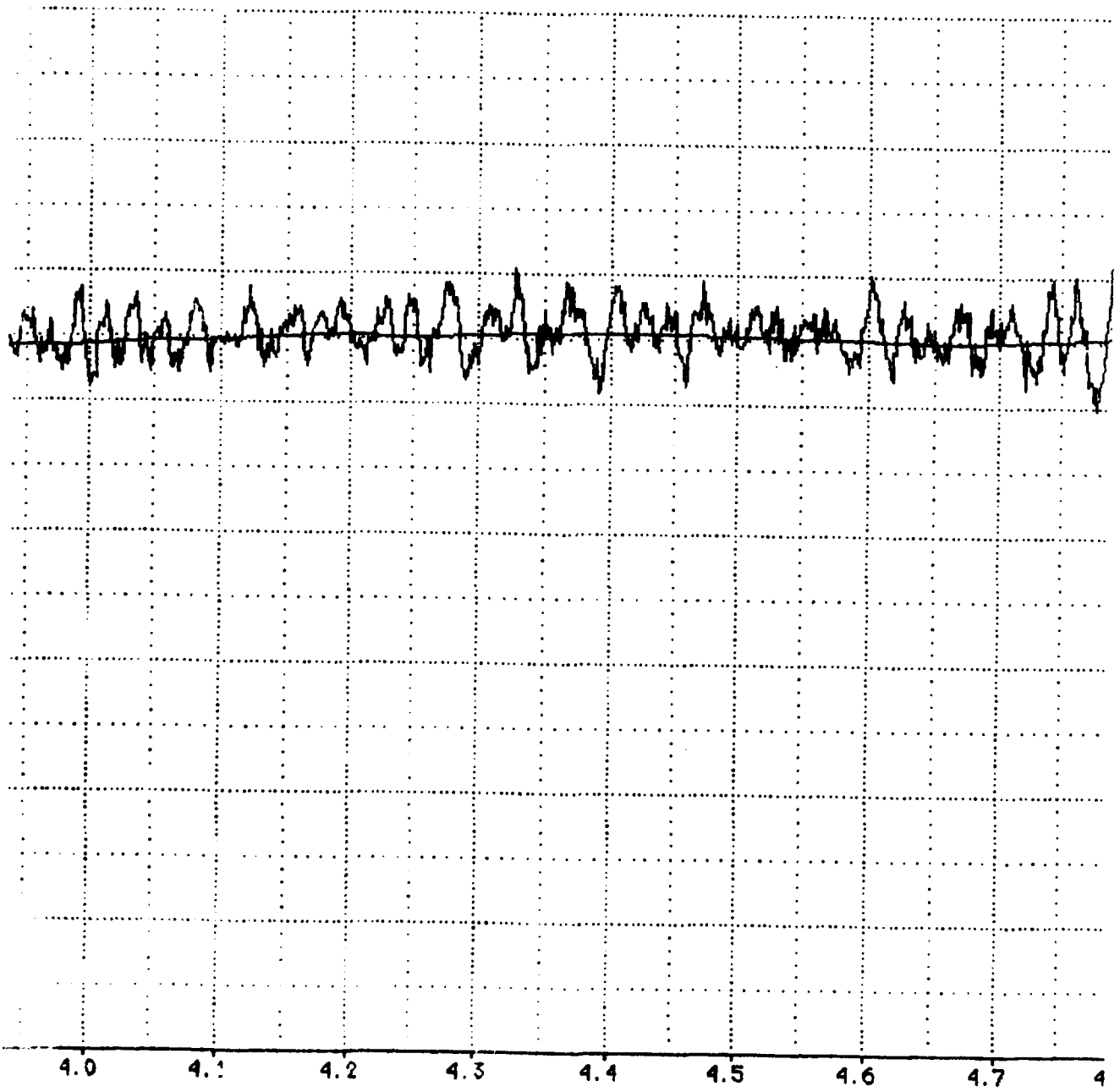
4.0
4.1
4.2
4.3
4.4
4.5
4.6
4.7

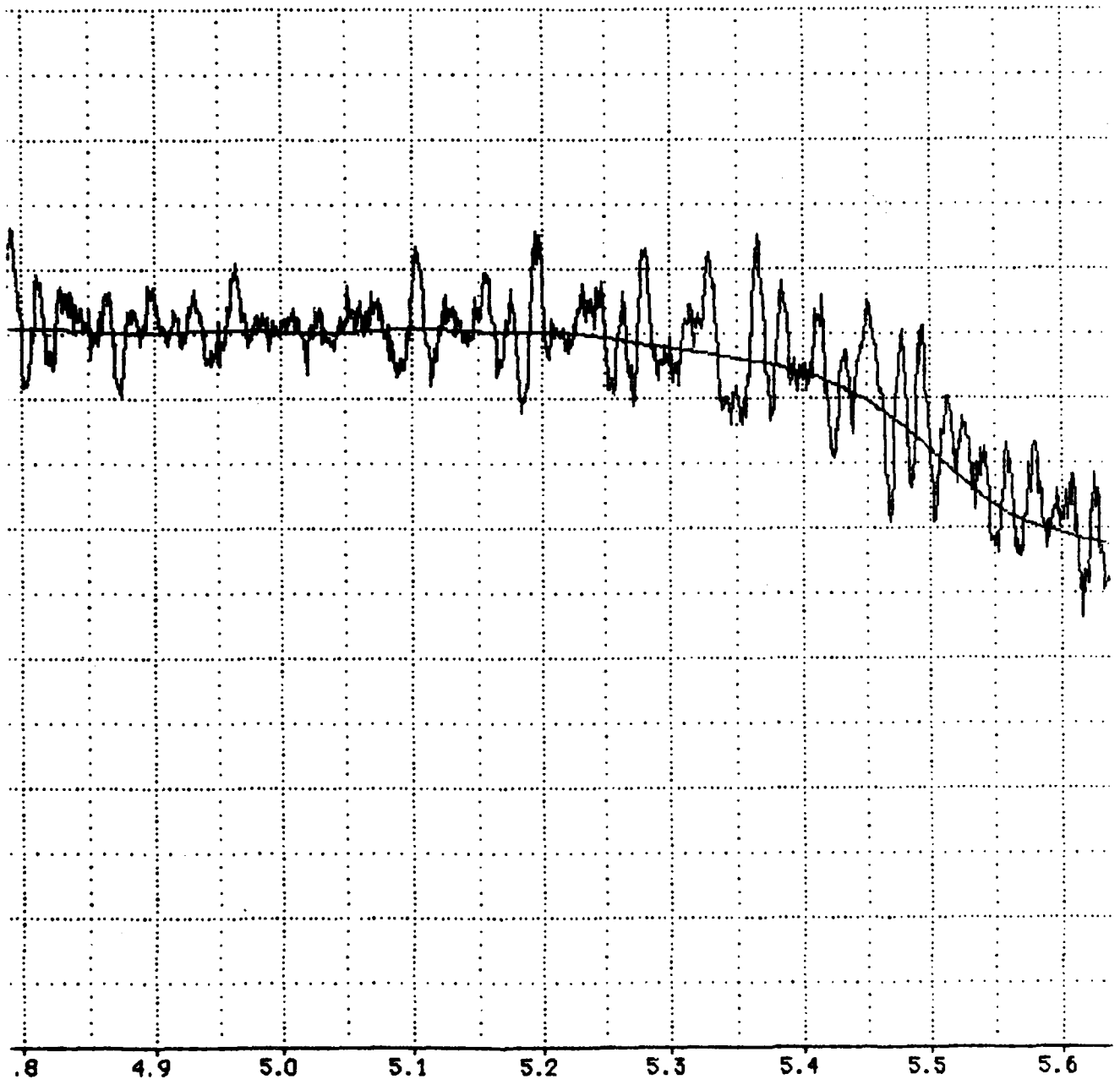
.8
4.9
5.0
5.1
5.2
5.3
5.4
5.5
5.6

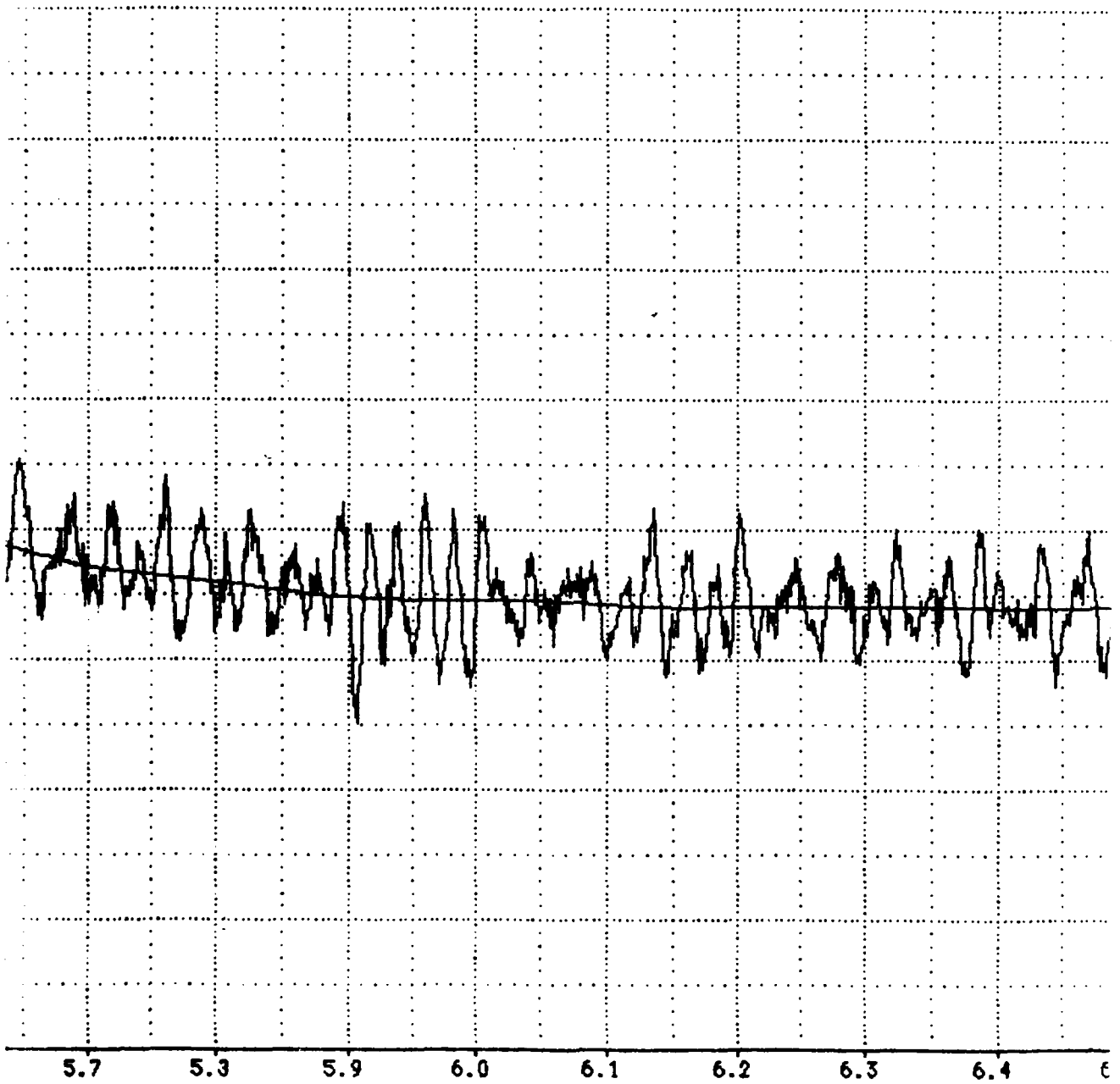
5.7
5.3
5.9
6.0
6.1
6.2
6.3
6.4

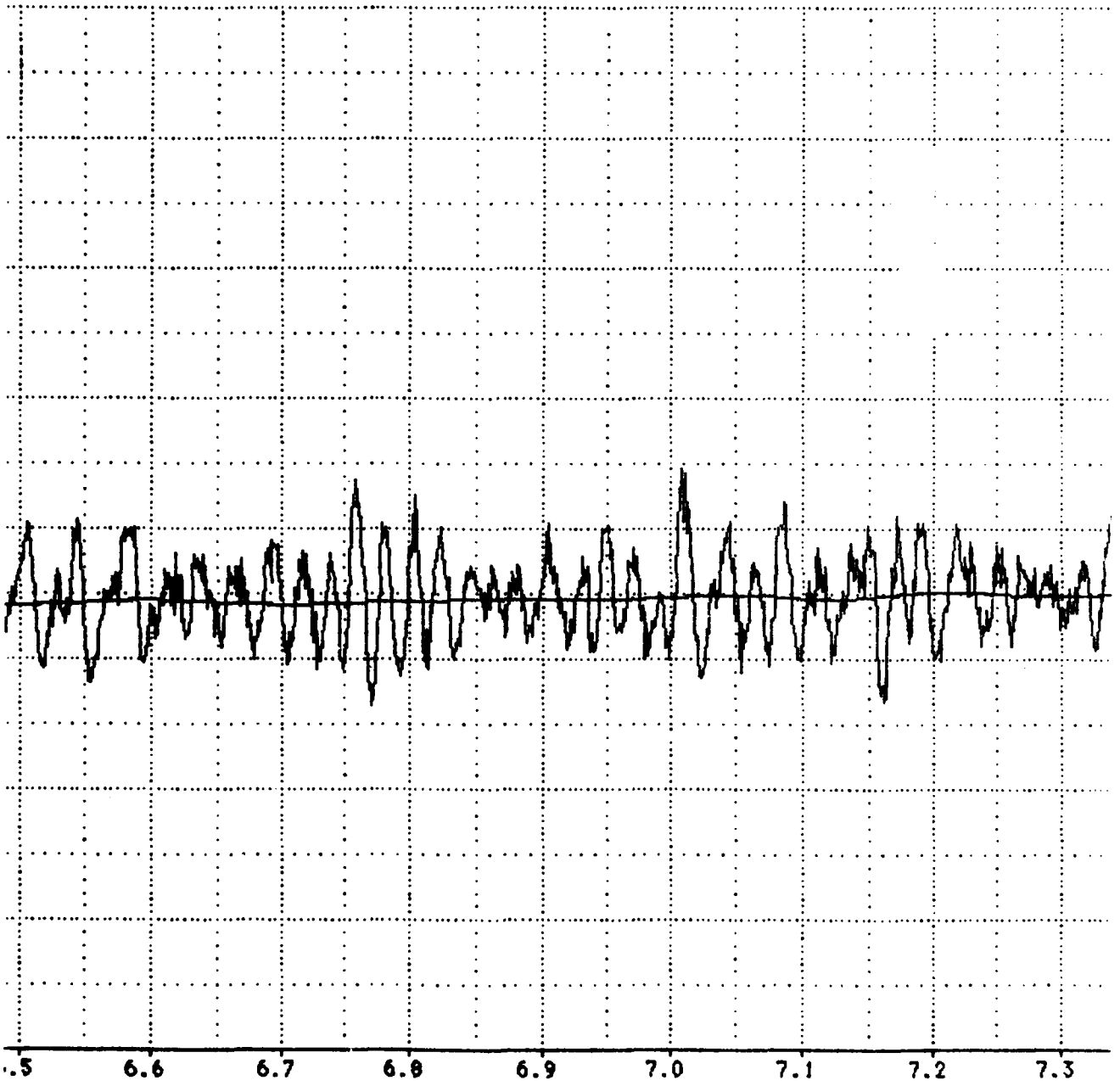
.5
6.6
6.7
6.8
6.9
7.0
7.1
7.2
7.3

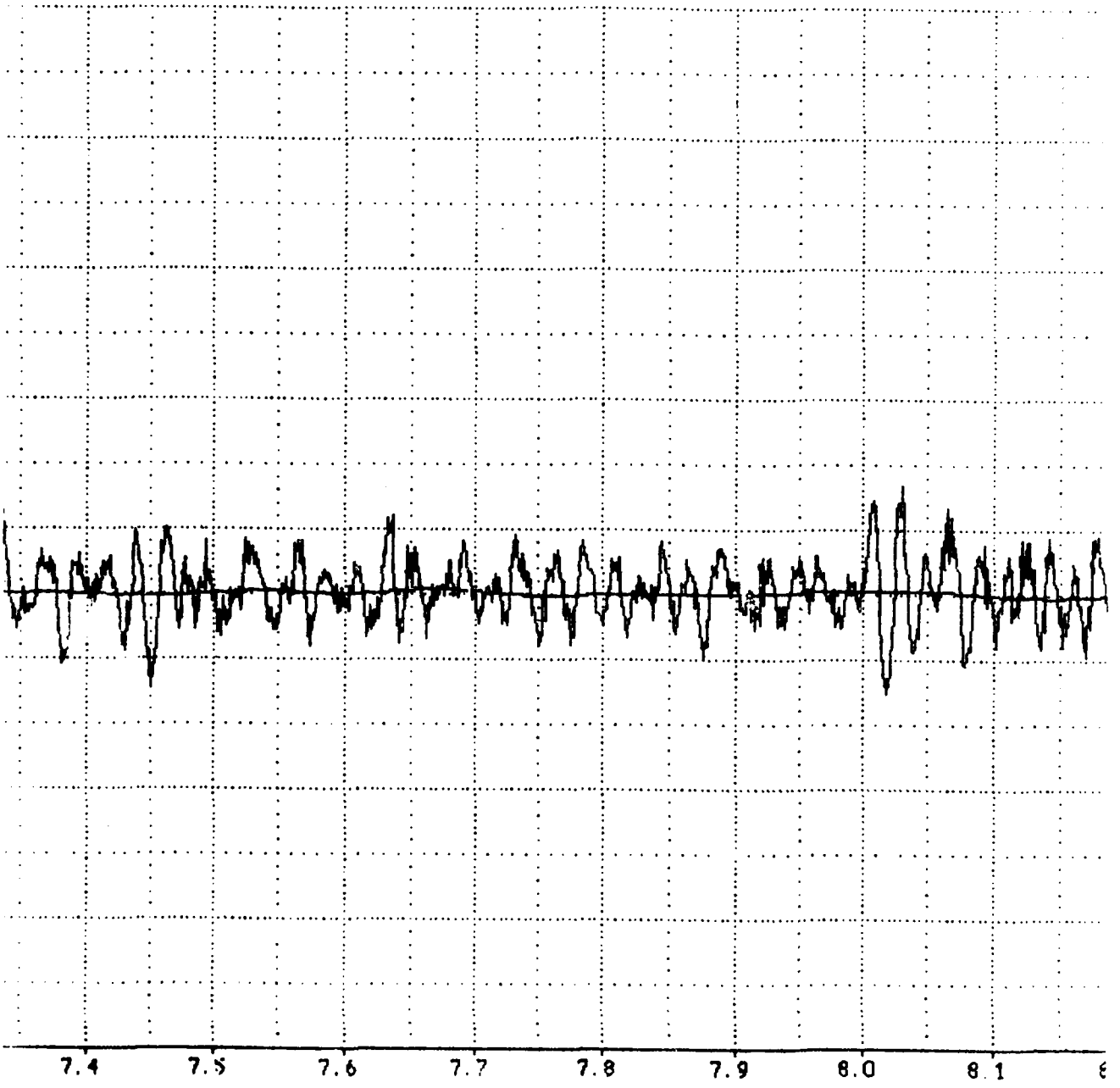
7.4
7.5
7.6
7.7
7.8
7.9
8.0
8.1

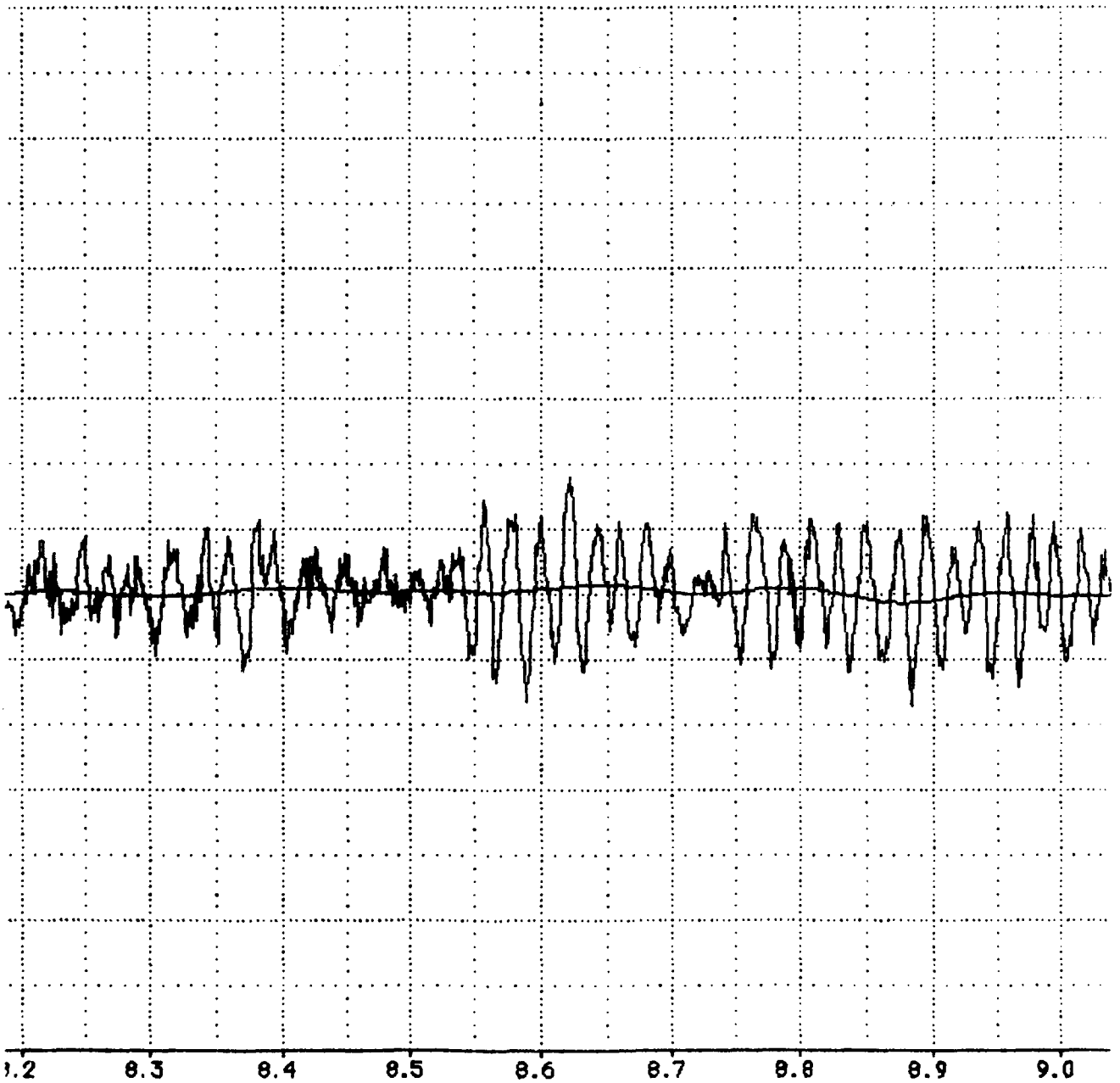
8.2
8.3
8.4
8.5
8.6
8.7
8.8
8.9
9.0

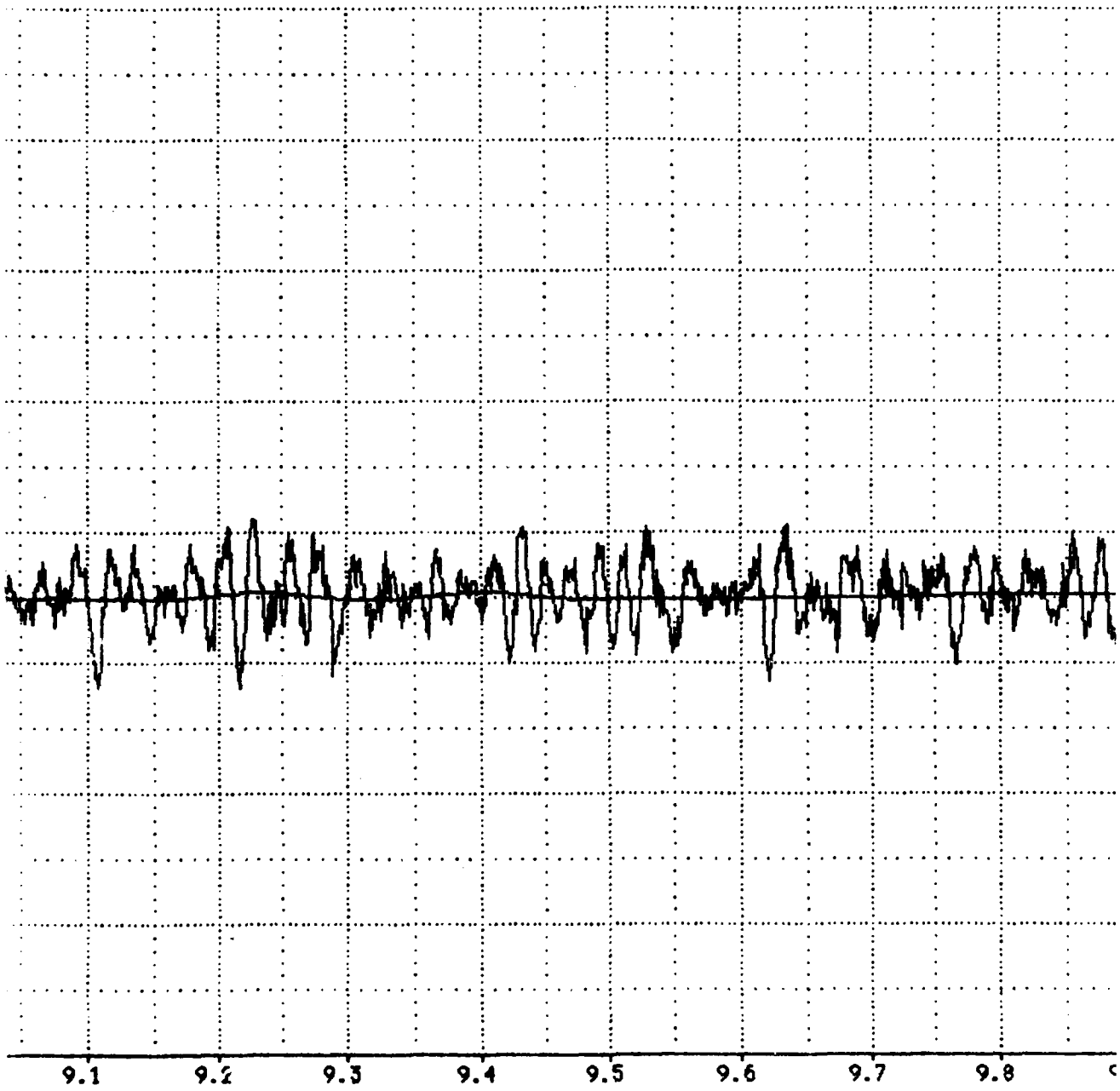
9.1
9.2
9.3
9.4
9.5
9.6
9.7
9.8

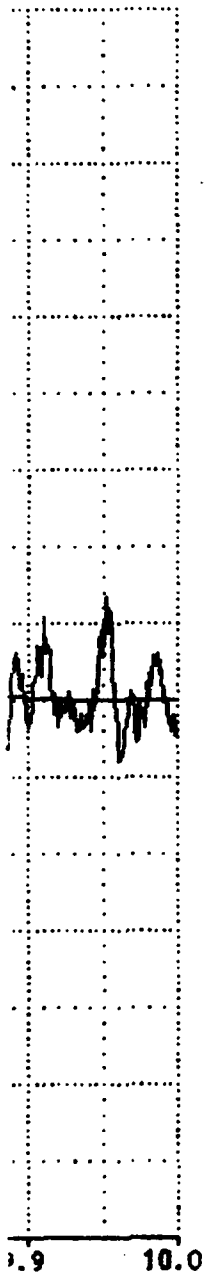
.9
10.0

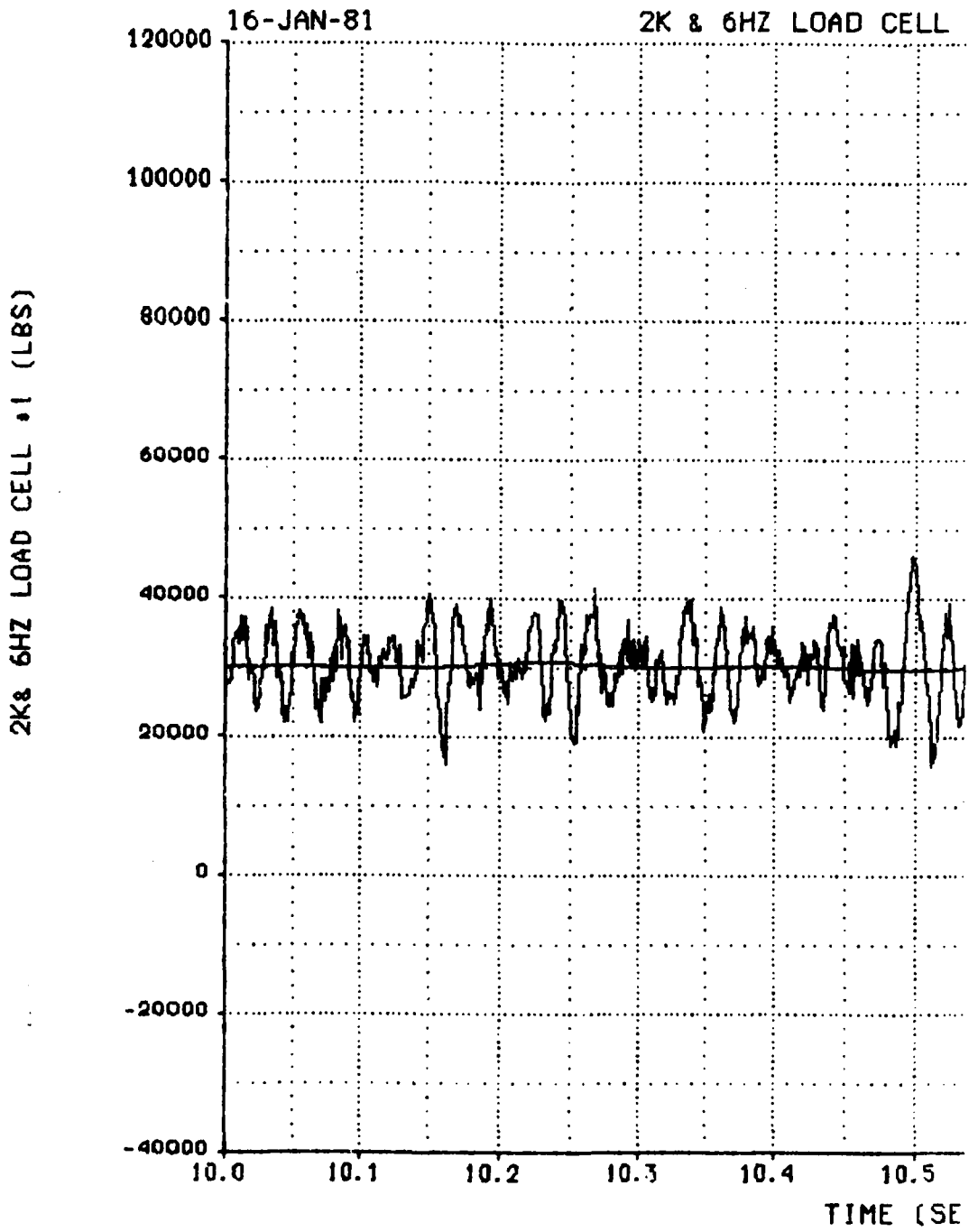
16-JAN-81
2K & 6HZ LOAD CELL
120000
100000
80000
60000
40000
20000
0
-20000
-40000
2K& 6HZ LOAD CELL #1 (LBS)
10.0
10.1
10.2
10.3
10.4
10.5
TIME (SE

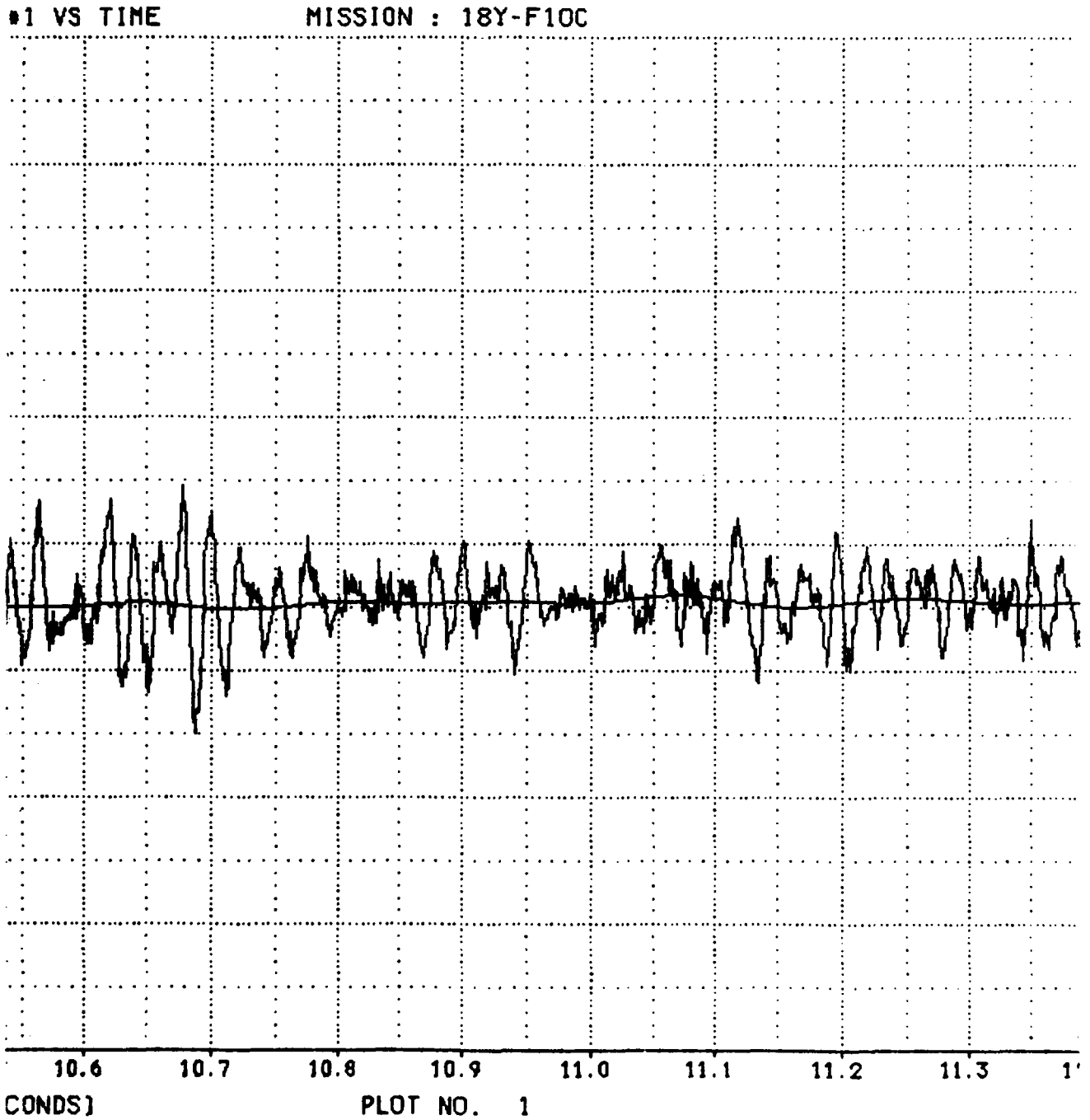
#1 VS TIME
MISSION : 18Y-F10C
10.6
10.7
10.8
10.9
11.0
11.1
11.2
11.3
CONDS)
PLOT NO. 1

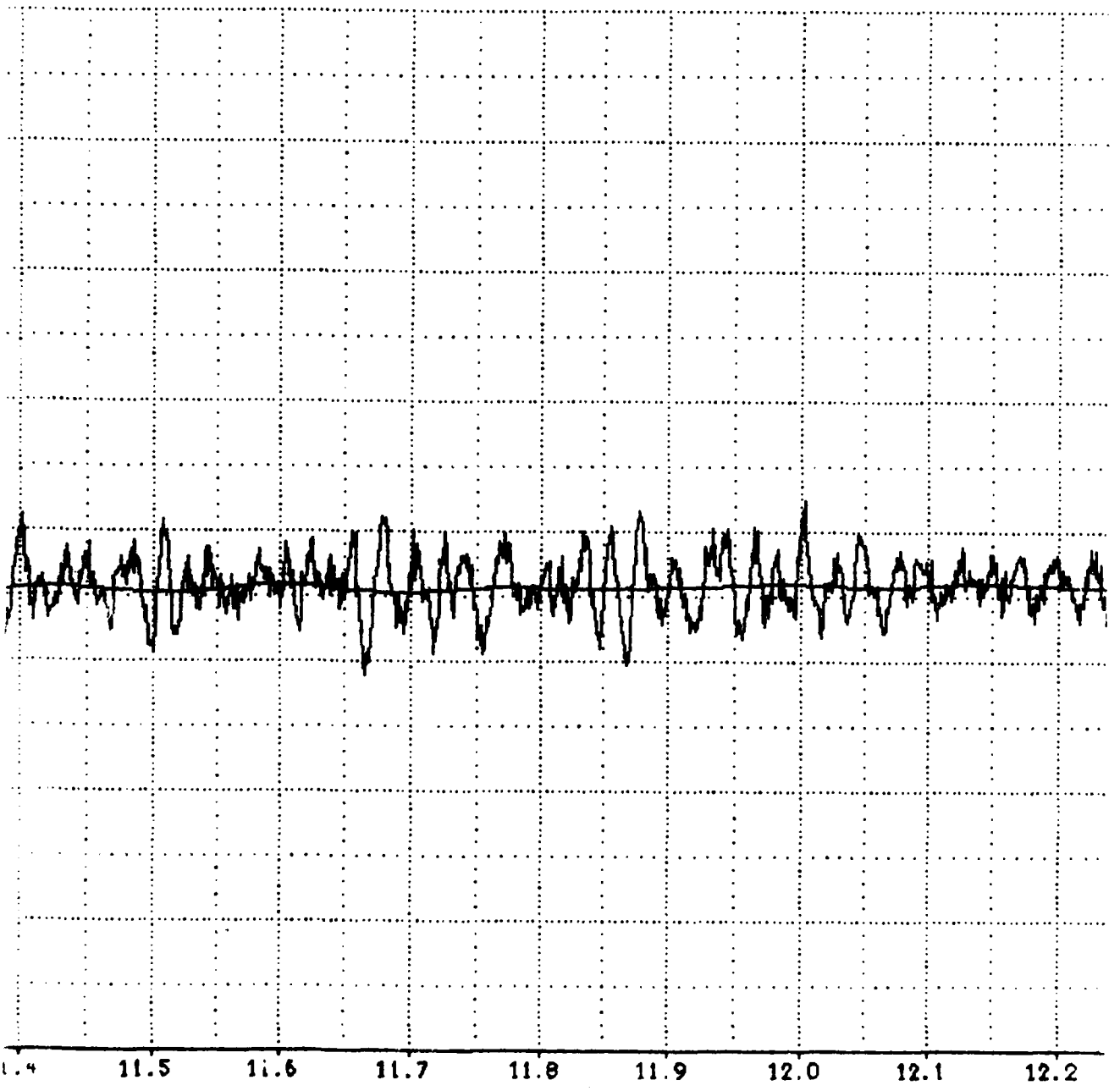
11.5
11.6
11.7
11.8
11.9
12.0
12.1
12.2

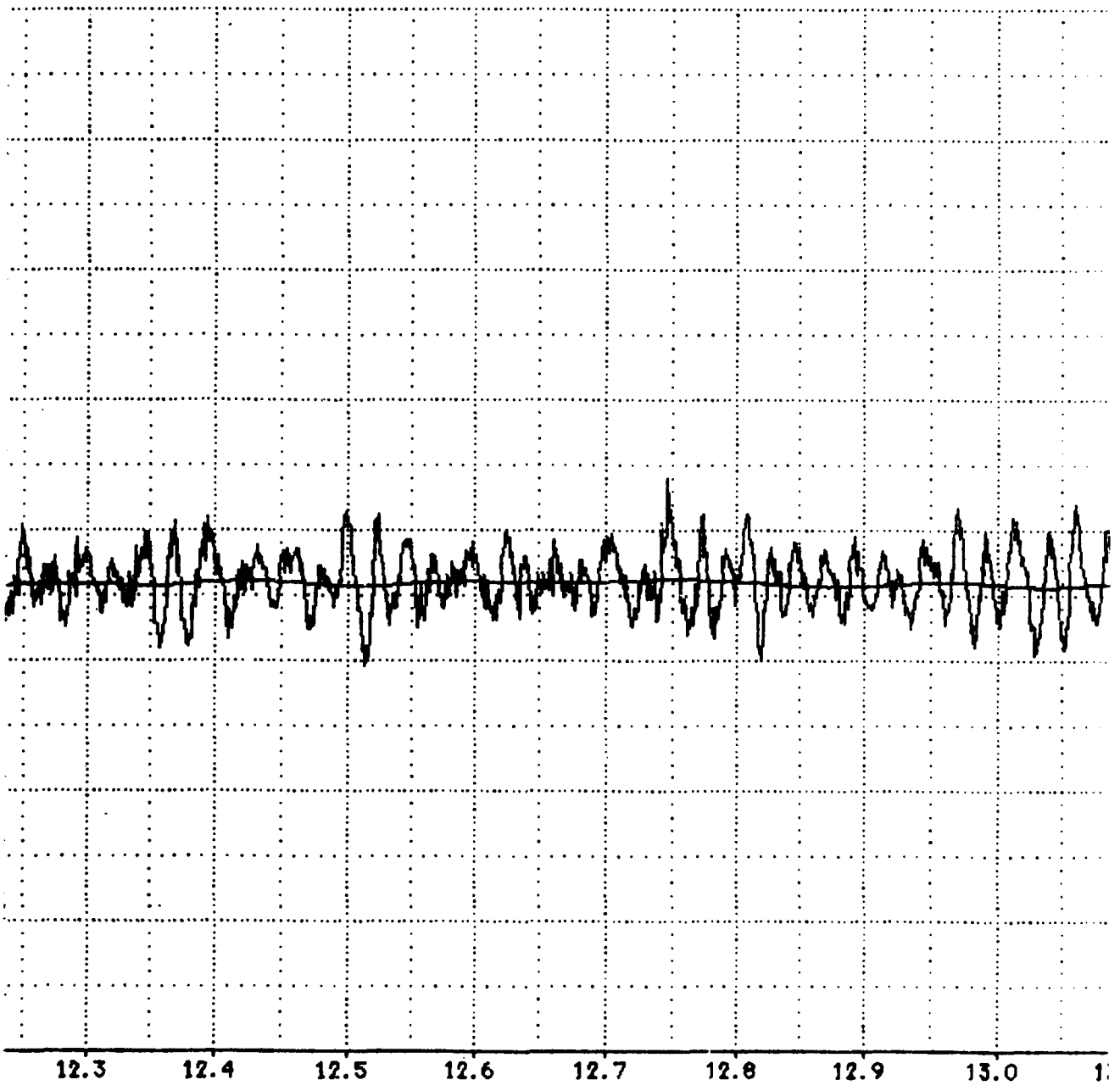
12.3
12.4
12.5
12.6
12.7
12.8
12.9
13.0

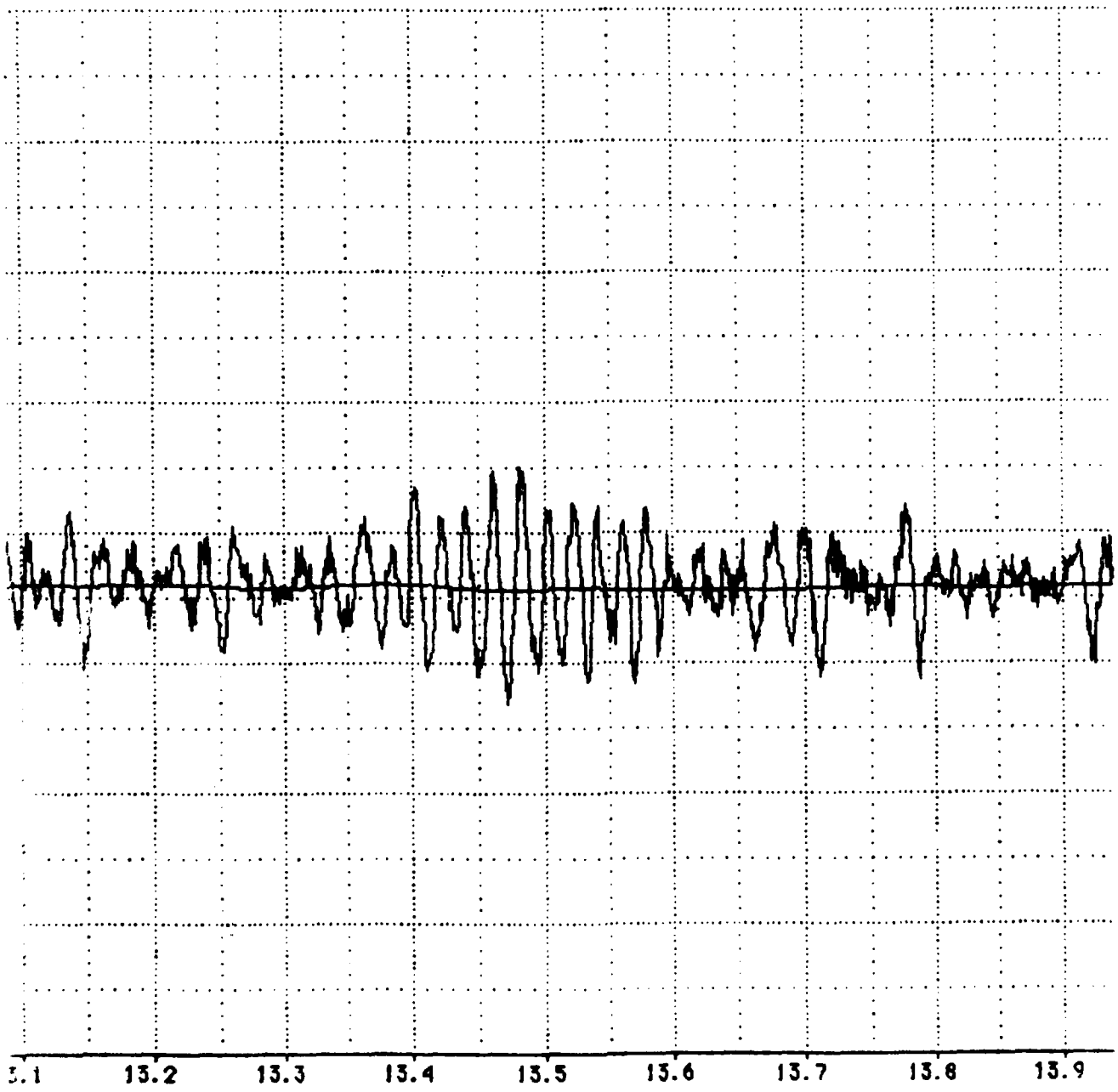
13.2
13.3
13.4
13.5
13.6
13.7
13.8
13.9

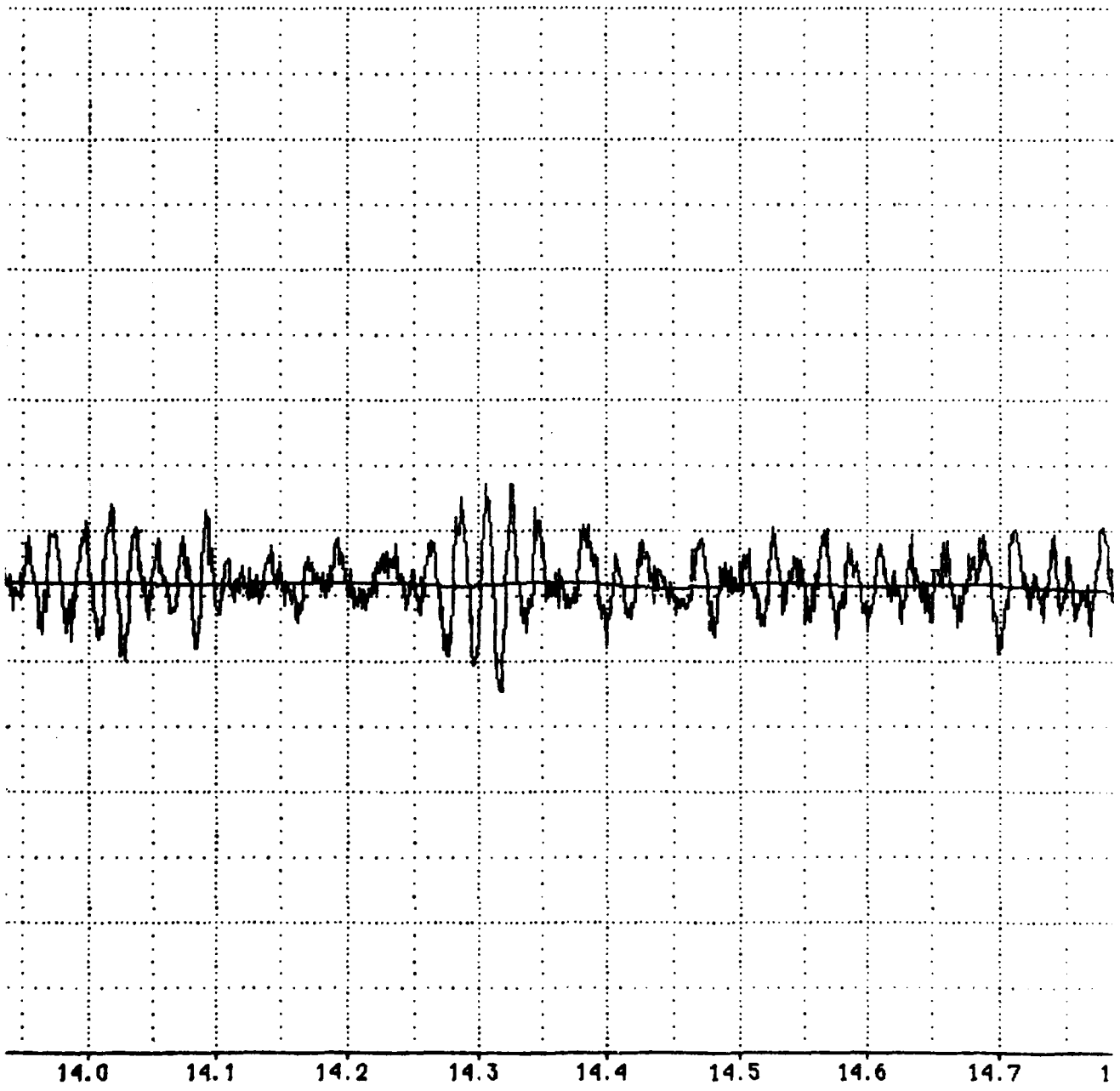
14.0
14.1
14.2
14.3
14.4
14.5
14.6
14.7
1

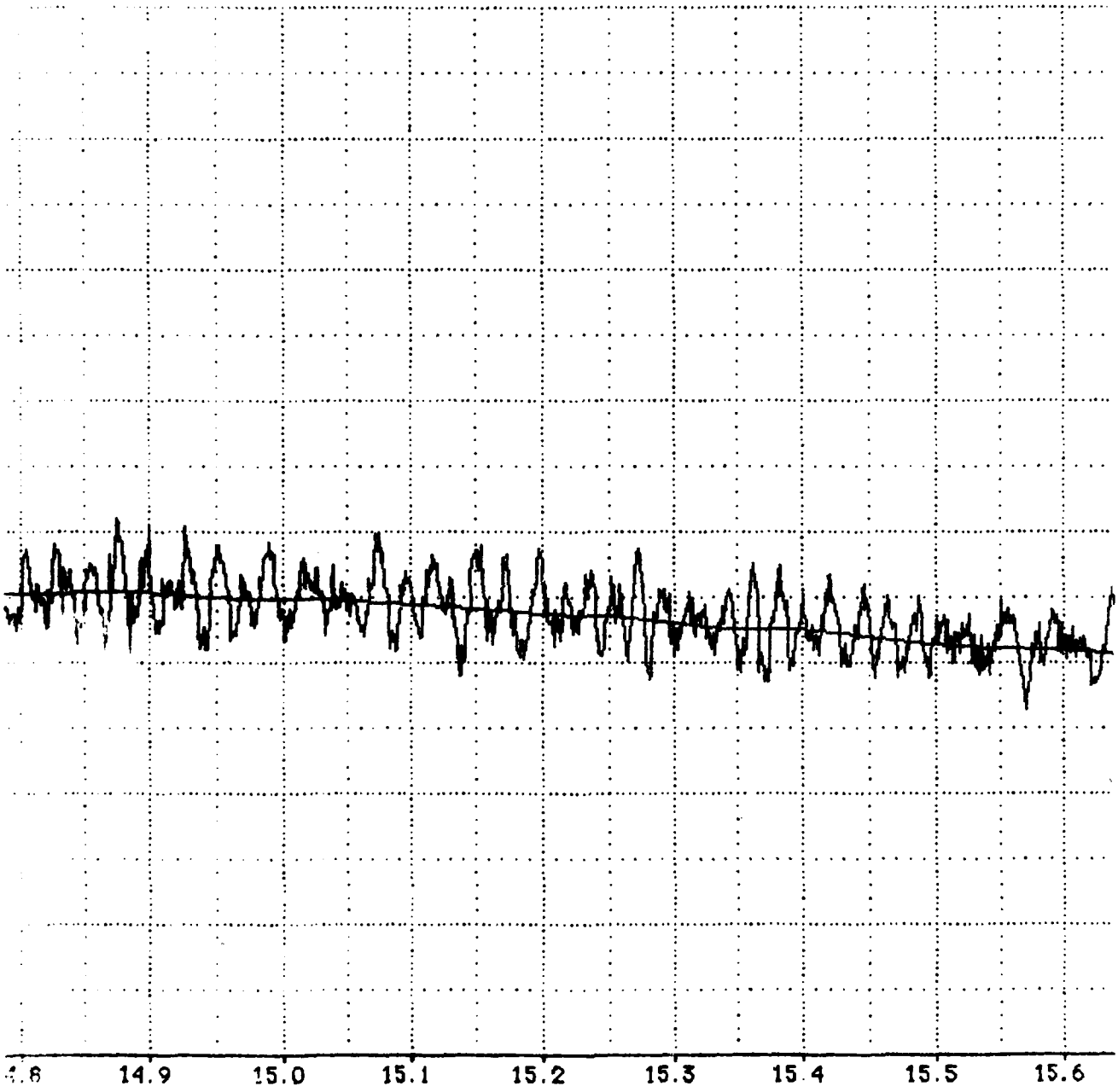
14.8
14.9
15.0
15.1
15.2
15.3
15.4
15.5
15.6

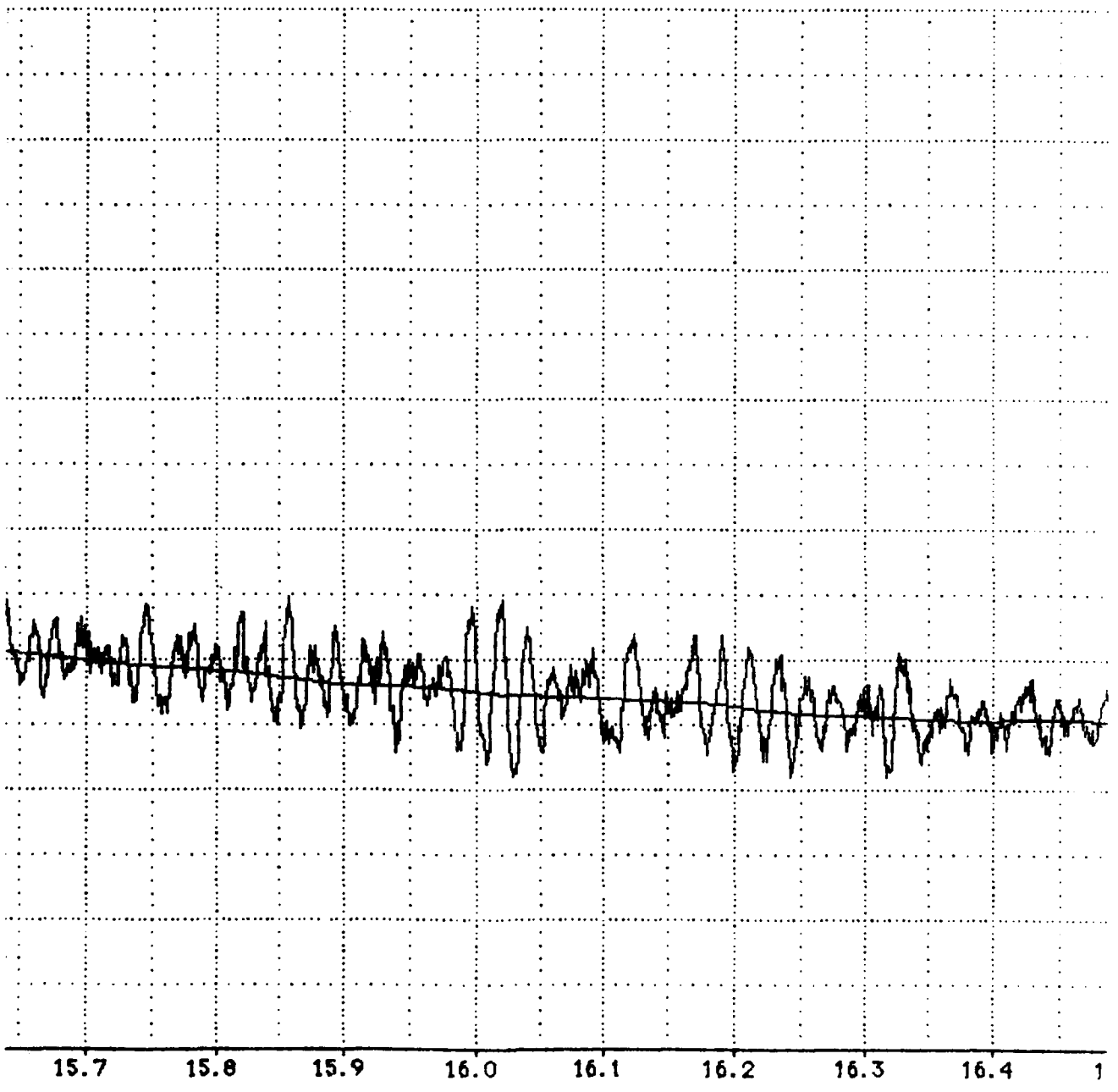
15.7
15.8
15.9
16.0
16.1
16.2
16.3
16.4

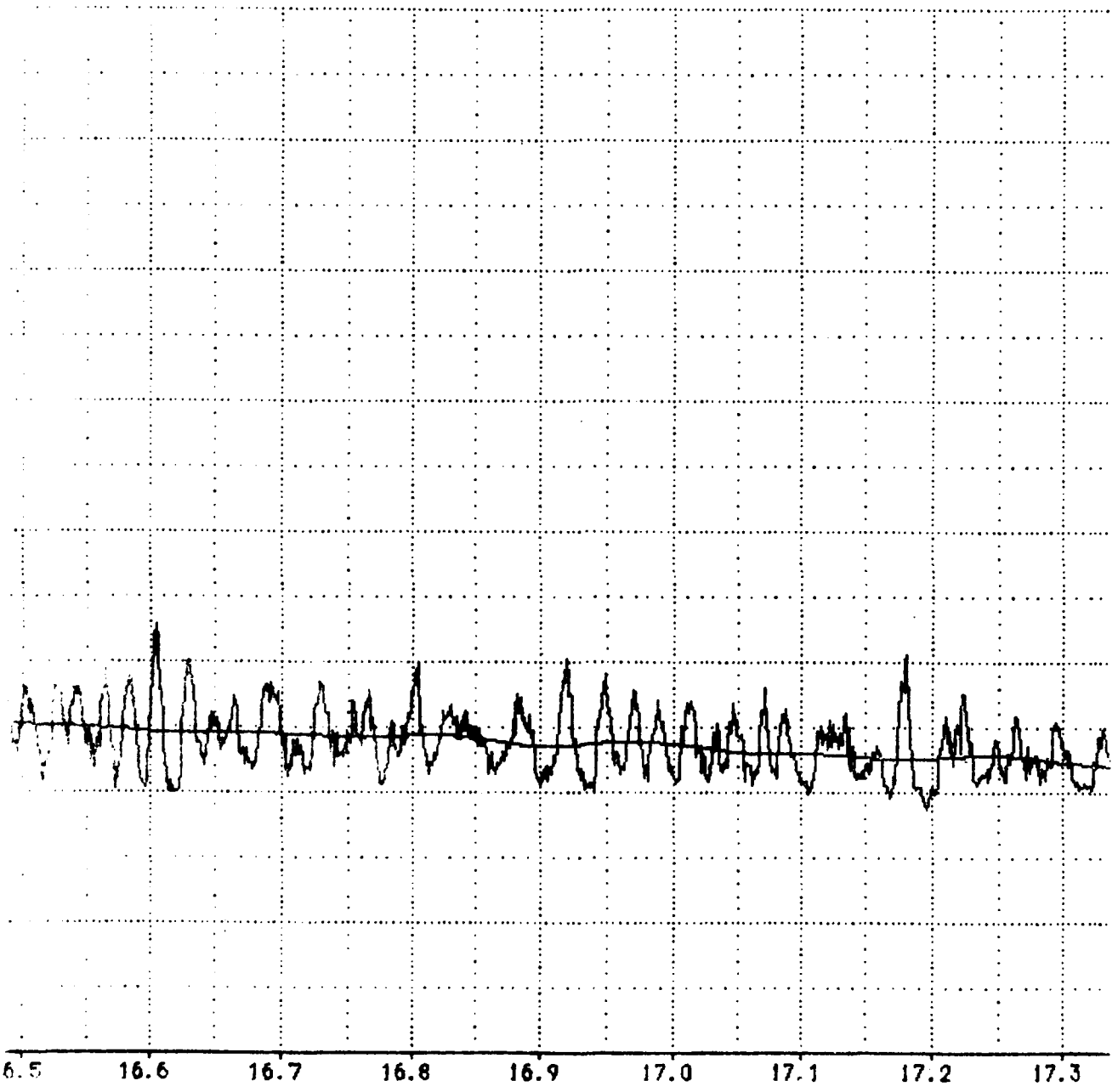
6.5
16.6
16.7
16.8
16.9
17.0
17.1
17.2
17.3

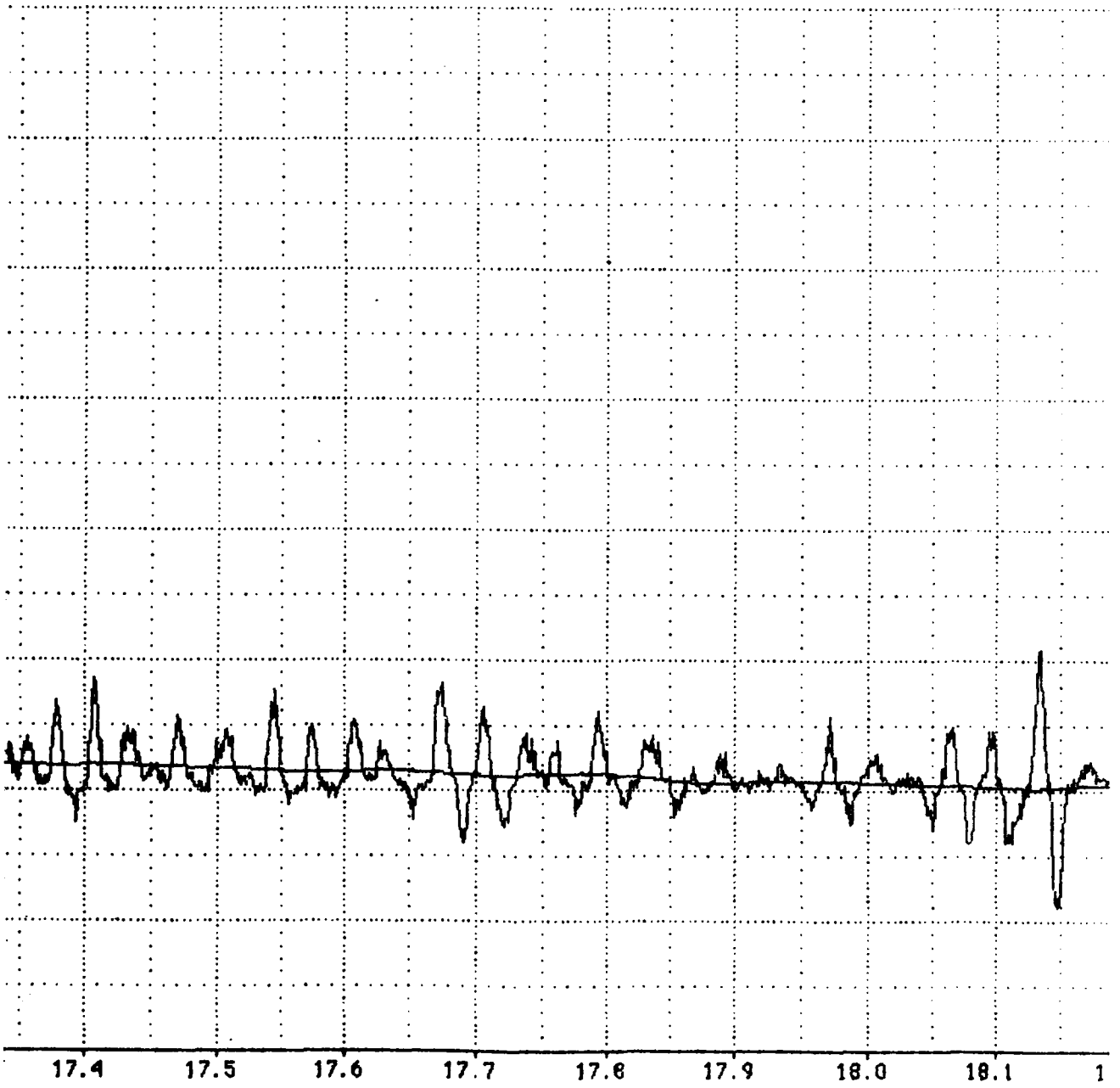
17.4
17.5
17.6
17.7
17.8
17.9
18.0
18.1
1

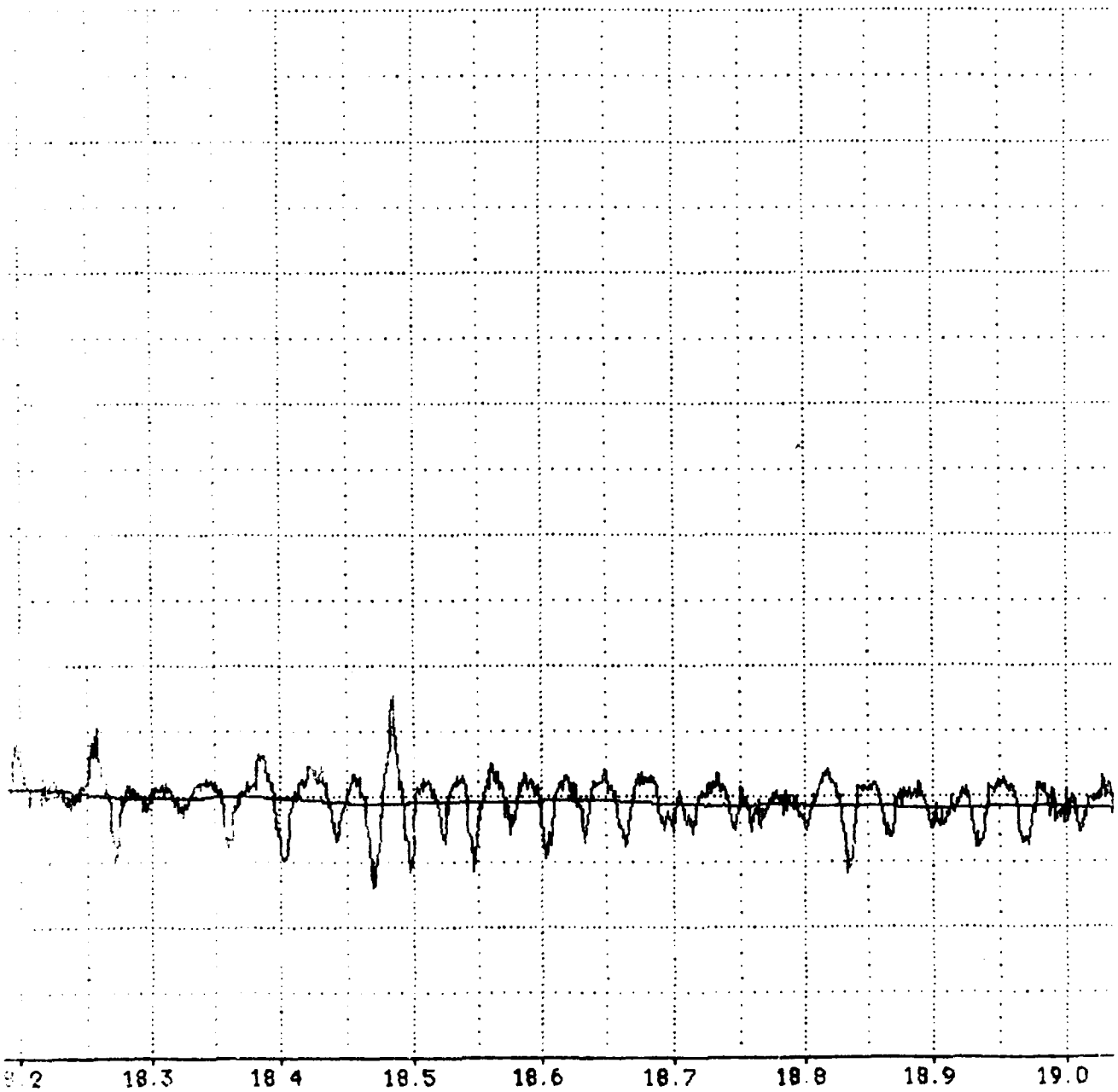
18.2
18.3
18.4
18.5
18.6
18.7
18.8
18.9
19.0

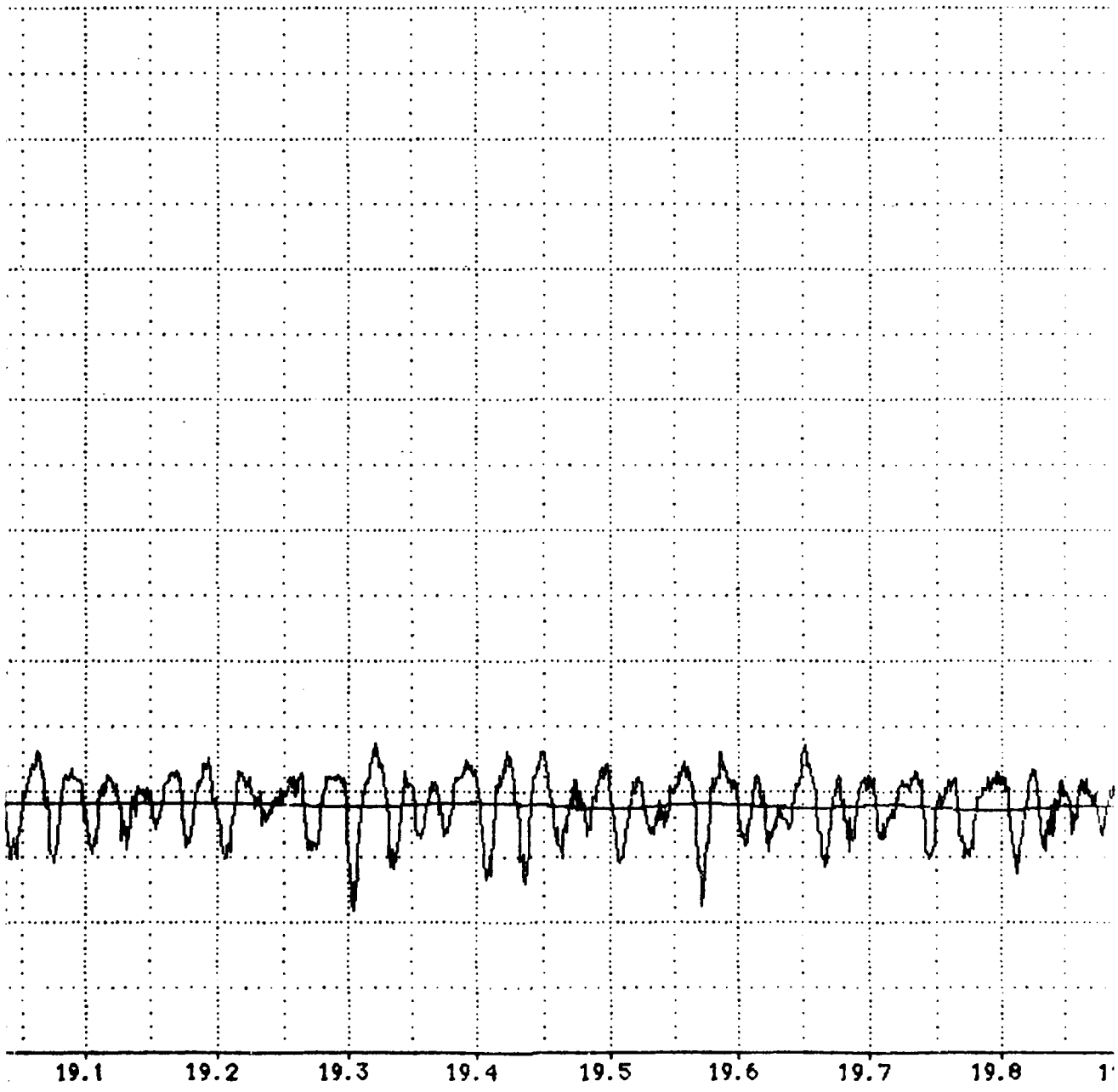
19.1
19.2
19.3
19.4
19.5
19.6
19.7
19.8

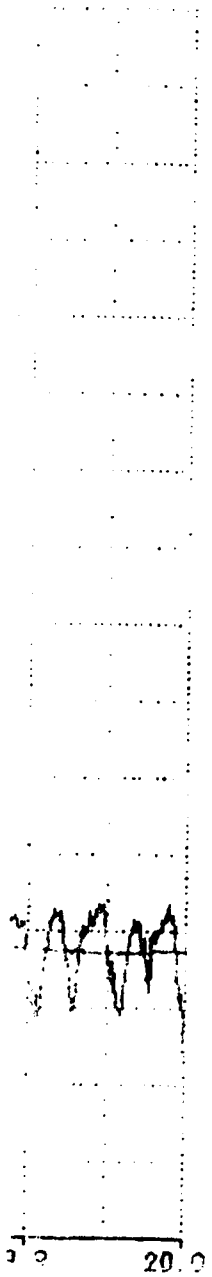
20.0

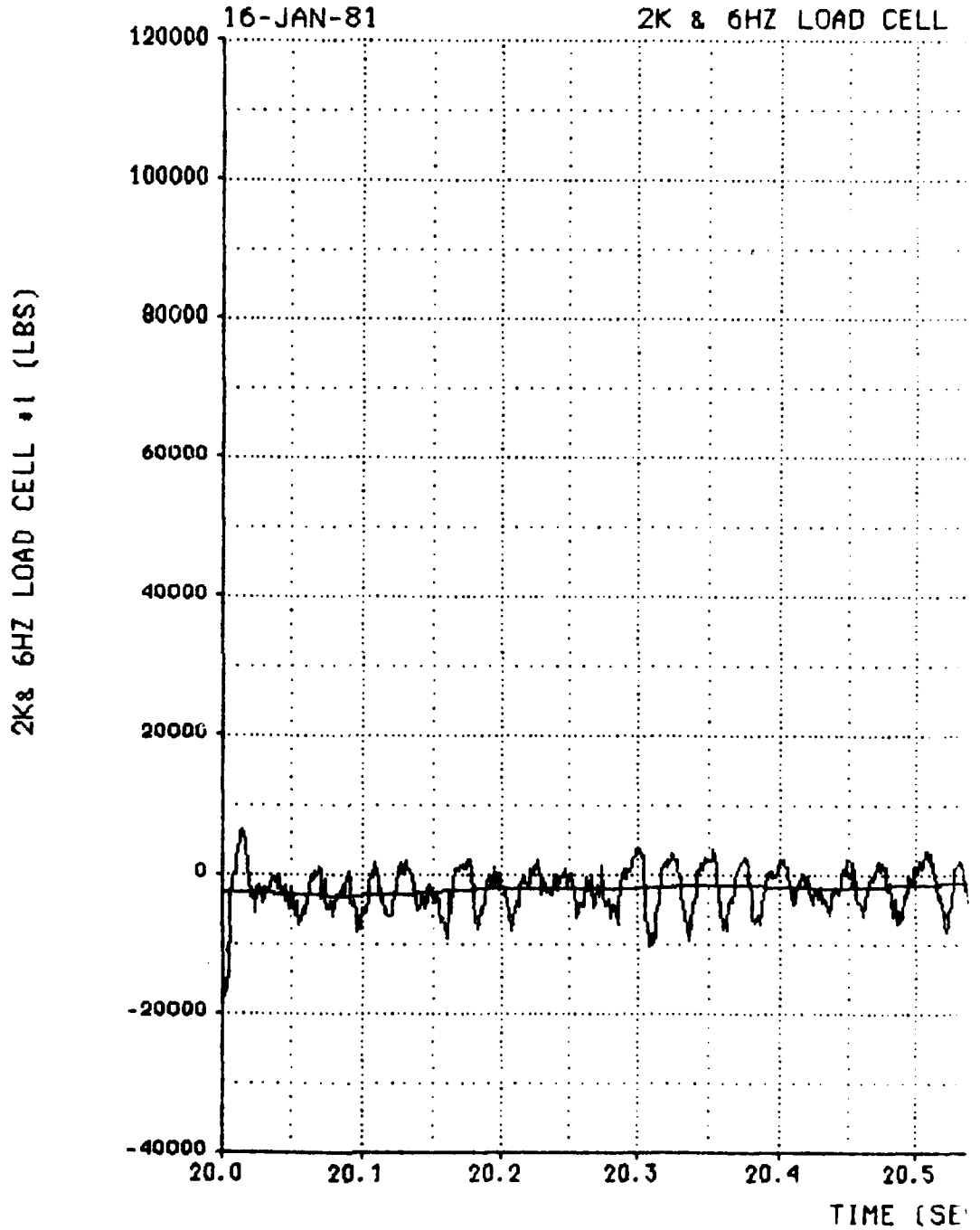
16-JAN-81
2K & 6HZ LOAD CELL
120000
100000
80000
60000
40000
20000
0
-20000
-40000
2K& 6HZ LOAD CELL #1 (LBS)
20.0
20.1
20.2
20.3
20.4
20.5
TIME (SE

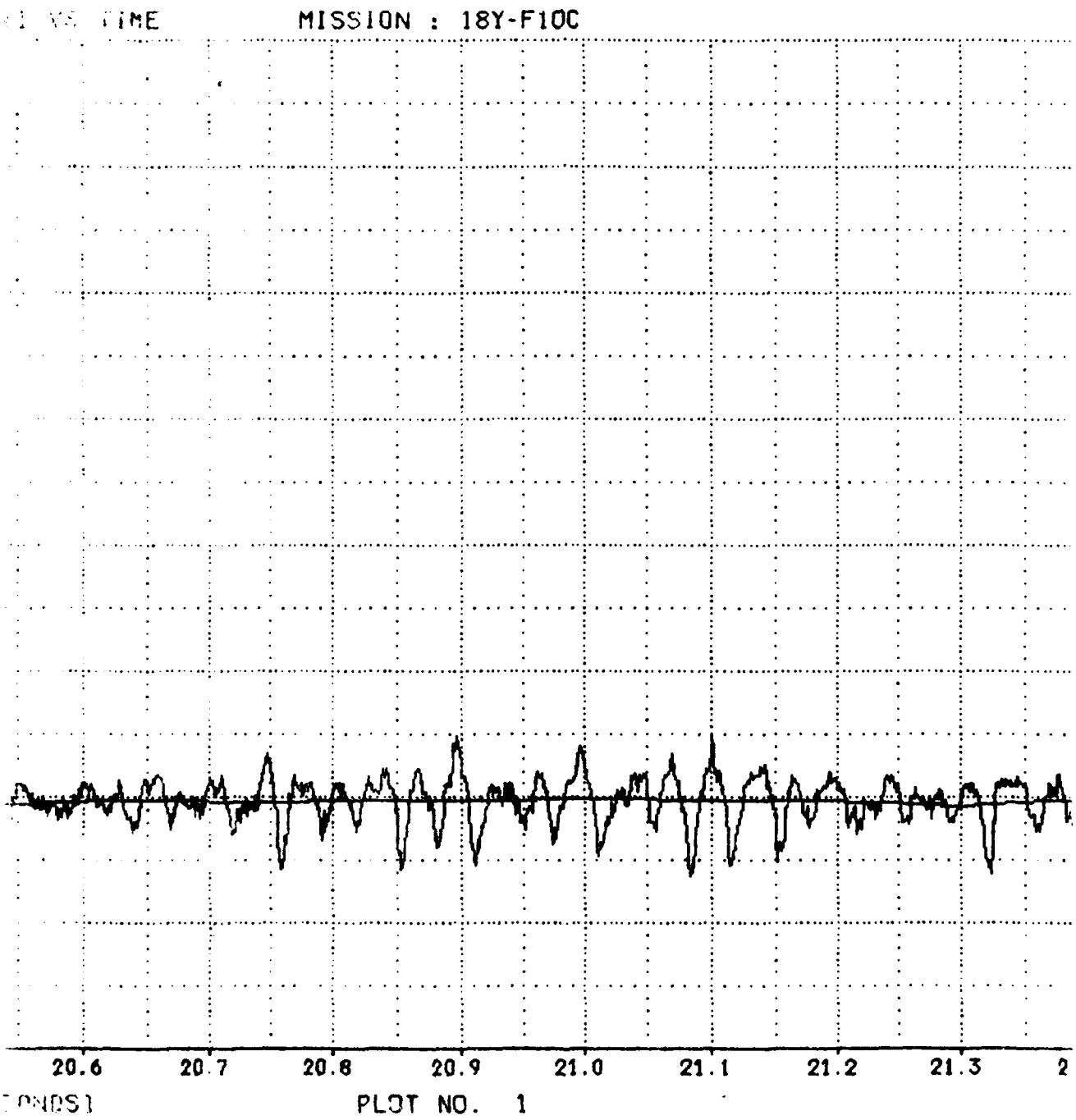
MISSION : 18Y-F10C
20.6
20.7
20.8
20.9
21.0
21.1
21.2
21.3
PLOT NO. 1

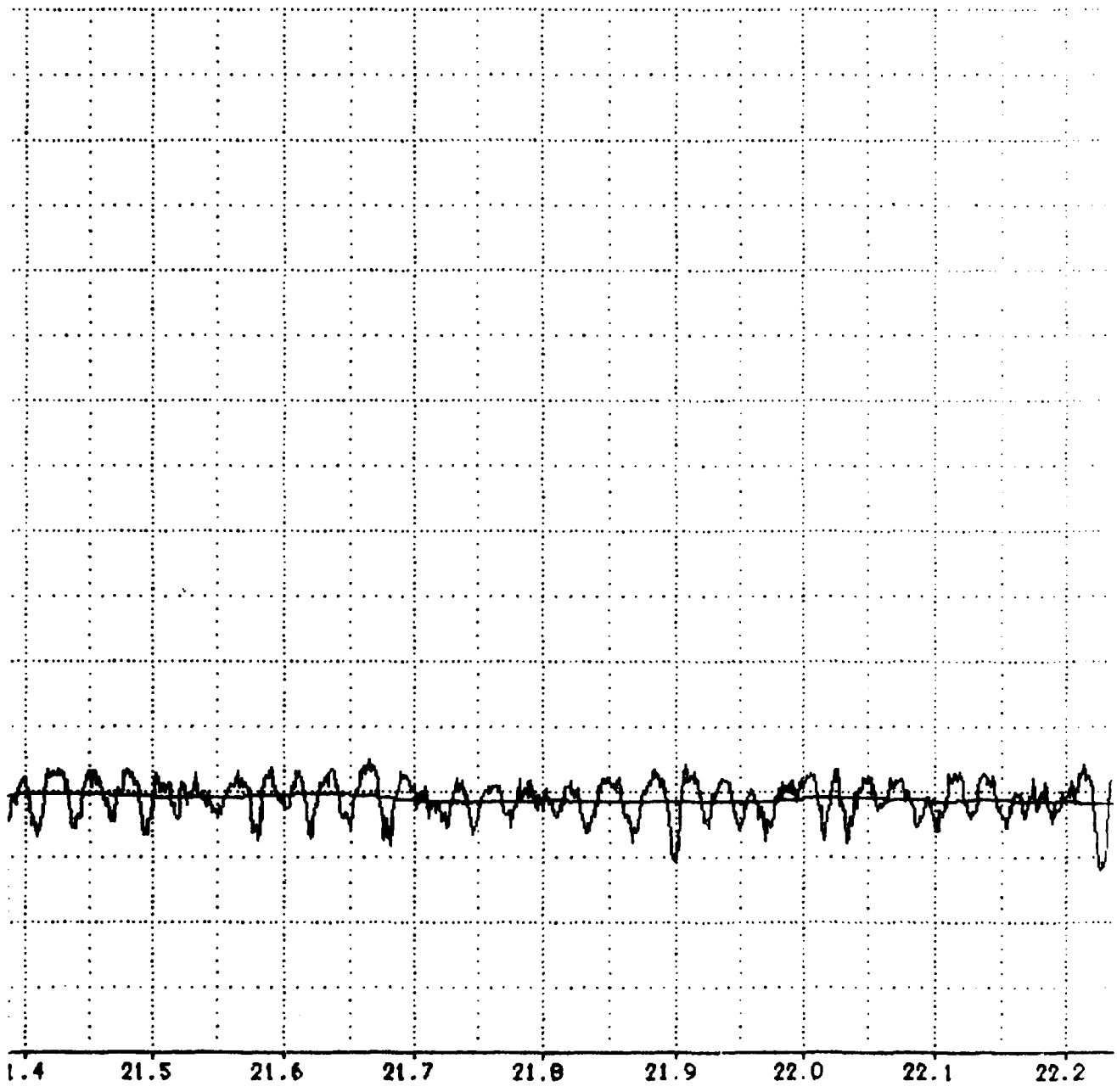
1.4
21.5
21.6
21.7
21.8
21.9
22.0
22.1
22.2

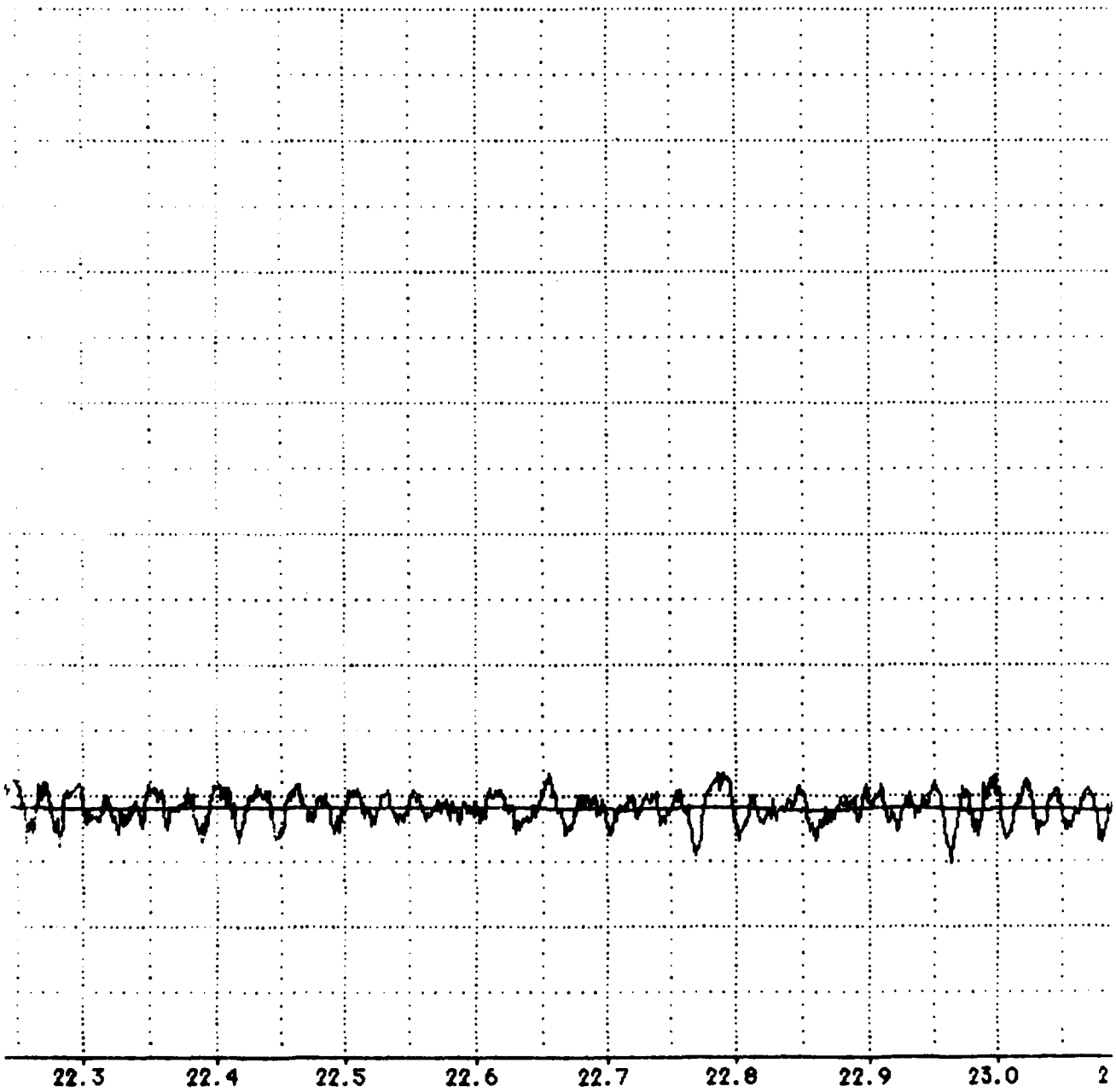
22.3
22.4
22.5
22.6
22.7
22.8
22.9
23.0

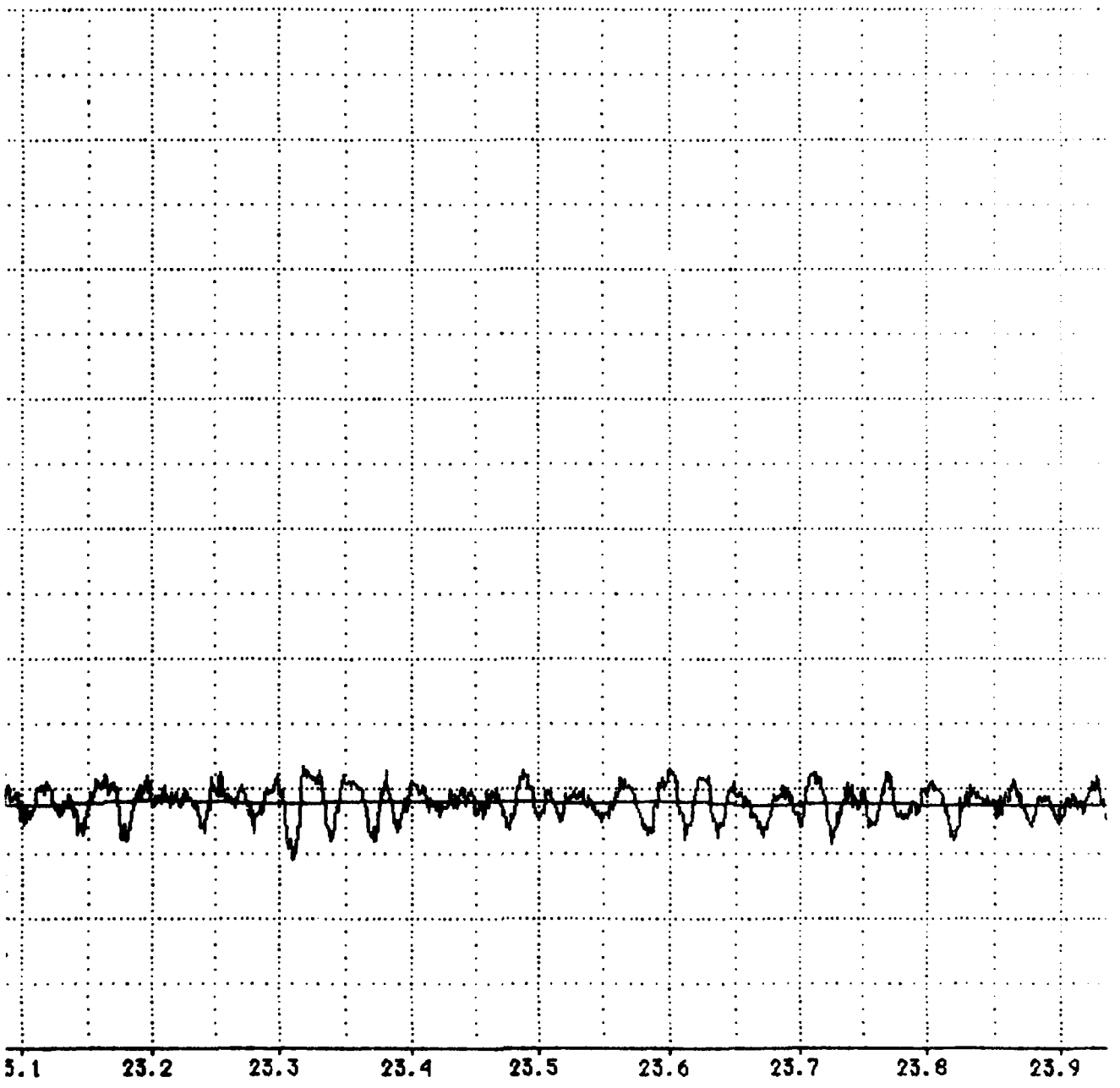
5.1
23.2
23.3
23.4
23.5
23.6
23.7
23.8
23.9

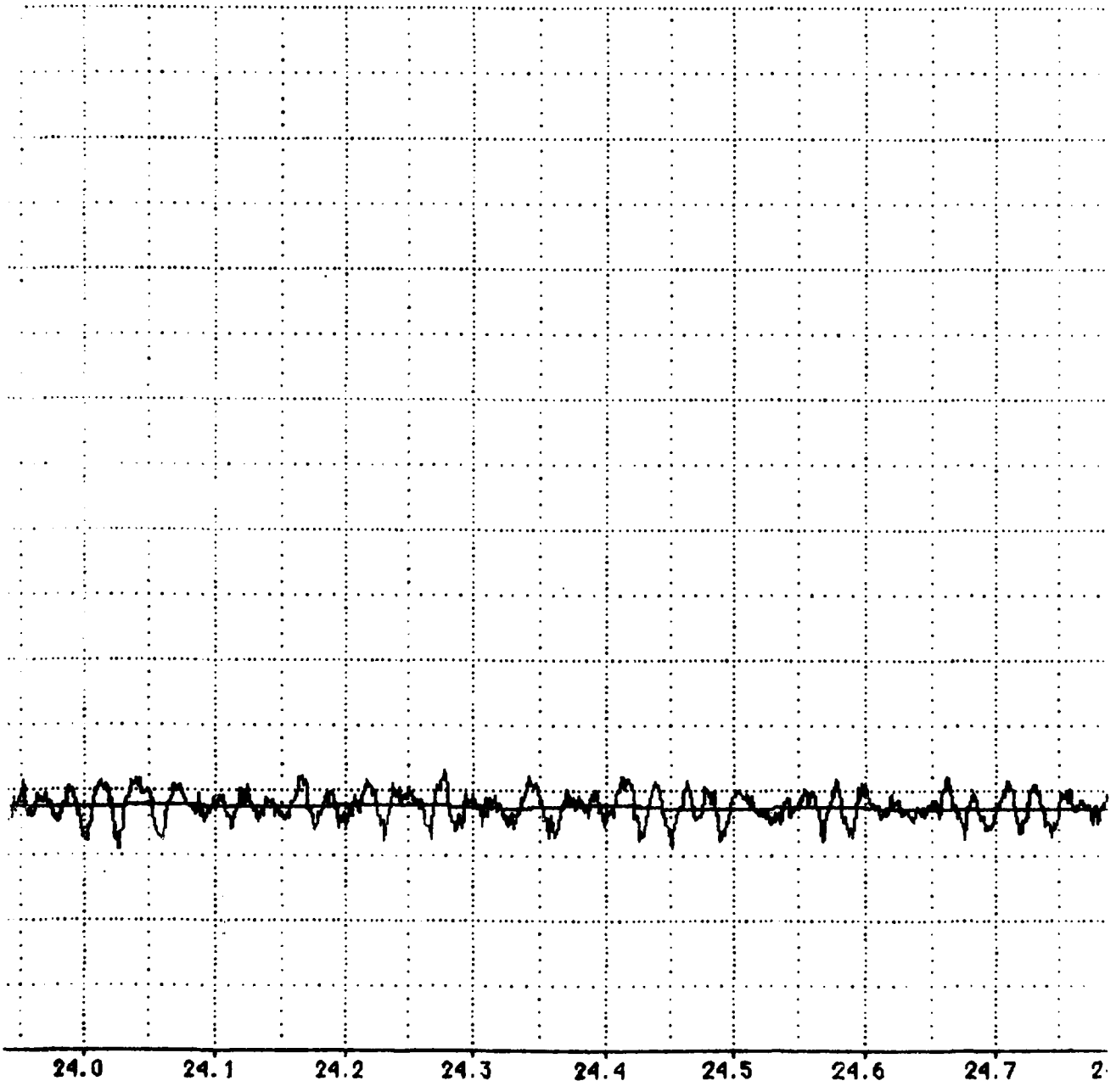
24.0
24.1
24.2
24.3
24.4
24.5
24.6
24.7
2

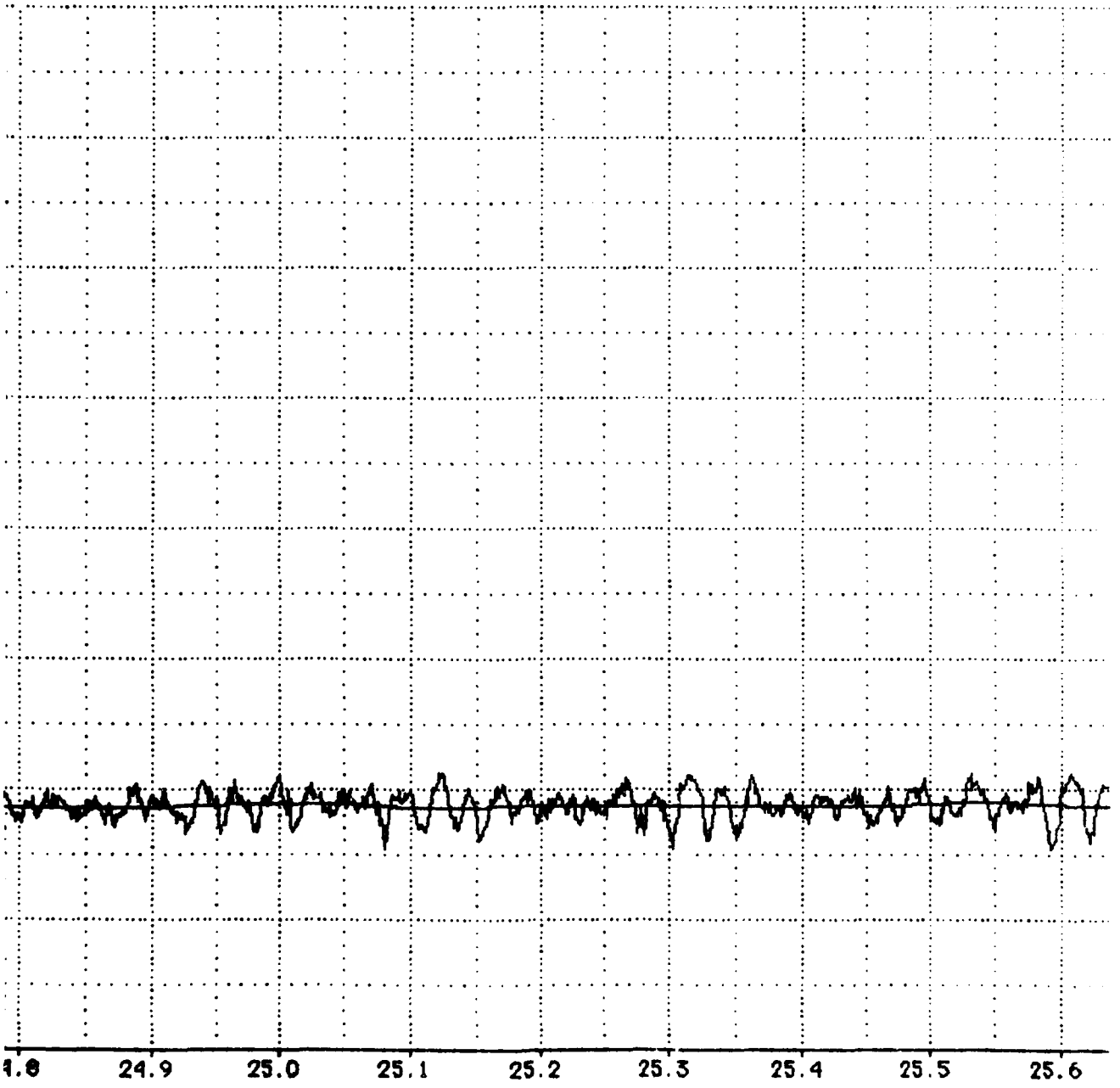
4.8
24.9
25.0
25.1
25.2
25.3
25.4
25.5
25.6

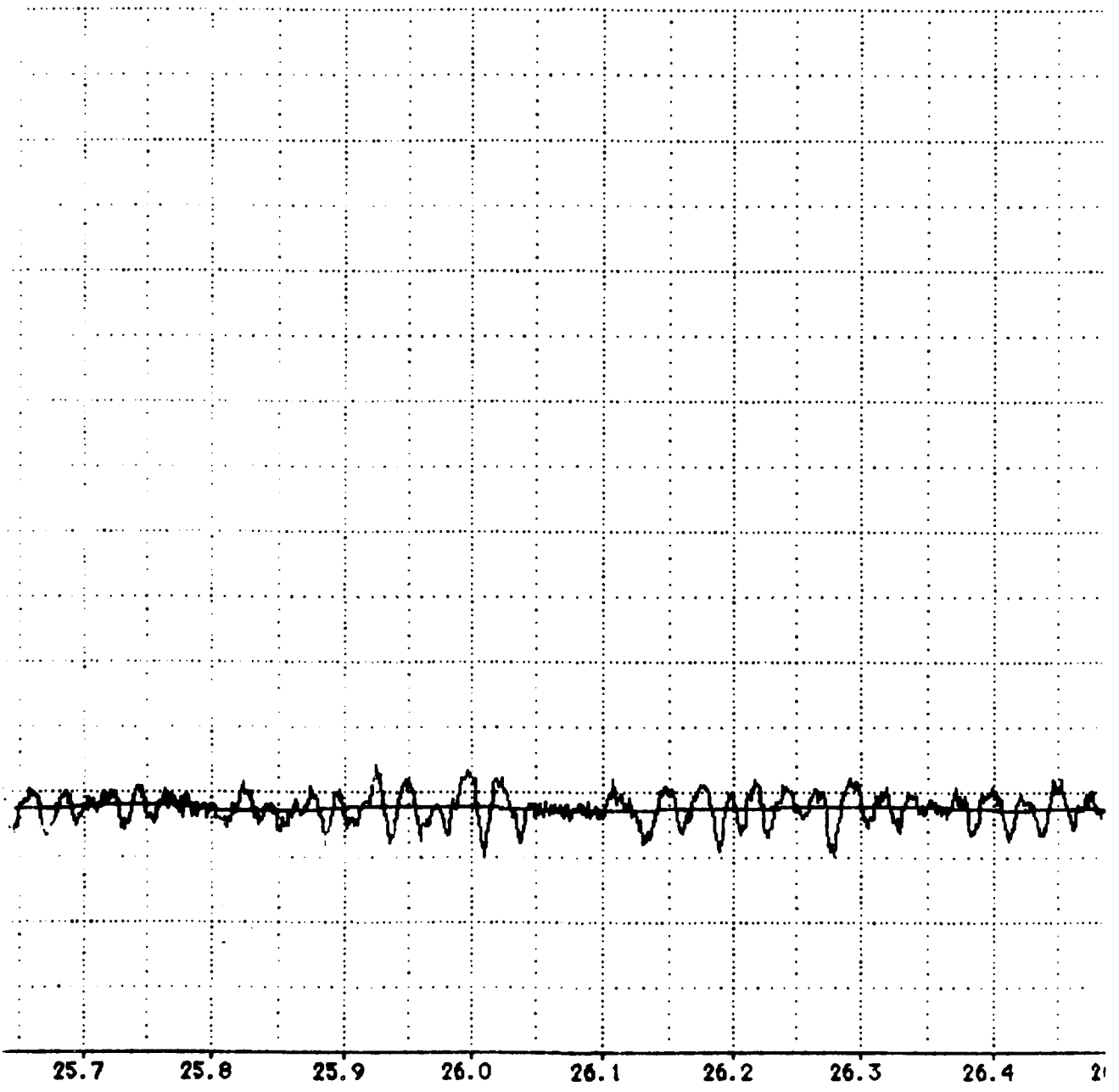
25.7
25.8
25.9
26.0
26.1
26.2
26.3
26.4

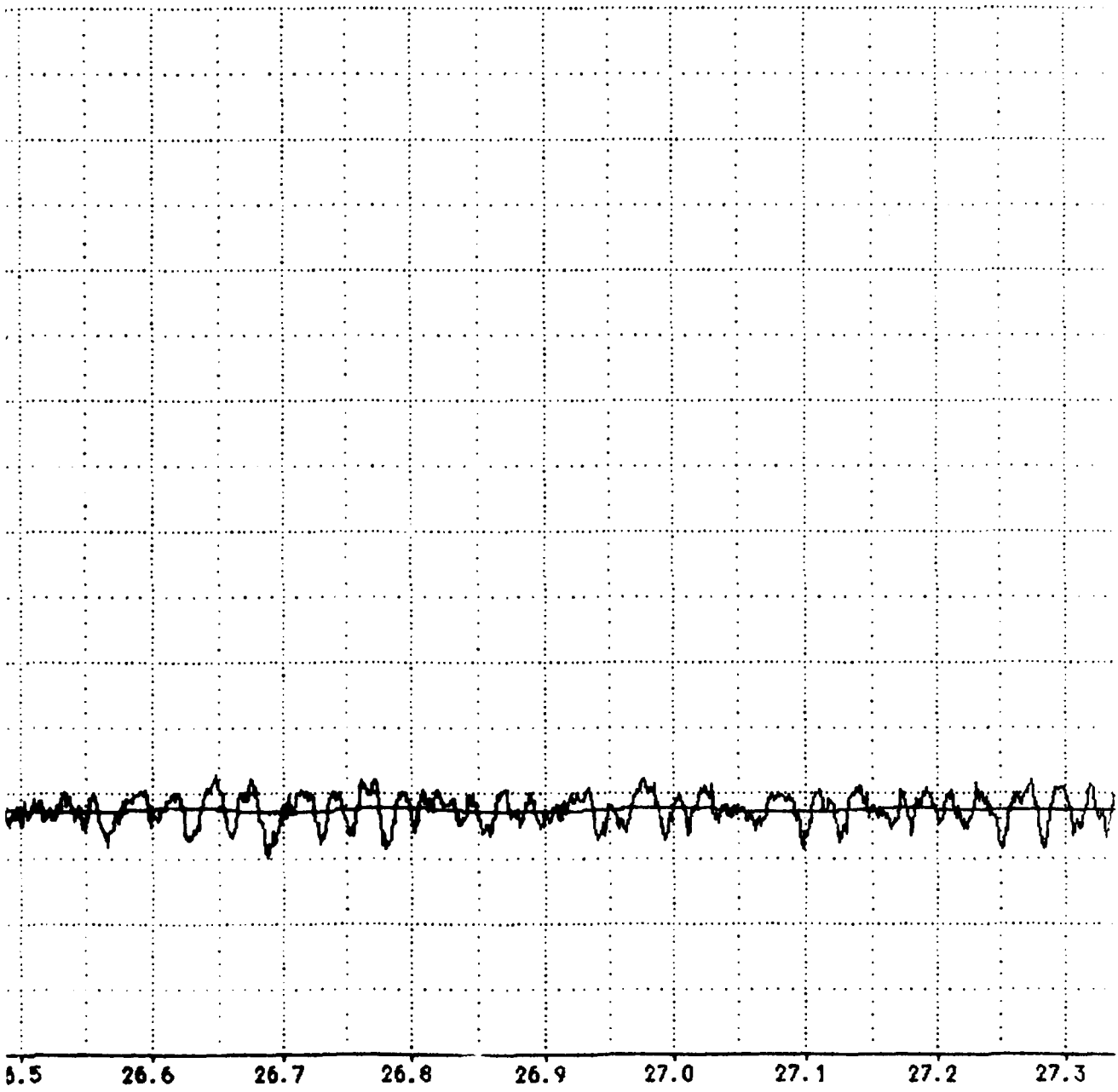
6.5
26.6
26.7
26.8
26.9
27.0
27.1
27.2
27.3

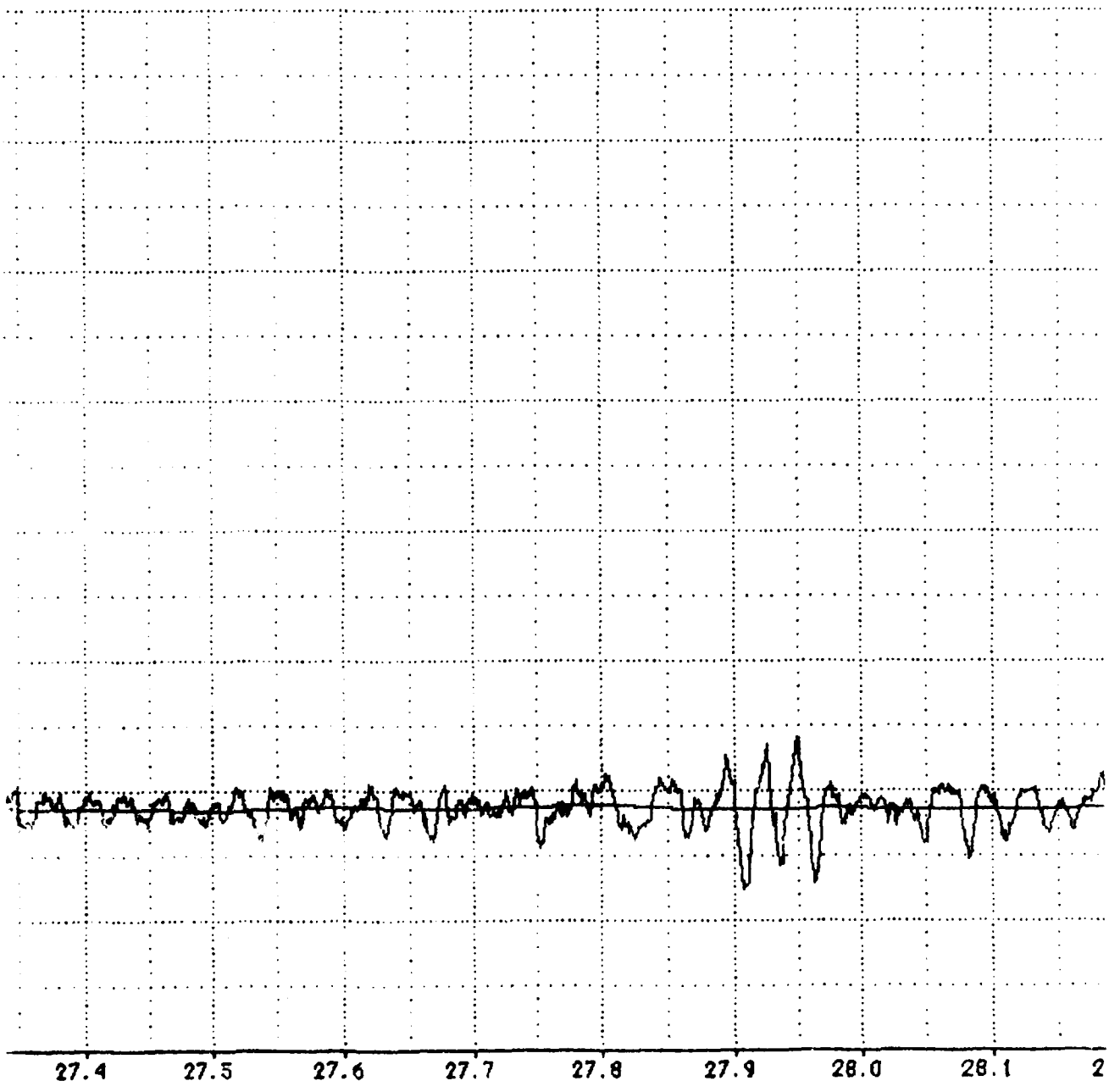
27.4
27.5
27.6
27.7
27.8
27.9
28.0
28.1
2

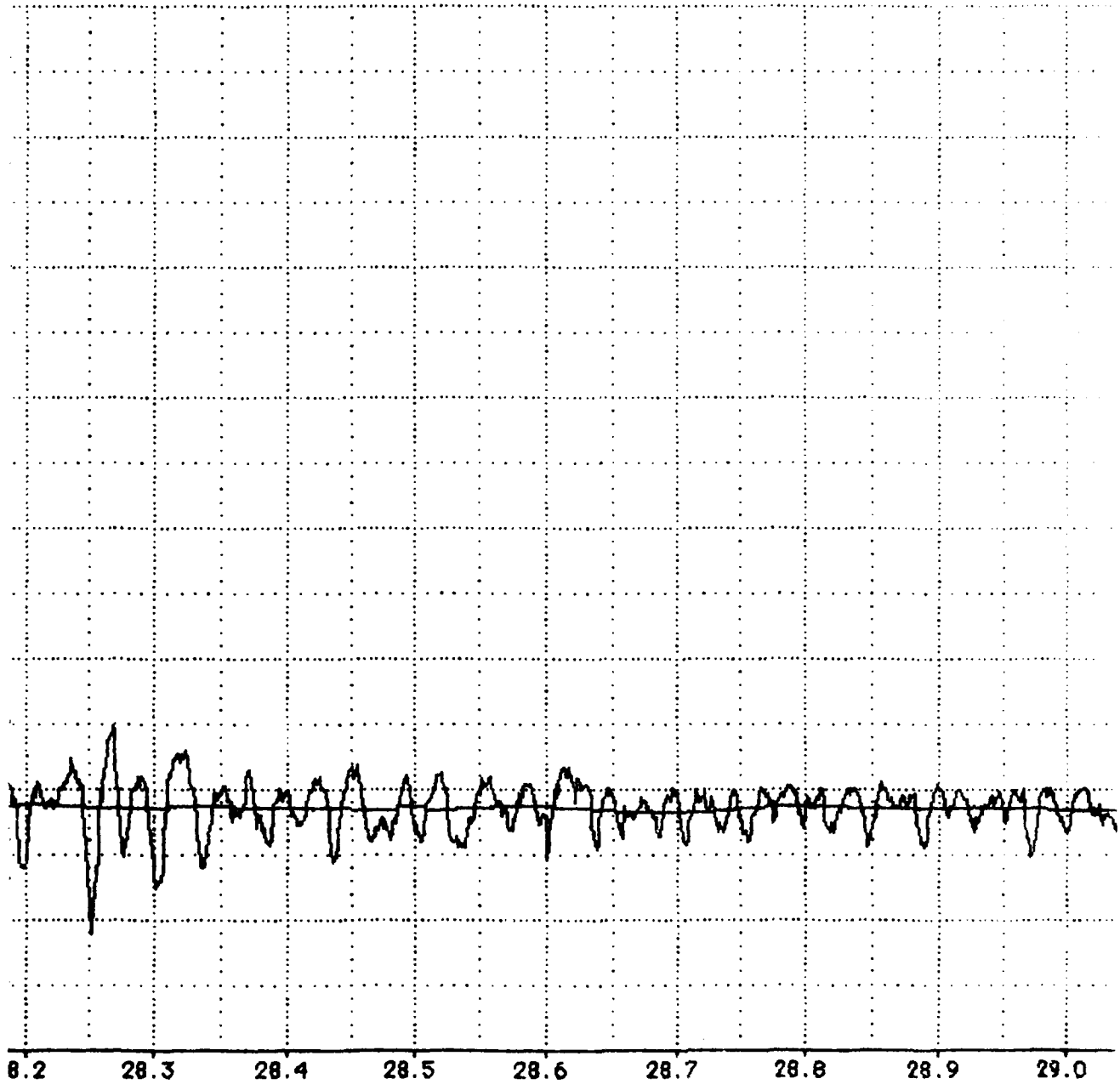
8.2
28.3
28.4
28.5
28.6
28.7
28.8
28.9
29.0

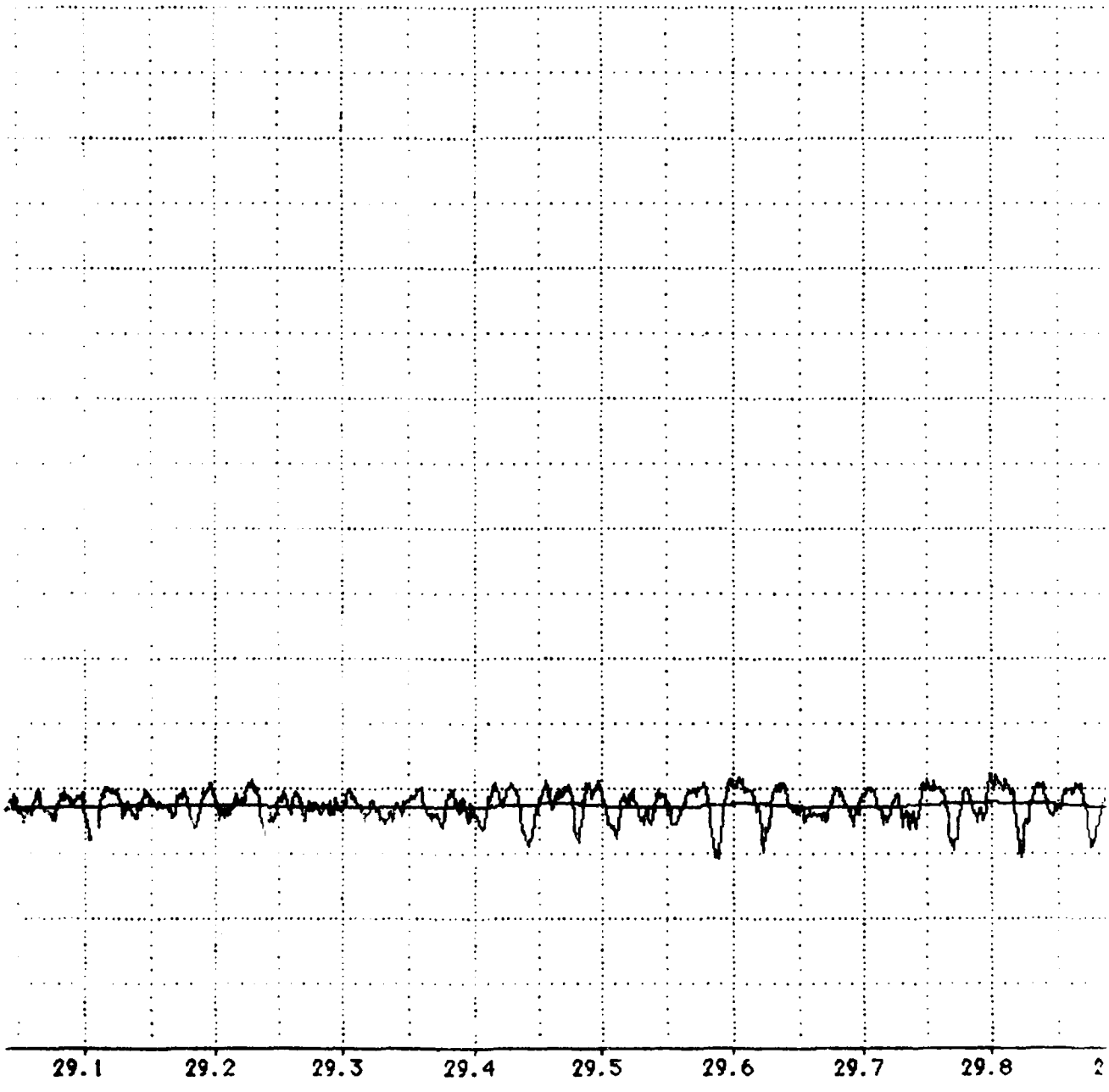
29.1
29.2
29.3
29.4
29.5
29.6
29.7
29.8

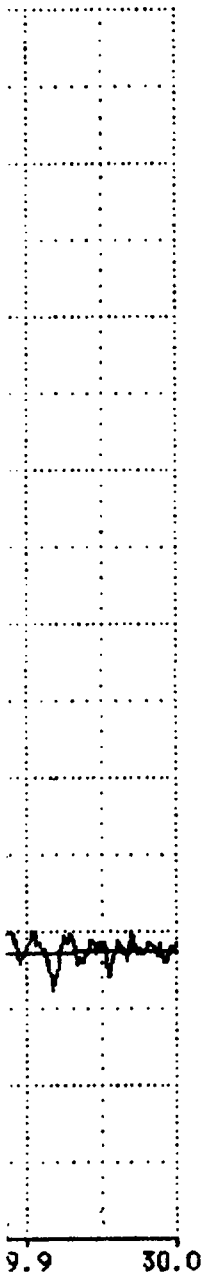
9.9
30.0

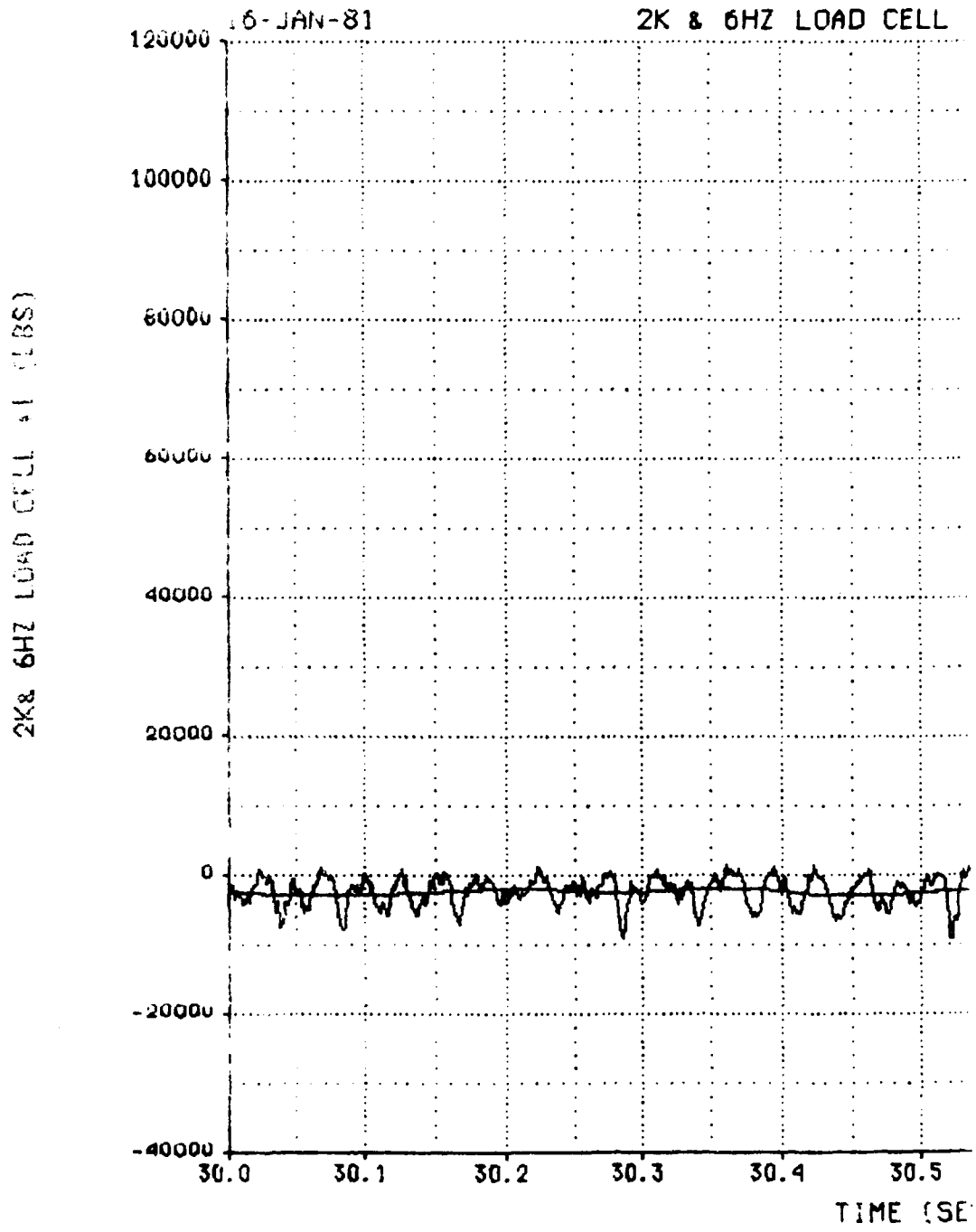
16-JAN-81
2K & 6HZ LOAD CELL
120000
100000
80000
60000
40000
20000
0
-20000
-40000
30.0
30.1
30.2
30.3
30.4
30.5
TIME (SE
2K& 6HZ LOAD CELL

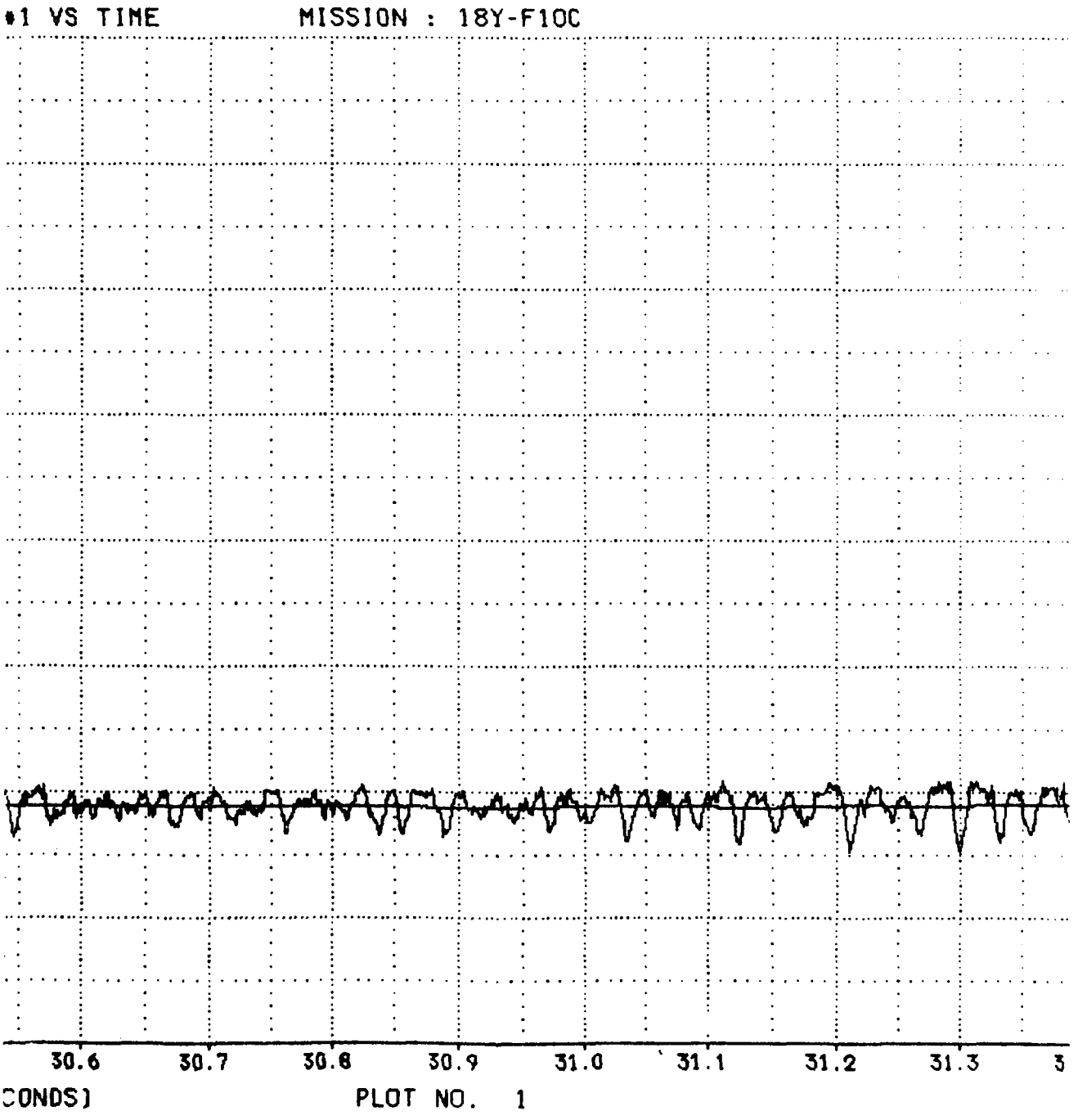
#1 VS TIME
MISSION : 18Y-F10C
30.6
30.7
30.8
30.9
31.0
31.1
31.2
31.3
CONDS)
PLOT NO. 1

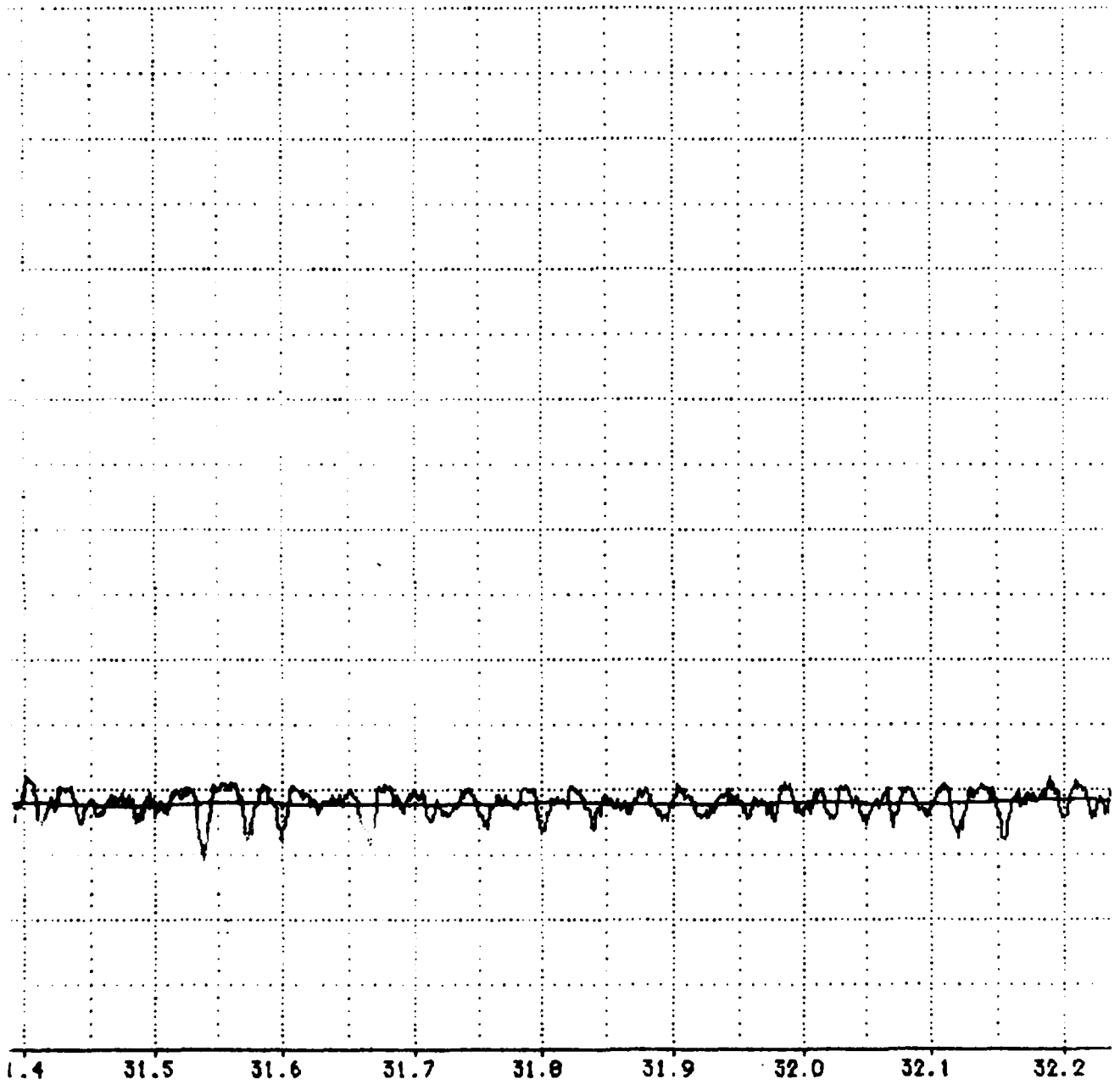
1.4
31.5
31.6
31.7
31.8
31.9
32.0
32.1
32.2

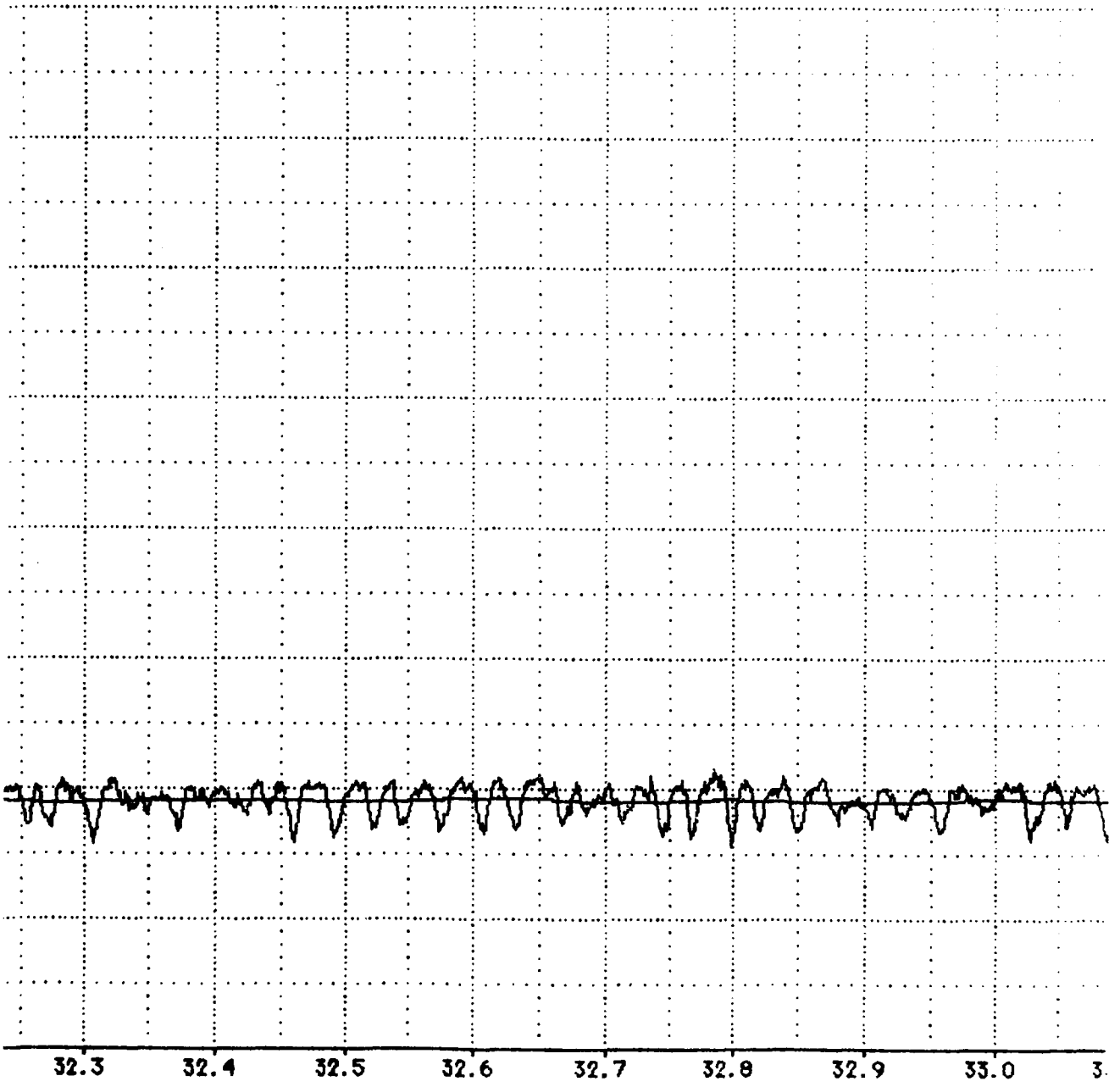
32.3
32.4
32.5
32.6
32.7
32.8
32.9
33.0

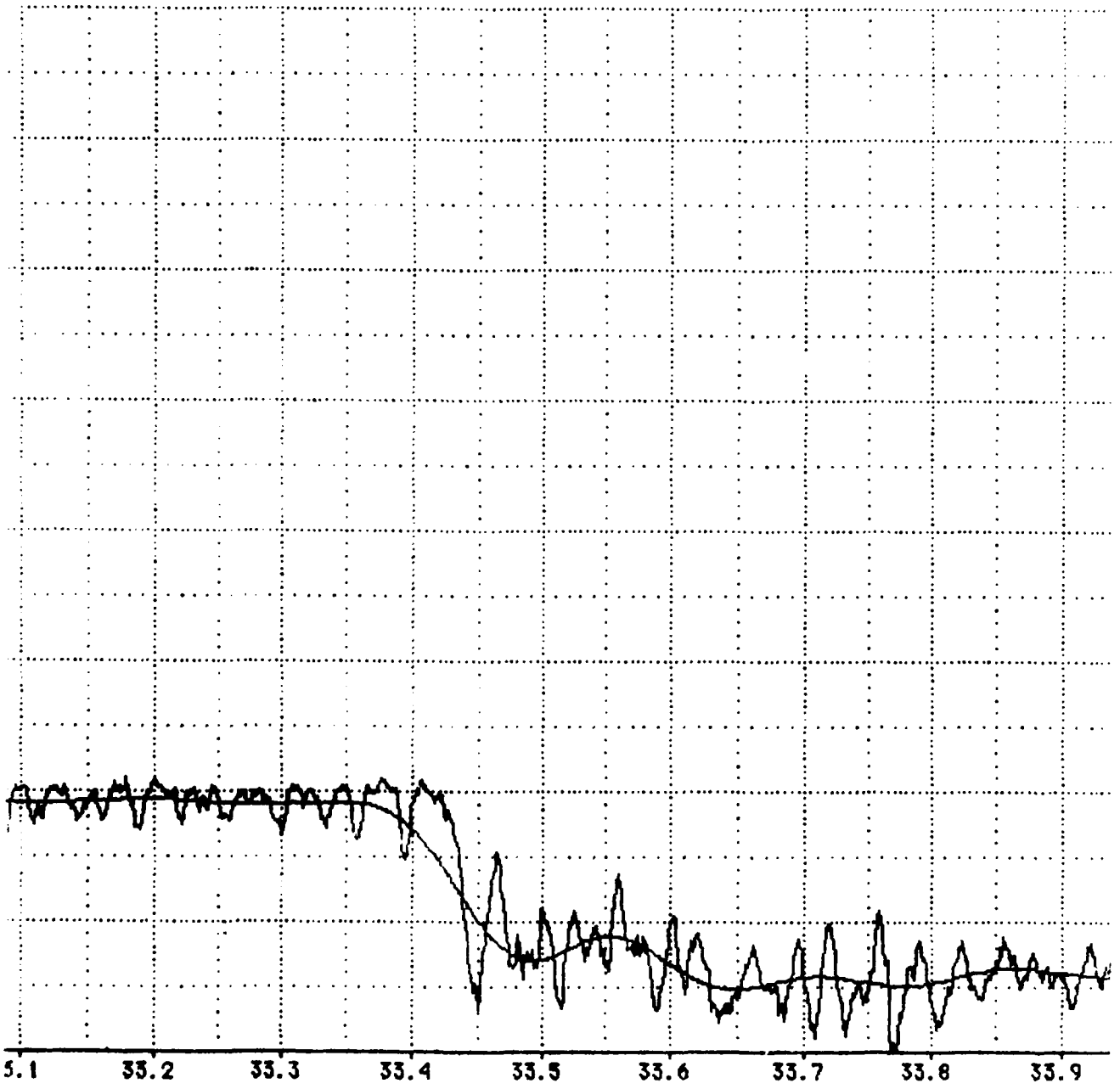
5.1
33.2
33.3
33.4
33.5
33.6
33.7
33.8
33.9

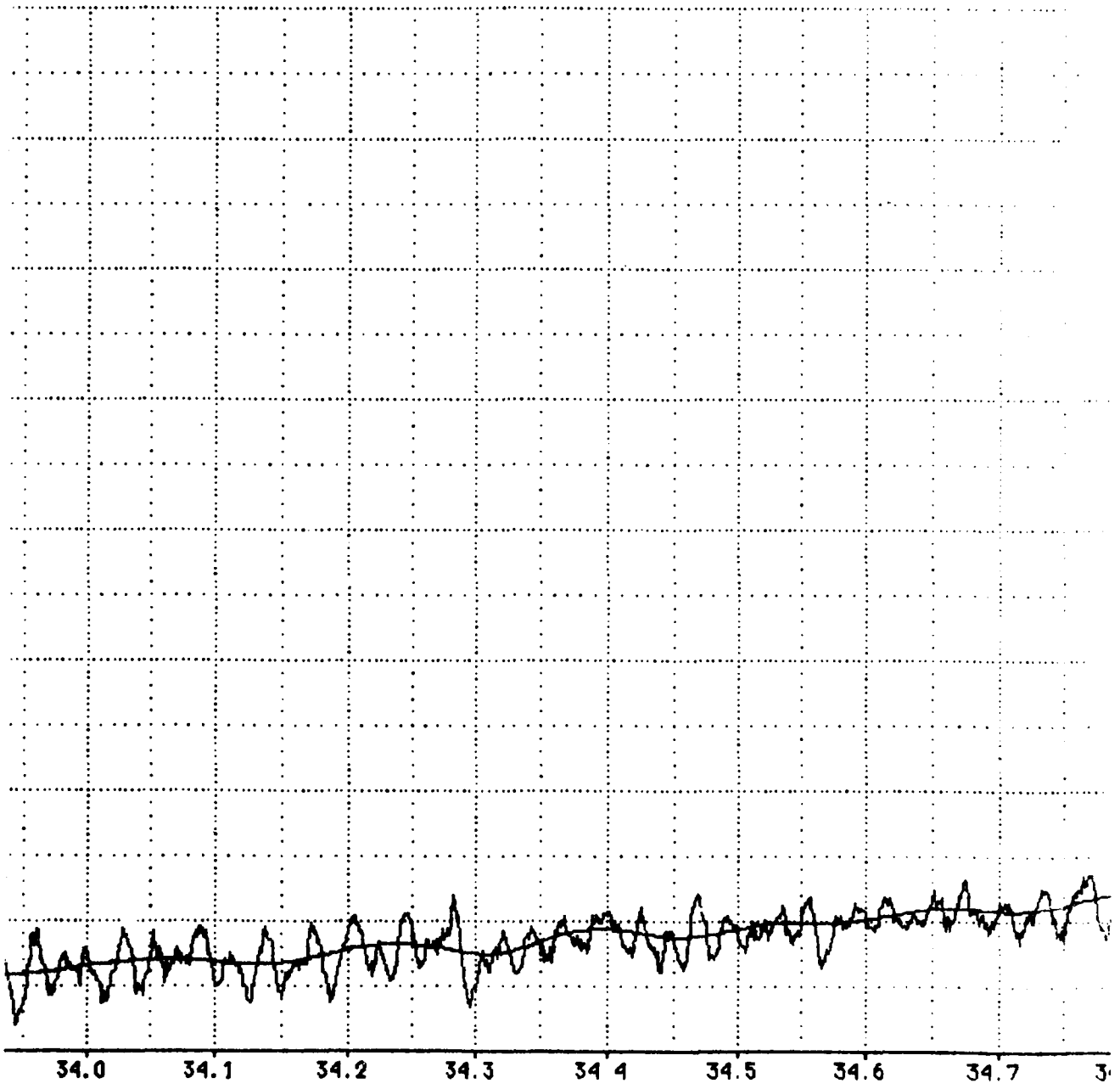
34.0
34.1
34.2
34.3
34 4
34.5
34.6
34.7

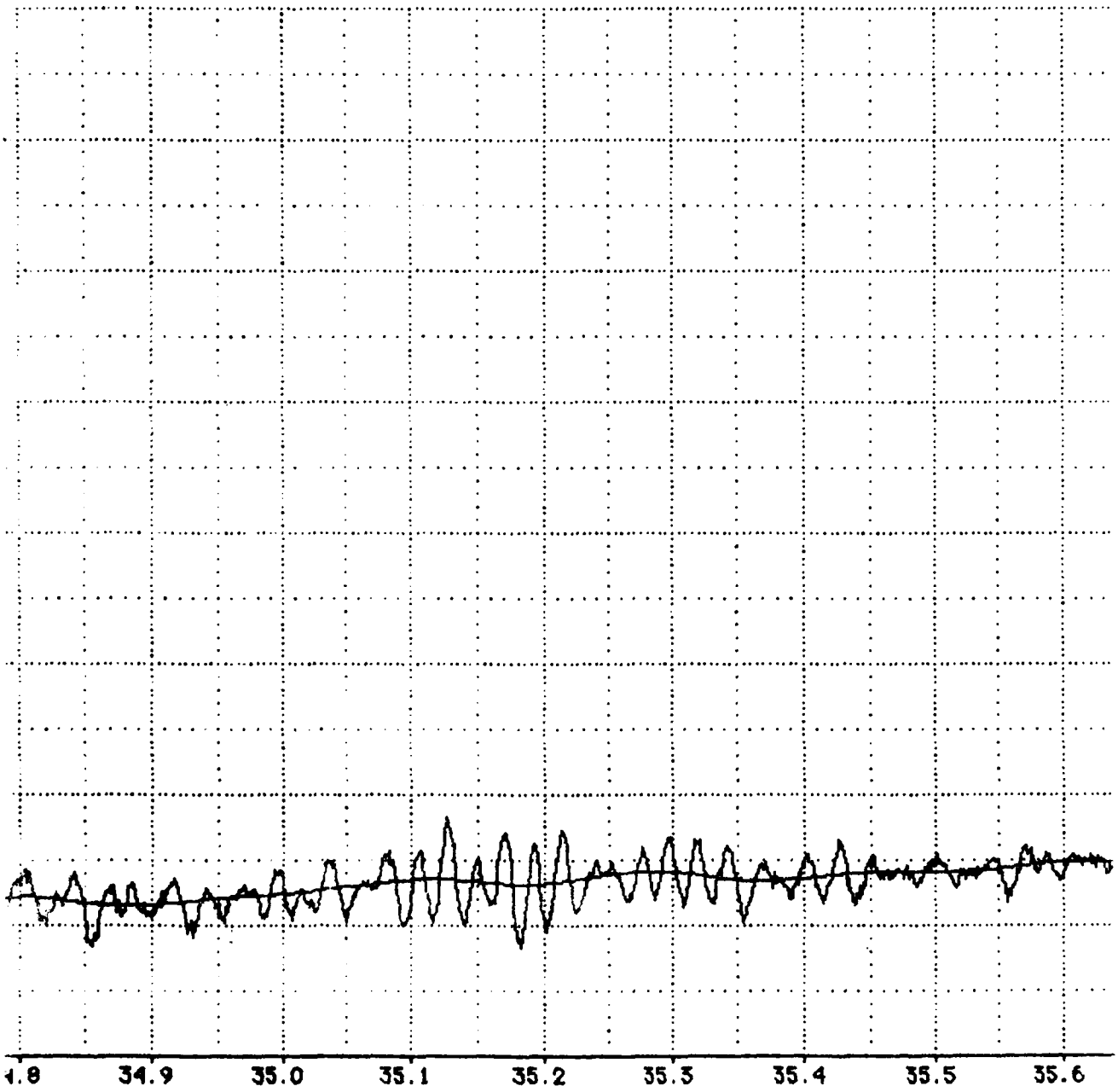
4.8
34.9
35.0
35.1
35.2
35.3
35.4
35.5
35.6

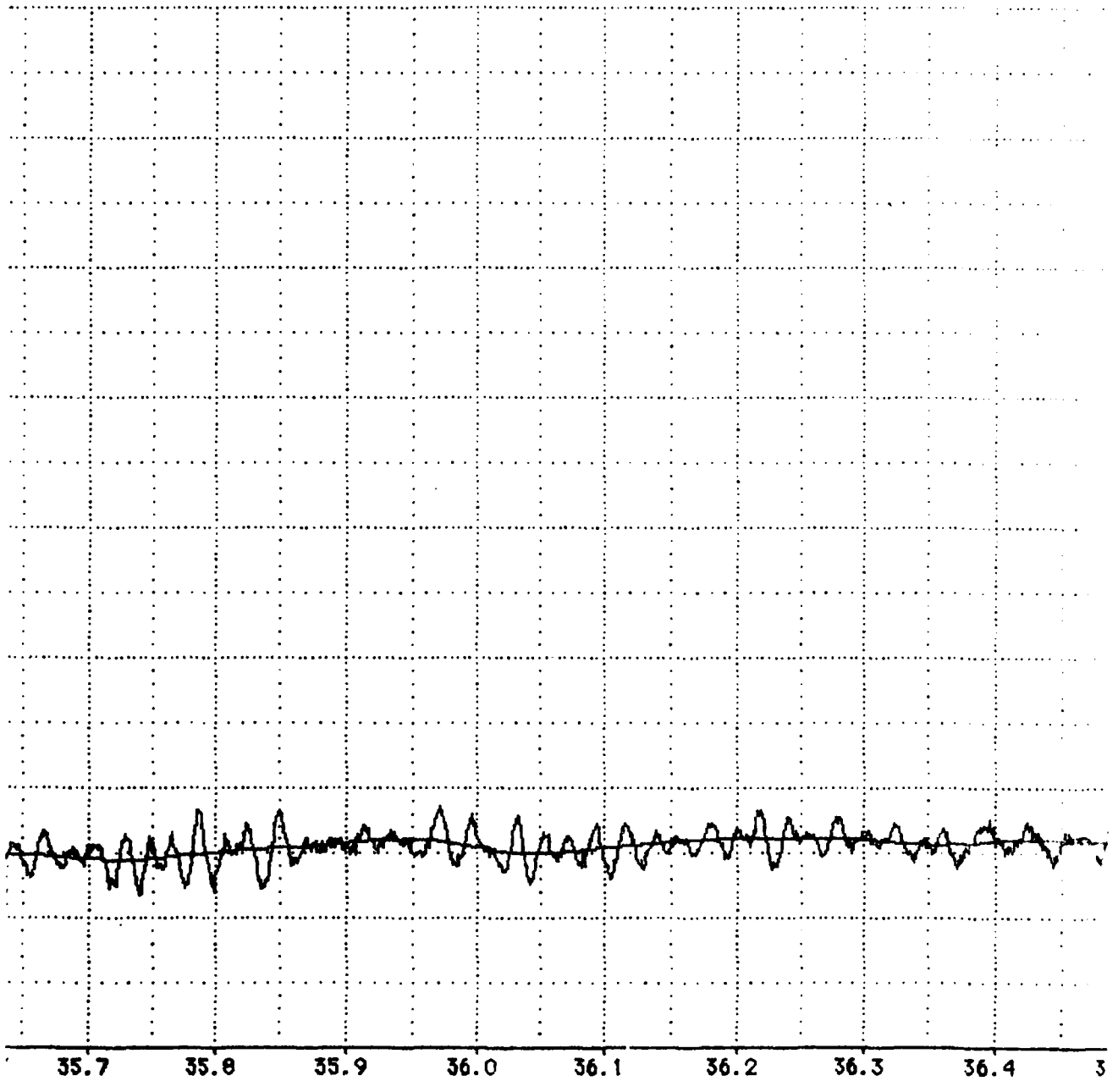
35.7
35.8
35.9
36.0
36.1
36.2
36.3
36.4

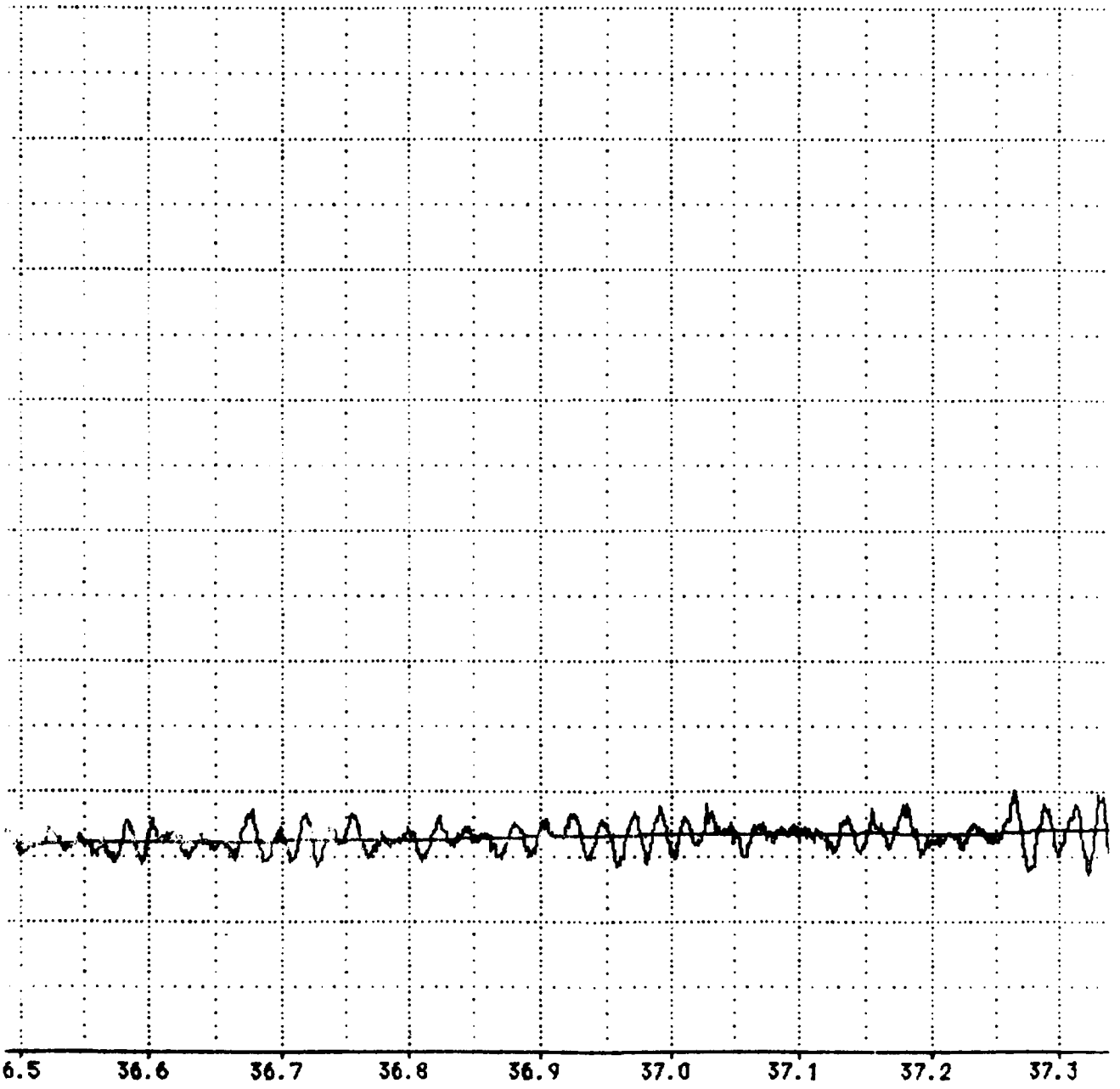
6.5
36.6
36.7
36.8
36.9
37.0
37.1
37.2
37.3

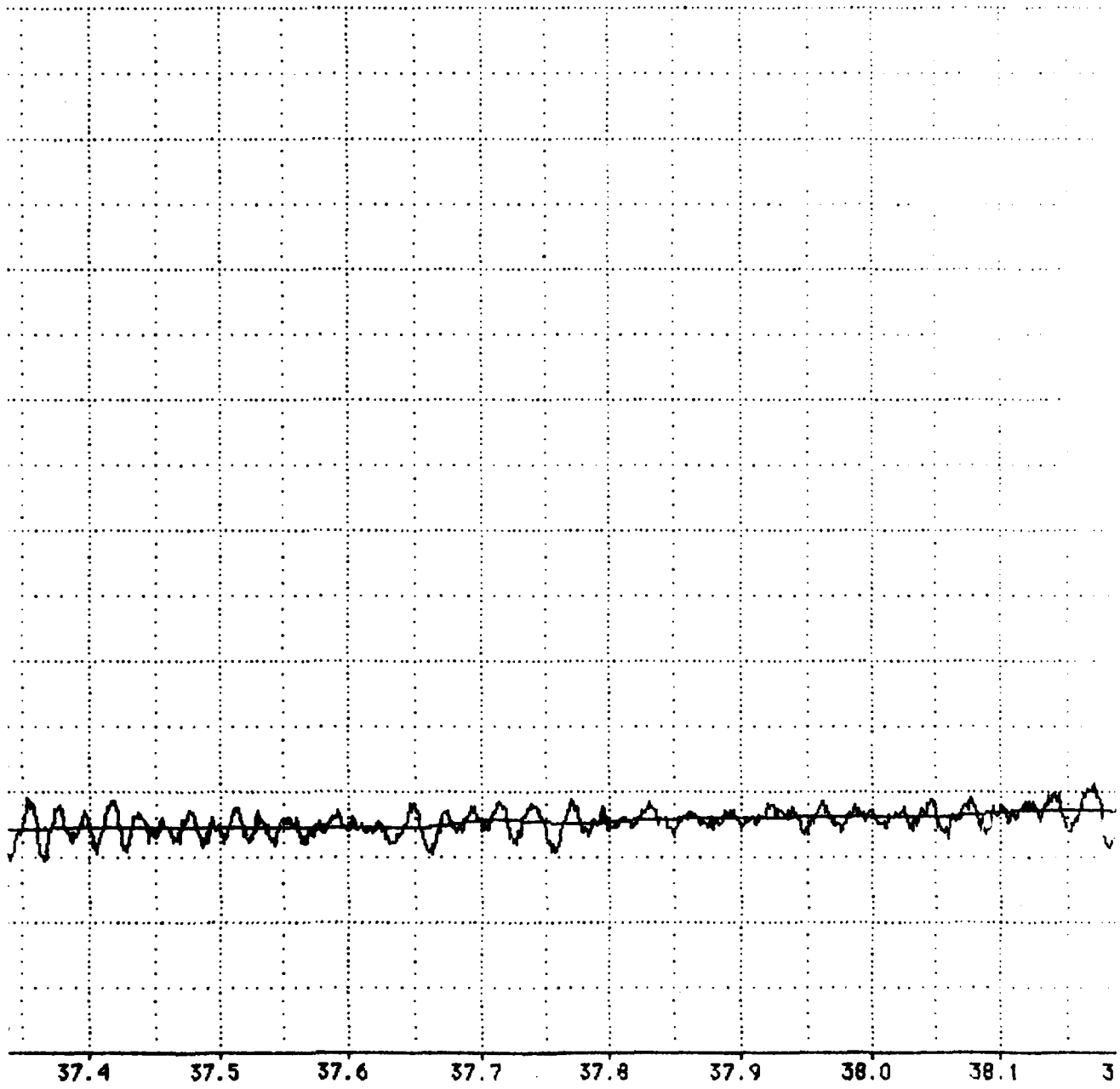
37.4
37.5
37.6
37.7
37.8
37.9
38.0
38.1
3

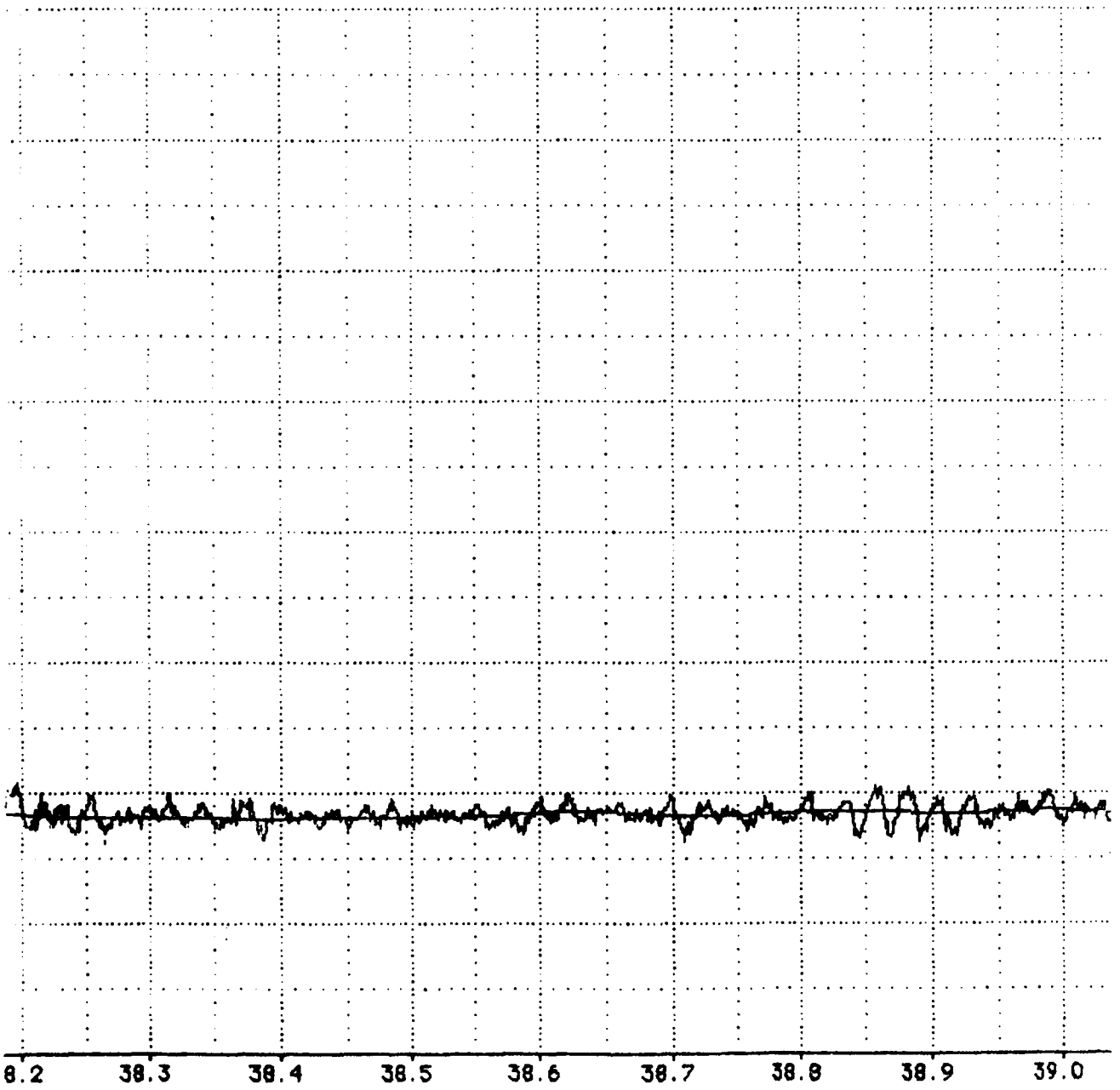
38.2
38.3
38.4
38.5
38.6
38.7
38.8
38.9
39.0

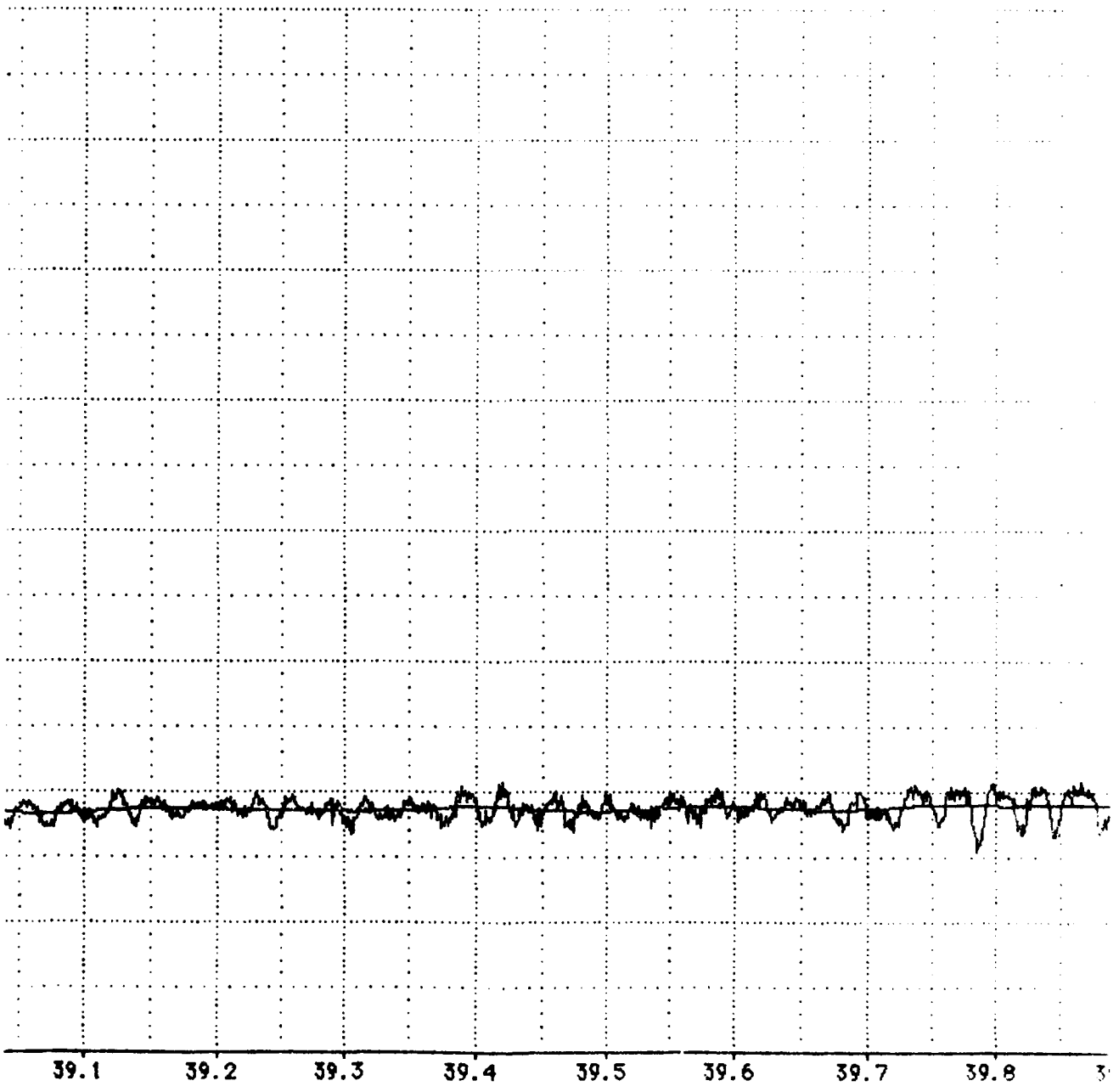
39.1
39.2
39.3
39.4
39.5
39.6
39.7
39.8

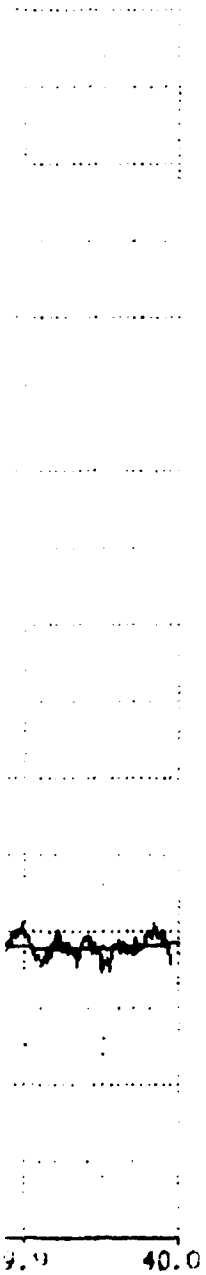
40.0

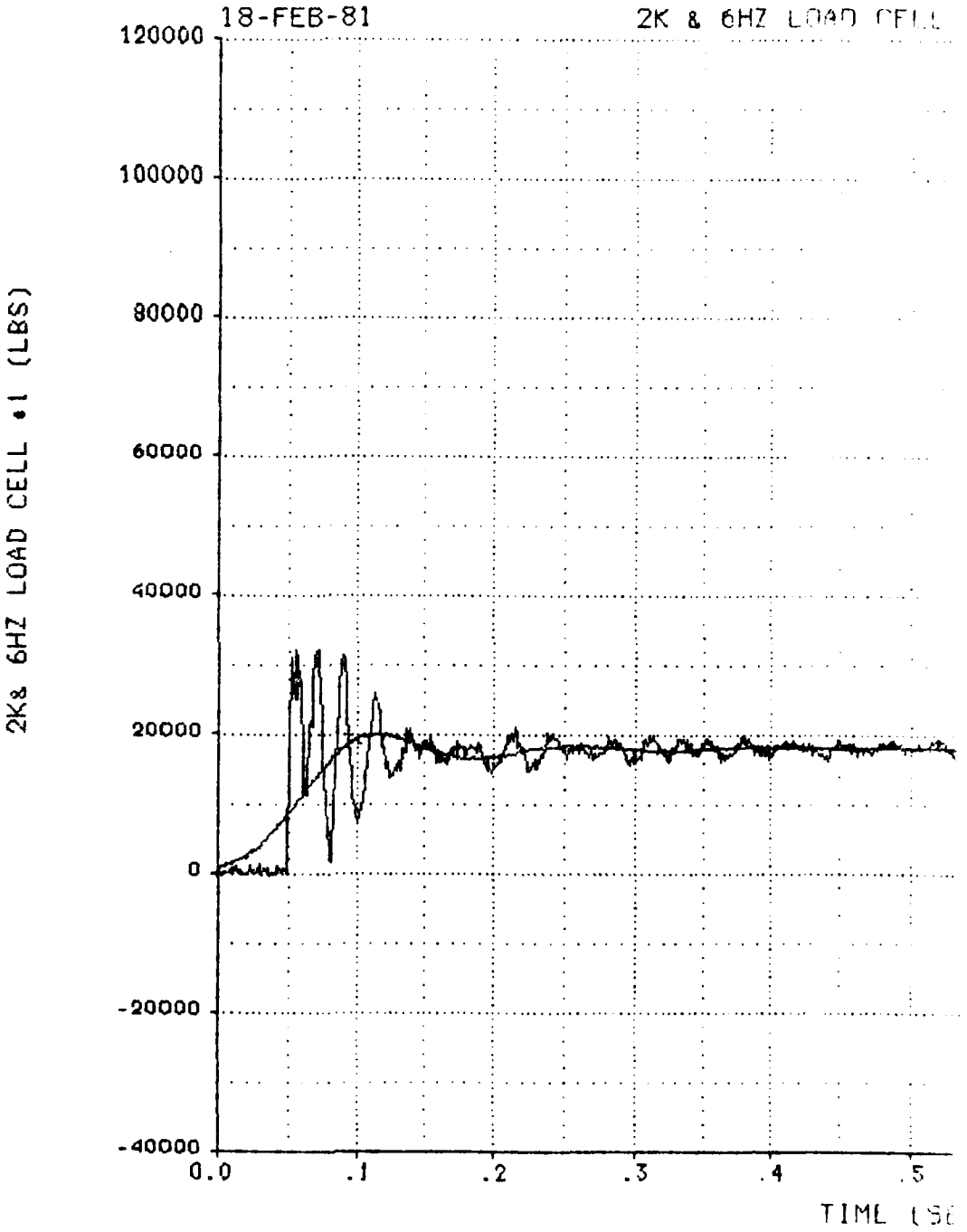
18-FEB-81
2K & 6HZ LOAD CELL
120000
100000
80000
60000
40000
20000
0
-20000
-40000
0.0
.1
.2
.3
.4
.5
2K& 6HZ LOAD CELL •1 (LBS)
TIME (SE

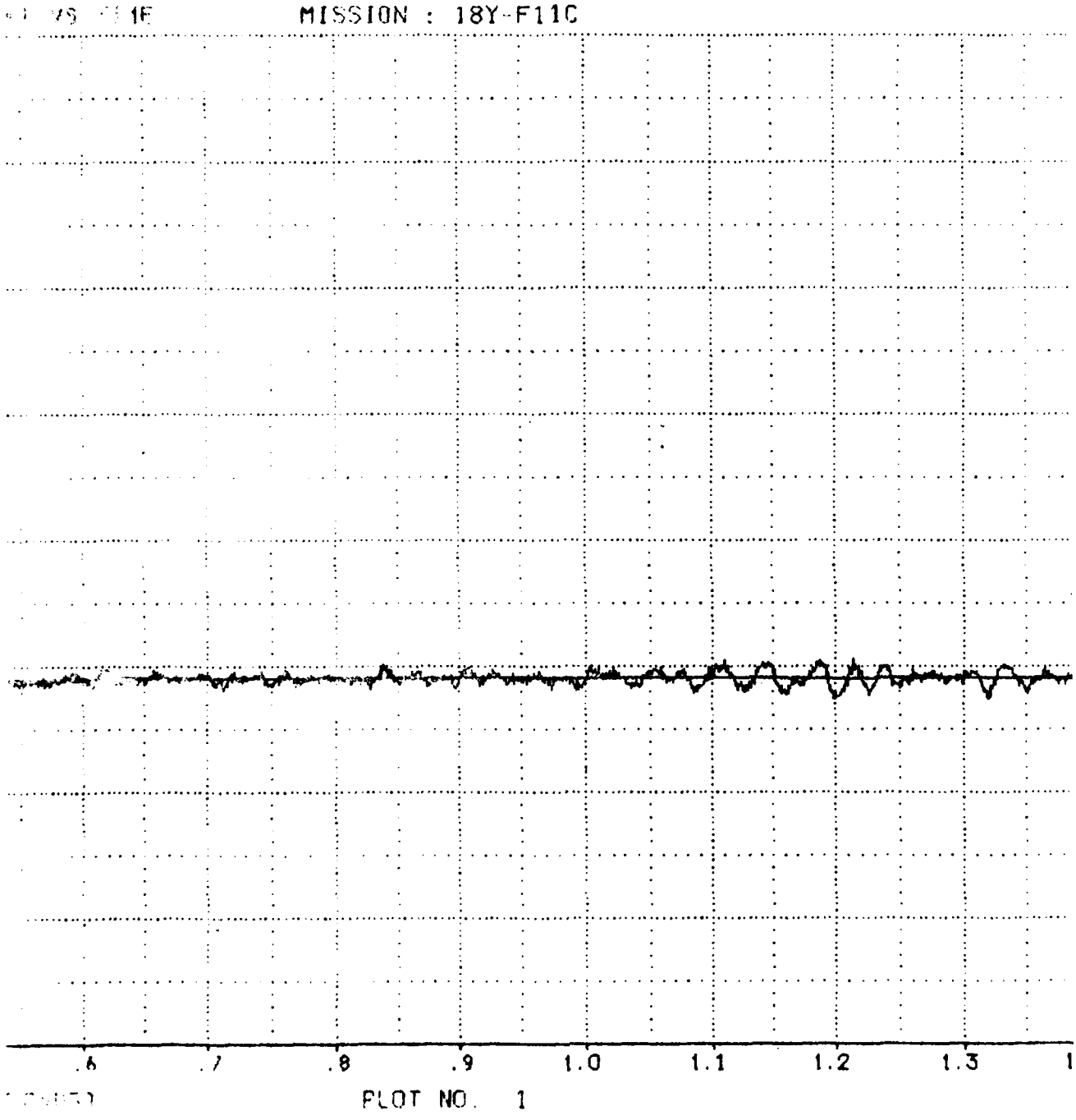
MISSION : 18Y-F11C
.6
.7
.8
.9
1.0
1.1
1.2
1.3
PLOT NO. 1

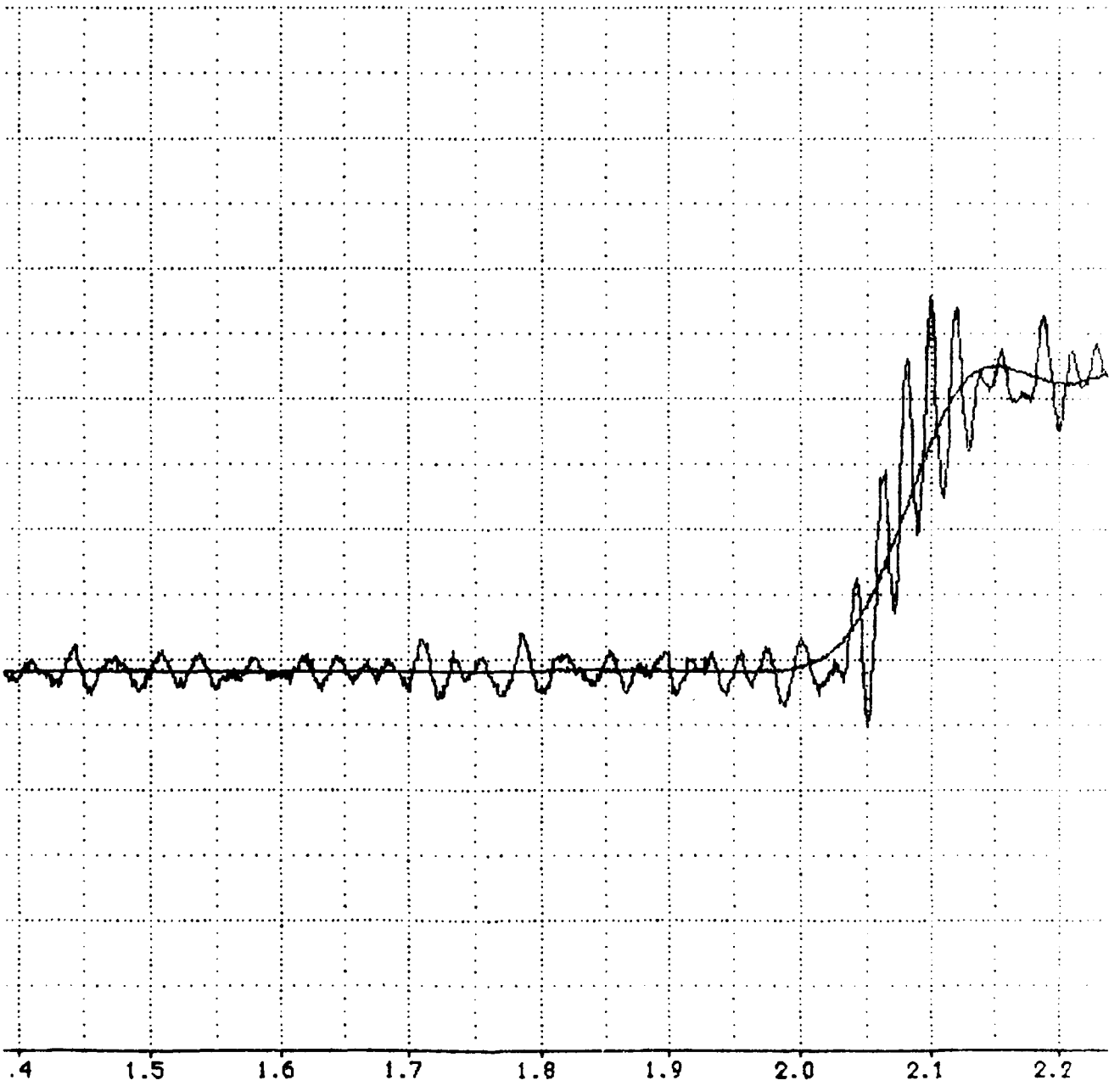
.4
1.5
1.6
1.7
1.8
1.9
2.0
2.1
2.2

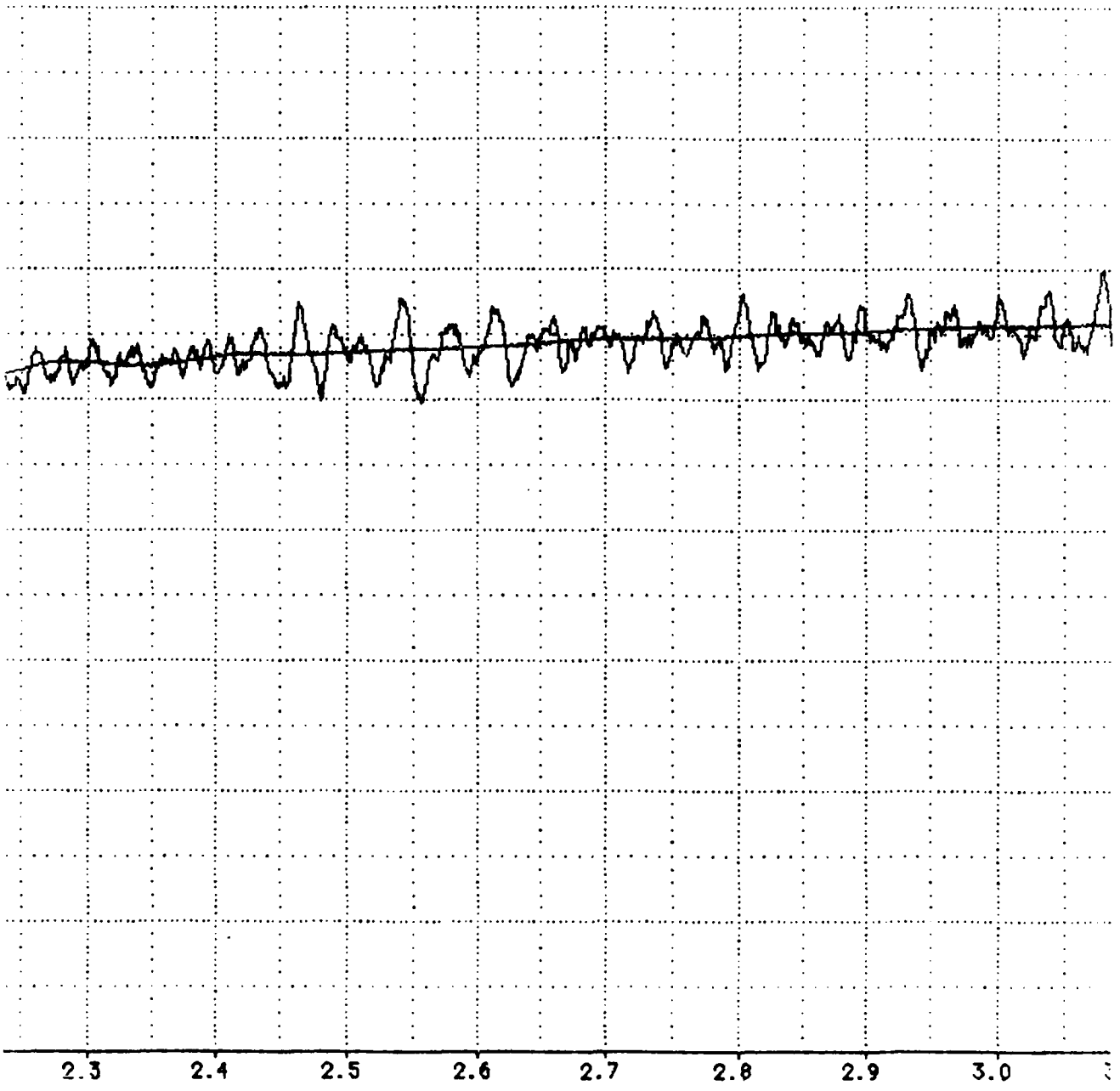
2.3
2.4
2.5
2.6
2.7
2.8
2.9
3.0

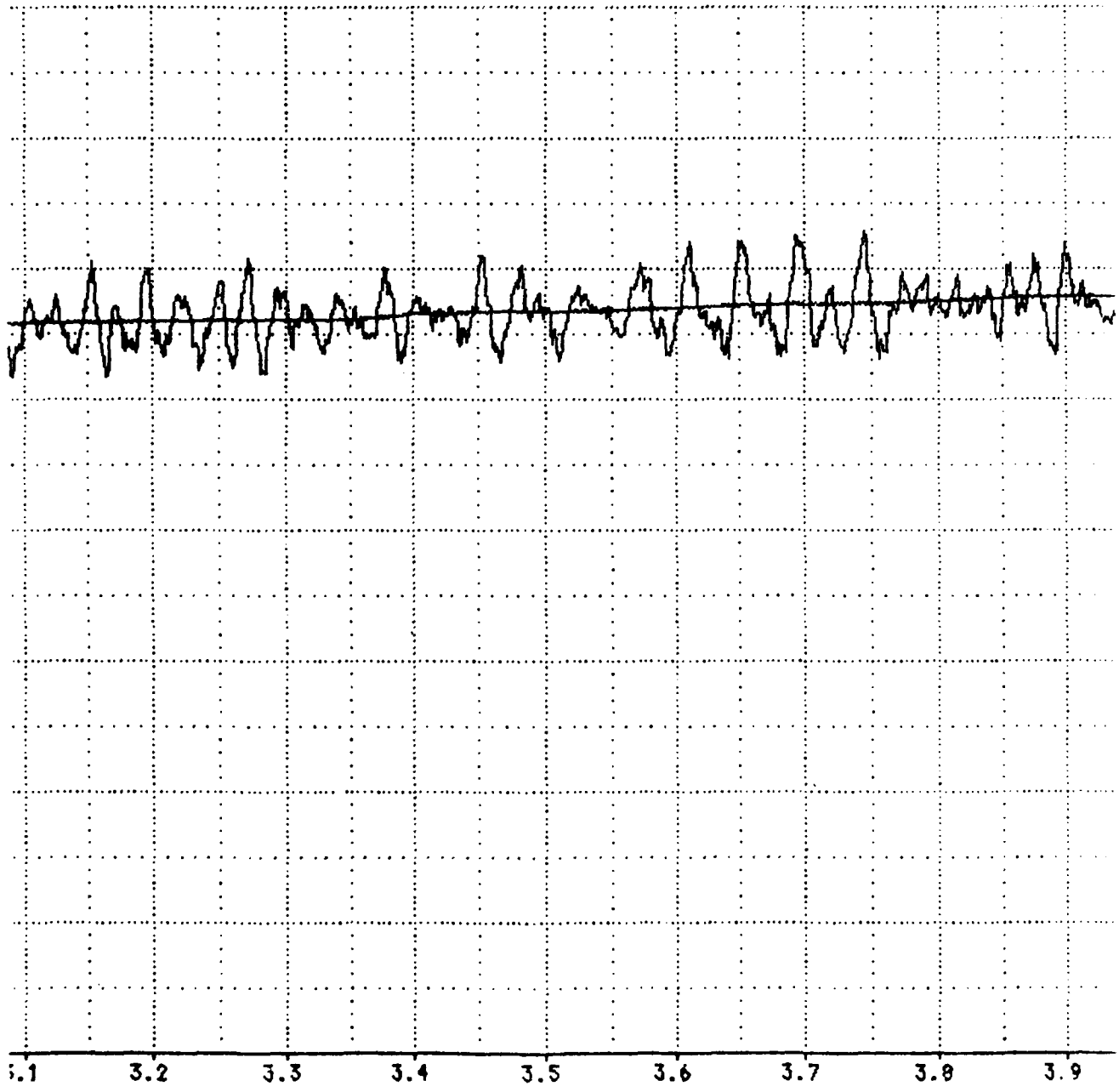
3.1
3.2
3.3
3.4
3.5
3.6
3.7
3.8
3.9

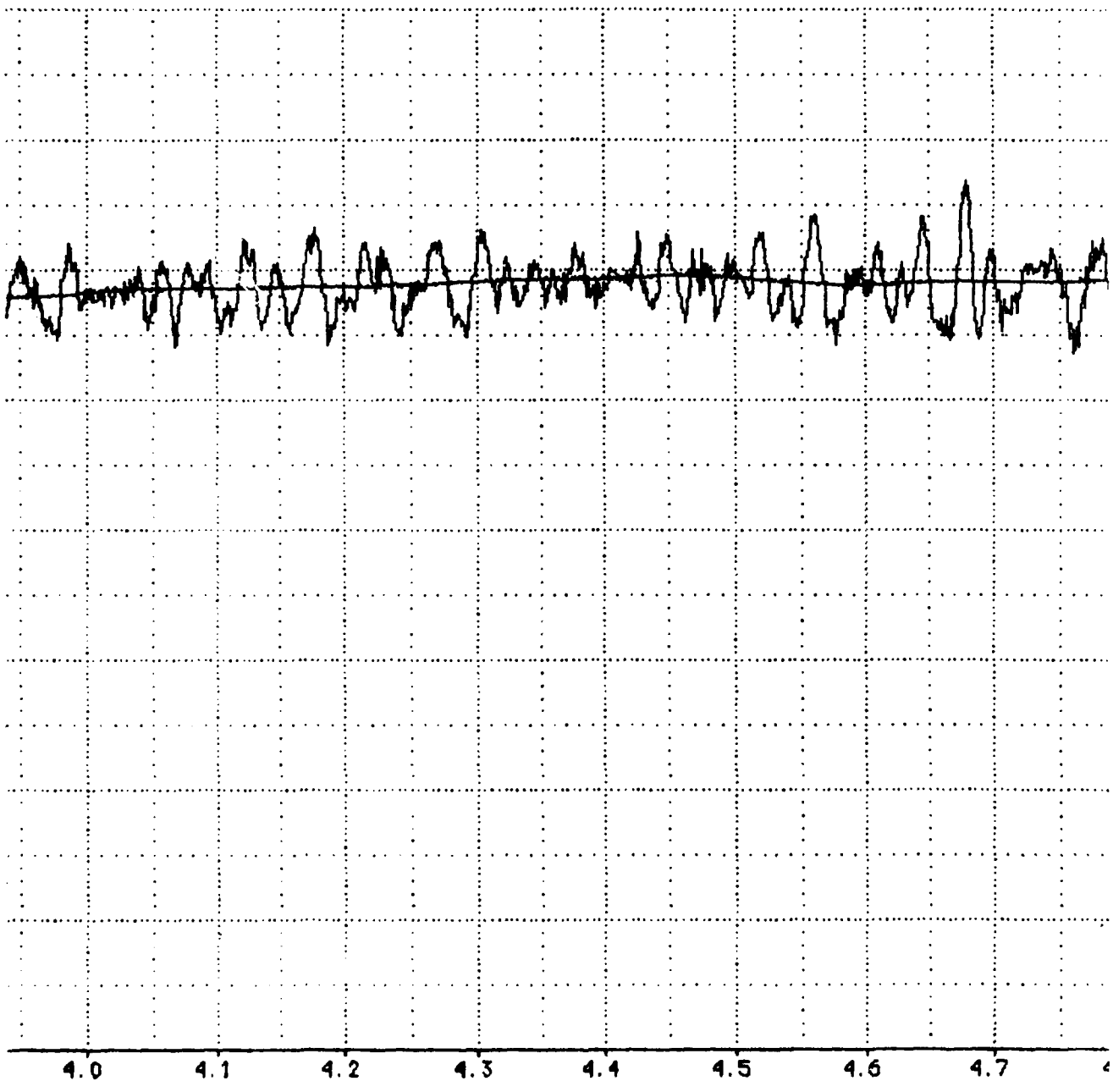
4.0
4.1
4.2
4.3
4.4
4.5
4.6
4.7

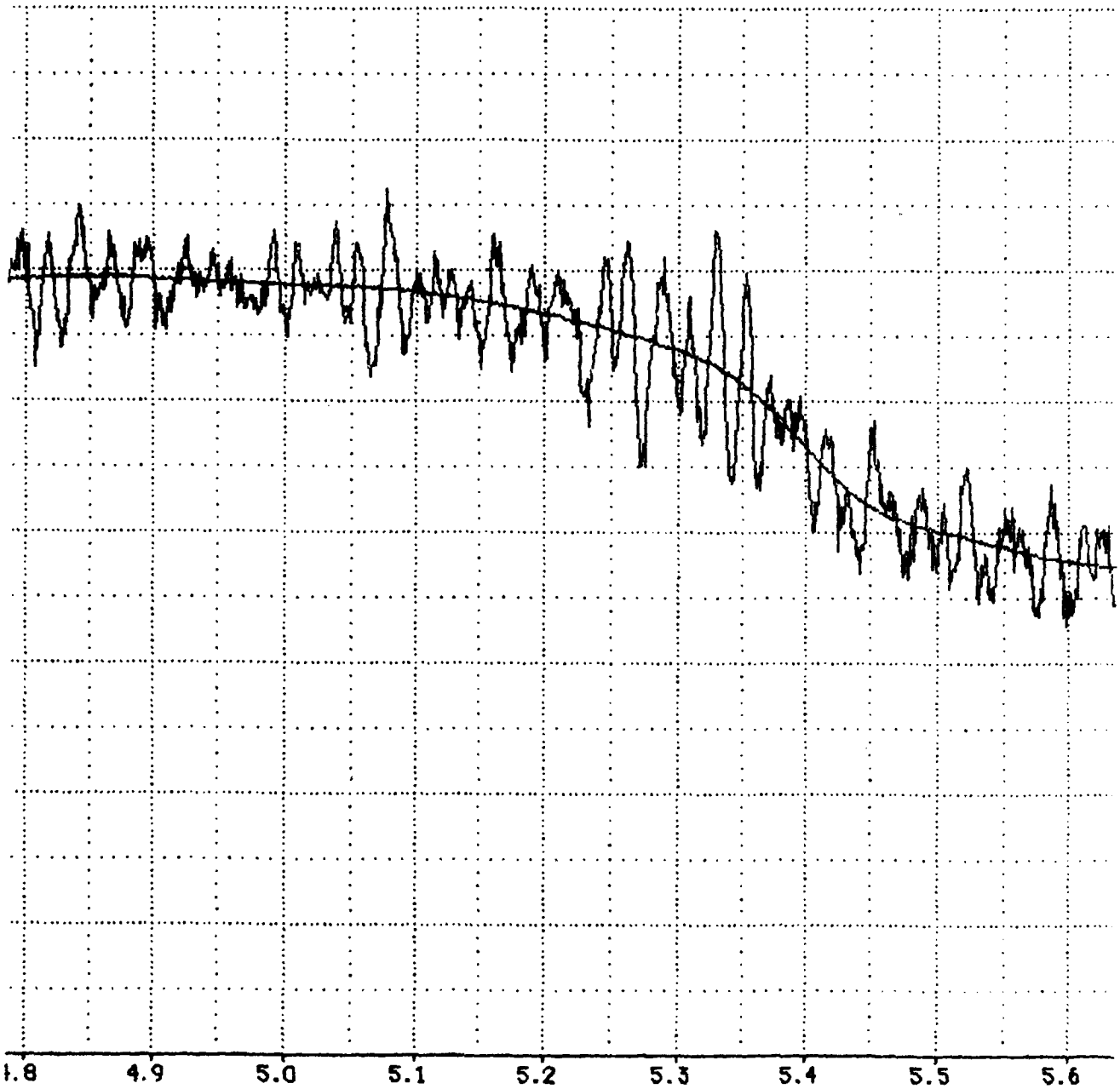
4.8
4.9
5.0
5.1
5.2
5.3
5.4
5.5
5.6

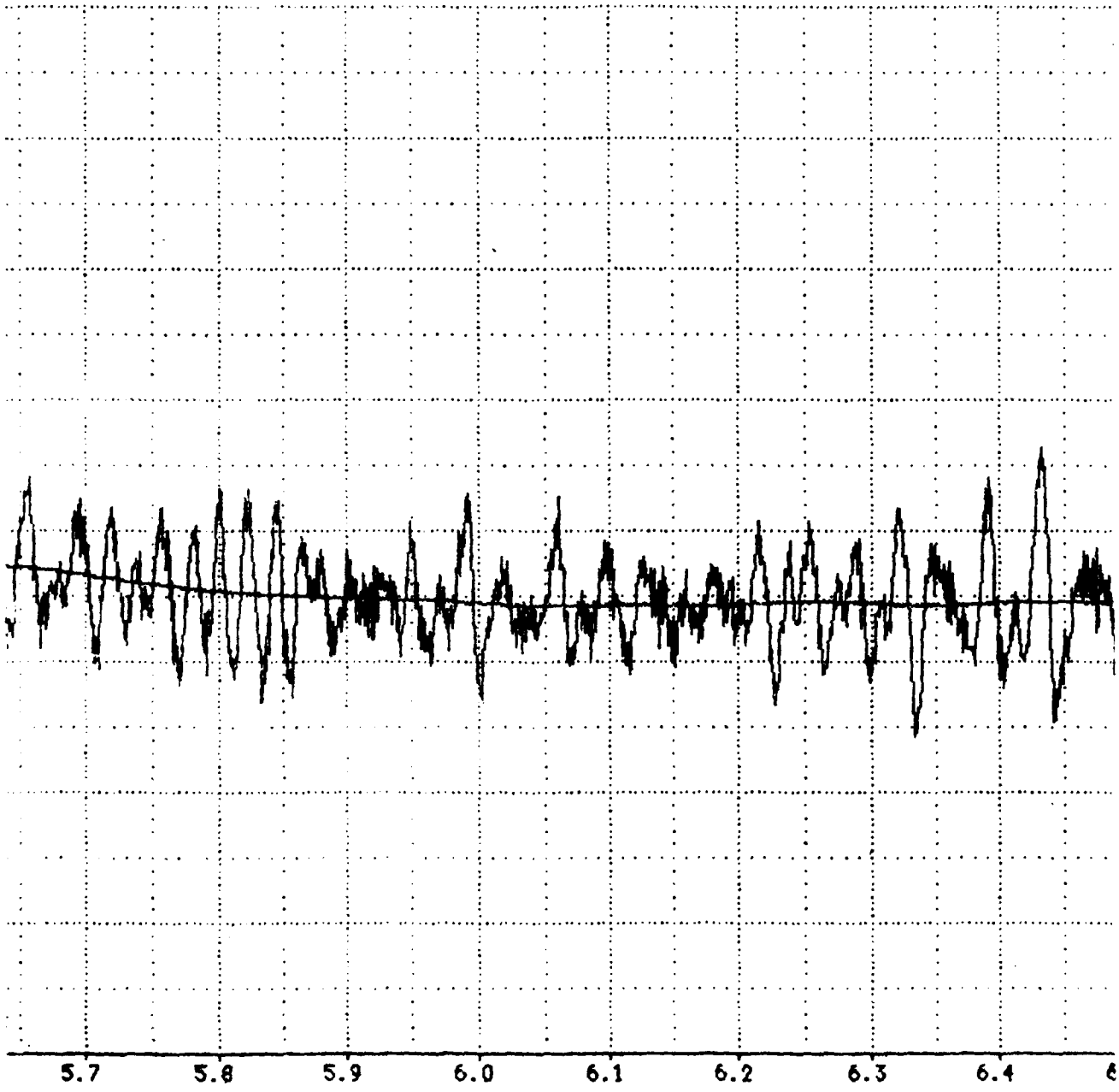
5.7
5.8
5.9
6.0
6.1
6.2
6.3
6.4

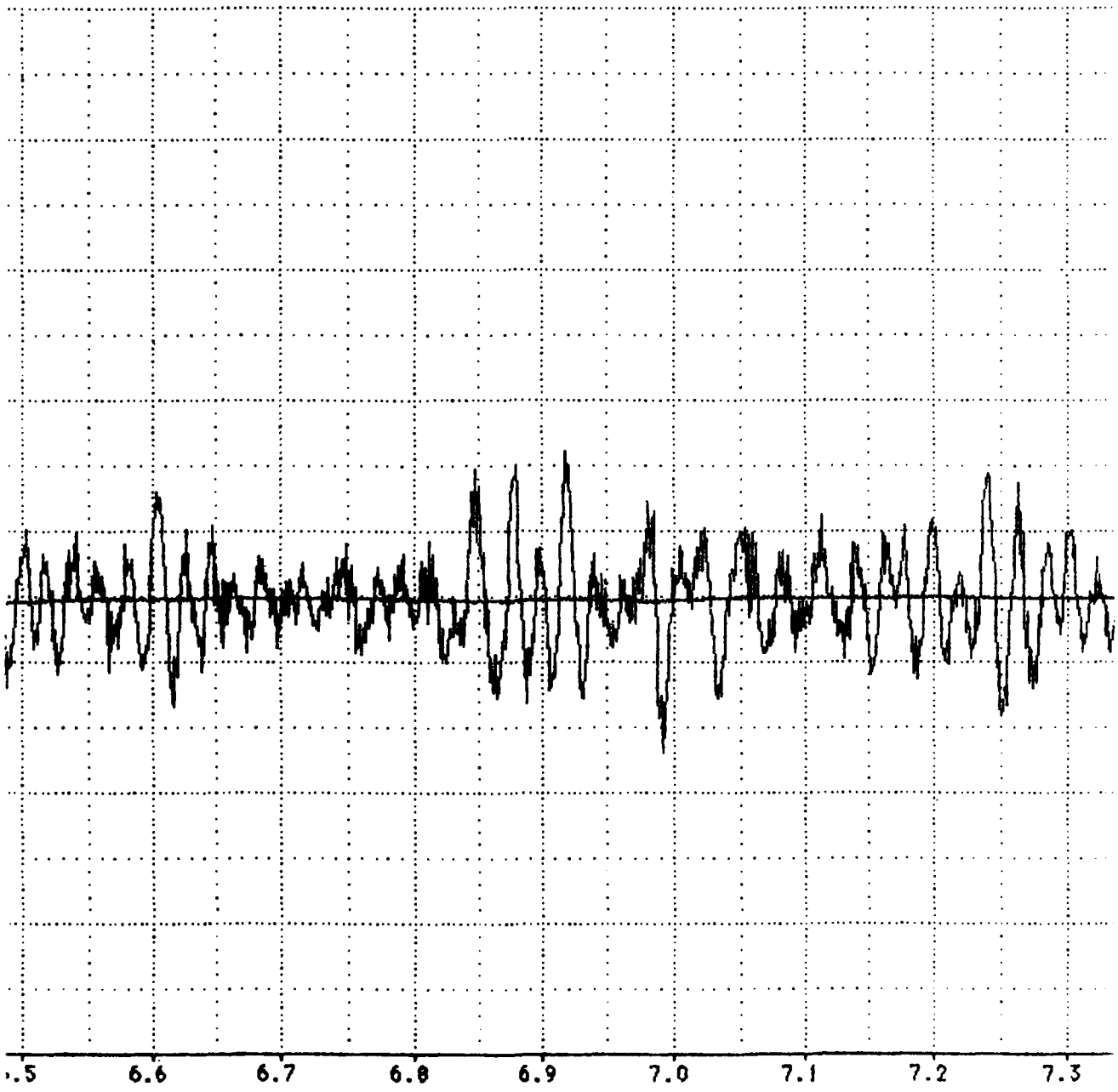
.5
6.6
6.7
6.8
6.9
7.0
7.1
7.2
7.3

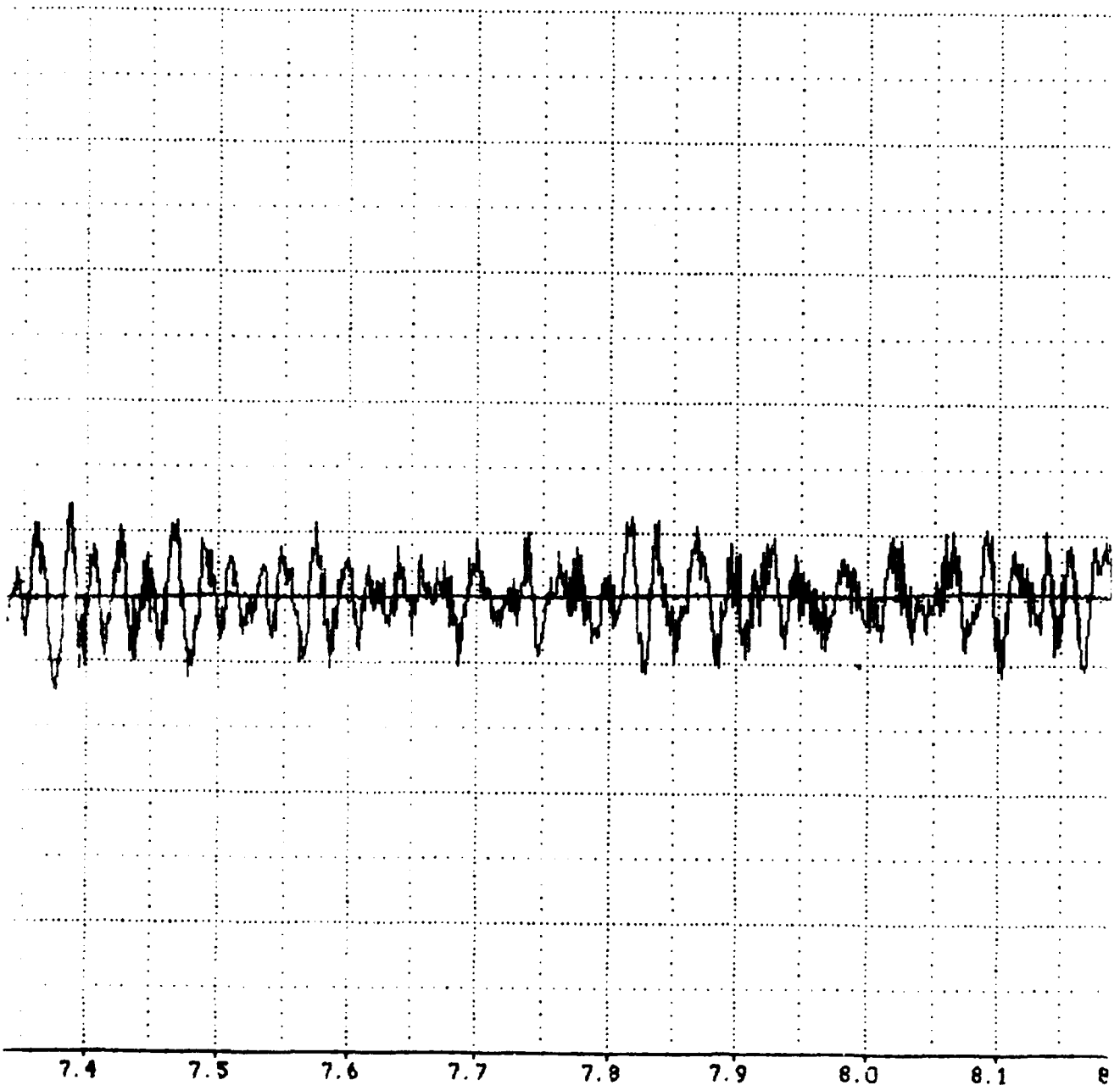
7.4
7.5
7.6
7.7
7.8
7.9
8.0
8.1

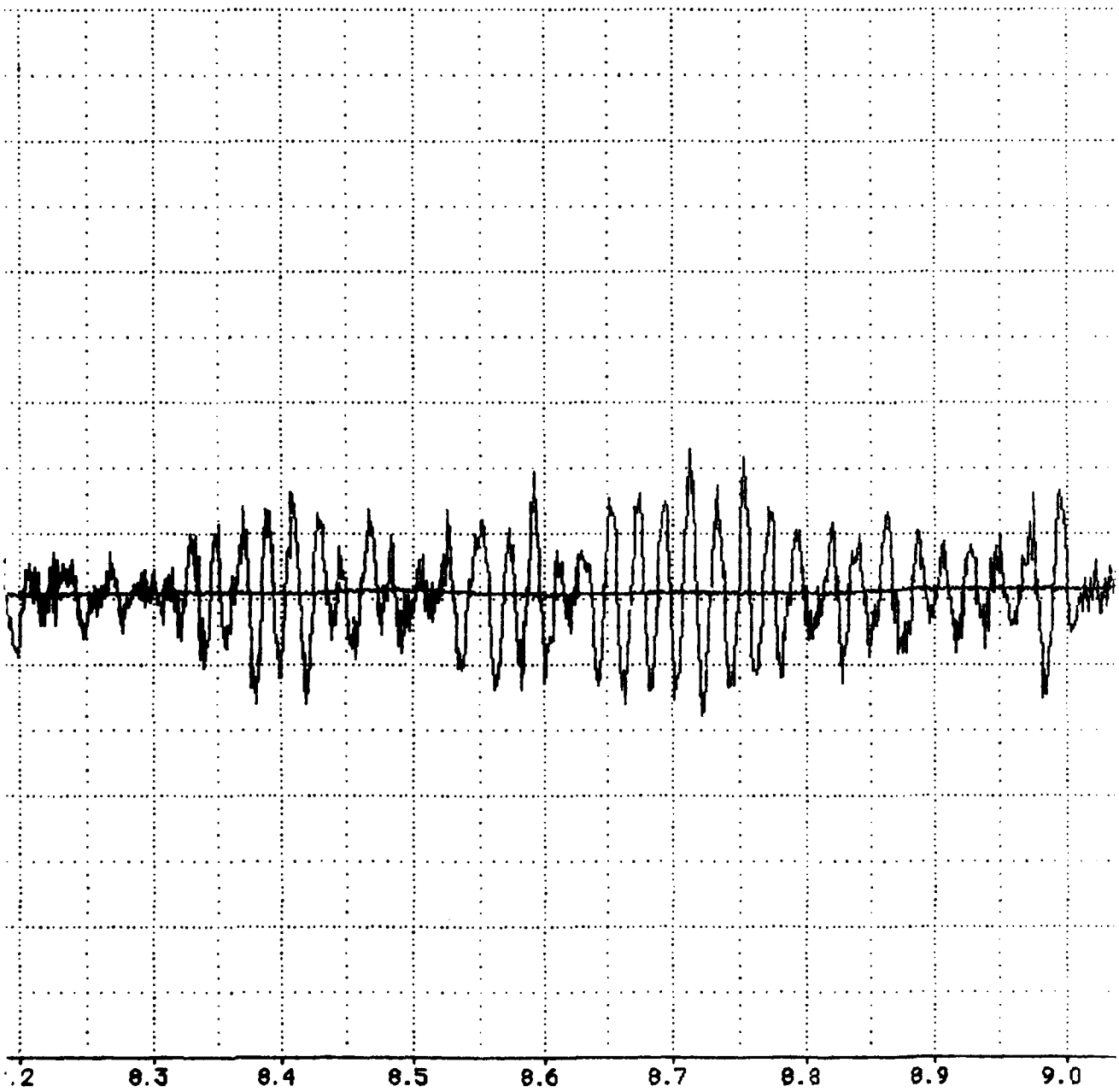
.2
8.3
8.4
8.5
8.6
8.7
8.8
8.9
9.0

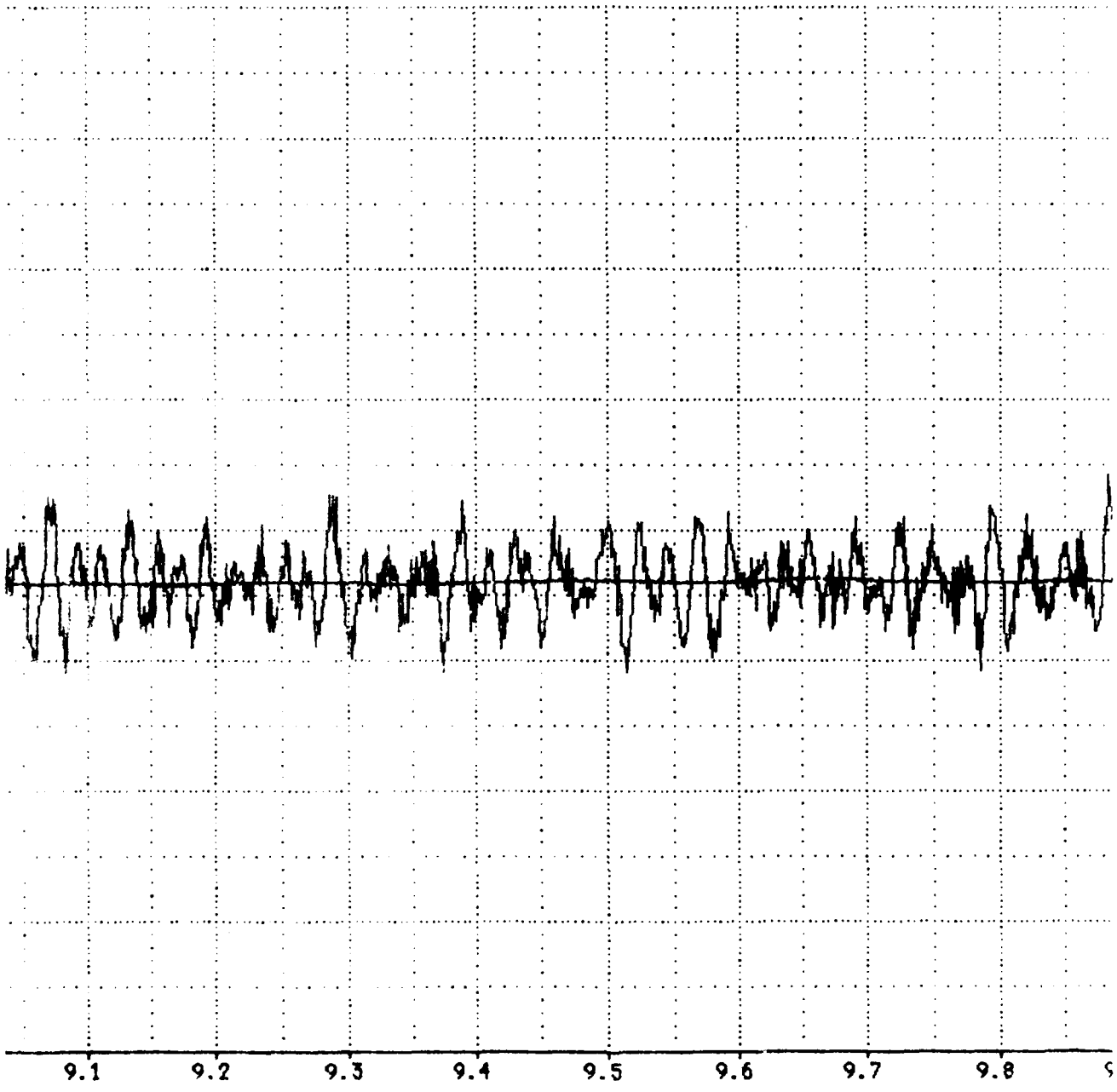
9.1
9.2
9.3
9.4
9.5
9.6
9.7
9.8

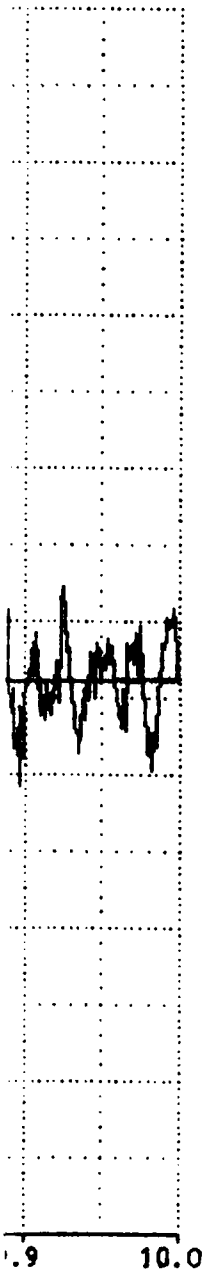
.9
10.0

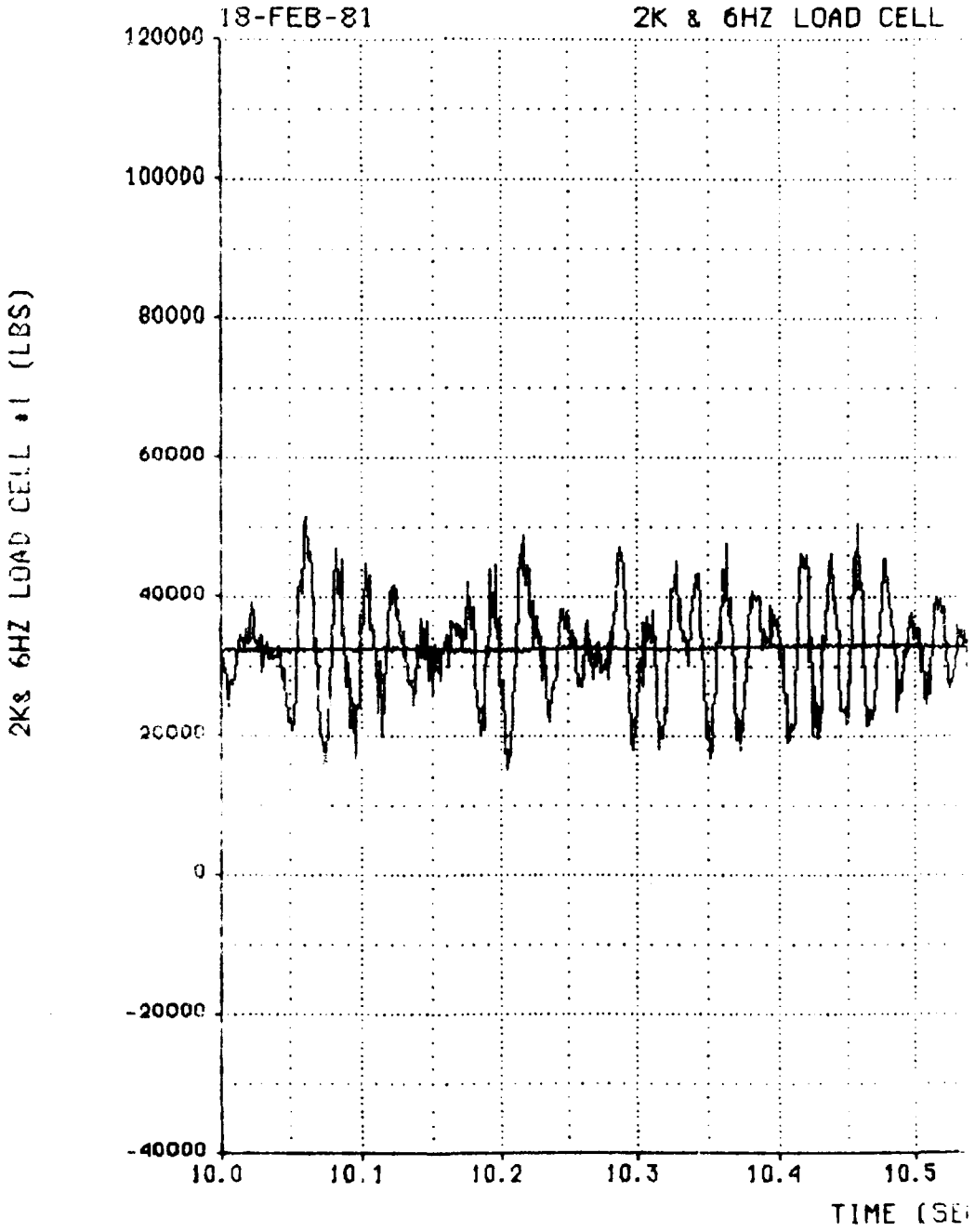
18-FEB-81
2K & 6HZ LOAD CELL
120000
100000
80000
60000
40000
20000
0
-20000
-40000
2K& 6HZ LOAD CELL *1 (LBS)
10.0
10.1
10.2
10.3
10.4
10.5
TIME (SE

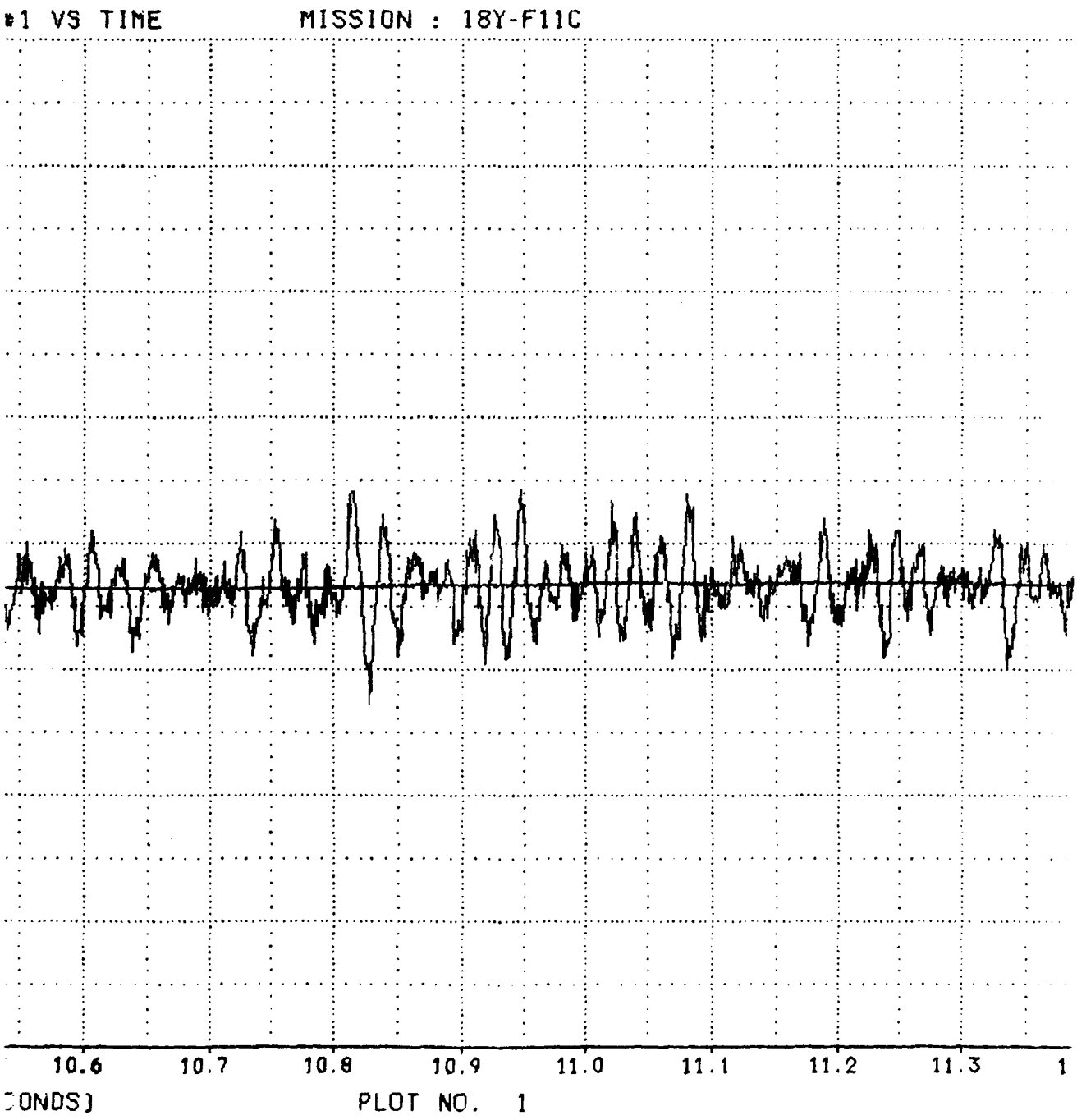
#1 VS TIME
MISSION : 18Y-F11C
10.6
10.7
10.8
10.9
11.0
11.1
11.2
11.3
1
ONDS)
PLOT NO. 1

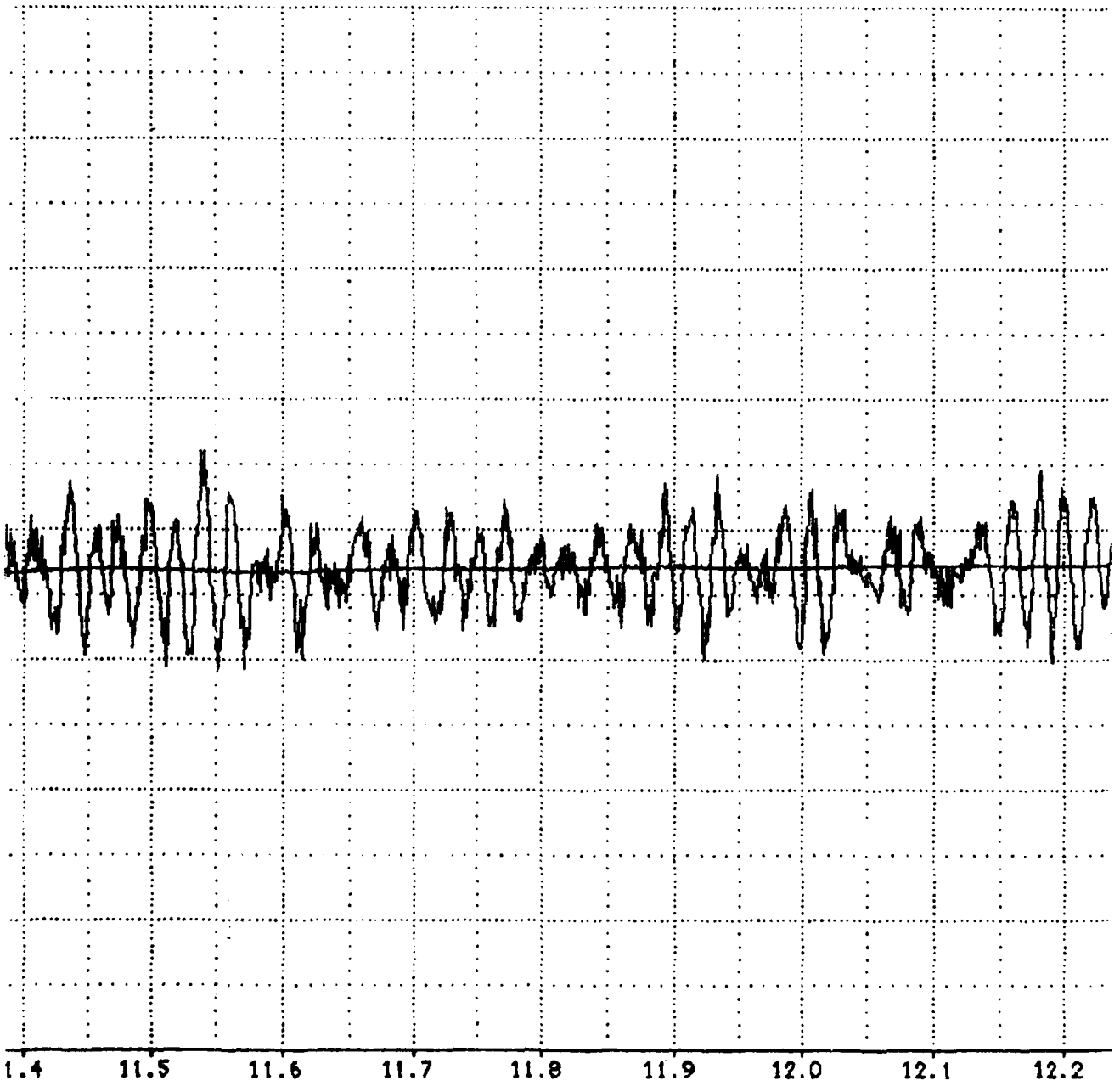
1.4
11.5
11.6
11.7
11.8
11.9
12.0
12.1
12.2

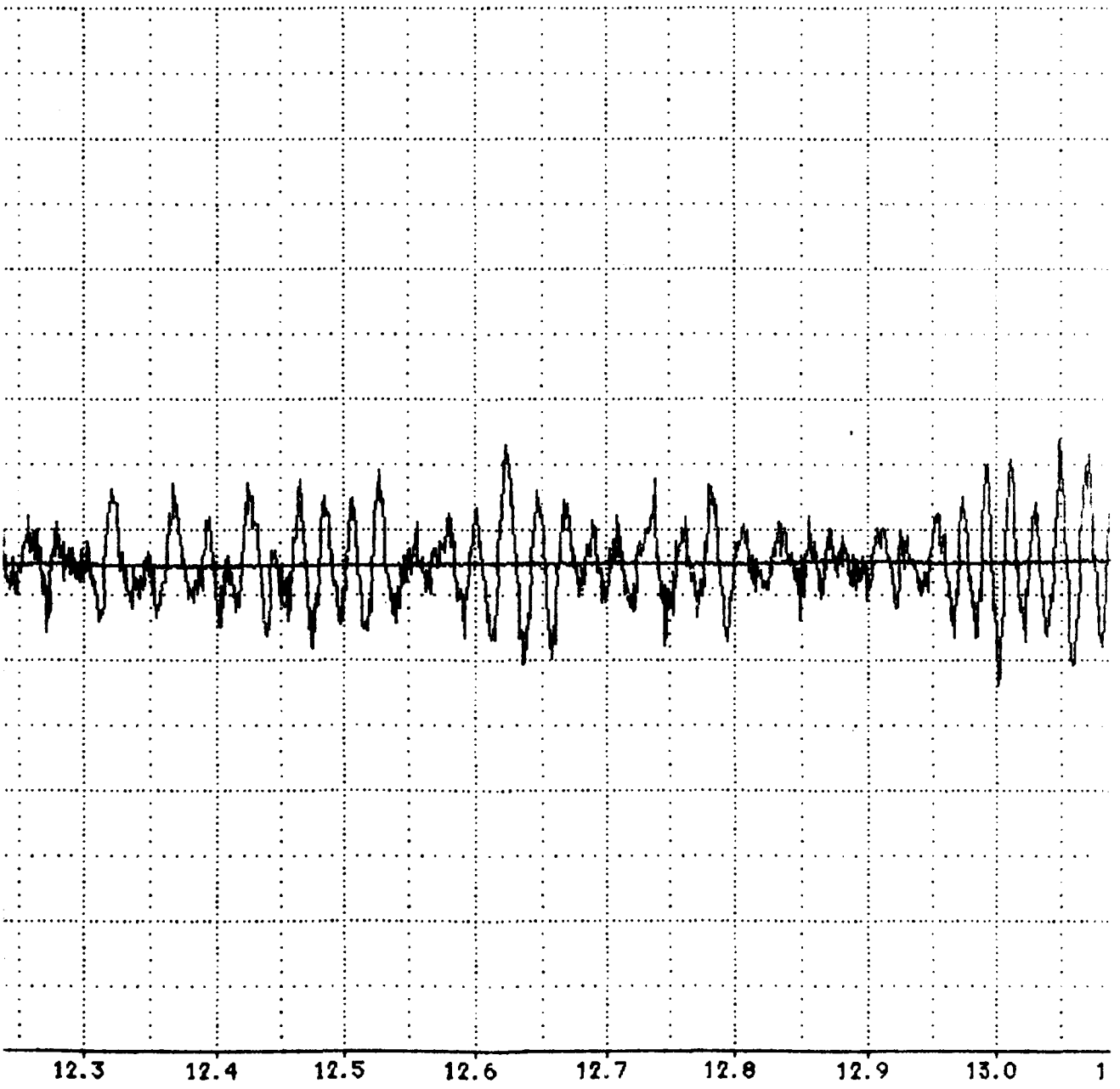
12.3
12.4
12.5
12.6
12.7
12.8
12.9
13.0
1

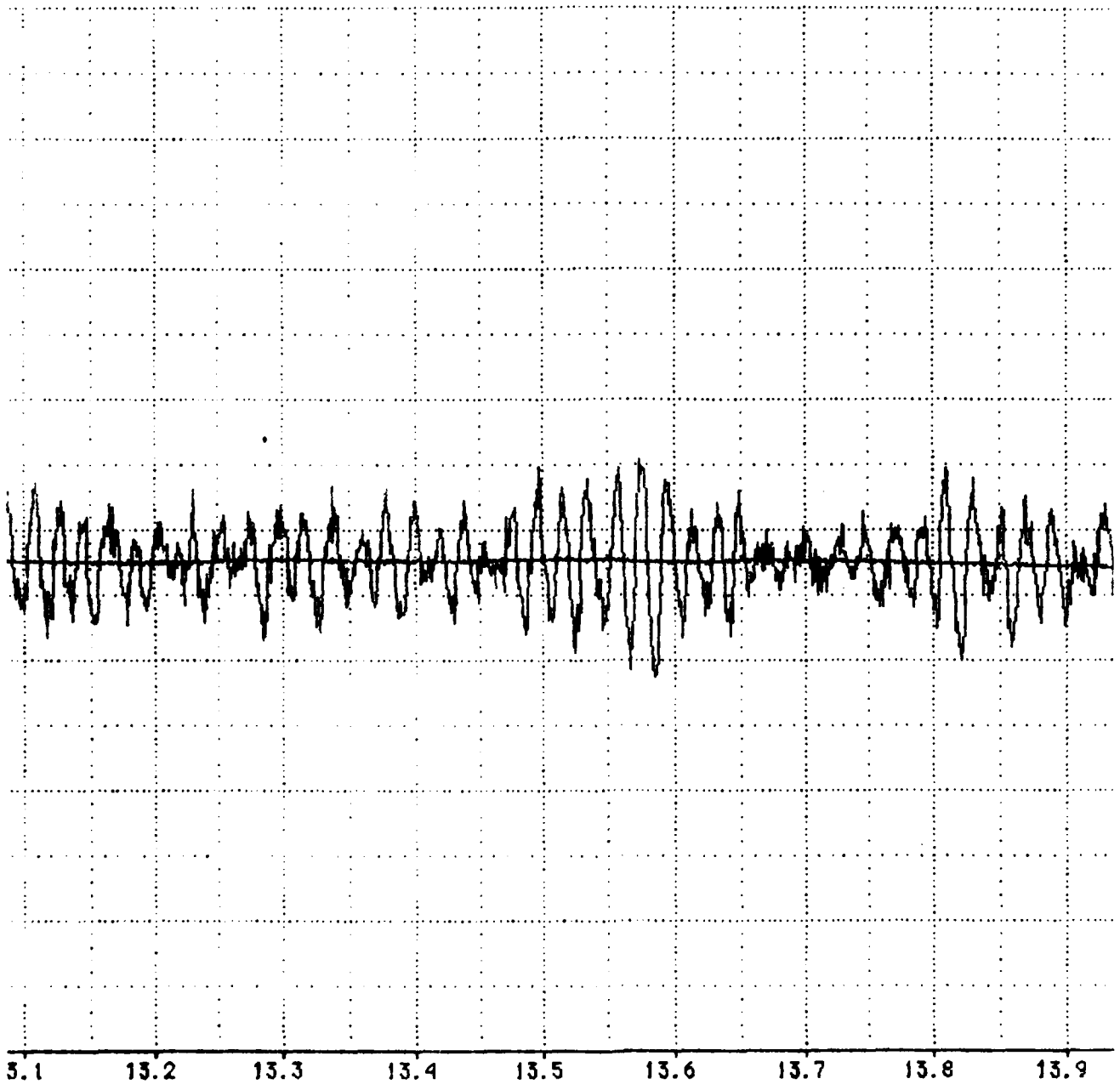
13.1
13.2
13.3
13.4
13.5
13.6
13.7
13.8
13.9

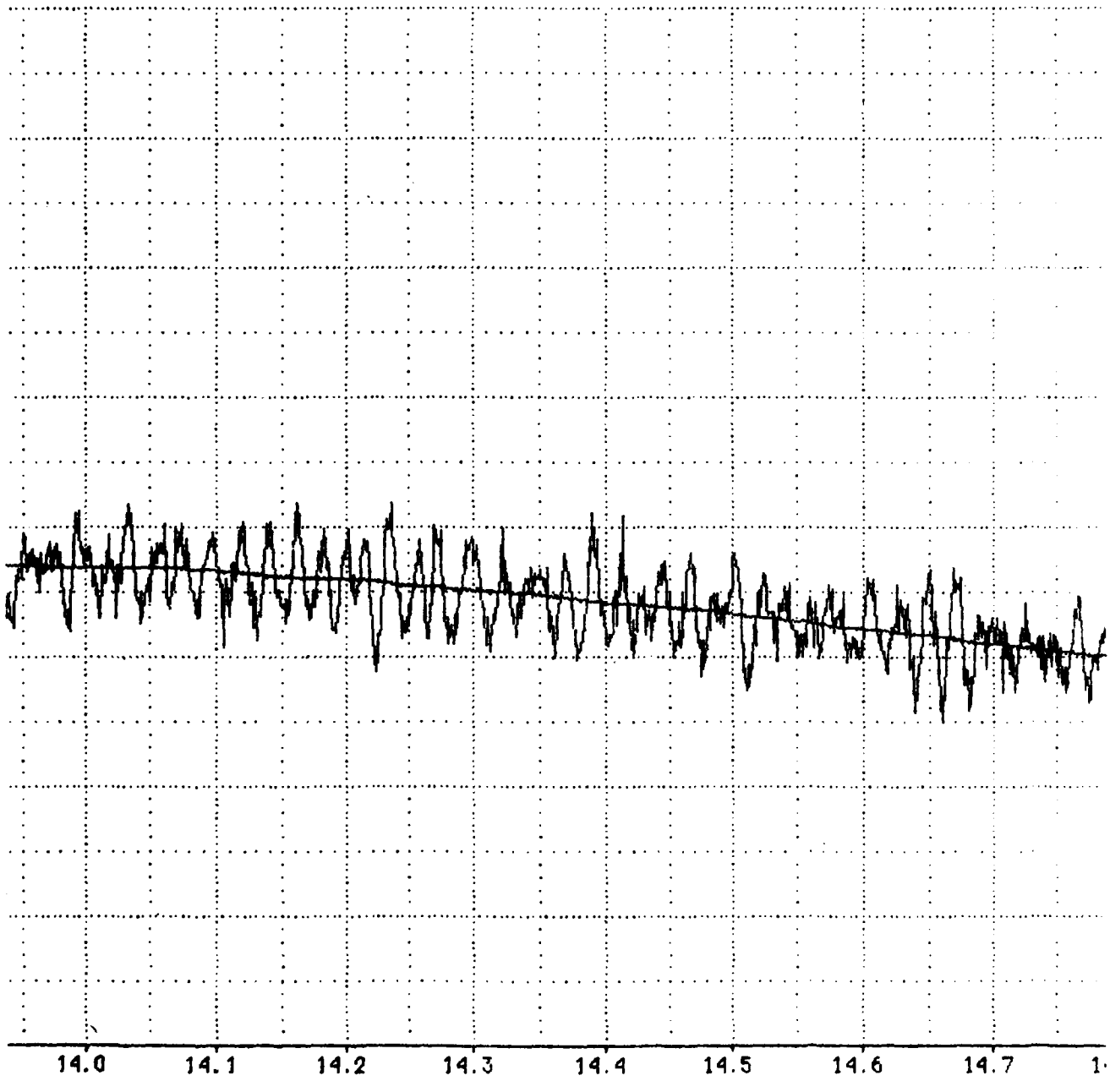
14.0
14.1
14.2
14.3
14.4
14.5
14.6
14.7

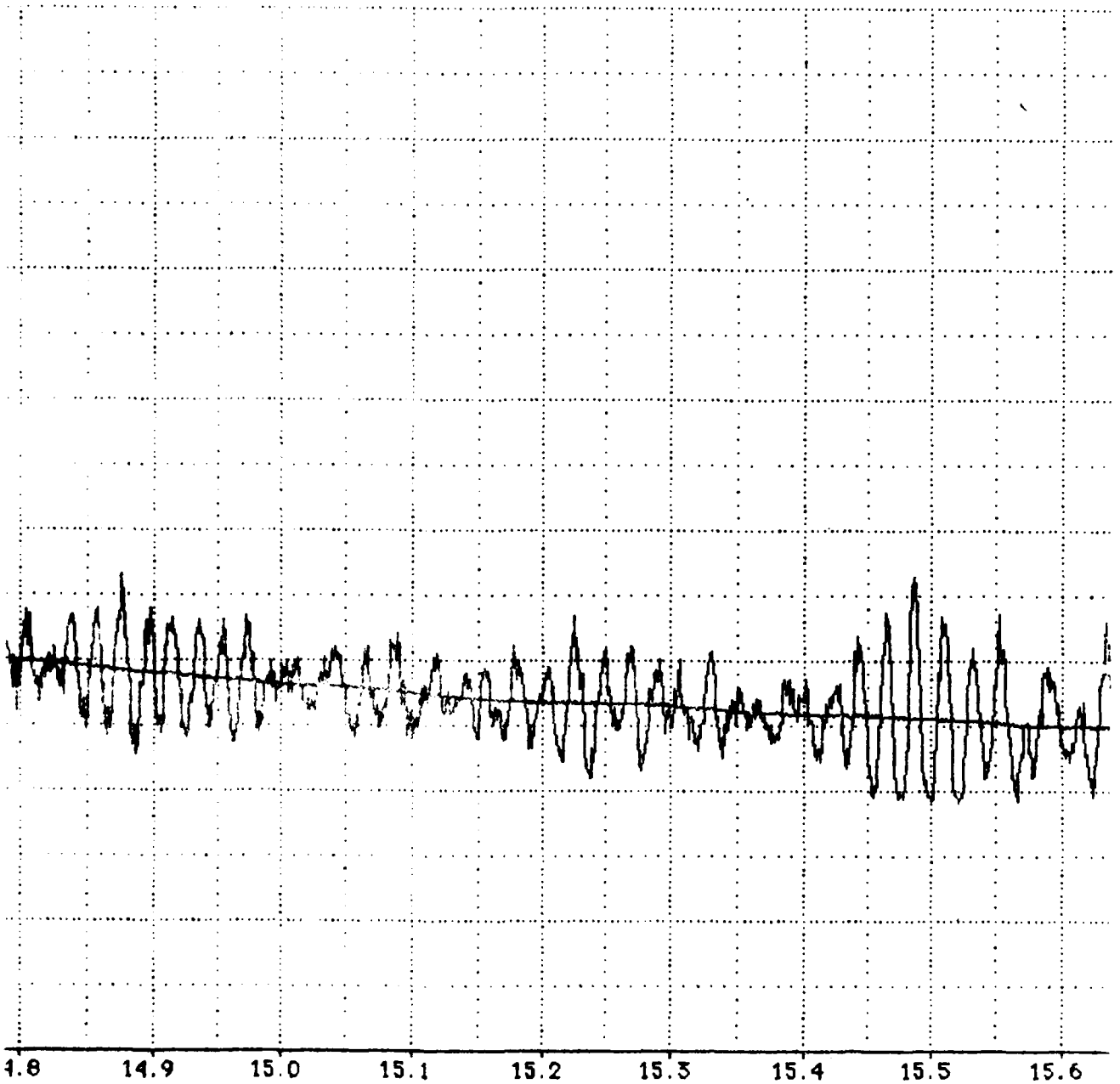
14.8
14.9
15.0
15.1
15.2
15.3
15.4
15.5
15.6

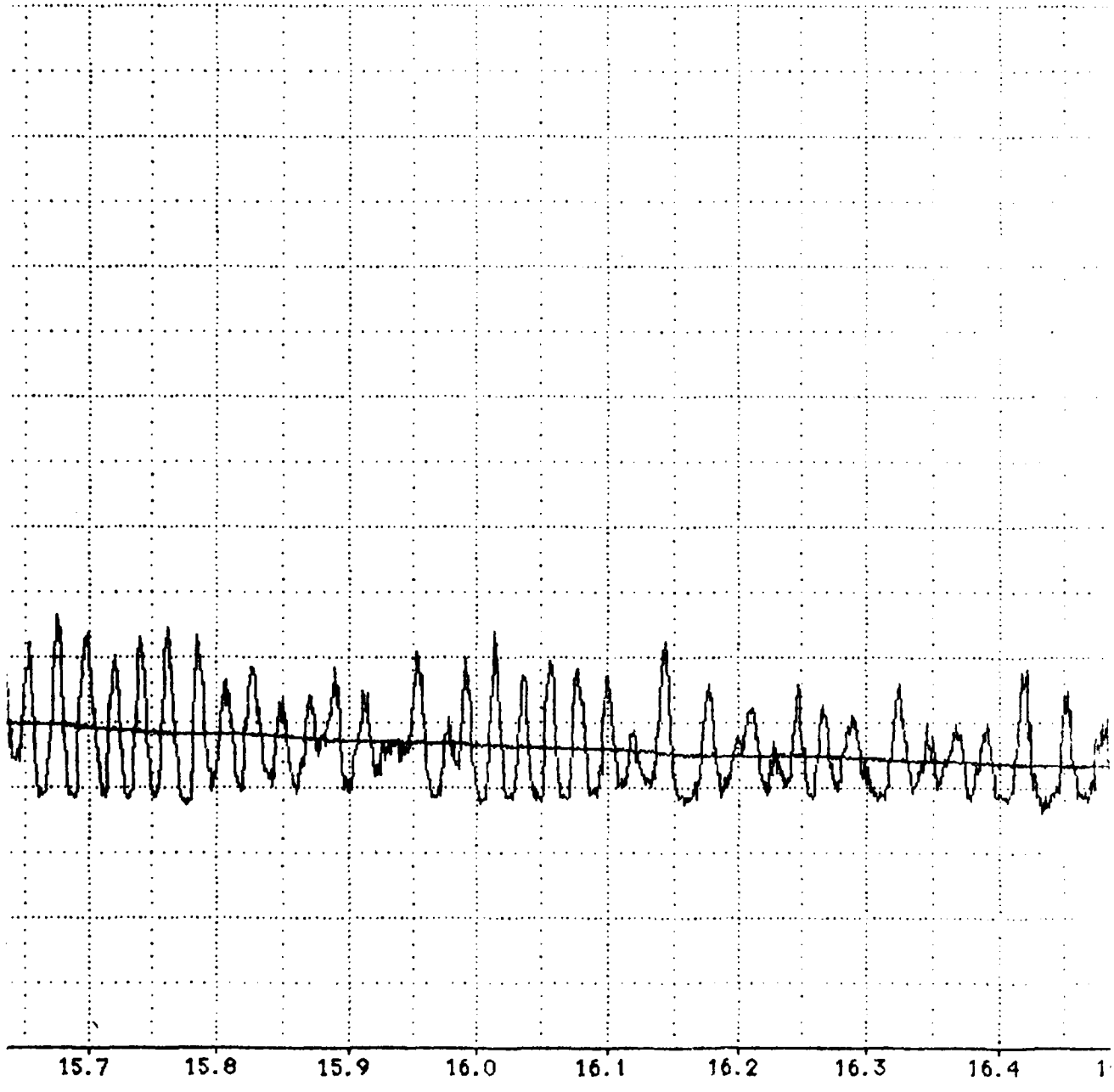
15.7
15.8
15.9
16.0
16.1
16.2
16.3
16.4

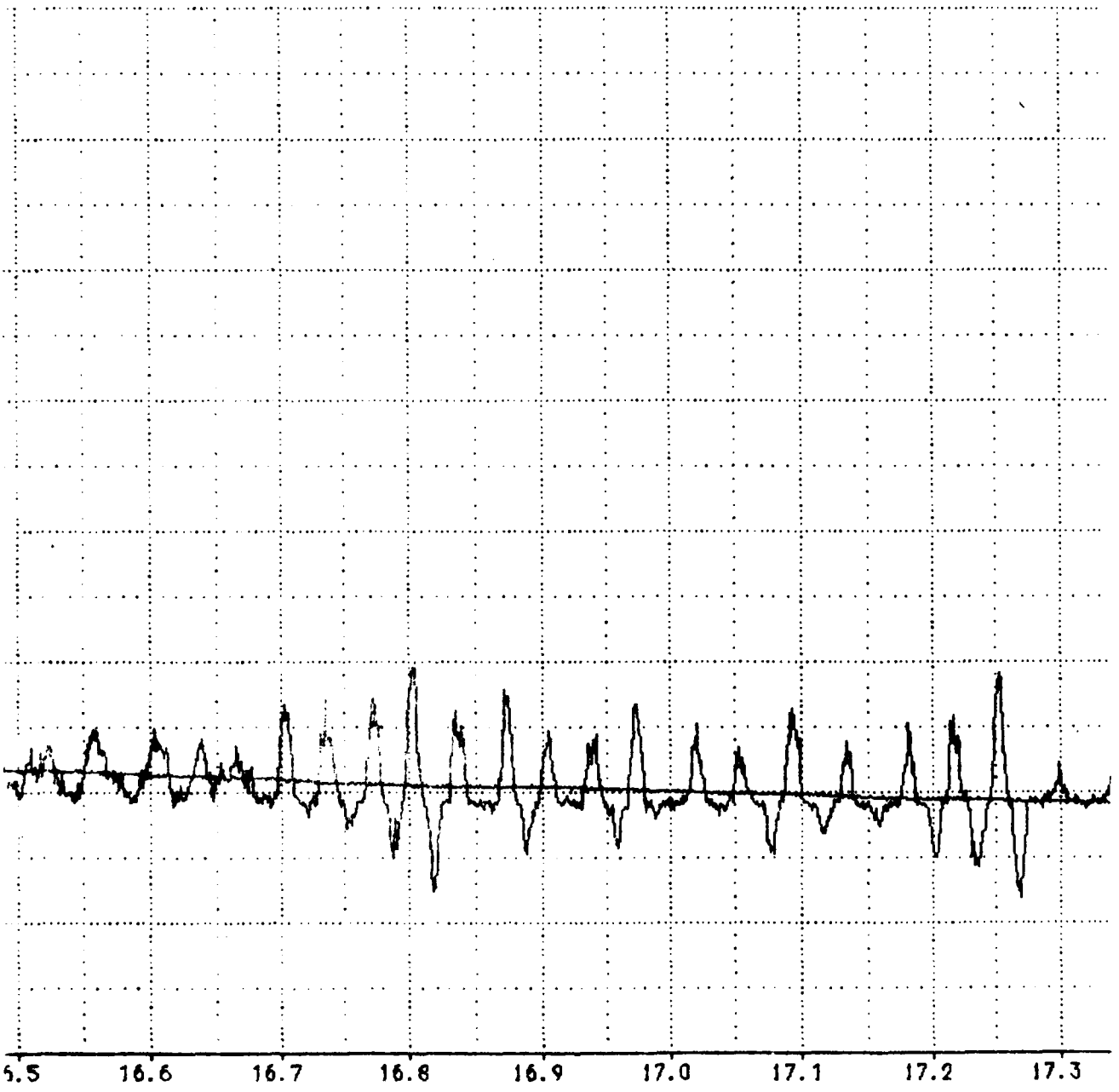
16.5
16.6
16.7
16.8
16.9
17.0
17.1
17.2
17.3

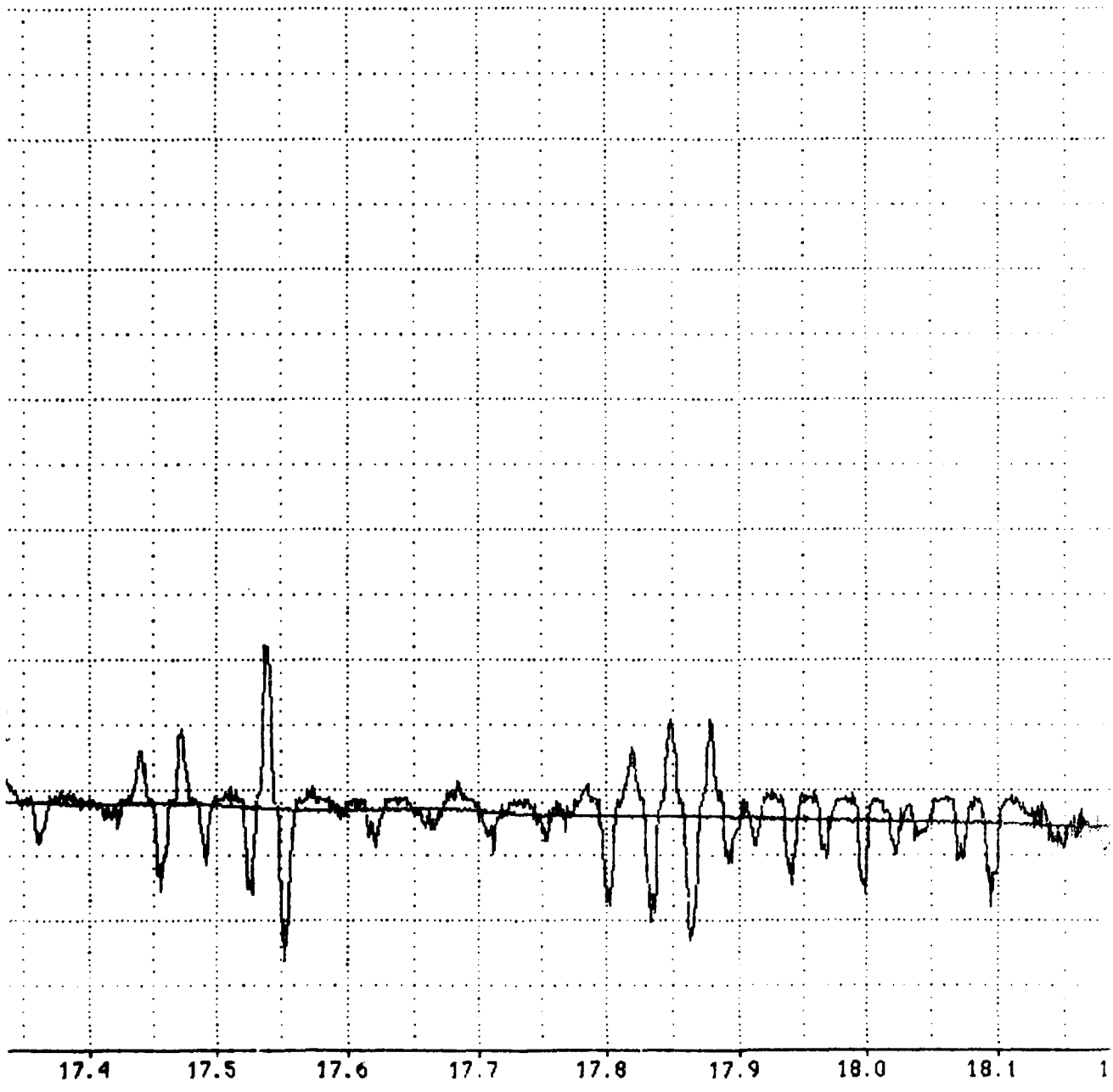
17.4
17.5
17.6
17.7
17.8
17.9
18.0
18.1
1

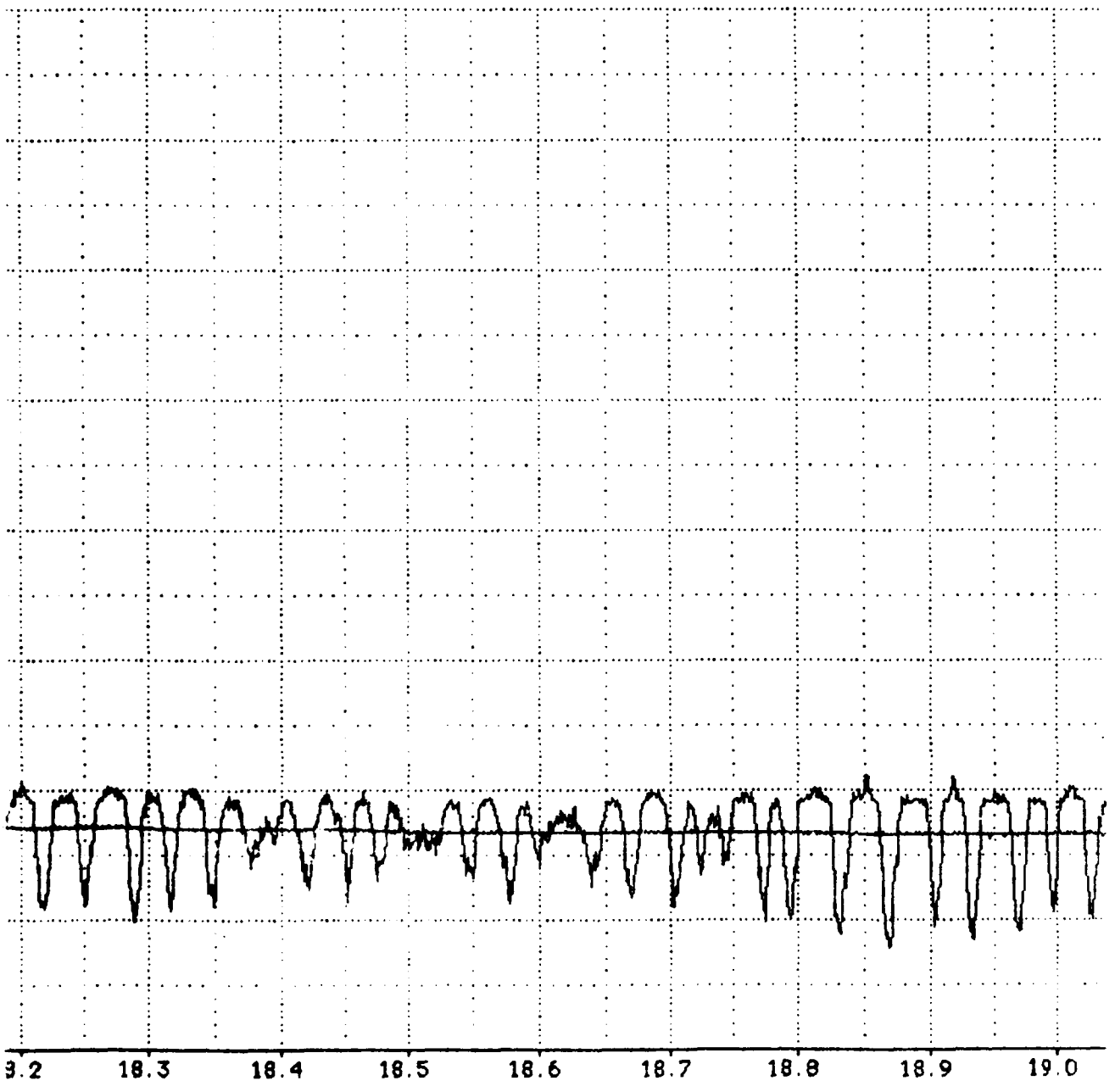
3.2
18.3
18.4
18.5
18.6
18.7
18.8
18.9
19.0

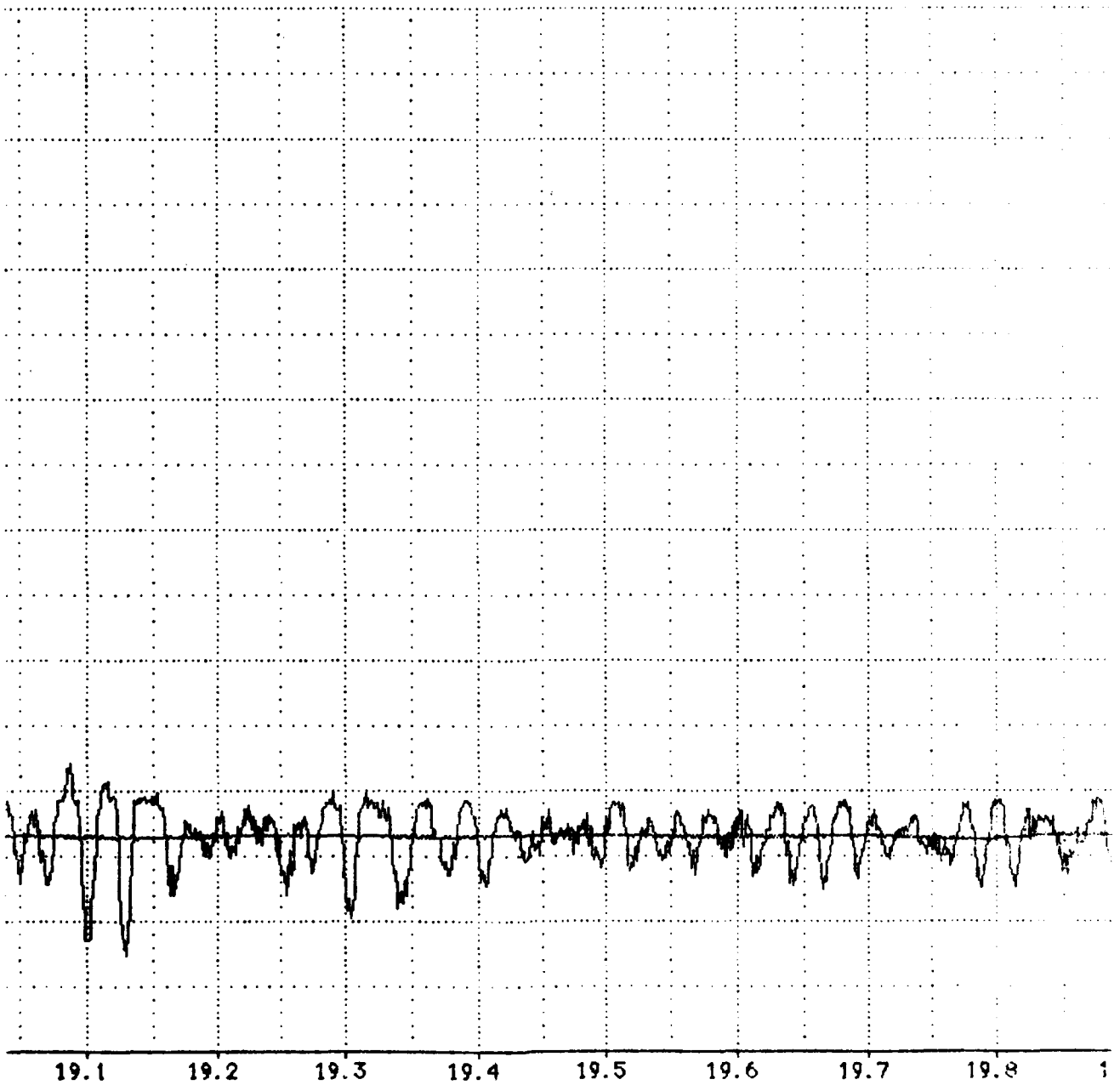
19.1
19.2
19.3
19.4
19.5
19.6
19.7
19.8

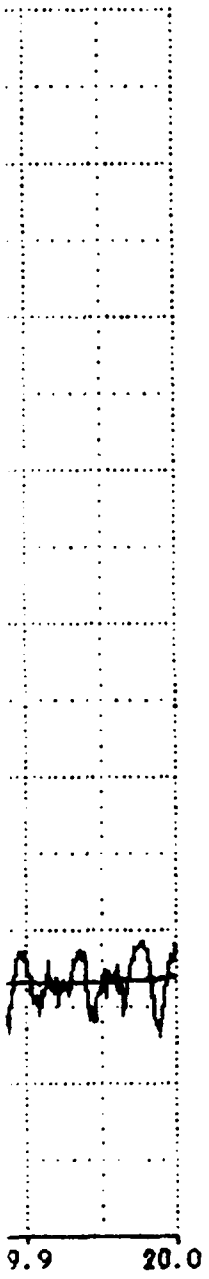
9.9
20.0

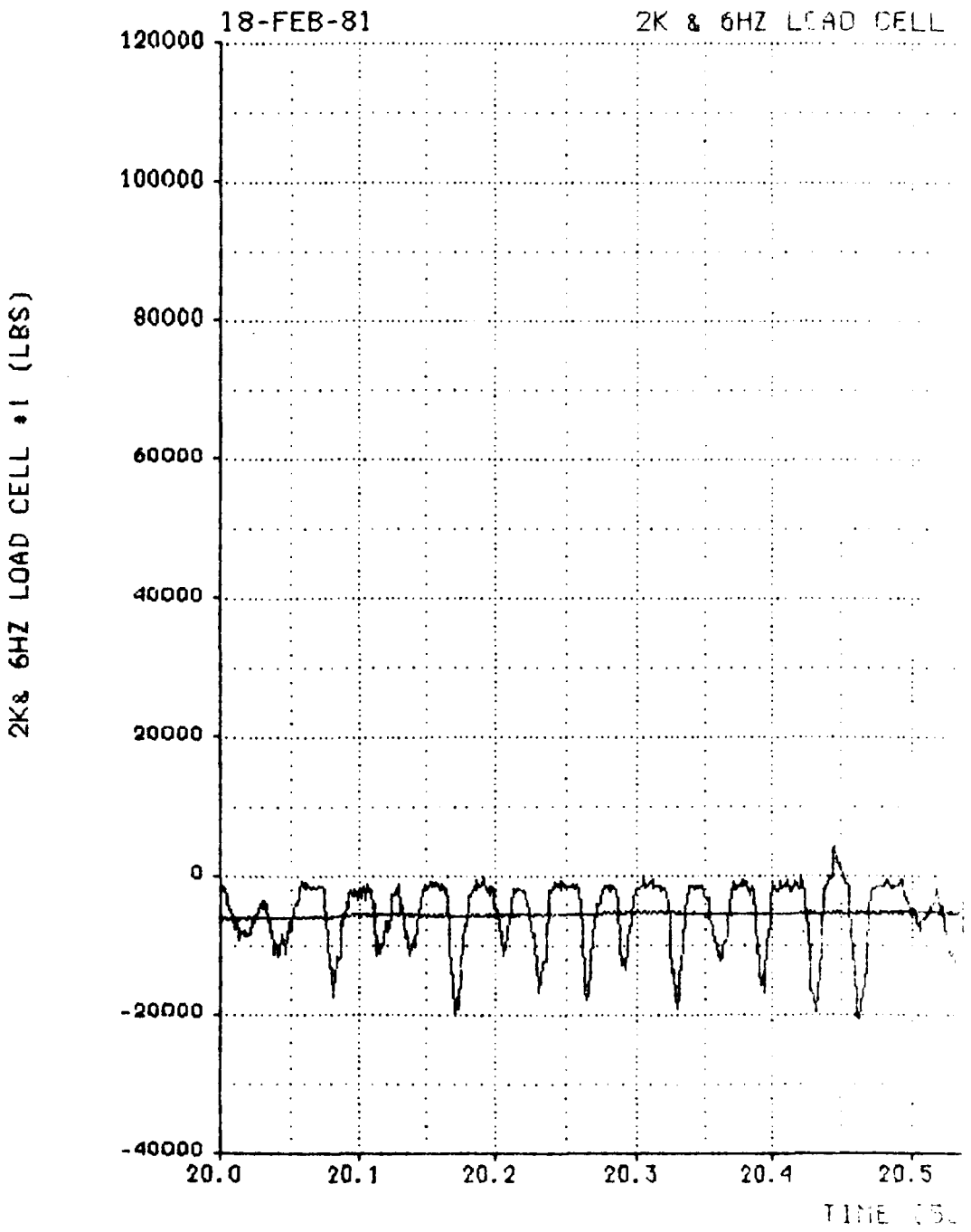
18-FEB-81
2K & 6HZ LOAD CELL
2K& 6HZ LOAD CELL #1 (LBS)
120000
100000
80000
60000
40000
20000
0
-20000
-40000
20.0
20.1
20.2
20.3
20.4
20.5
TIME (S

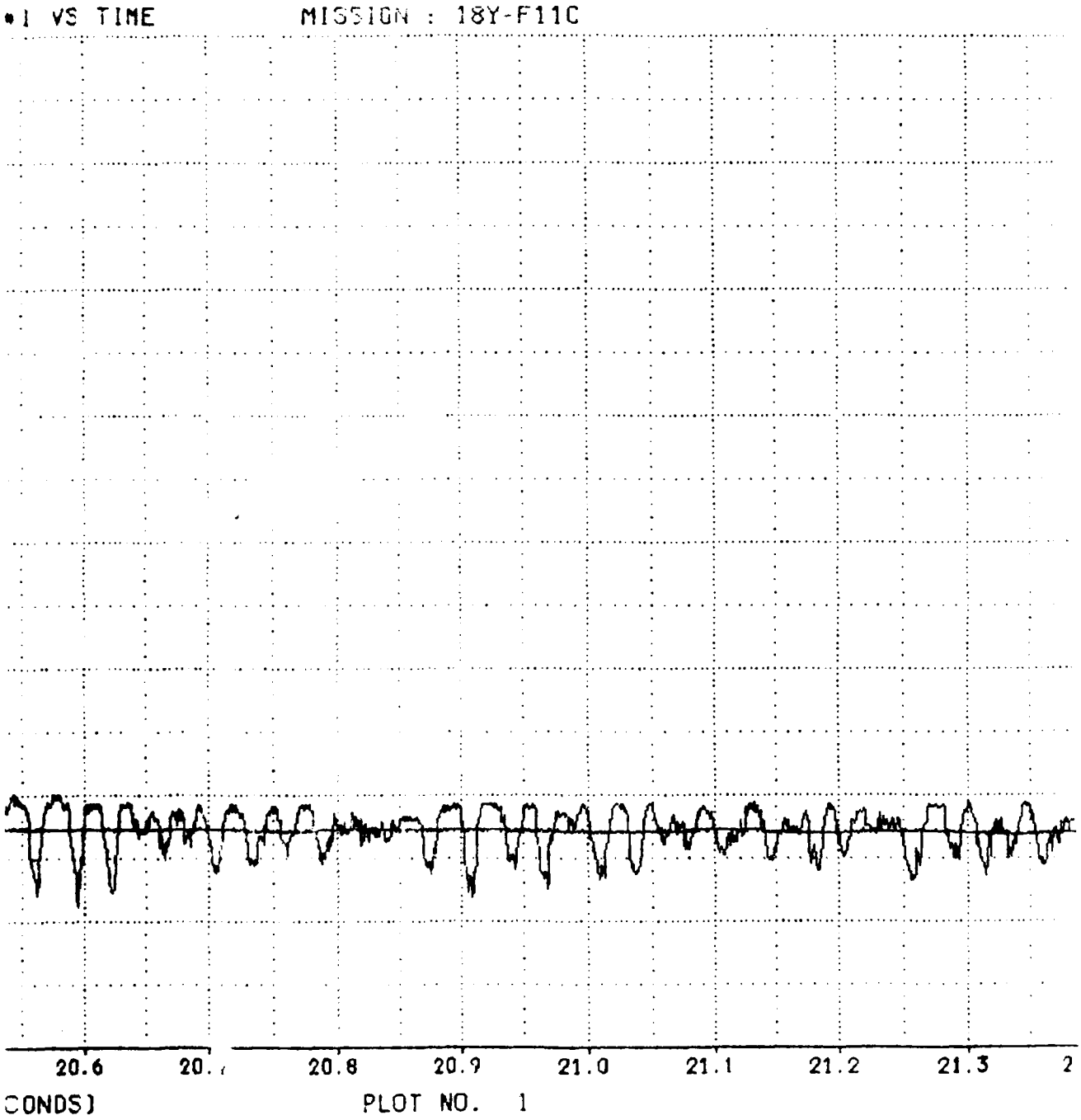
•I VS TIME
MISSION : 18Y-F11C
20.6
20.8
20.9
21.0
21.1
21.2
21.3
CONDS)
PLOT NO. 1

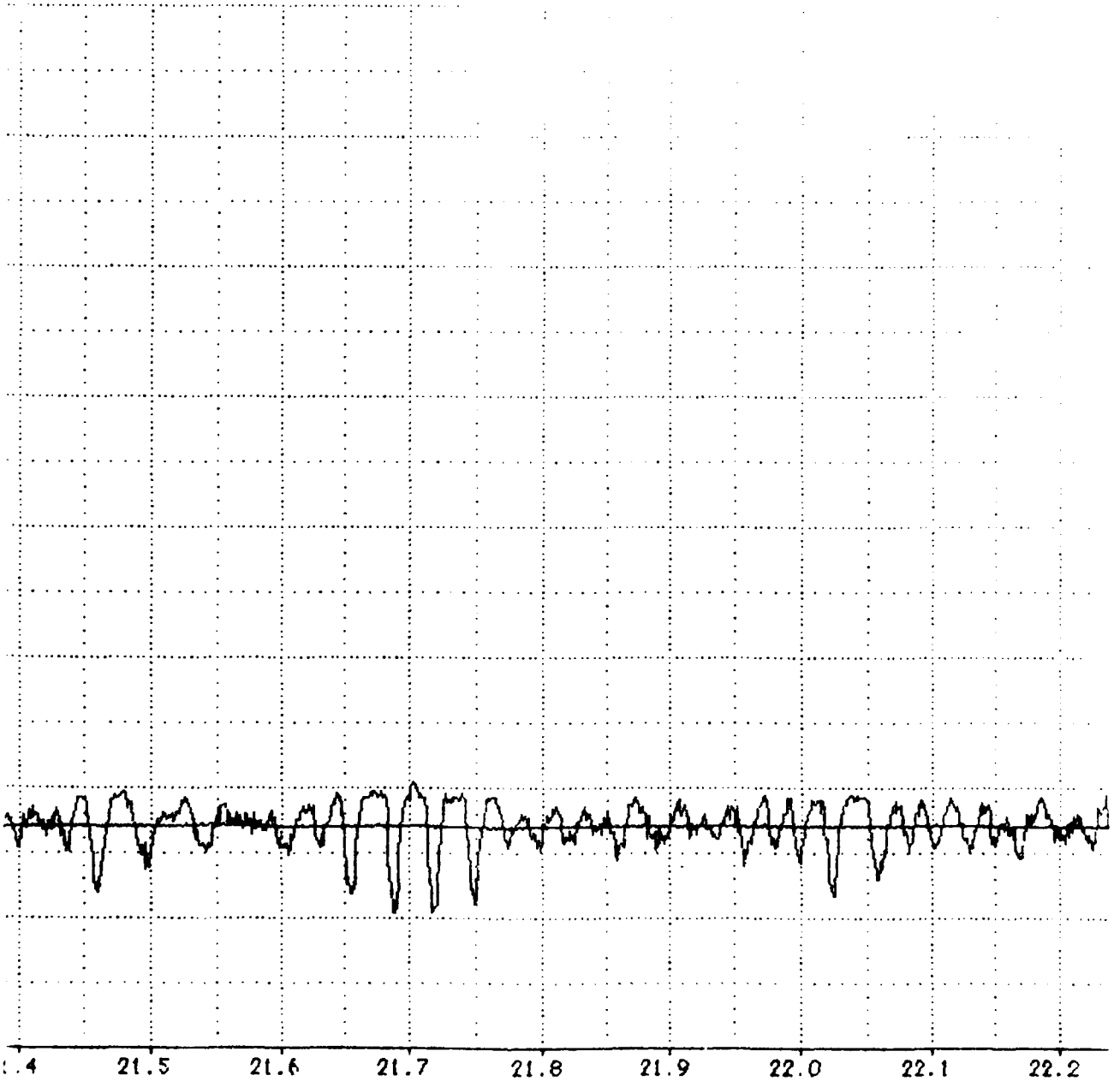
.4
21.5
21.6
21.7
21.8
21.9
22.0
22.1
22.2

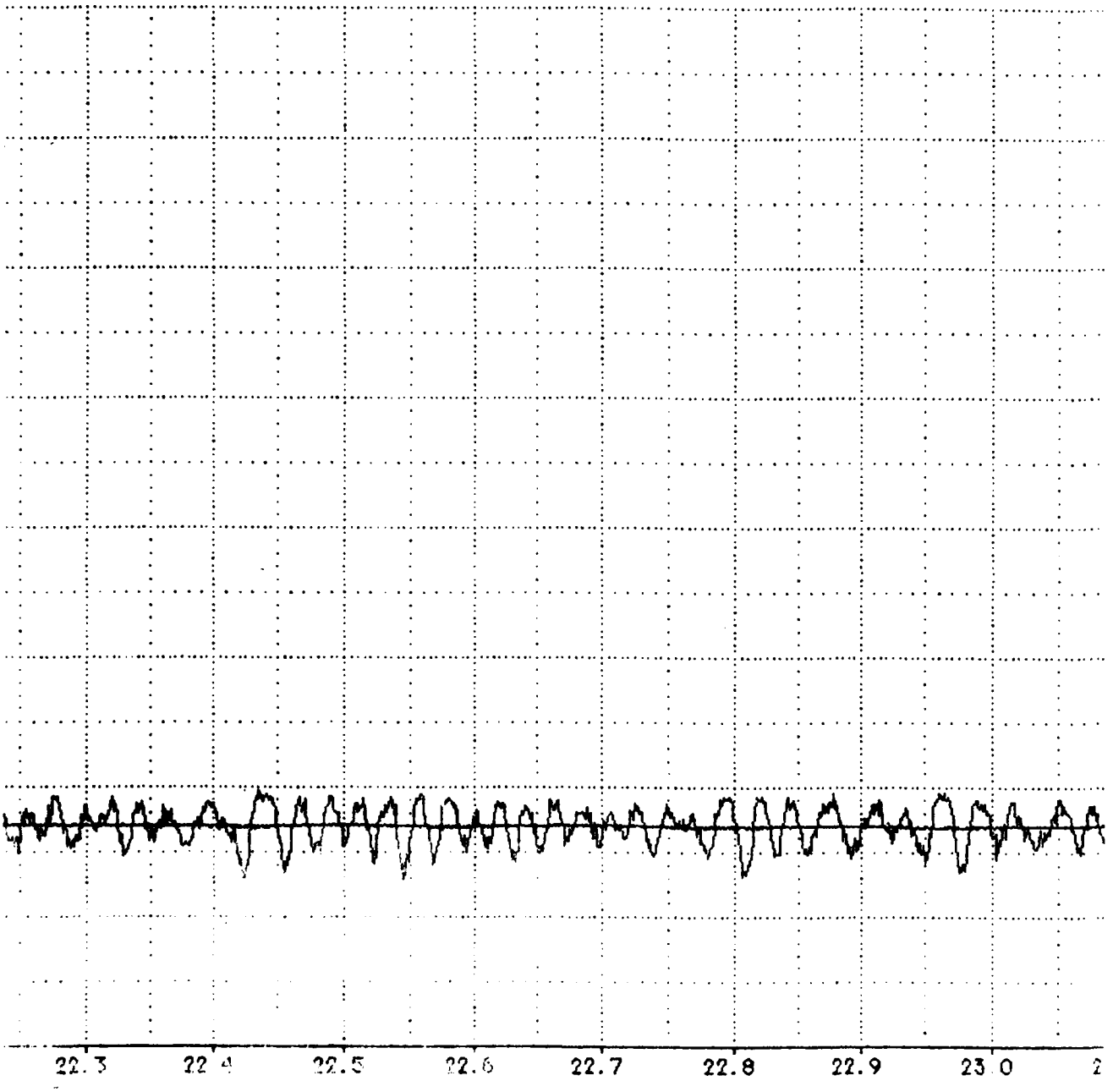
22.3
22.4
22.5
22.6
22.7
22.8
22.9
23.0

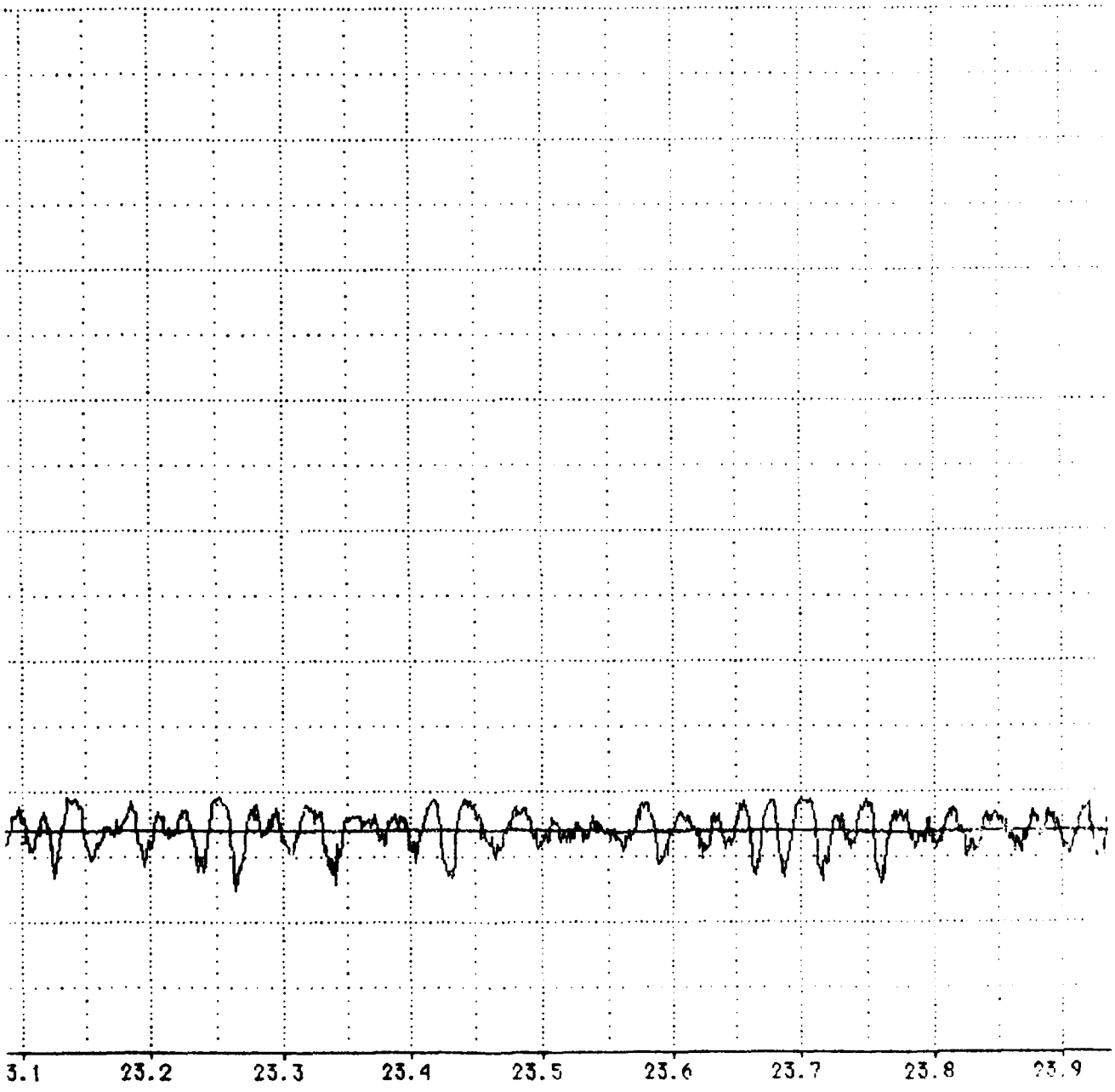
3.1
23.2
23.3
23.4
23.5
23.6
23.7
23.8
23.9

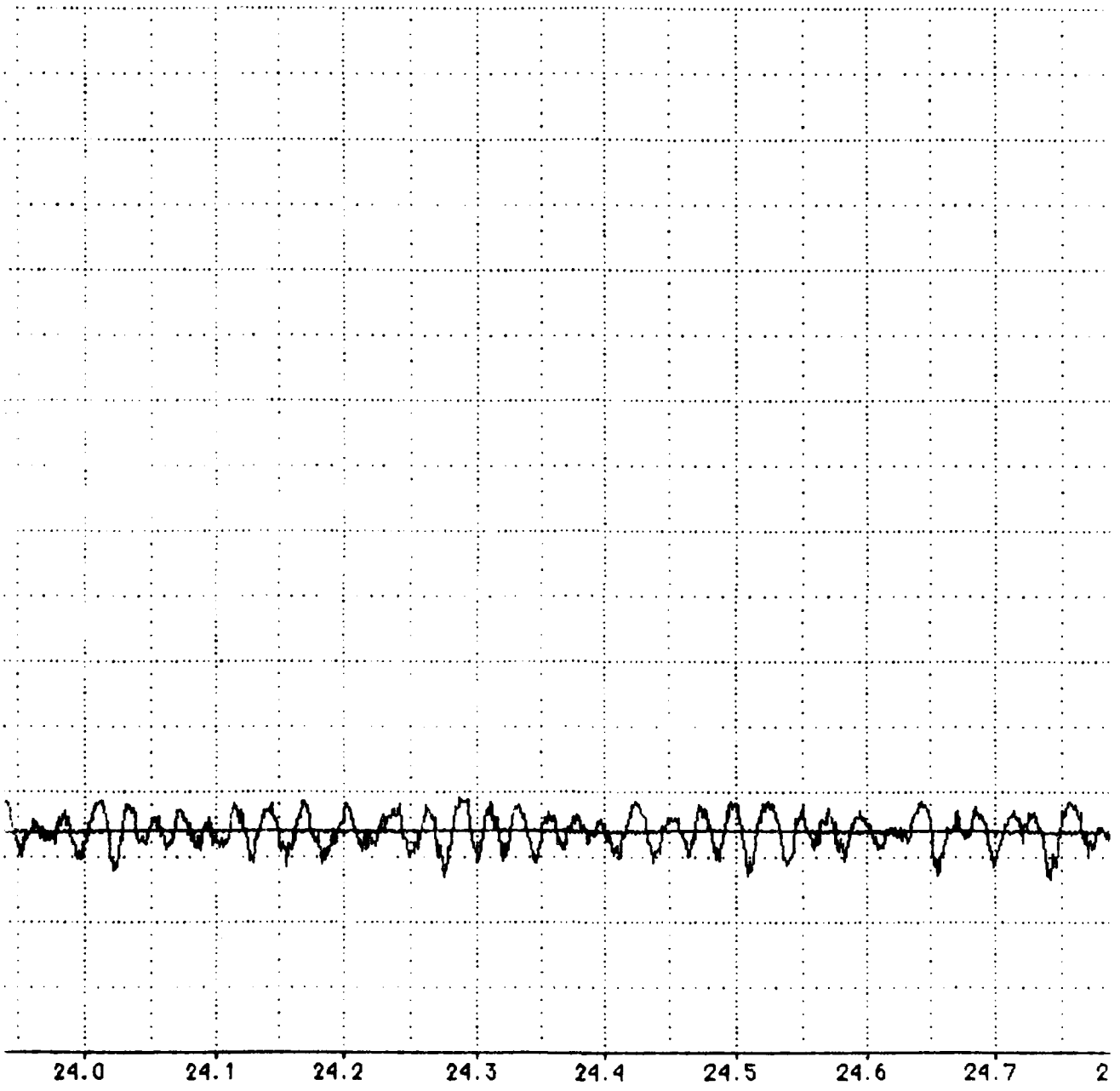
24.0
24.1
24.2
24.3
24.4
24.5
24.6
24.7
2

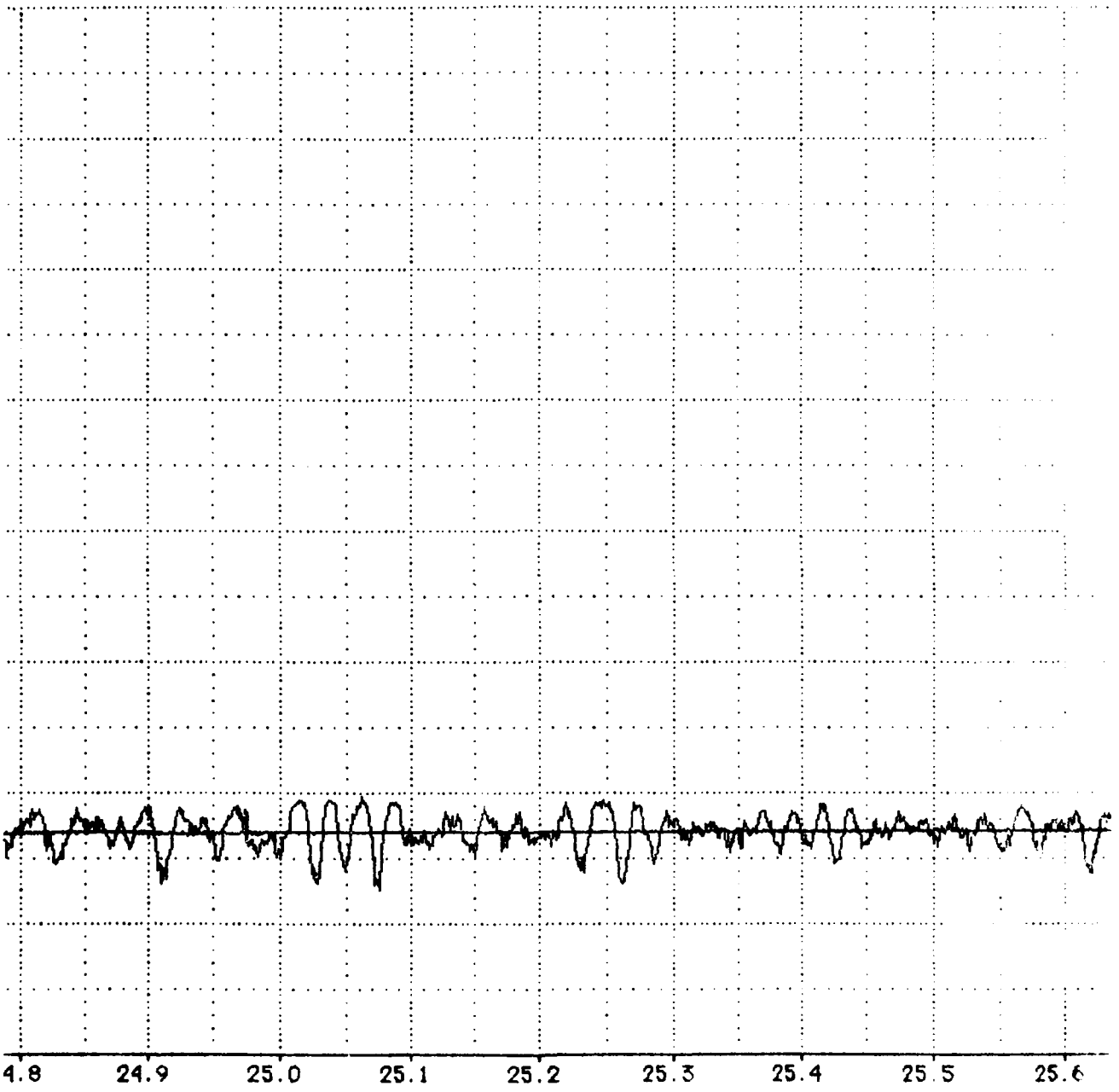
4.8
24.9
25.0
25.1
25.2
25.3
25.4
25.5
25.6

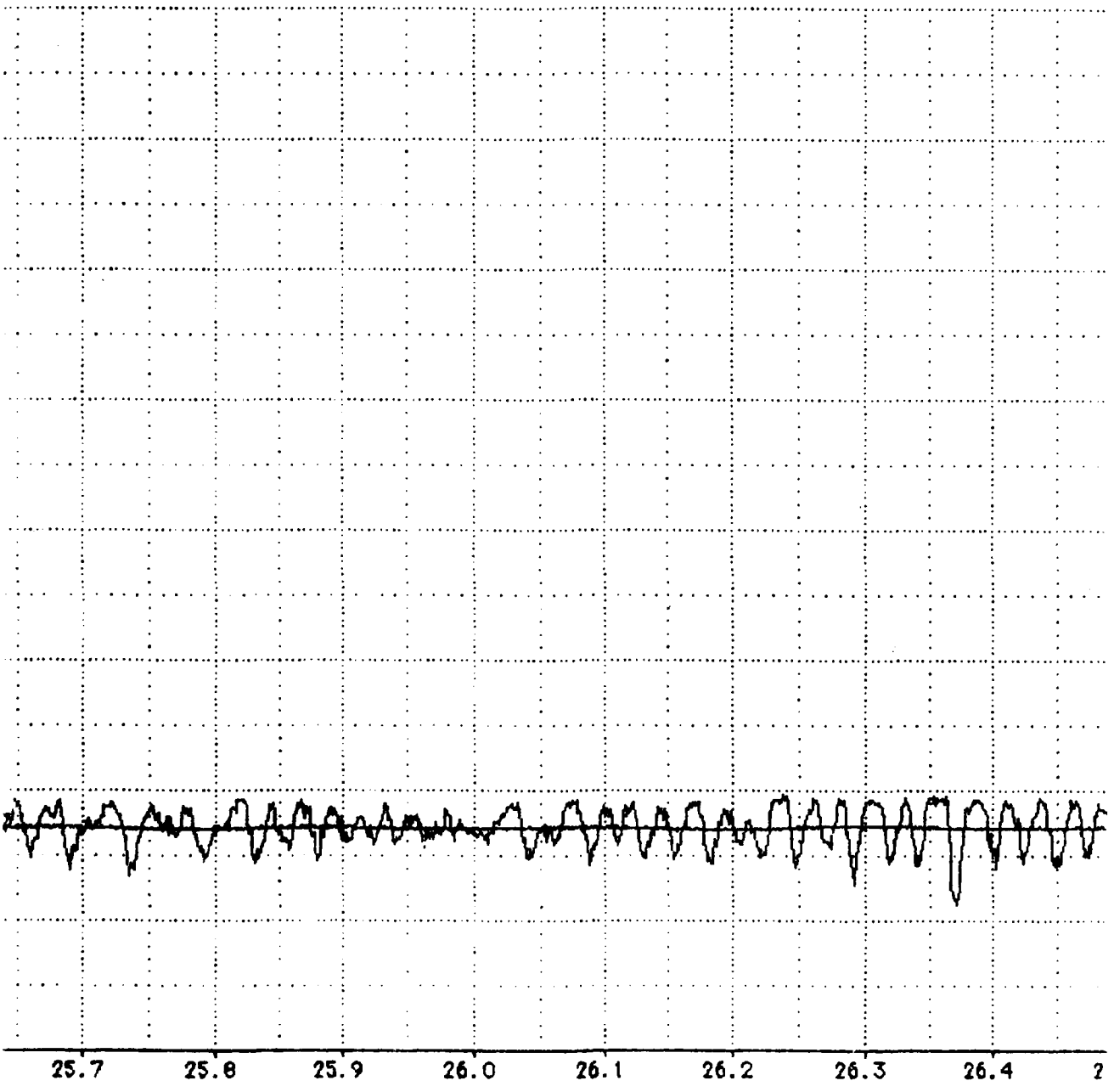
25.7
25.8
25.9
26.0
26.1
26.2
26.3
26.4

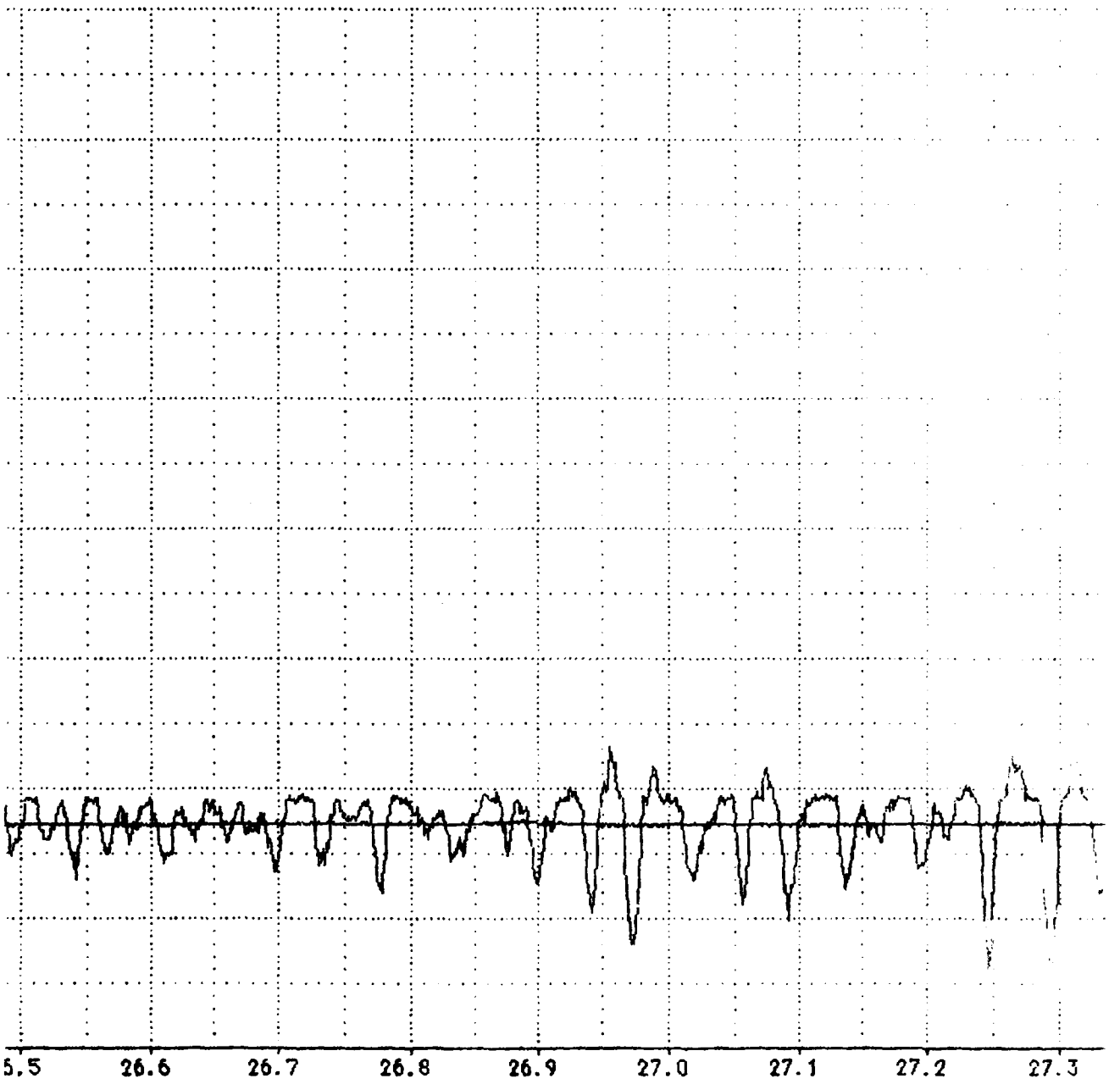
5.5
26.6
26.7
26.8
26.9
27.0
27.1
27.2
27.3

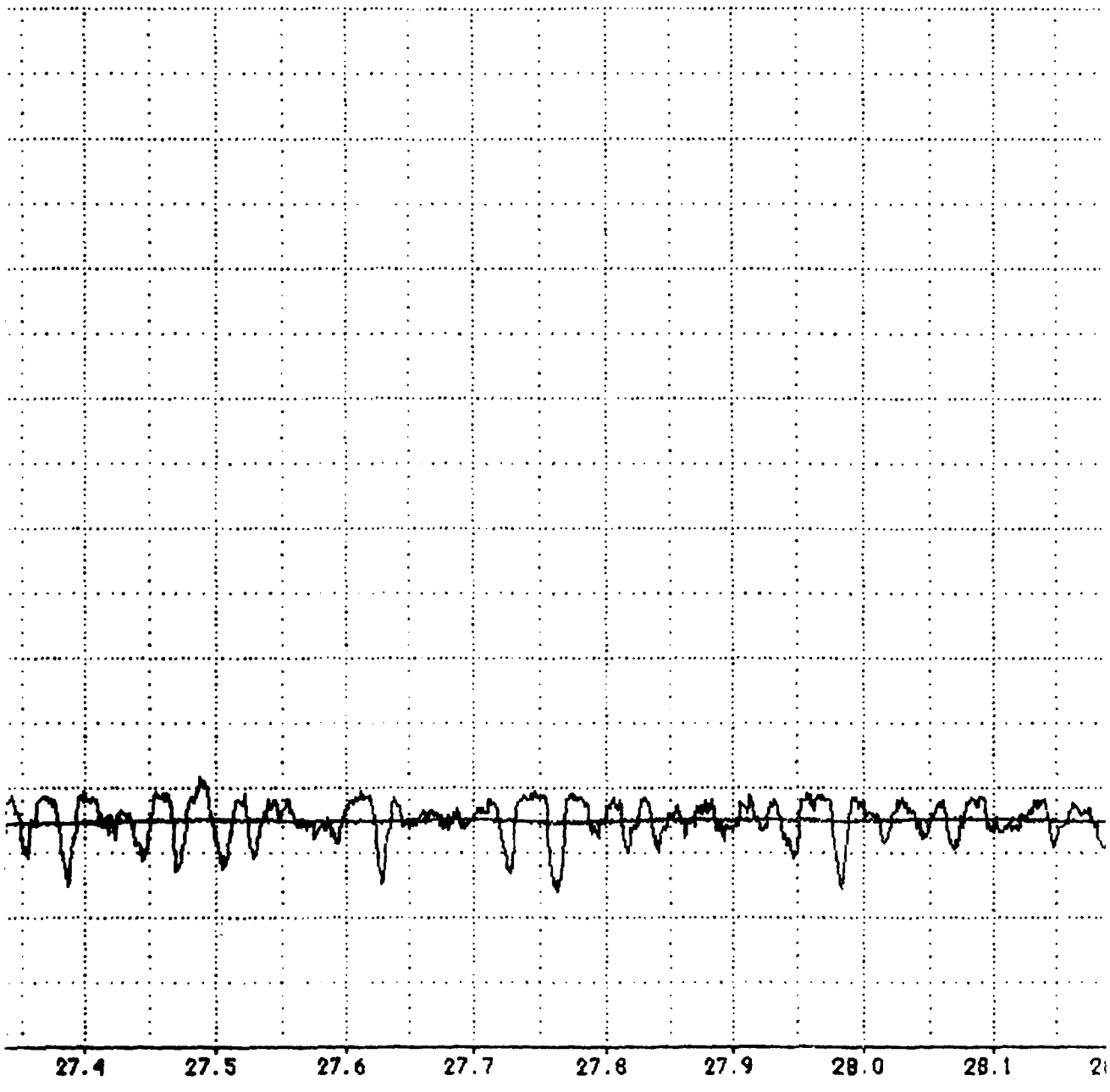
27.4
27.5
27.6
27.7
27.8
27.9
28.0
28.1

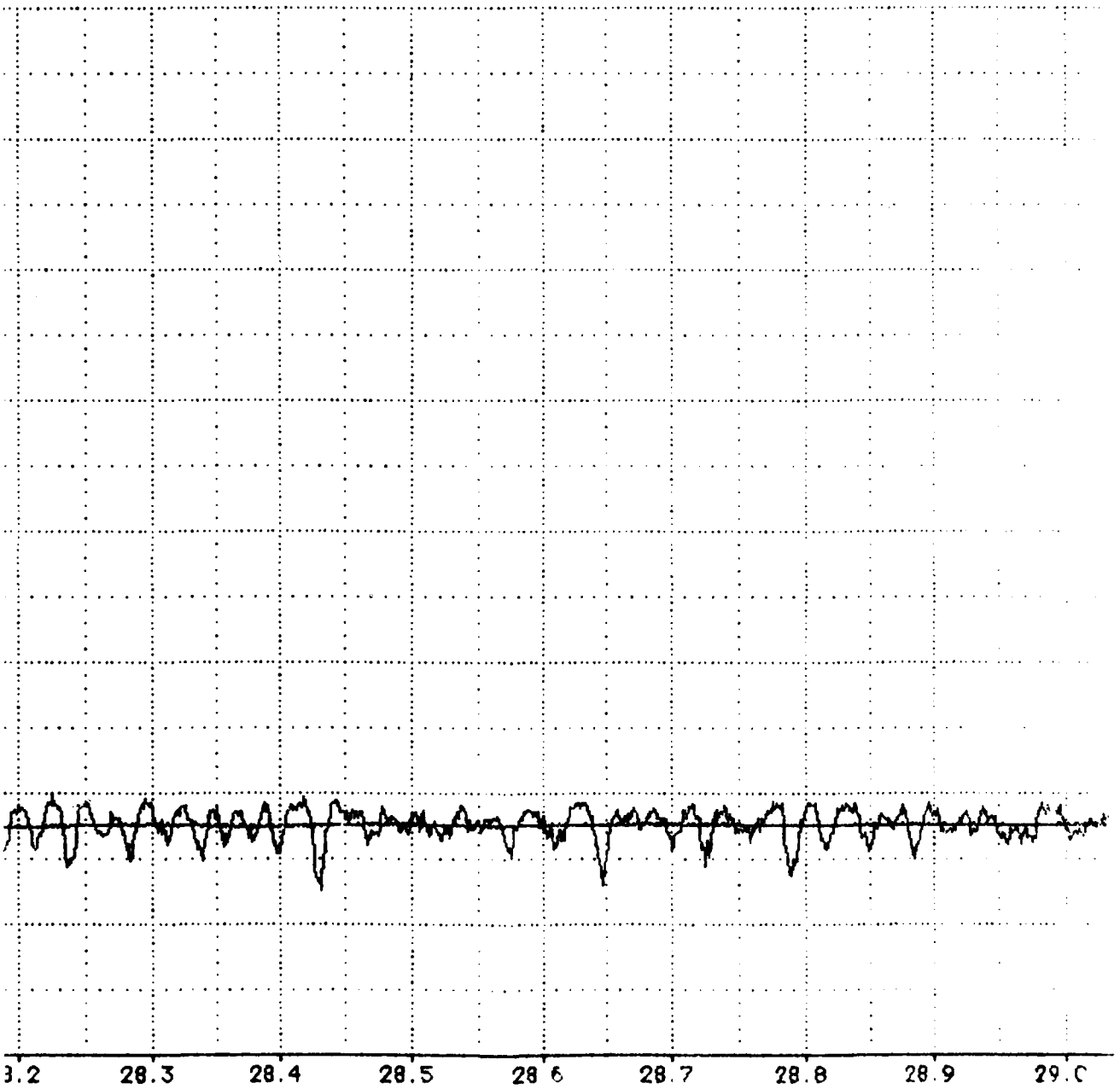
3.2
28.3
28.4
28.5
28 6
28.7
28.8
28.9
29.C

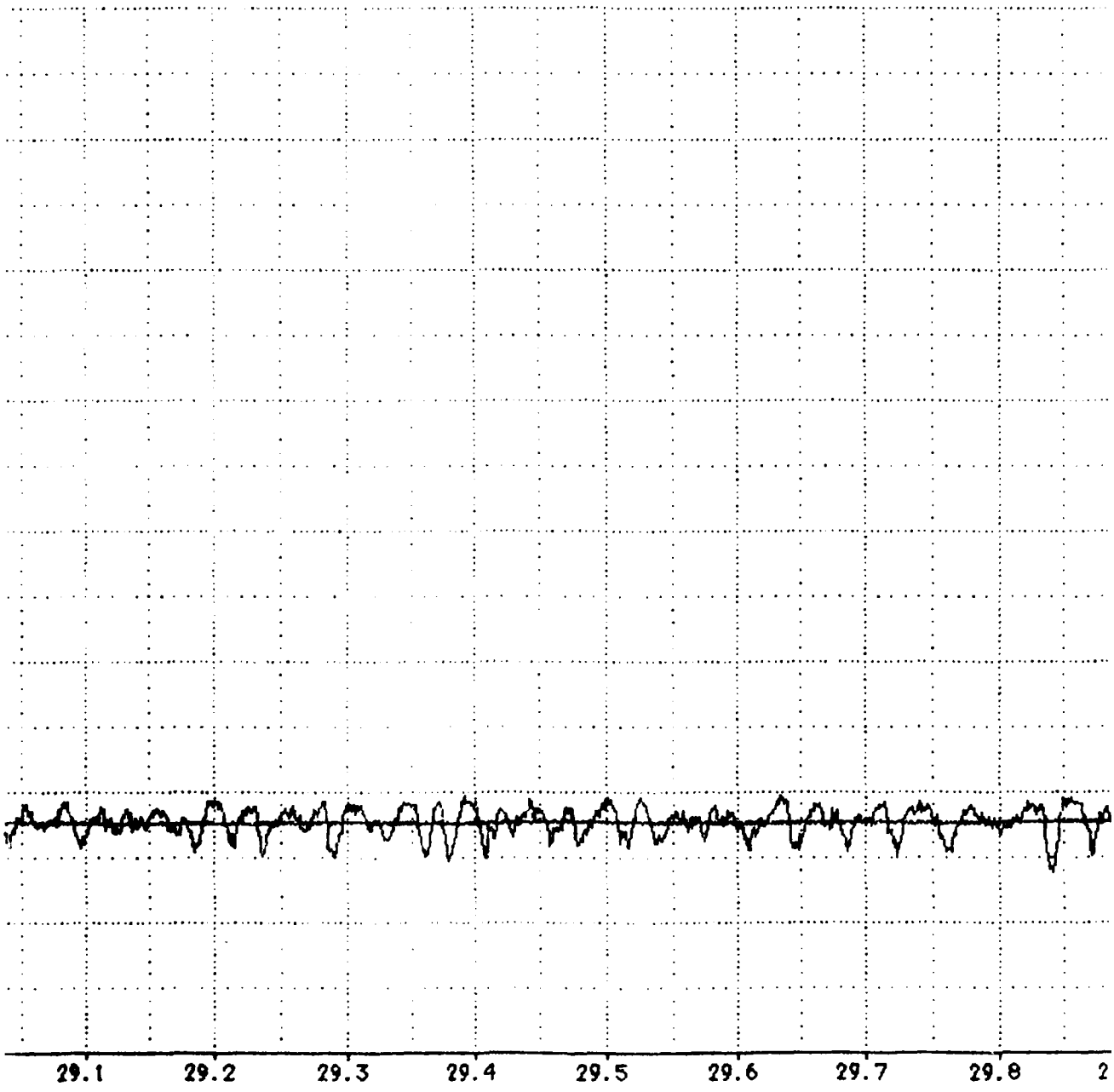
29.1
29.2
29.3
29.4
29.5
29.6
29.7
29.8
2

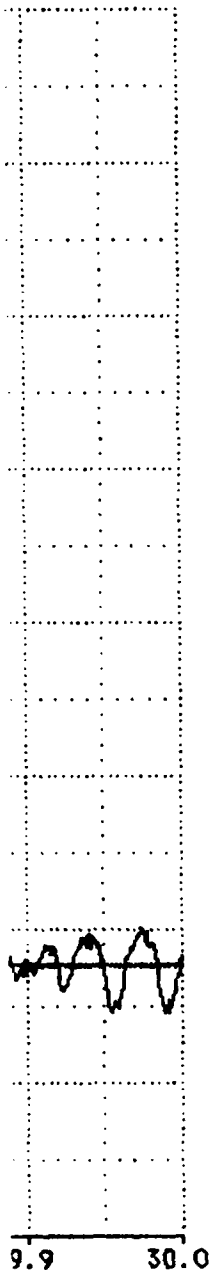
9.9
30.0

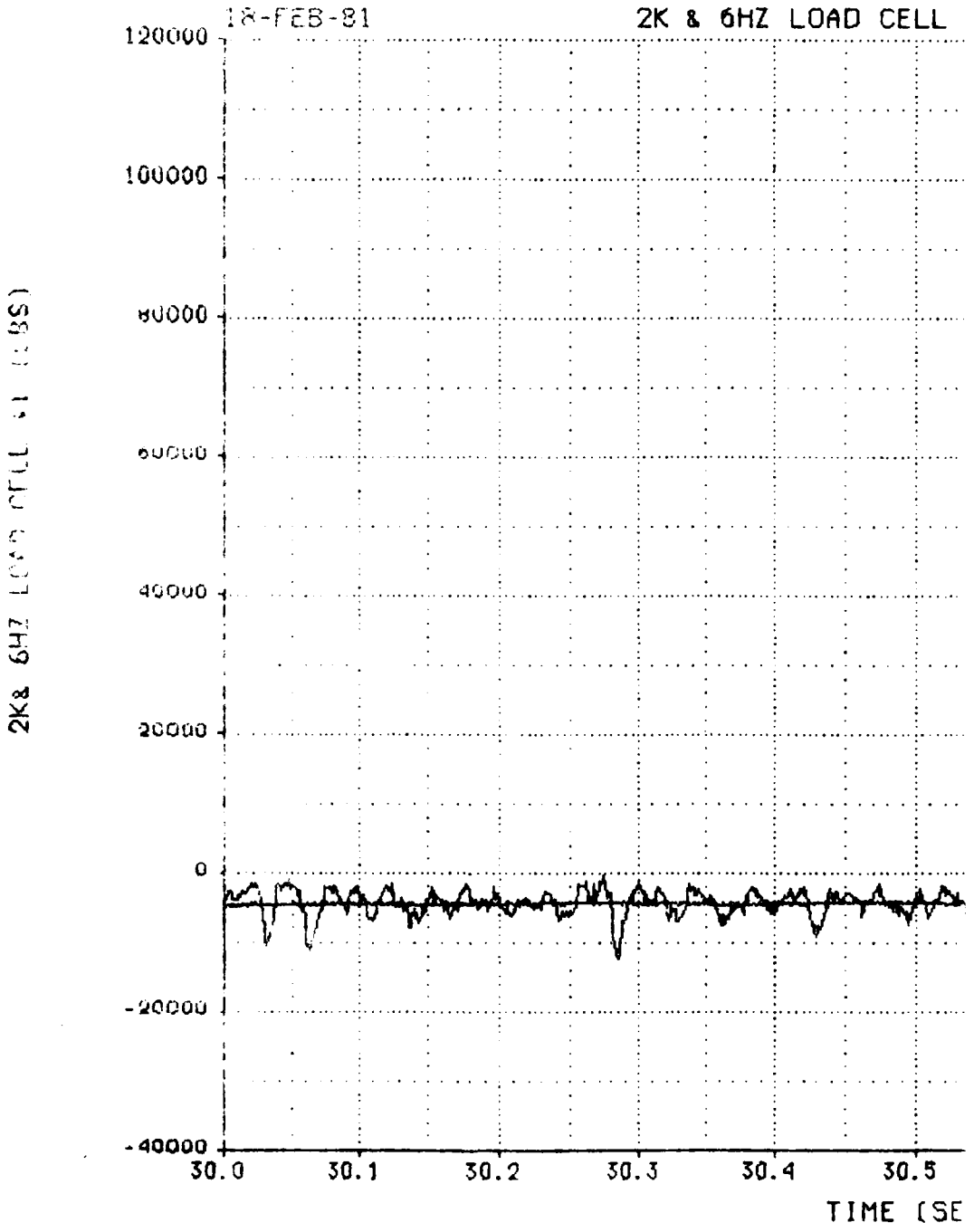
18-FEB-81
2K & 6HZ LOAD CELL
120000
100000
80000
60000
40000
20000
0
-20000
-40000
30.0
30.1
30.2
30.3
30.4
30.5
TIME (SE

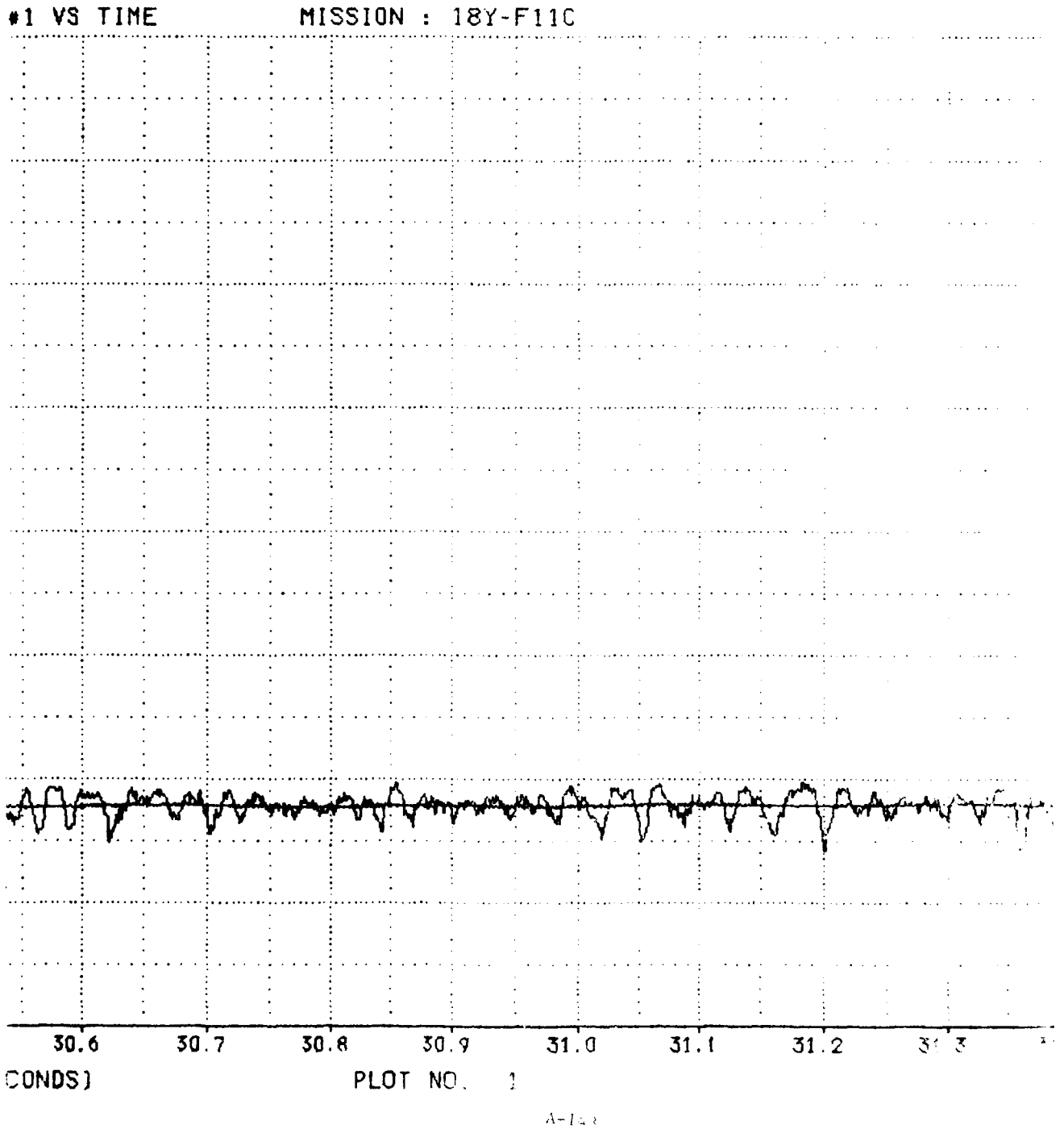
#1 VS TIME
MISSION : 18Y-F11C
30.6
30.7
30.8
30.9
31.0
31.1
31.2
CONDS)
PLOT NO. 1

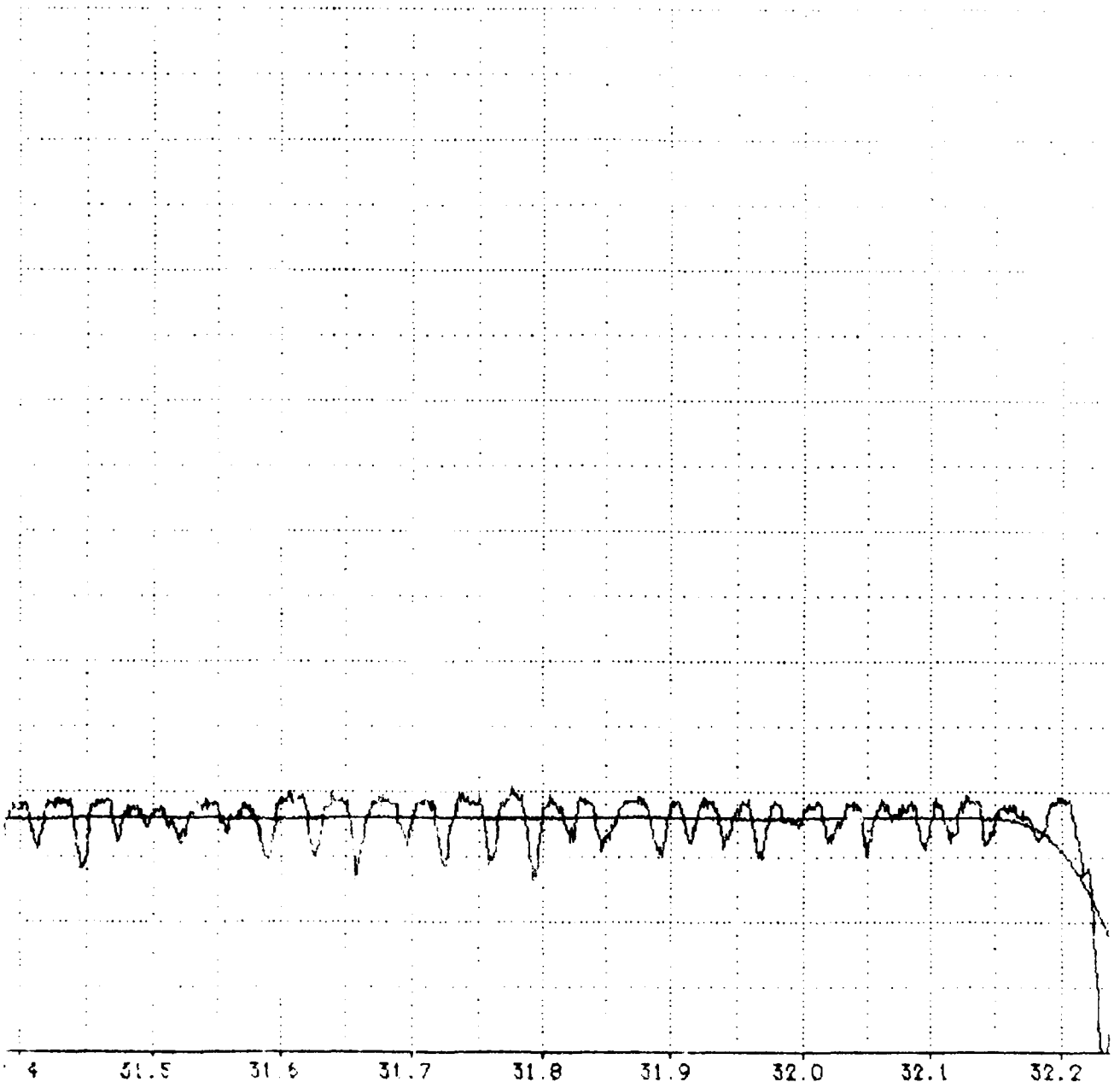
4
31.5
31.6
31.7
31.8
31.9
32.0
32.1
32.2

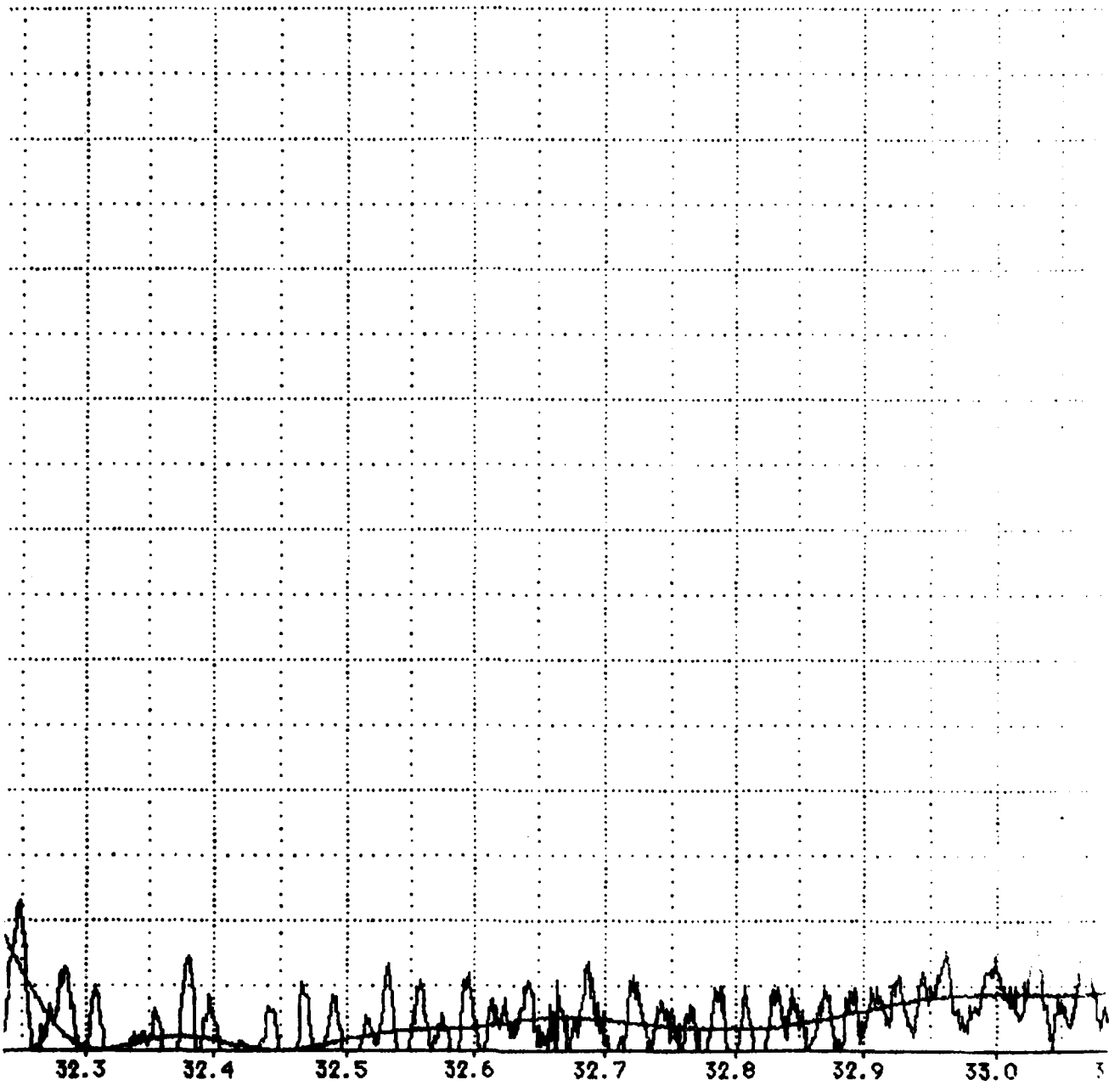
32.3
32.4
32.5
32.6
32.7
32.8
32.9
33.0

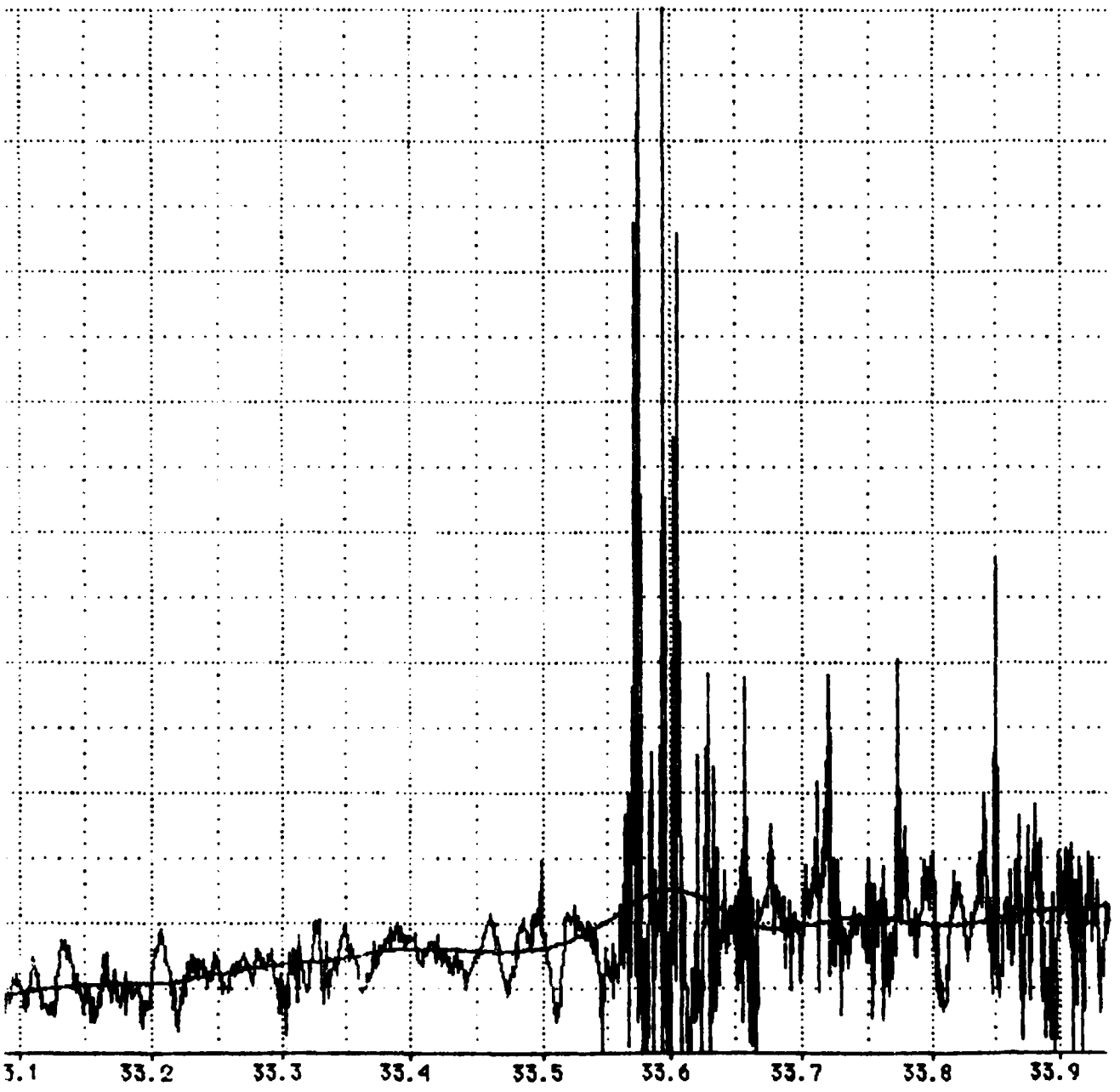
3.1
33.2
33.3
33.4
33.5
33.6
33.7
33.8
33.9

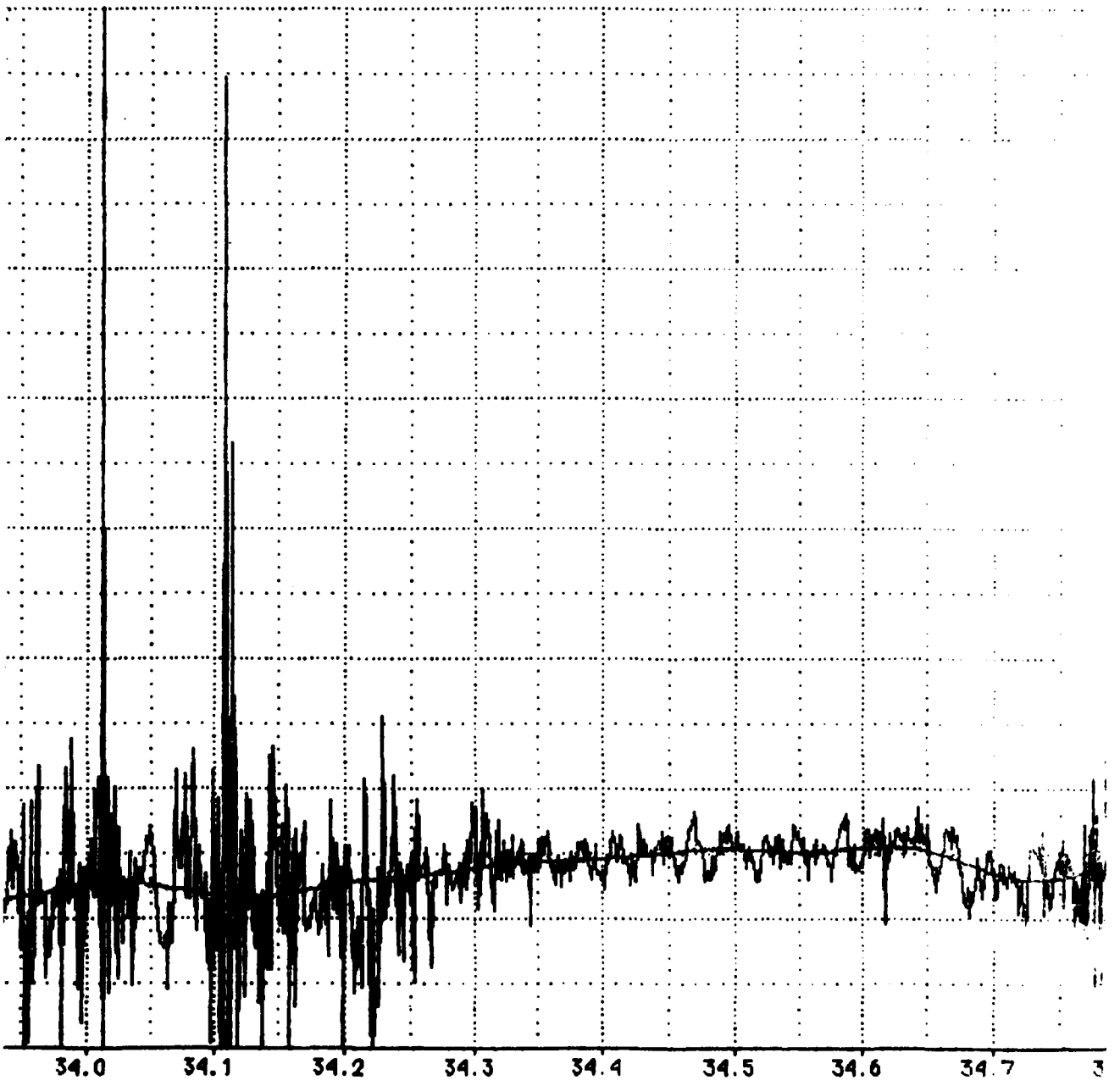
34.0
34.1
34.2
34.3
34.4
34.5
34.6
34.7

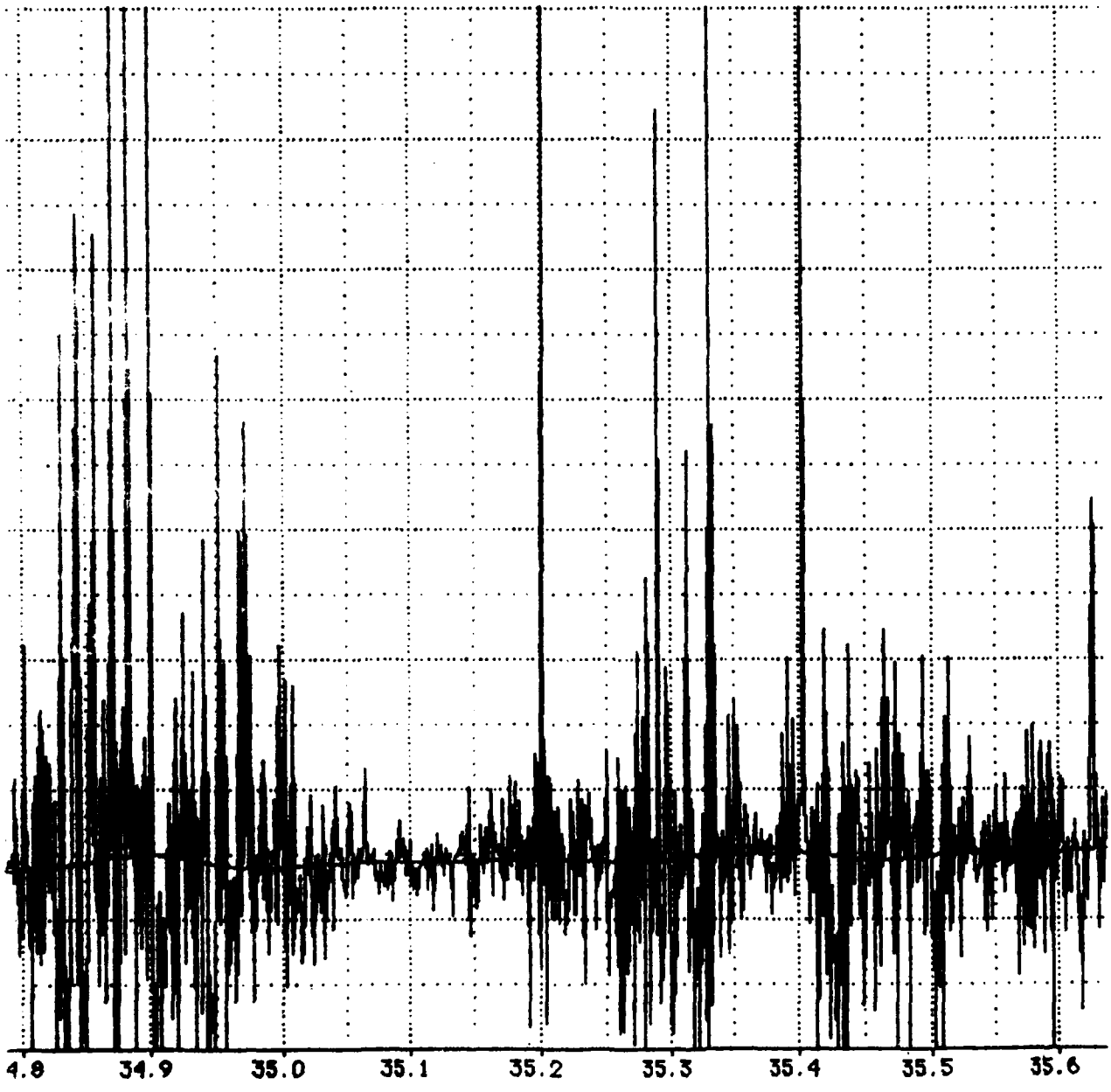
4.8
34.9
35.0
35.1
35.2
35.3
35.4
35.5
35.6

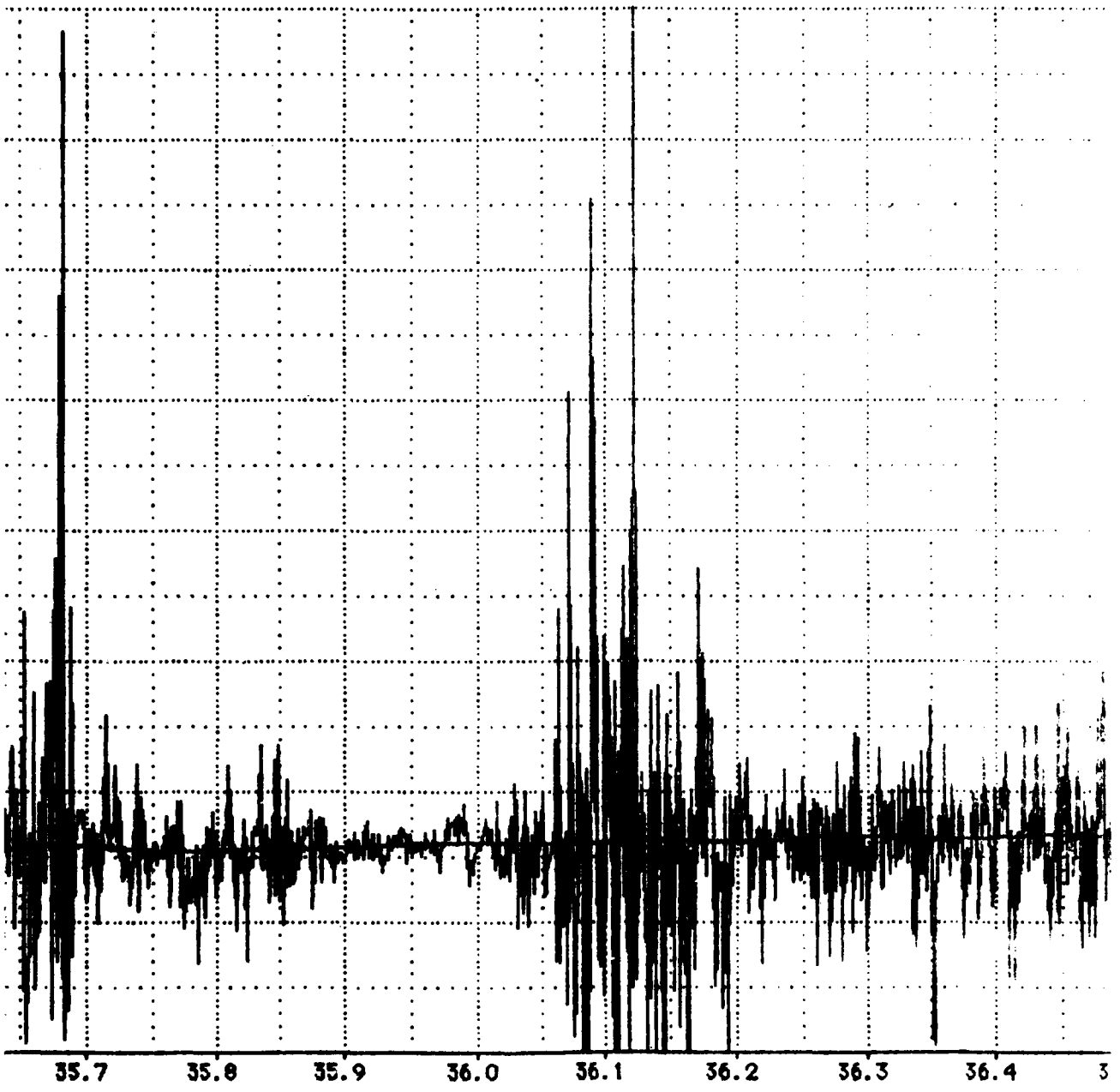
35.7
35.8
35.9
36.0
36.1
36.2
36.3
36.4

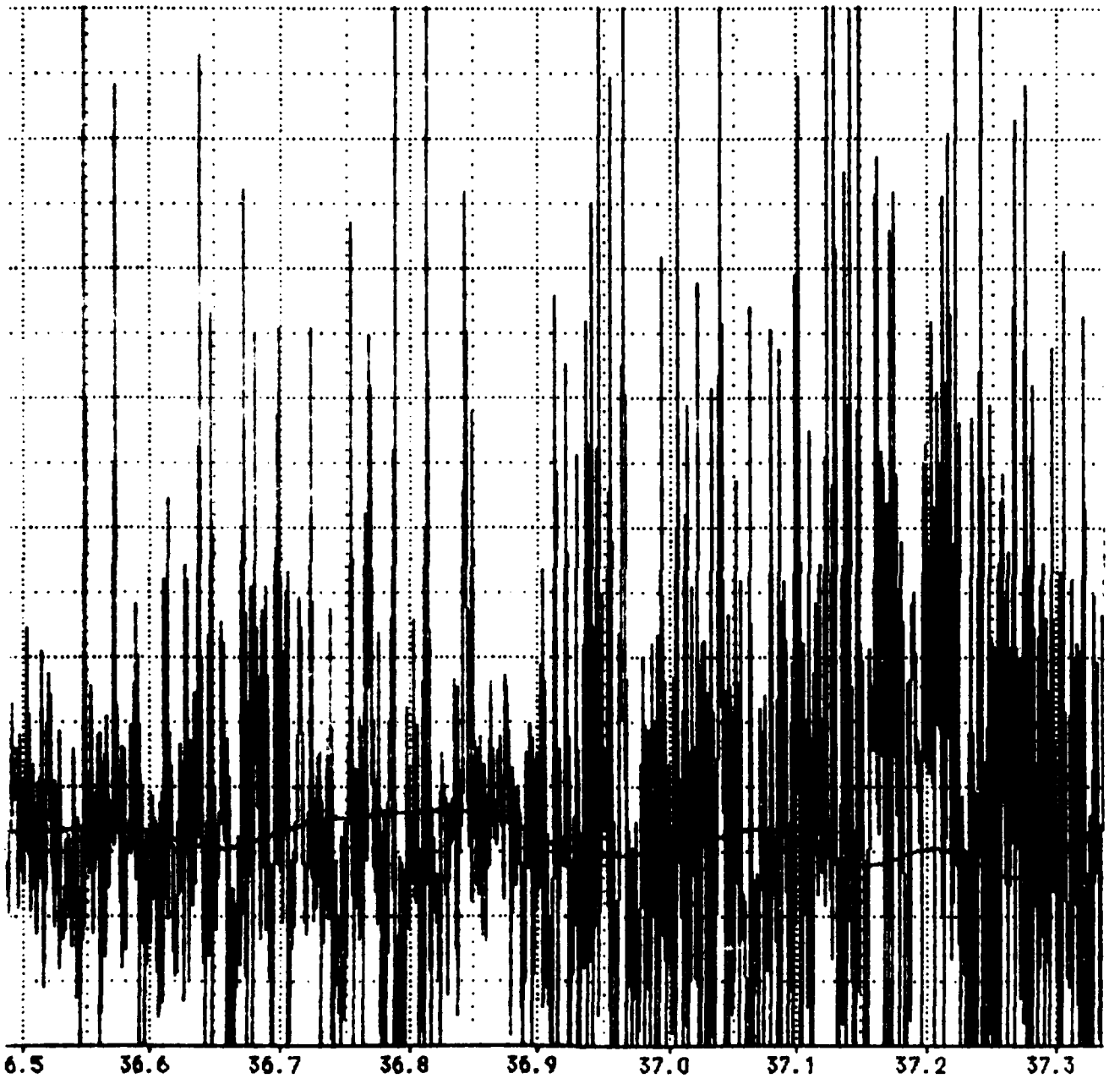
6.5
36.6
36.7
36.8
36.9
37.0
37.1
37.2
37.3

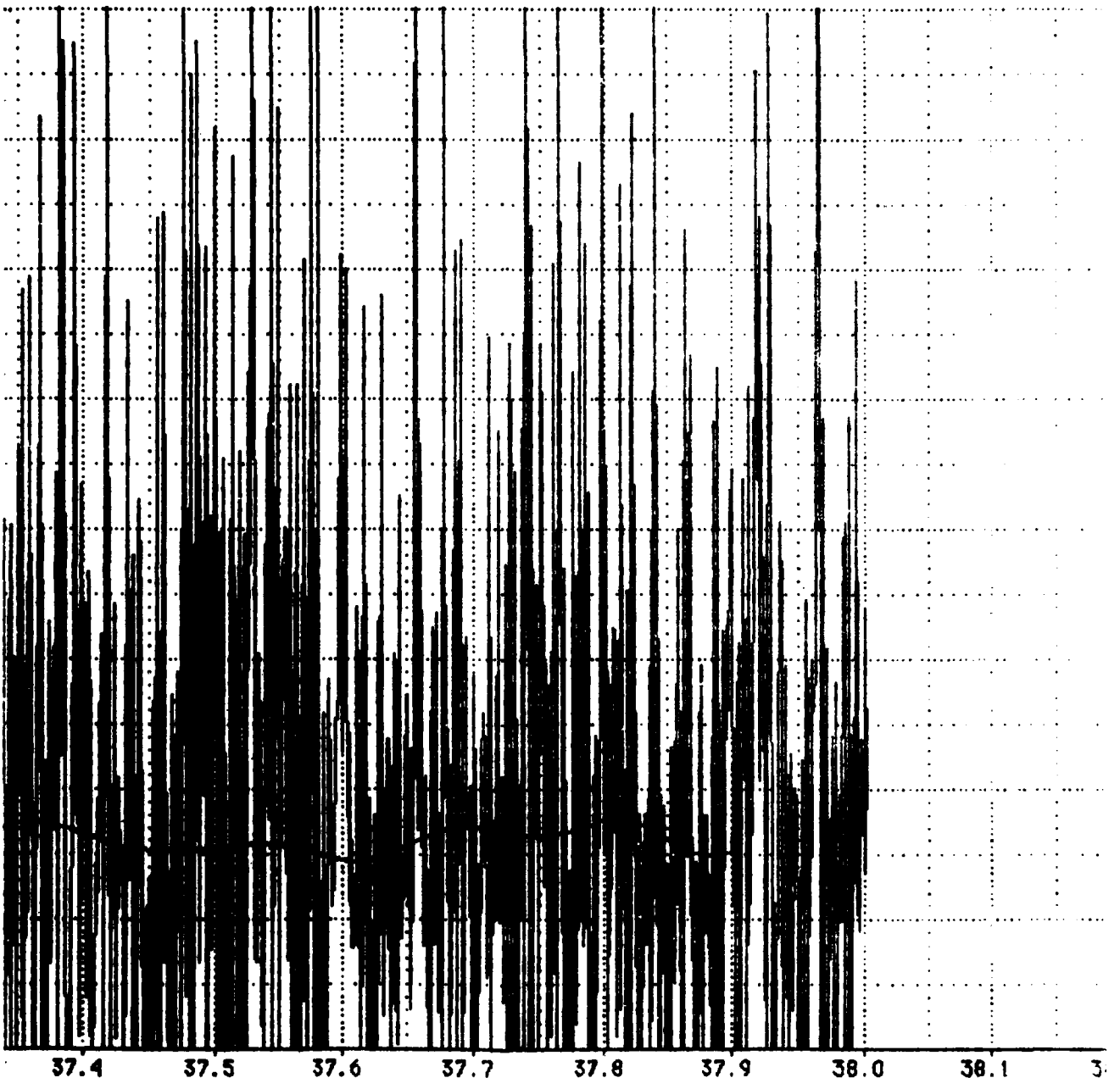
37.4
37.5
37.6
37.7
37.8
37.9
38.0
38.1

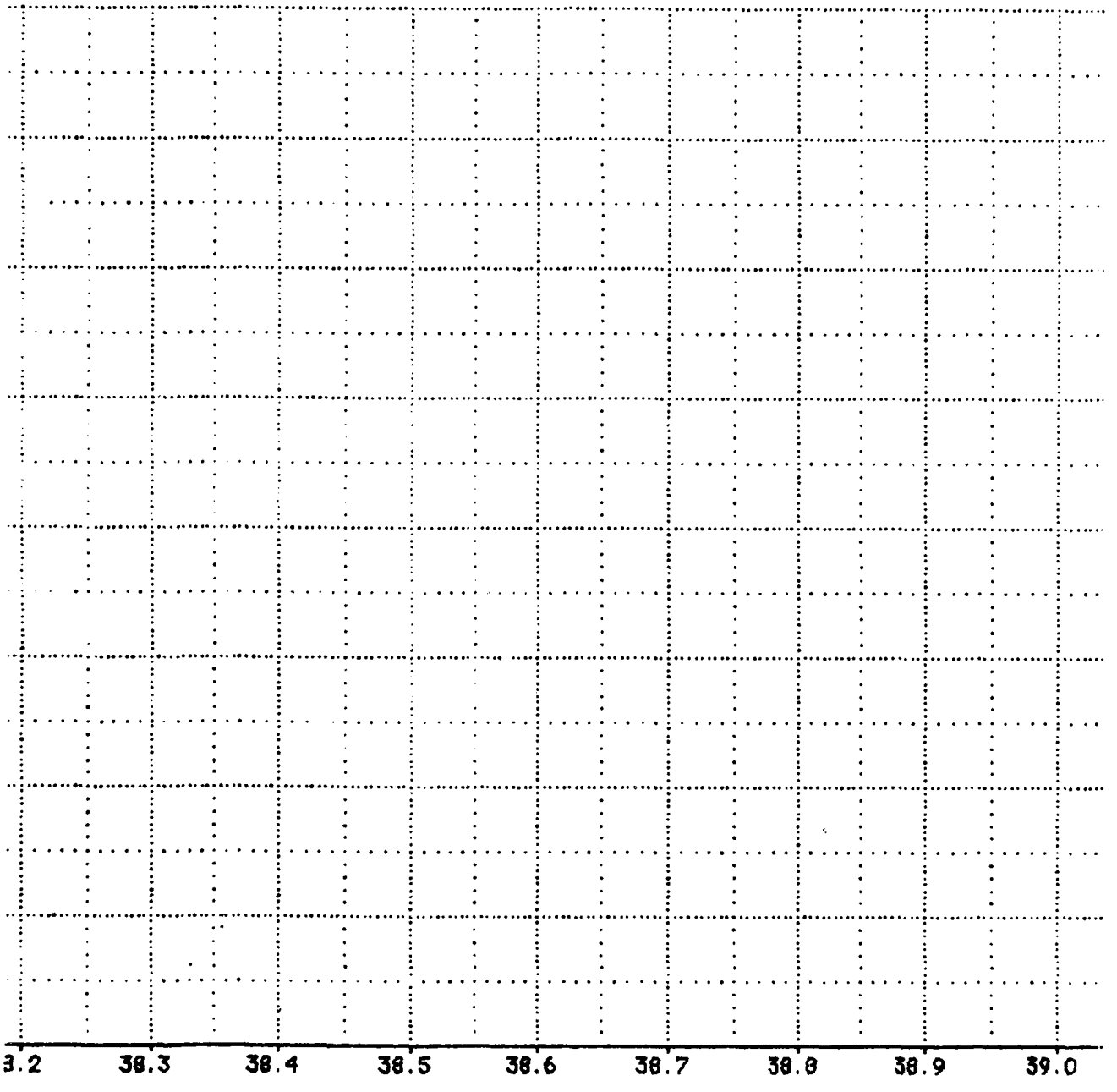
38.2
38.3
38.4
38.5
38.6
38.7
38.8
38.9
39.0

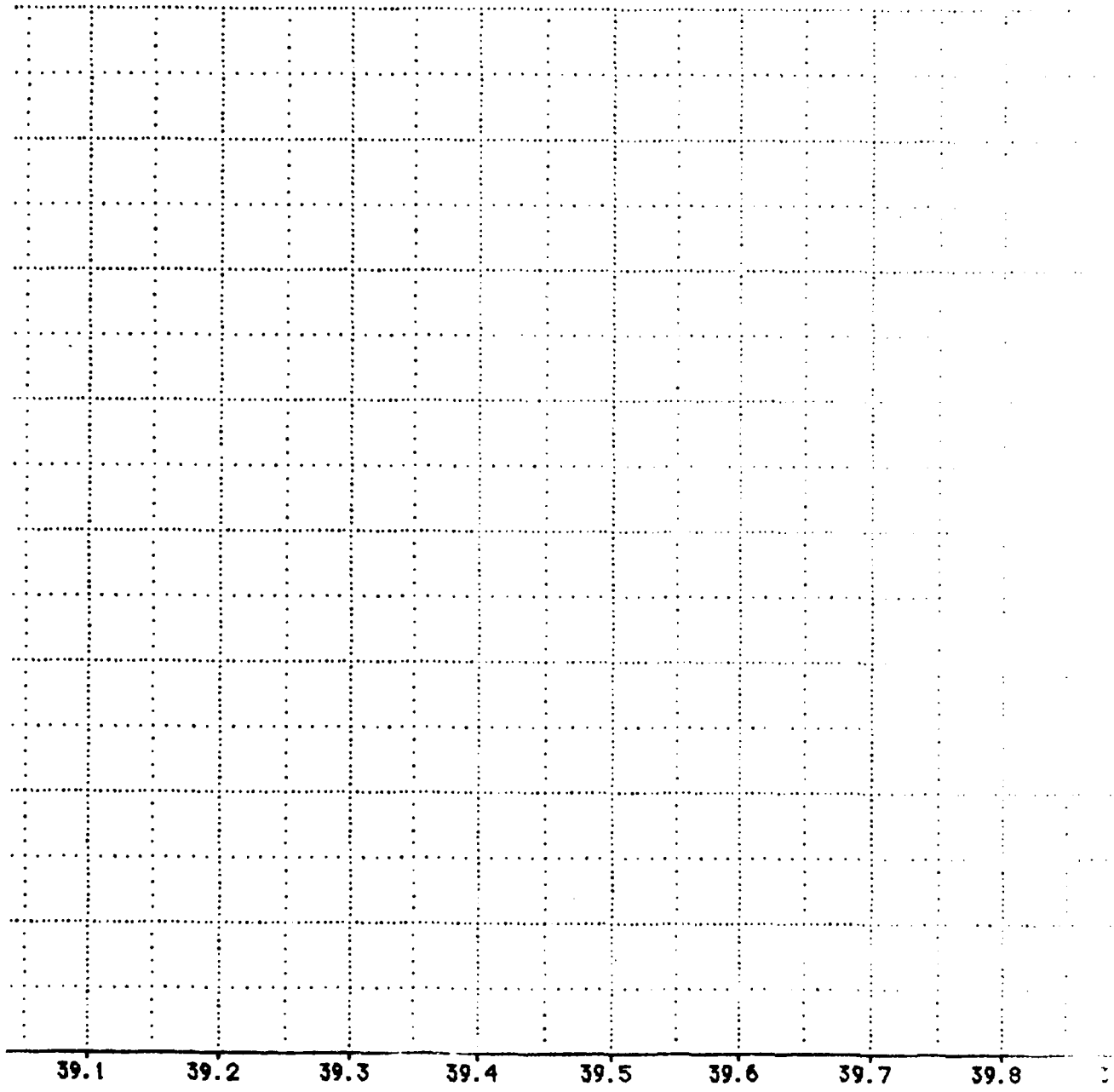
39.1
39.2
39.3
39.4
39.5
39.6
39.7
39.8

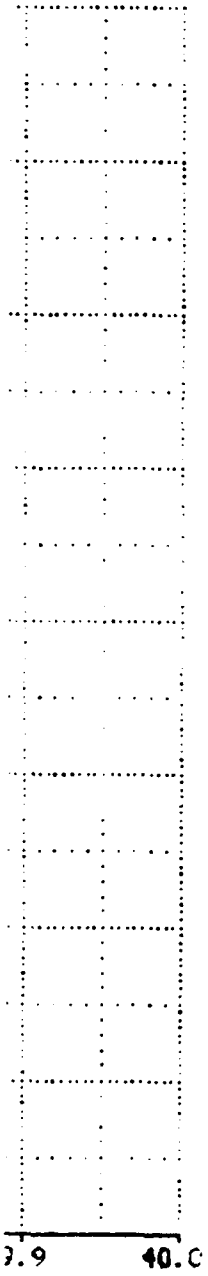
9.9
40.0

APPENDIX B

18Y-F9C RESIDUALS

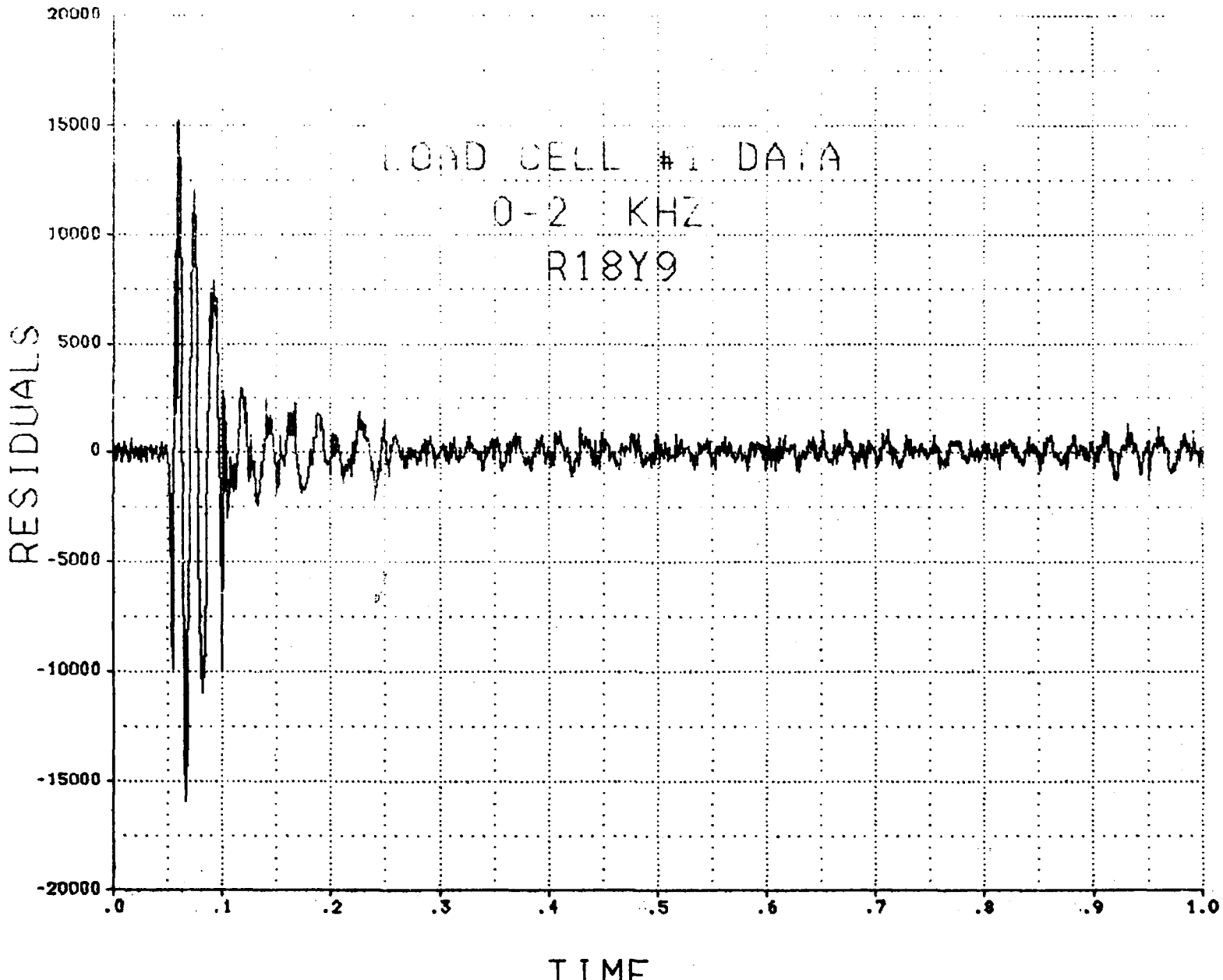
LOAD CELL #1 DATA
0-2 KHZ
R18Y9
RESIDUALS
TIME
20000
15000
10000
5000
0
-5000
-10000
-15000
-20000
.0
.1
.2
.3
.4
.5
.6
.7
.8
.9
1.0

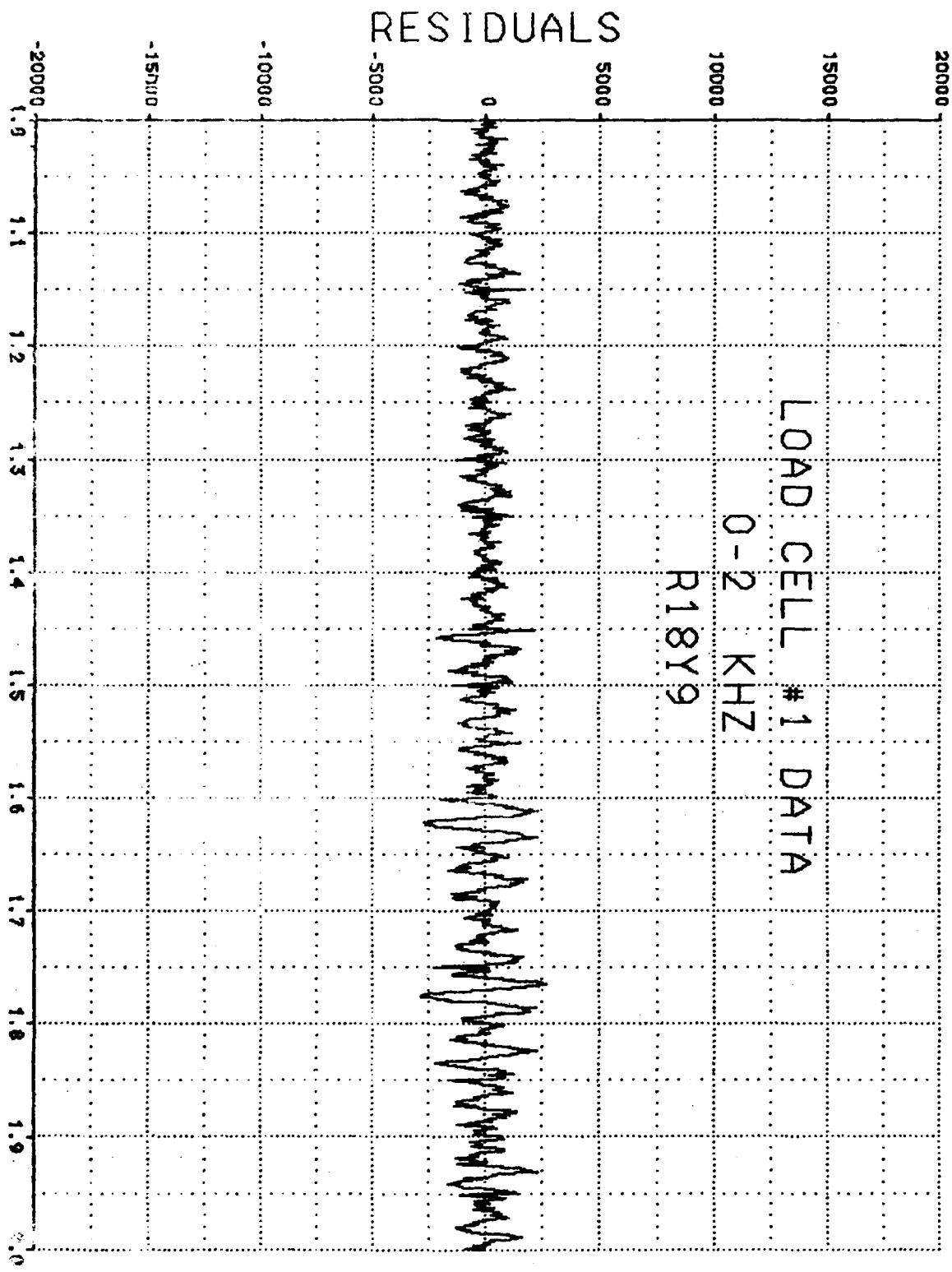
RESIDUALS
-20000
-15000
-10000
-5000
0
5000
10000
15000
20000
1.0
1.1
1.2
1.3
1.4
1.5
1.6
1.7
1.8
1.9
2.0
TIME
LOAD CELL #1 DATA
0-2 KHZ
R18Y9

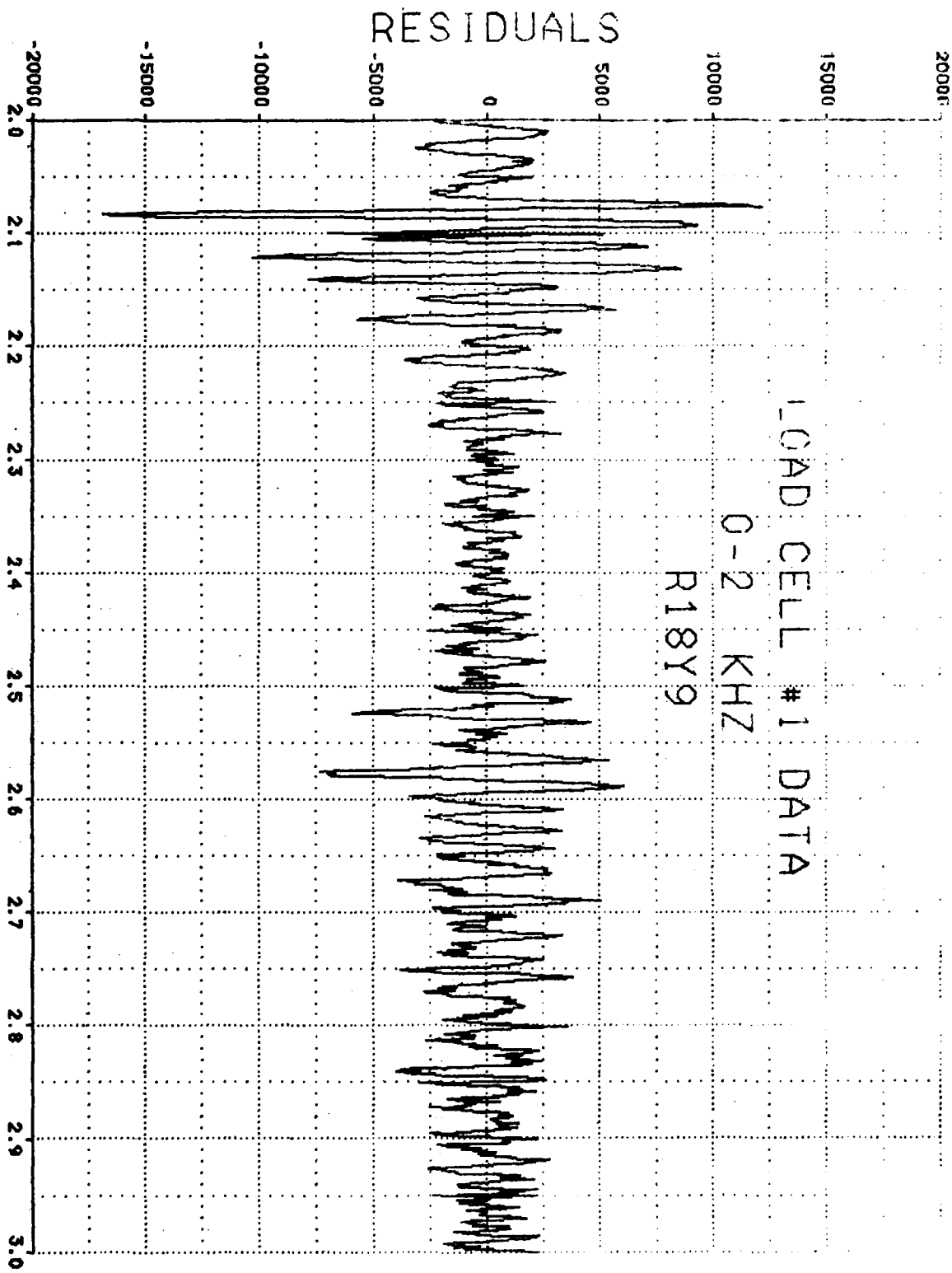
RESIDUALS
-20000
-15000
-10000
-5000
0
5000
10000
15000
20000
2.0
2.1
2.2
2.3
2.4
2.5
2.6
2.7
2.8
2.9
3.0
TIME
LOAD CELL #1 DATA
0-2 KHZ
R18Y9

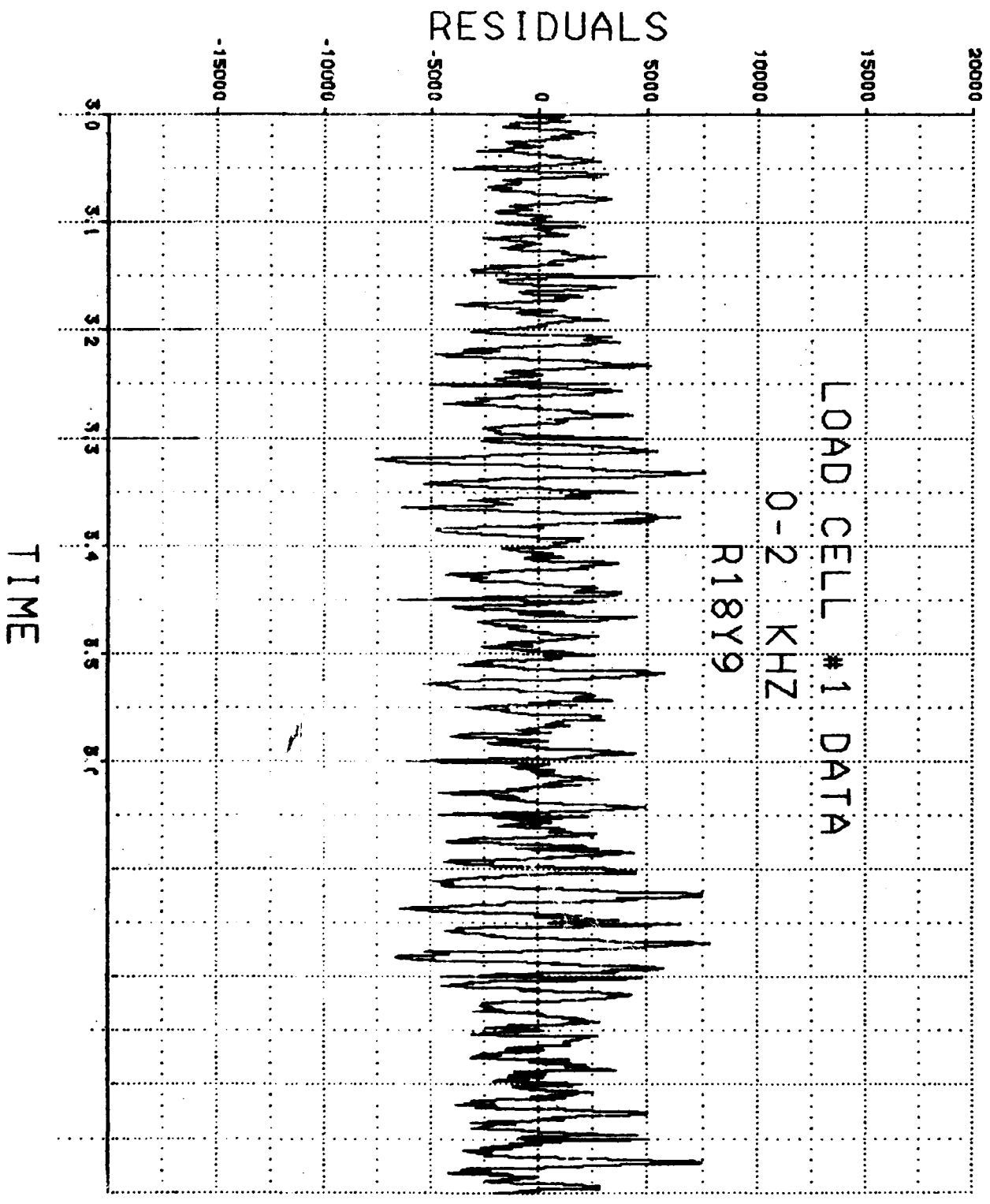
RESIDUALS
-15000
-10000
-5000
0
5000
10000
15000
20000
3.0
3.1
3.2
3.3
3.4
3.5
3.6
TIME
LOAD CELL #1 DATA
0-2 KHZ
R18Y9

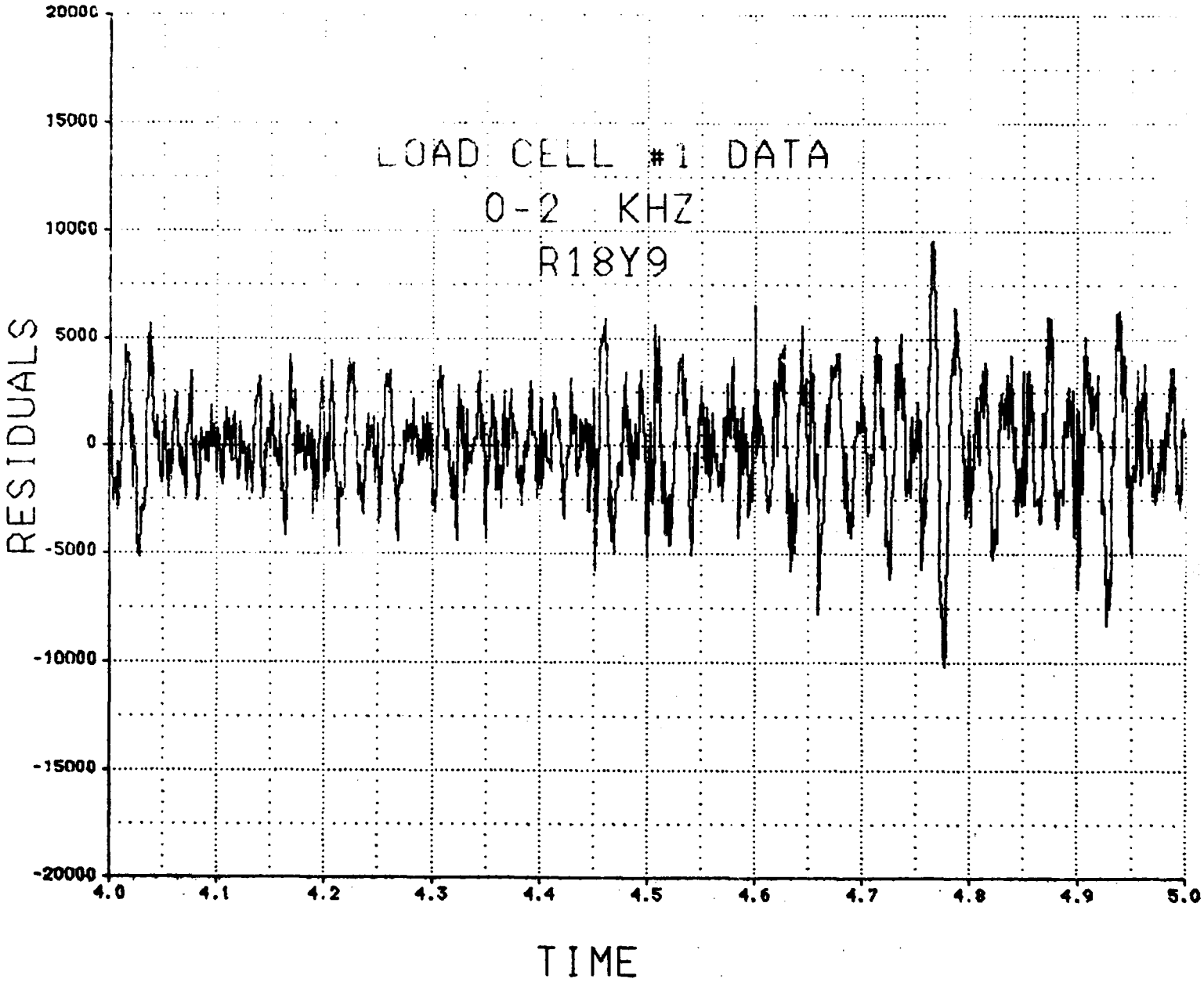
LOAD CELL #1 DATA
0-2 KHZ
R18Y9
RESIDUALS
TIME
20000
15000
10000
5000
0
-5000
-10000
-15000
-20000
4.0
4.1
4.2
4.3
4.4
4.5
4.6
4.7
4.8
4.9
5.0

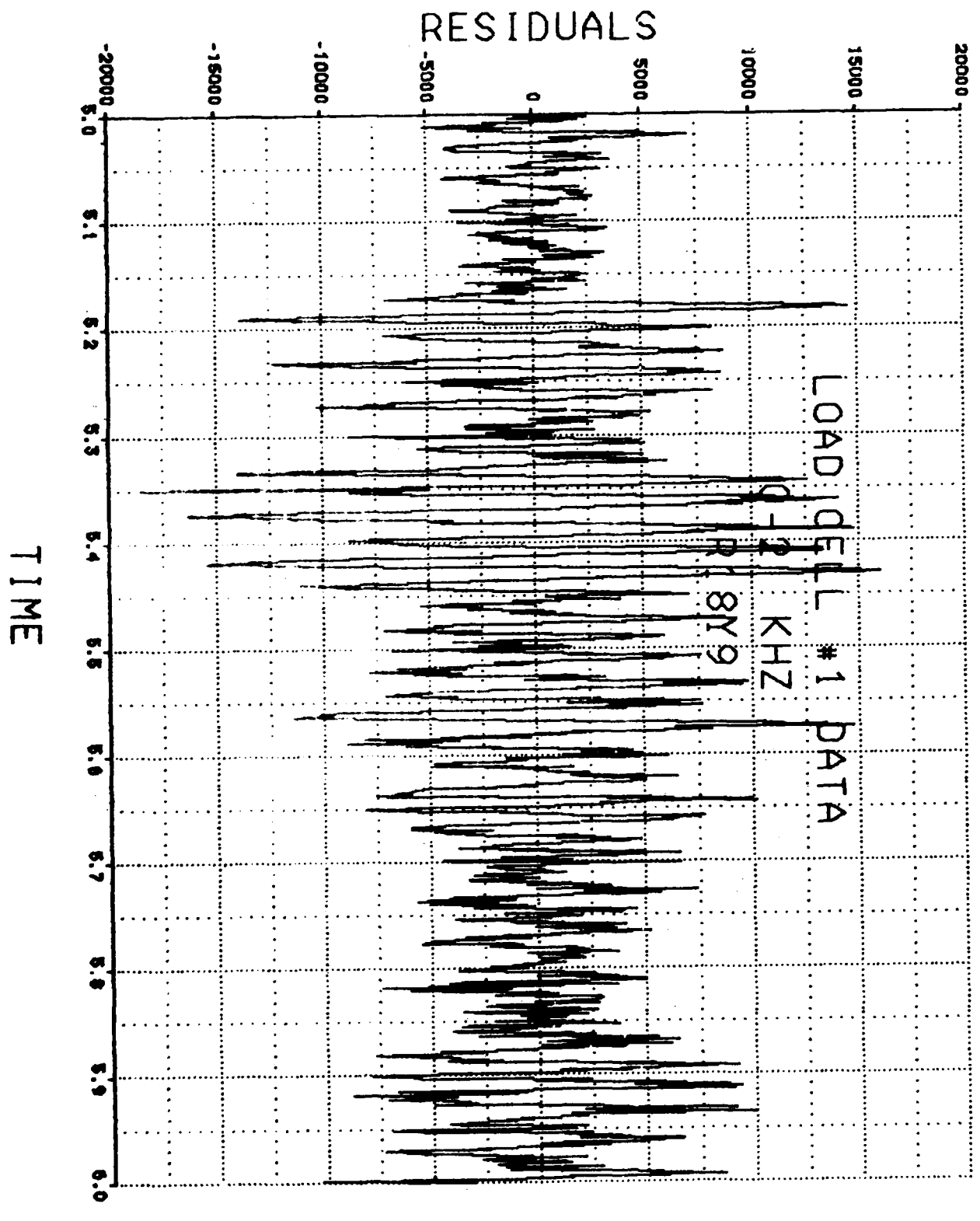
RESIDUALS
-20000
-15000
-10000
-5000
0
5000
10000
15000
20000
5.0
5.1
5.2
5.3
5.4
5.5
5.6
5.7
5.8
5.9
6.0
TIME
LOAD CELL #1 DATA
RUN 8Y6
KHZ

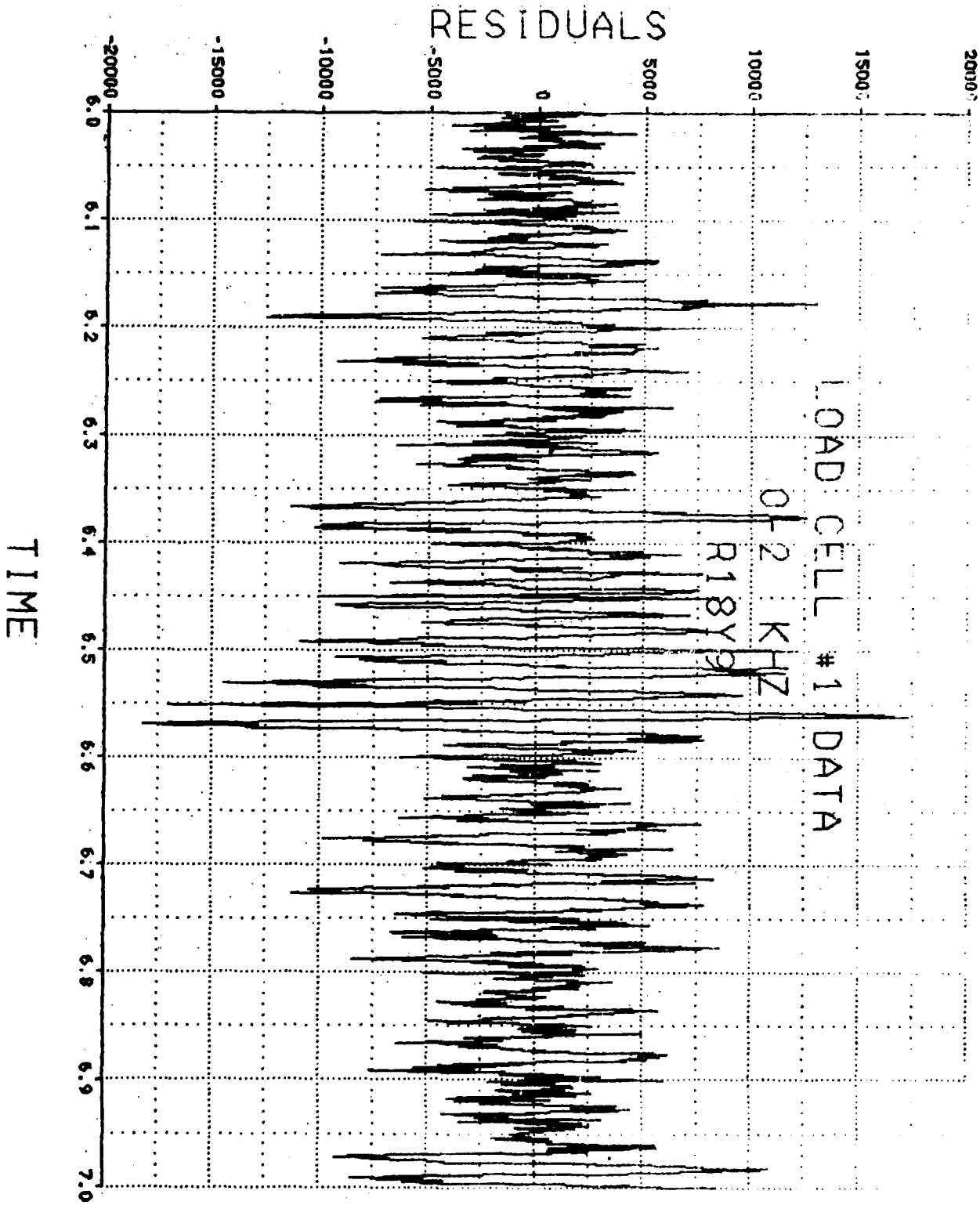
RESIDUALS
-20000
-15000
-10000
-5000
0
5000
10000
15000
20000
6.0
6.1
6.2
6.3
6.4
6.5
6.6
6.7
6.8
6.9
7.0
TIME
LOAD CELL #1 DATA
OF 2 KHZ
R18Y9

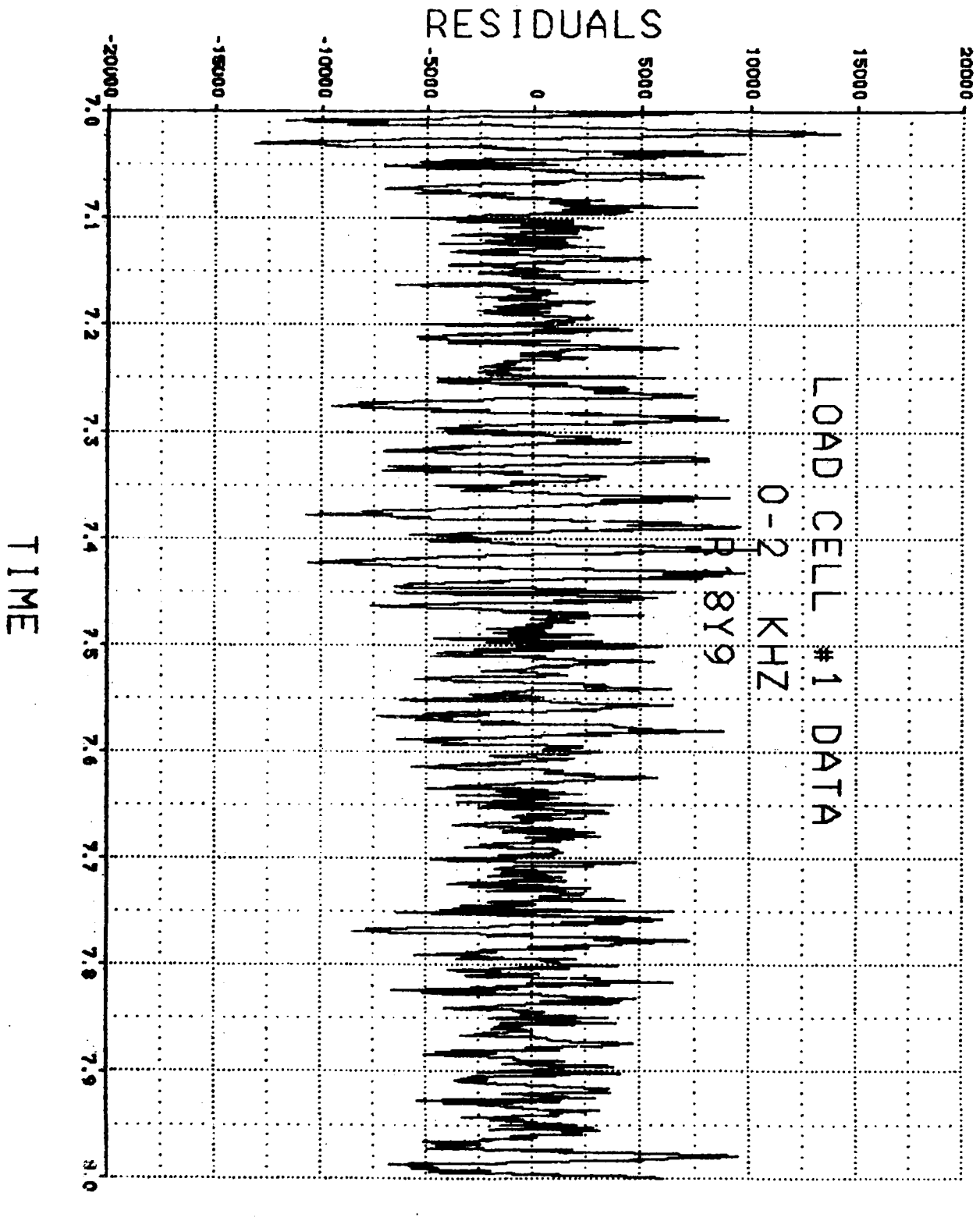
RESIDUALS
-20000
-15000
-10000
-5000
0
5000
10000
15000
20000
7.0
7.1
7.2
7.3
7.4
7.5
7.6
7.7
7.8
7.9
8.0
TIME
LOAD CELL #1 DATA
0-2 KHZ
R18Y9

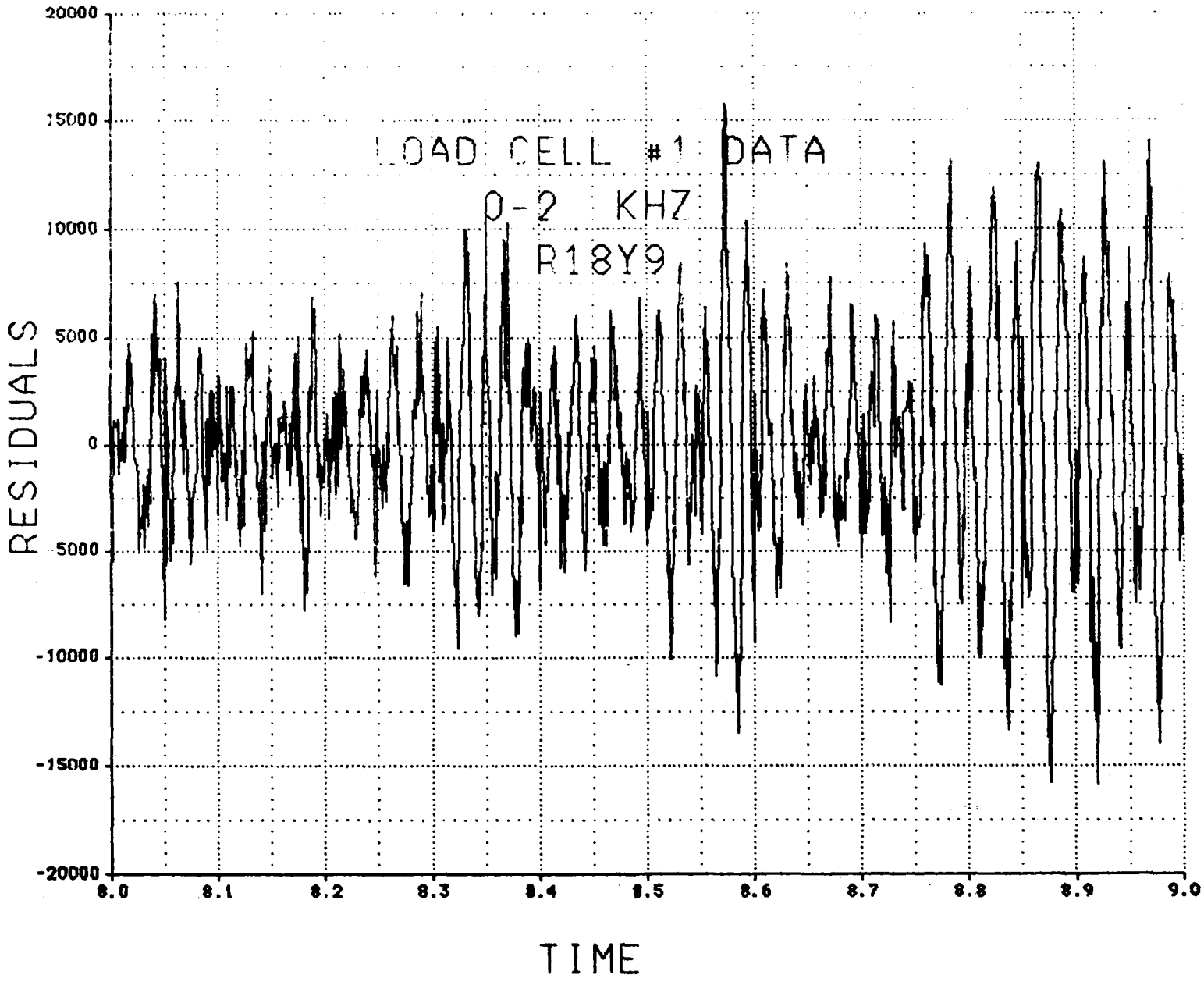
LOAD CELL #1 DATA
0-2 KHZ
R18Y9
RESIDUALS
TIME
20000
15000
10000
5000
0
-5000
-10000
-15000
-20000
8.0
8.1
8.2
8.3
8.4
8.5
8.6
8.7
8.8
8.9
9.0

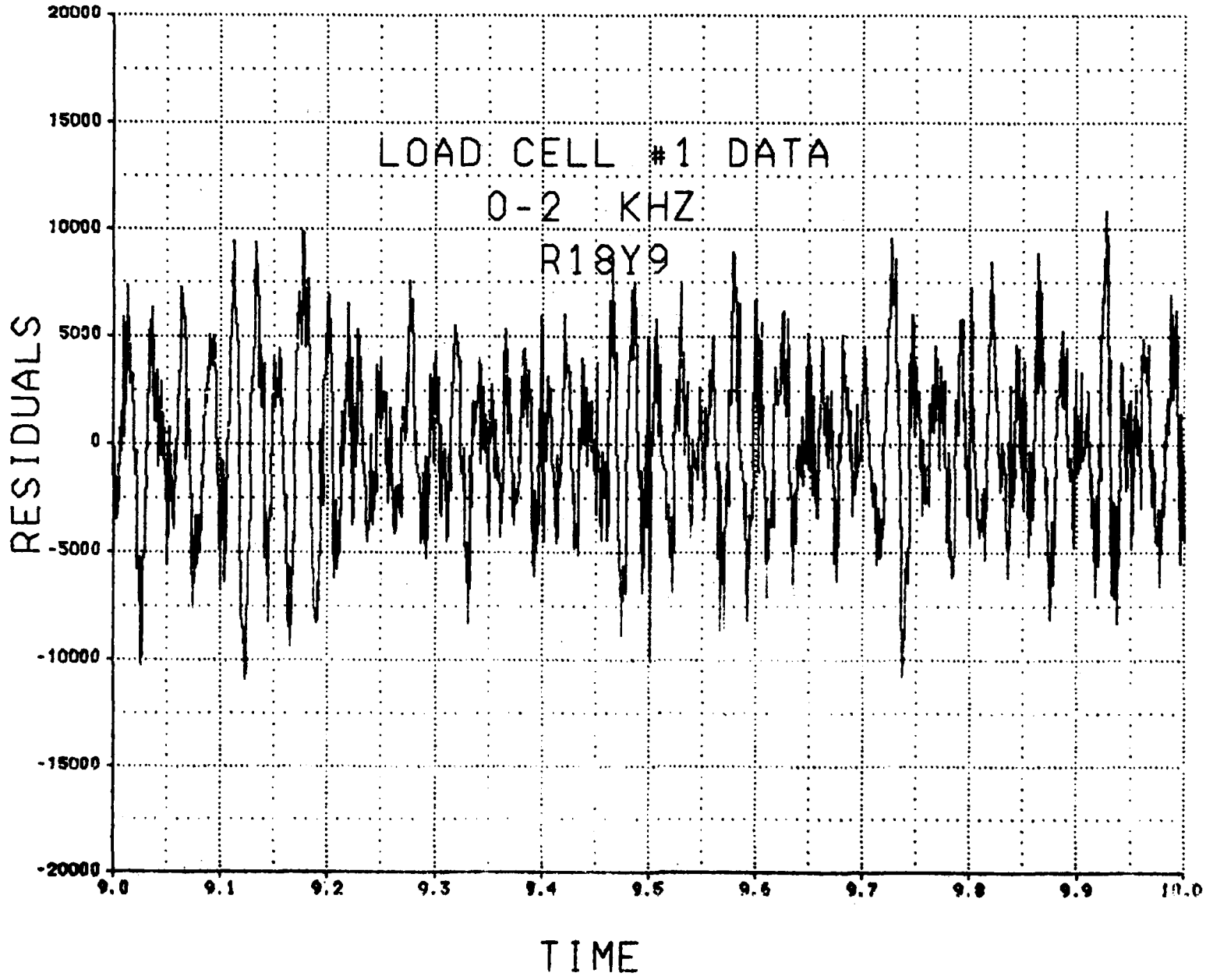
LOAD CELL #1 DATA
0-2 KHZ
R18Y9
RESIDUALS
TIME
20000
15000
10000
5000
0
-5000
-10000
-15000
-20000
9.0
9.1
9.2
9.3
9.4
9.5
9.6
9.7
9.8
9.9
10.0

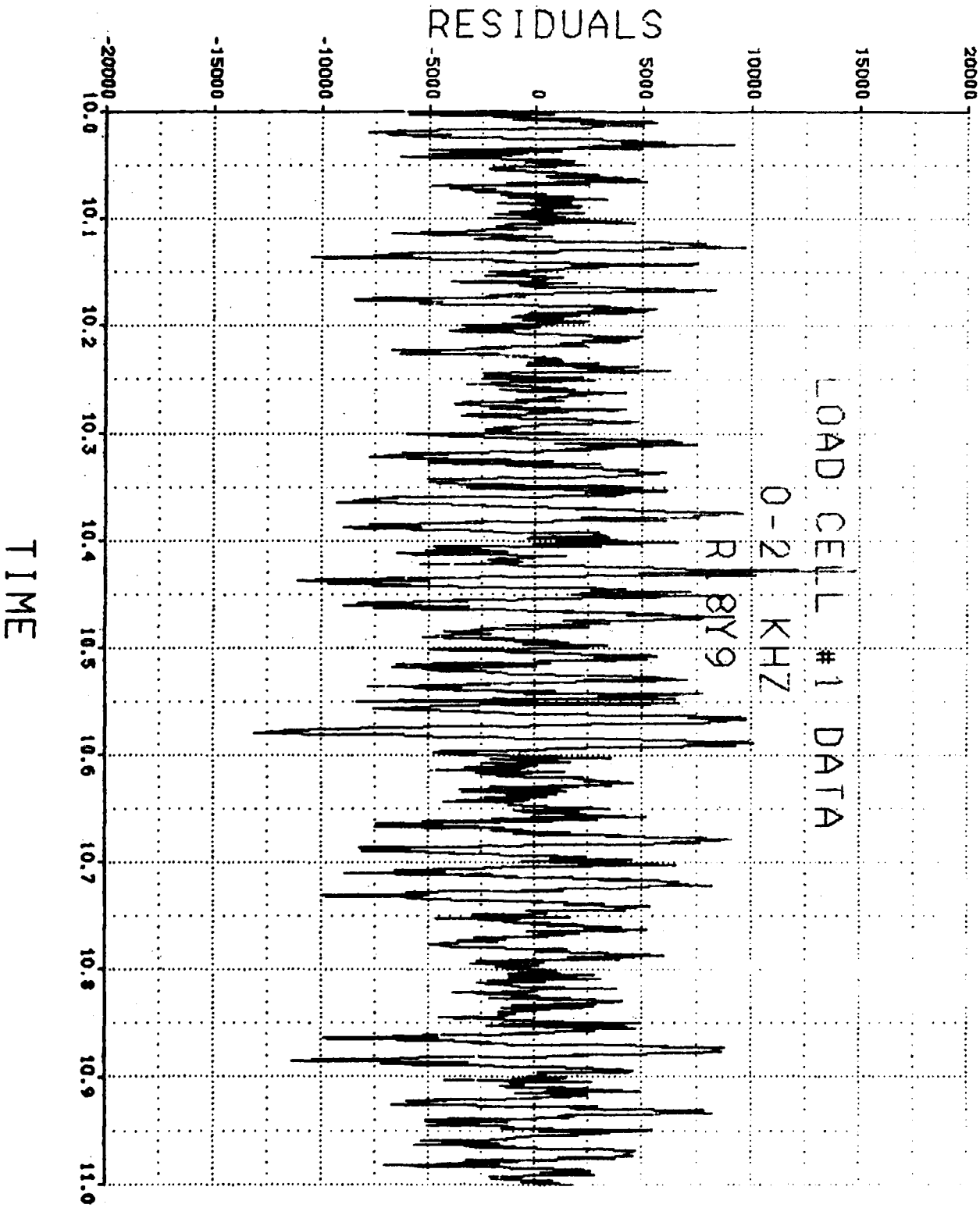
RESIDUALS
-20000
-15000
-10000
-5000
0
5000
10000
15000
20000
10.0
10.1
10.2
10.3
10.4
10.5
10.6
10.7
10.8
10.9
11.0
TIME
LOAD CELL #1 DATA
0-2 KHZ
R 8Y9

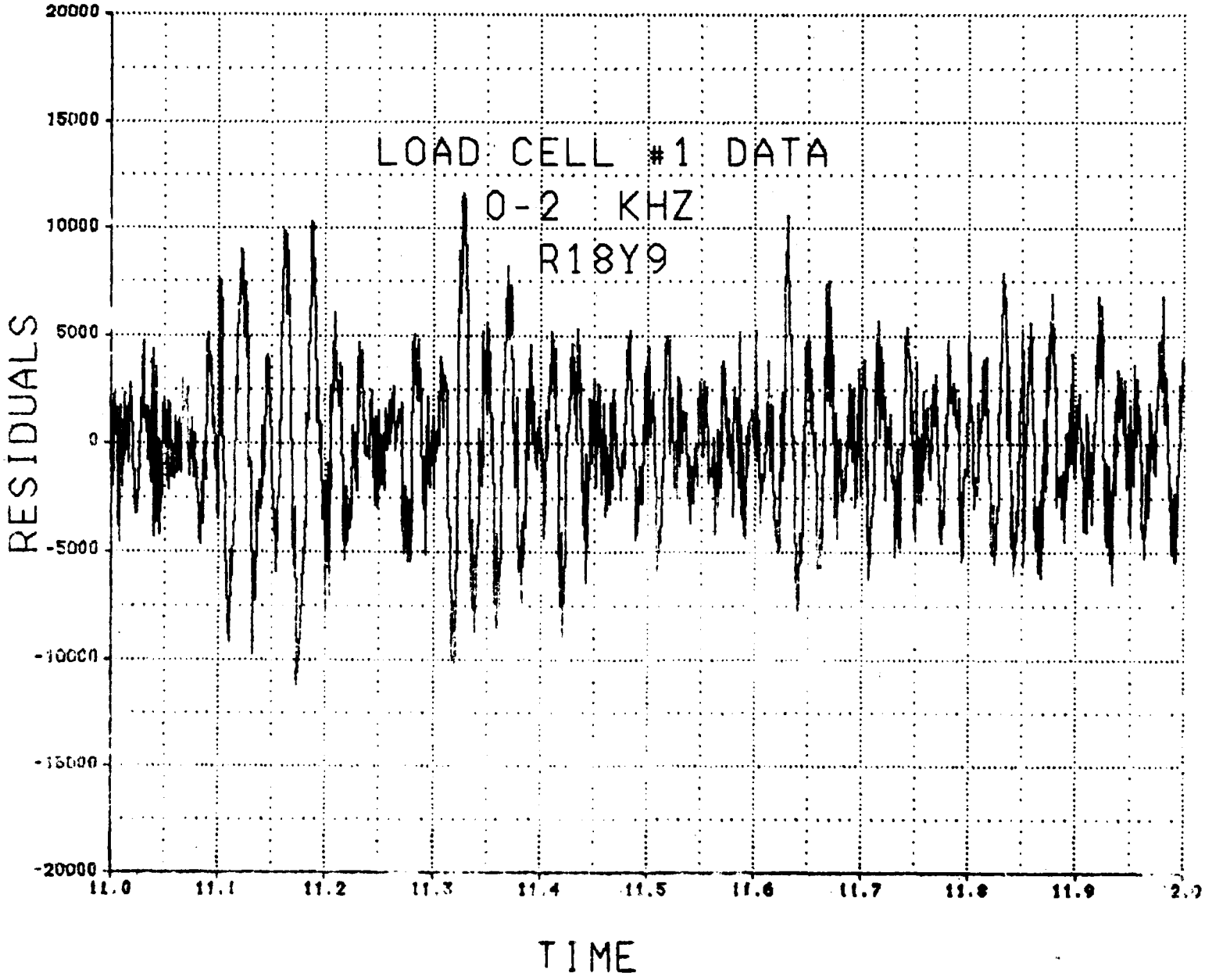
LOAD CELL #1 DATA
0-2 KHZ
R18Y9
RESIDUALS
TIME
20000
15000
10000
5000
0
-5000
-10000
-15000
-20000
11.0
11.1
11.2
11.3
11.4
11.5
11.6
11.7
11.8
11.9
2.0

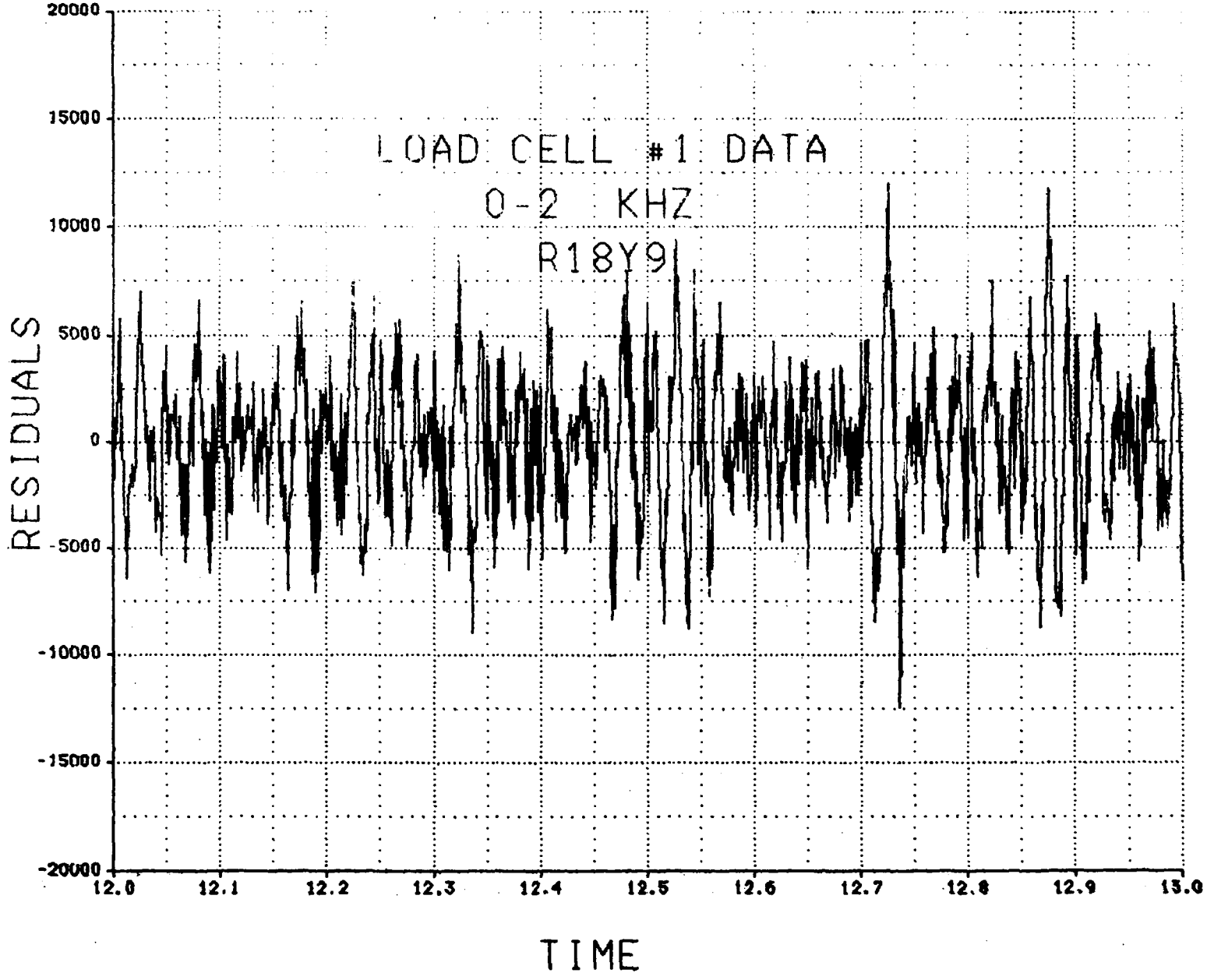
LOAD CELL #1 DATA
0-2 KHZ
R18Y9
RESIDUALS
20000
15000
10000
5000
0
-5000
-10000
-15000
-20000
12.0
12.1
12.2
12.3
12.4
12.5
12.6
12.7
12.8
12.9
13.0
TIME

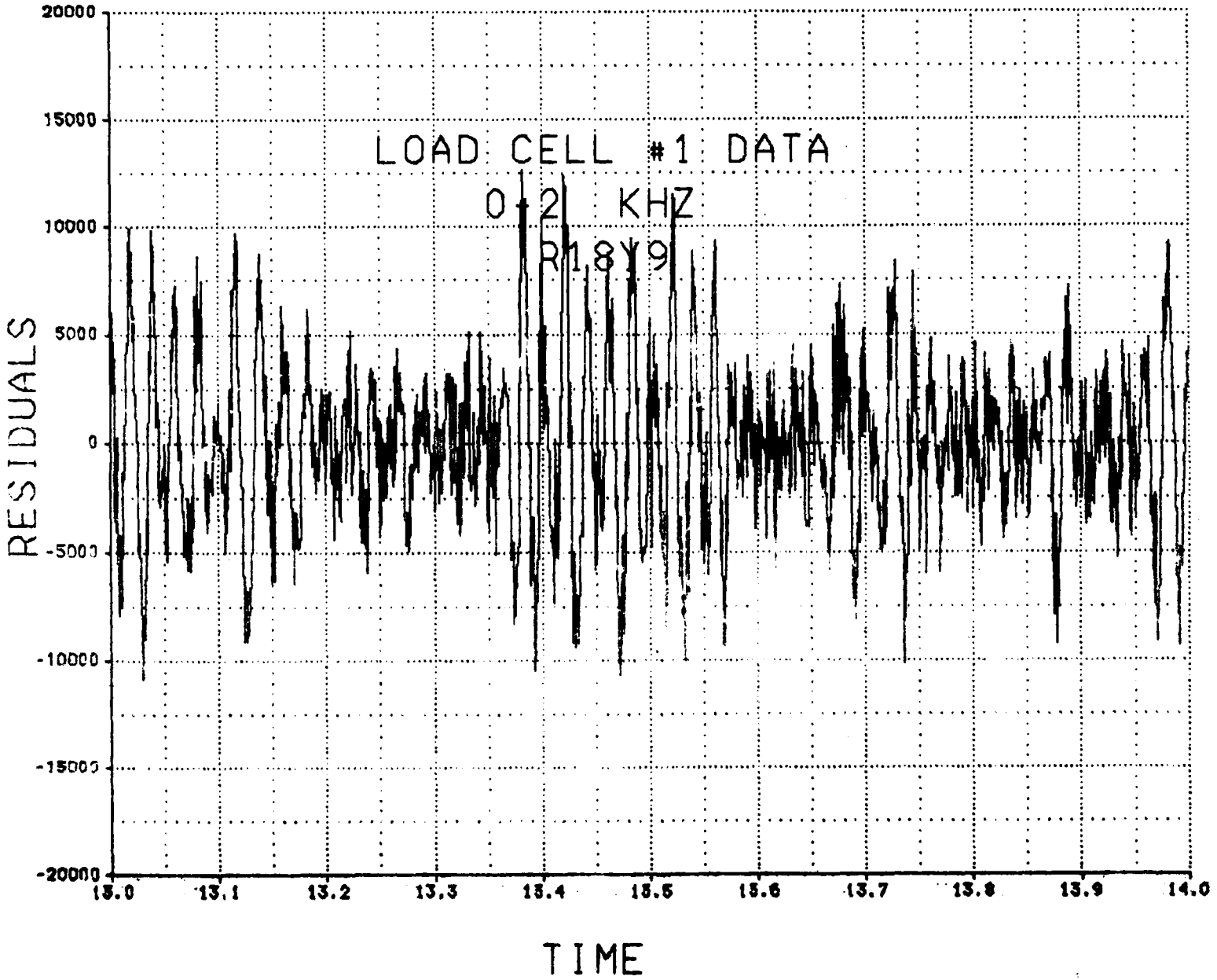
LOAD CELL #1 DATA
0.2 KHZ
R18Y9
RESIDUALS
TIME
20000
15000
10000
5000
0
-5000
-10000
-15000
-20000
13.0
13.1
13.2
13.3
13.4
13.5
13.6
13.7
13.8
13.9
14.0

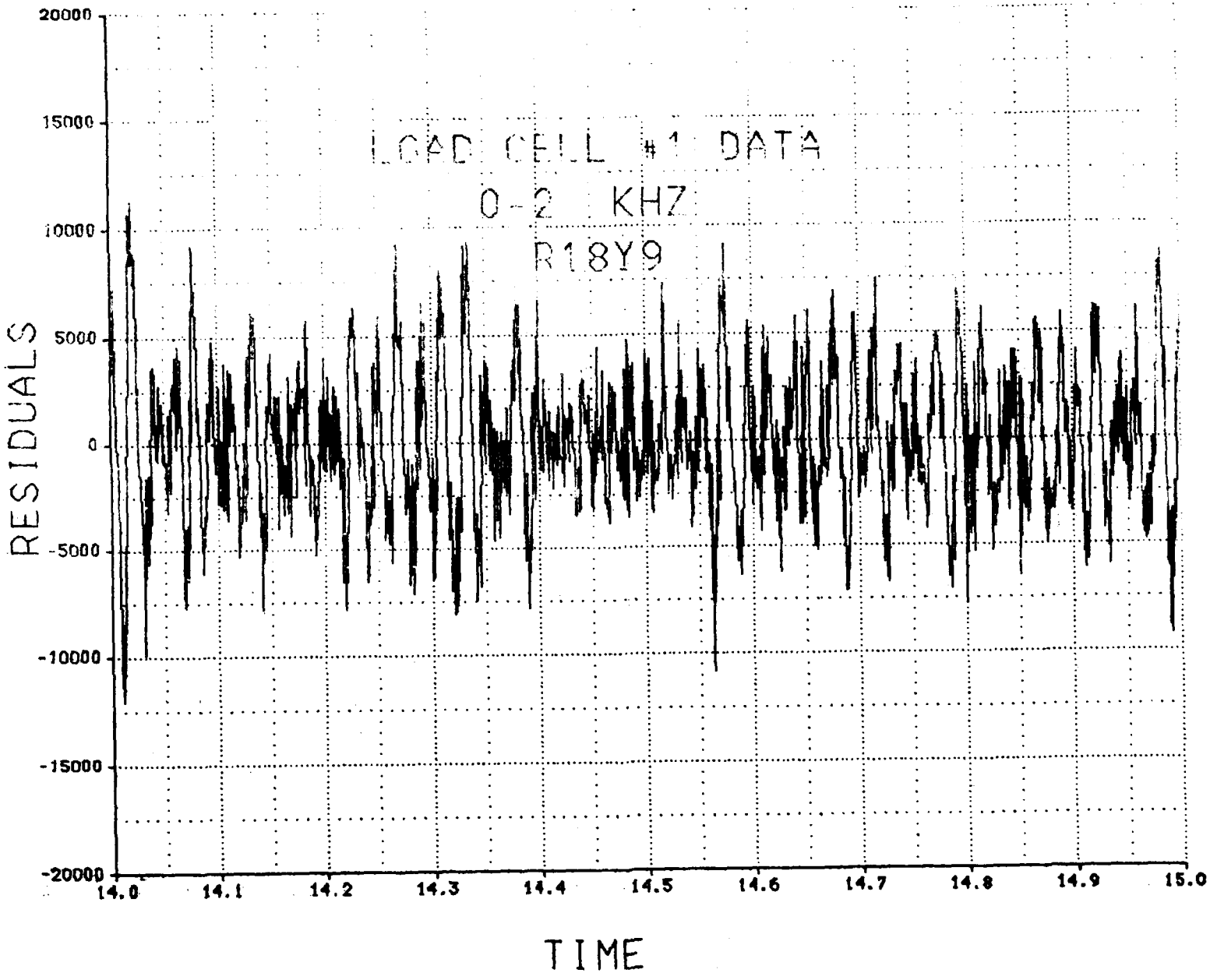
LOAD CELL #1 DATA
0-2 KHZ
R18Y9
RESIDUALS
TIME
20000
15000
10000
5000
0
-5000
-10000
-15000
-20000
14.0
14.1
14.2
14.3
14.4
14.5
14.6
14.7
14.8
14.9
15.0

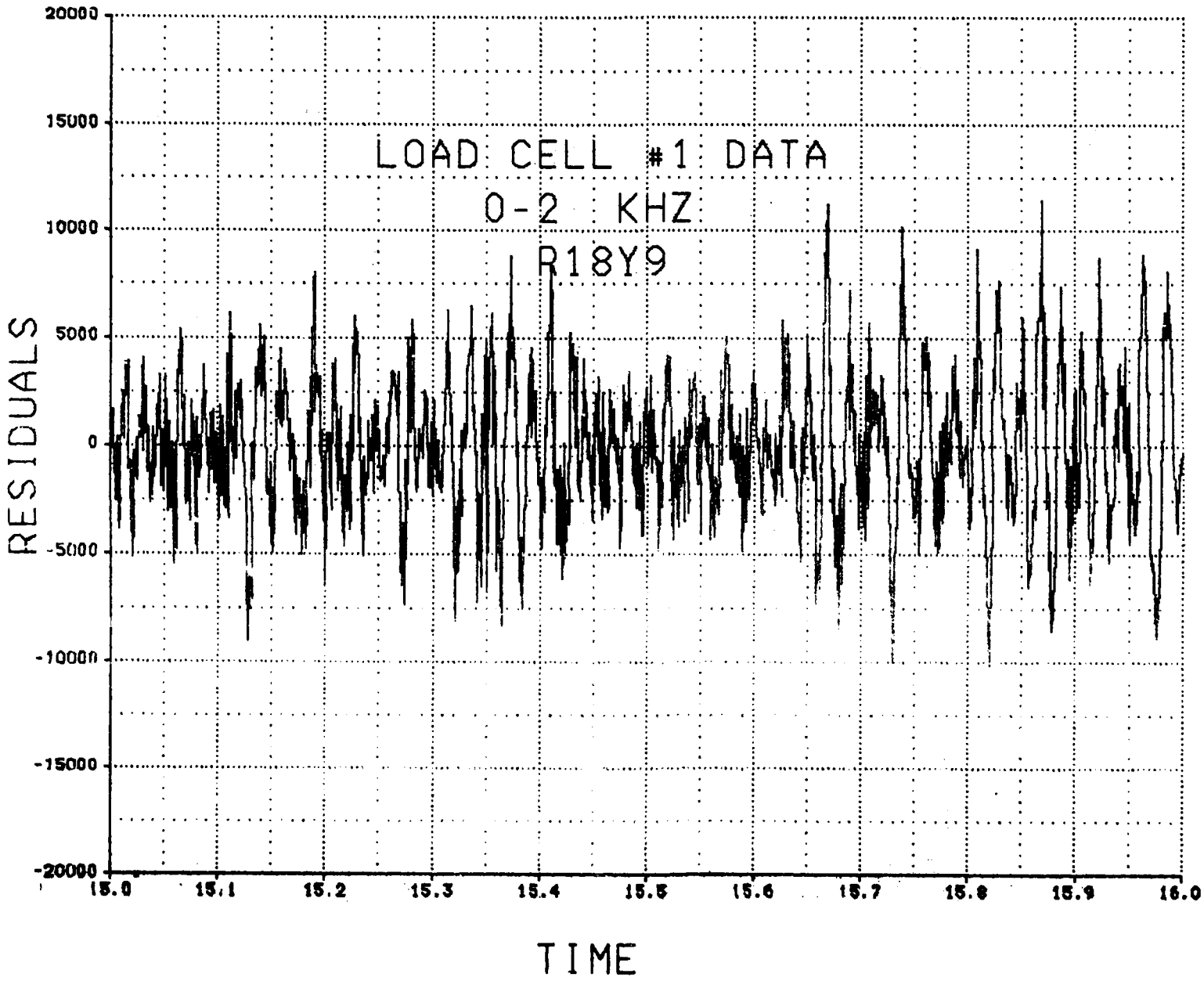
LOAD CELL #1 DATA
0-2 KHZ
R18Y9
RESIDUALS
TIME
20000
15000
10000
5000
0
-5000
-10000
-15000
-20000
15.0
15.1
15.2
15.3
15.4
15.5
15.6
15.7
15.8
15.9
16.0

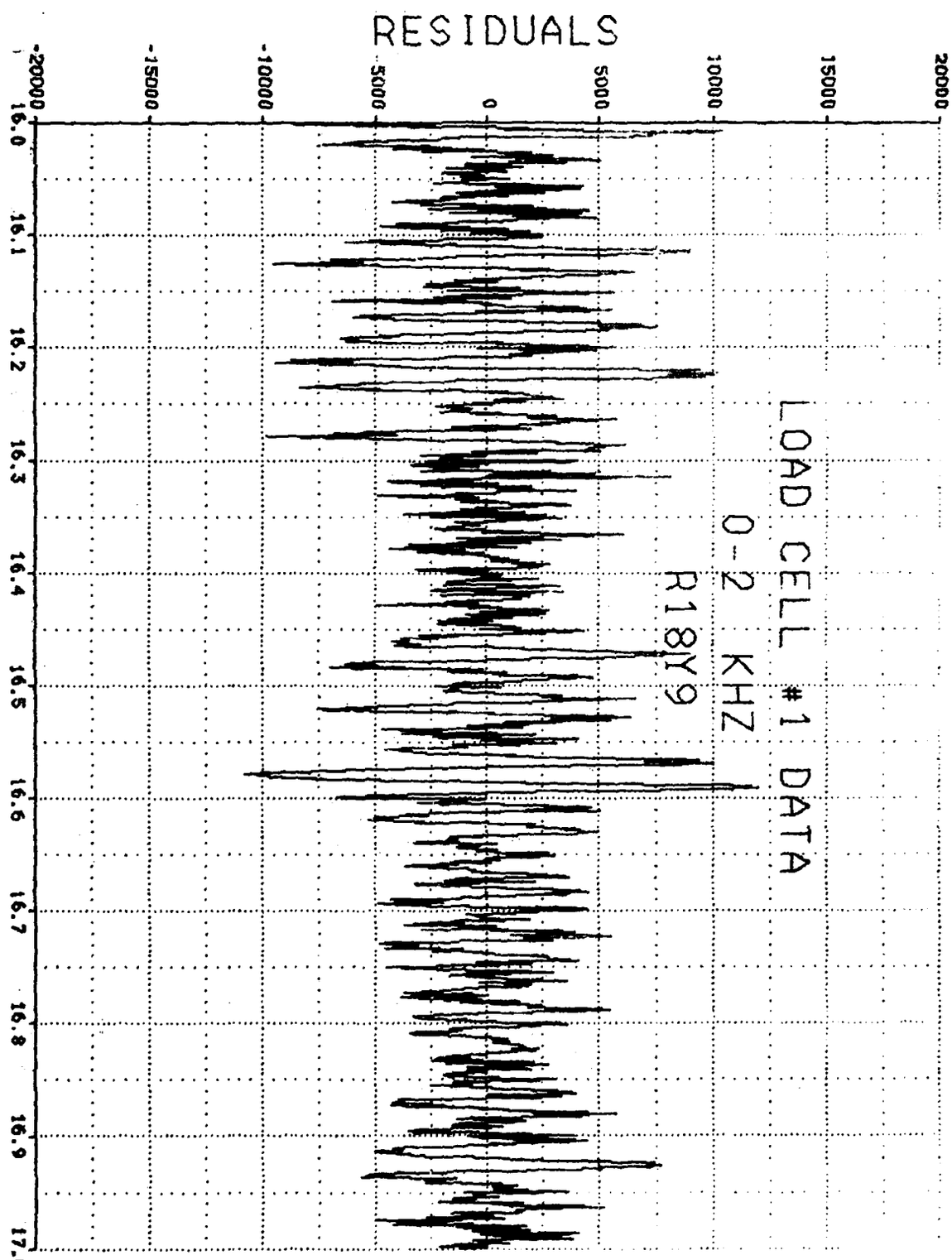
RESIDUALS
-20000
-15000
-10000
-5000
0
5000
10000
15000
20000
16.0
16.1
16.2
16.3
16.4
16.5
16.6
16.7
16.8
16.9
17.0
TIME
LOAD CELL #1 DATA
0-2 KHZ
R18Y9

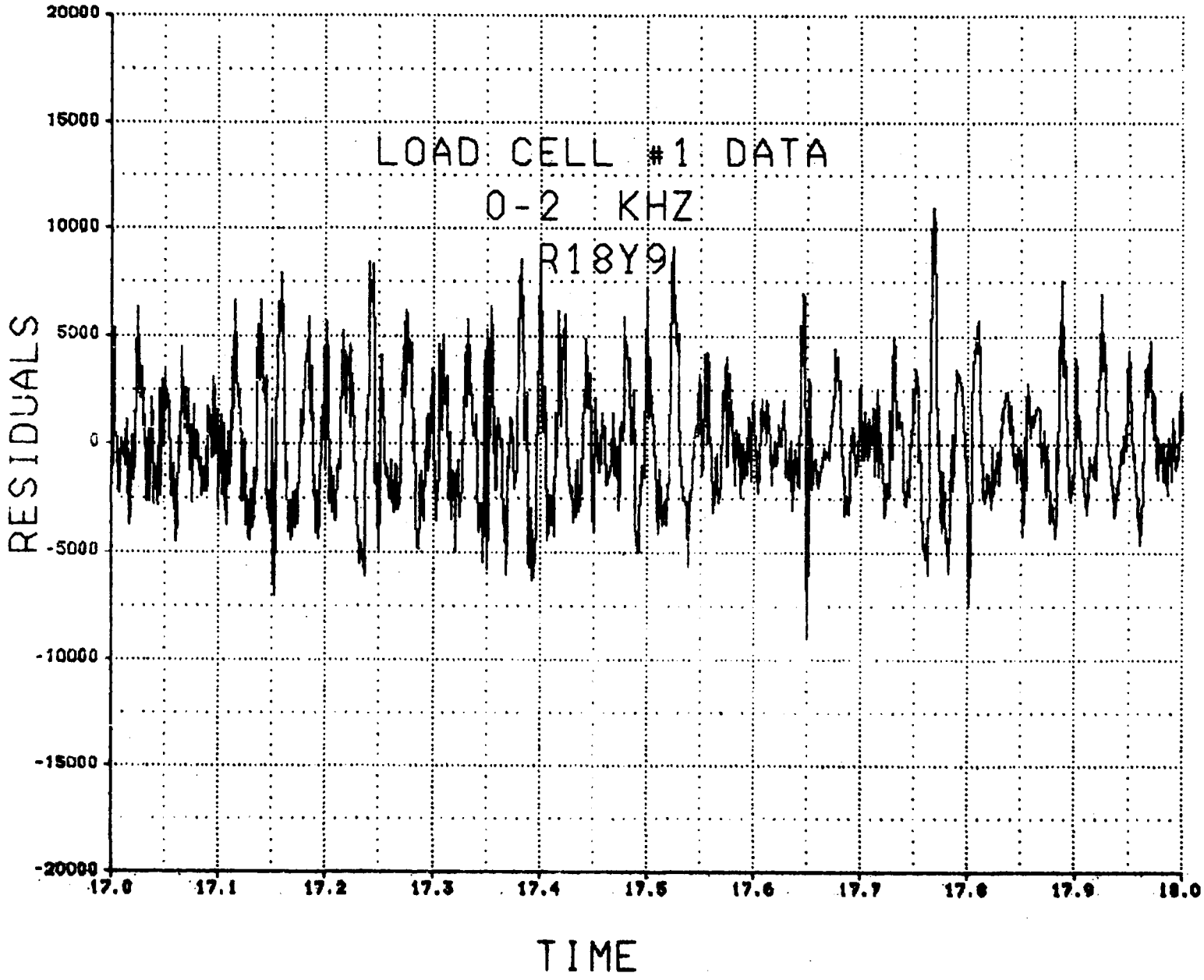
LOAD CELL #1 DATA
0-2 KHZ
R18Y9
RESIDUALS
TIME
20000
15000
10000
5000
0
-5000
-10000
-15000
-20000
17.0
17.1
17.2
17.3
17.4
17.5
17.6
17.7
17.8
17.9
18.0

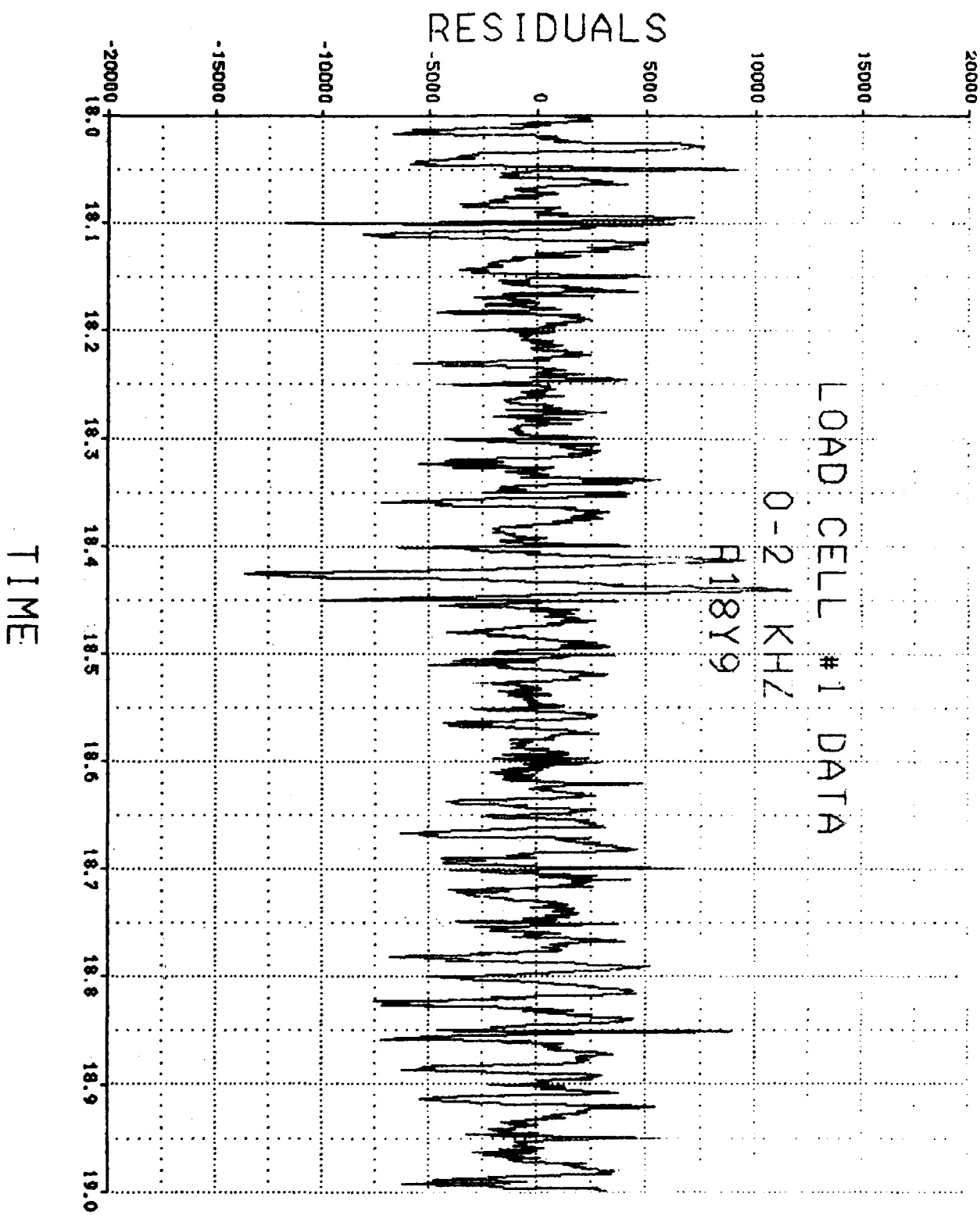
RESIDUALS
-20000
-15000
-10000
-5000
0
5000
10000
15000
20000
18.0
18.1
18.2
18.3
18.4
18.5
18.6
18.7
18.8
18.9
19.0
TIME
LOAD CELL #1 DATA
0-2 KHZ
R18Y9

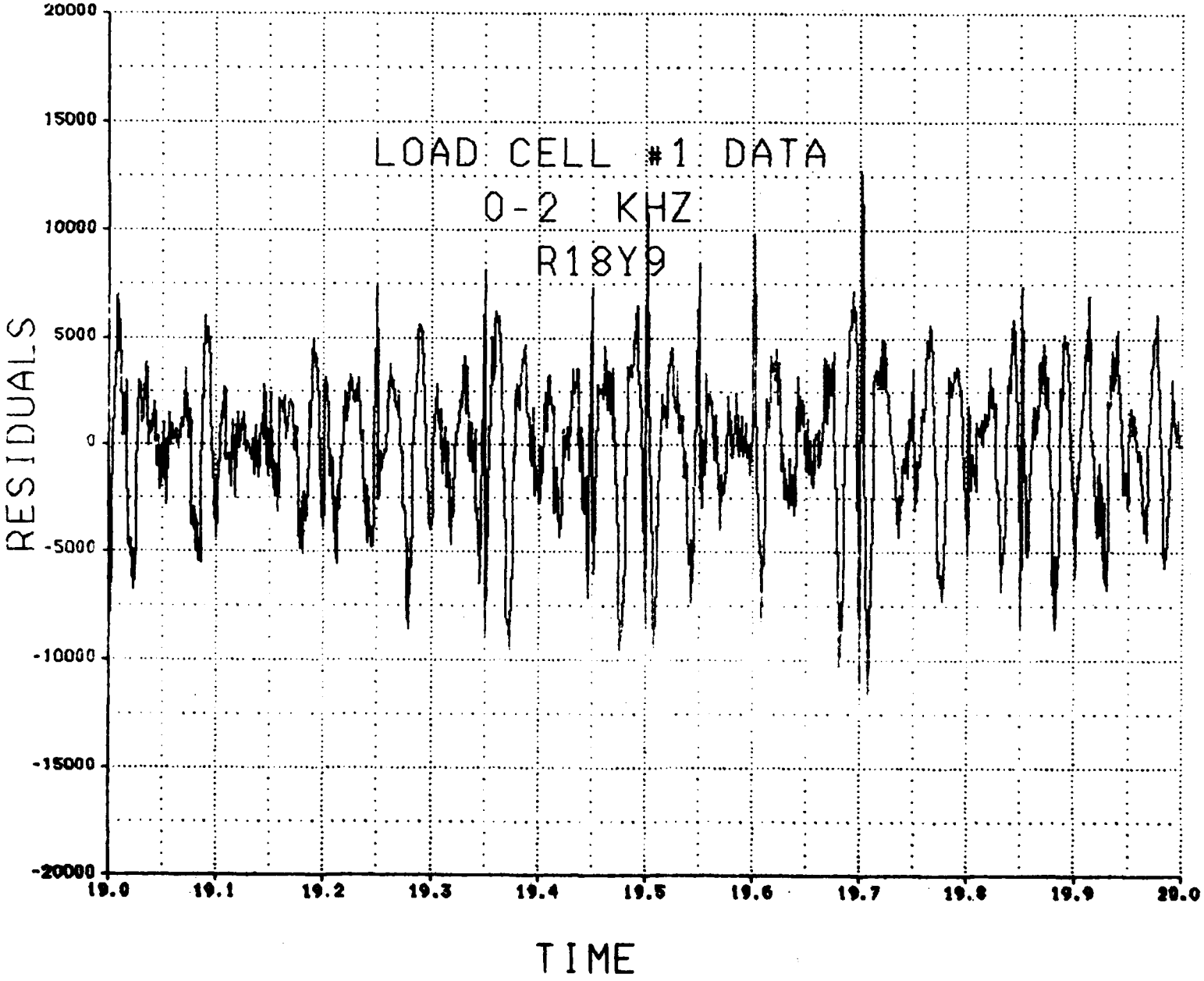
LOAD CELL #1 DATA
0-2 KHZ
R18Y9
RESIDUALS
TIME
20000
15000
10000
5000
0
-5000
-10000
-15000
-20000
19.0
19.1
19.2
19.3
19.4
19.5
19.6
19.7
19.8
19.9
20.0

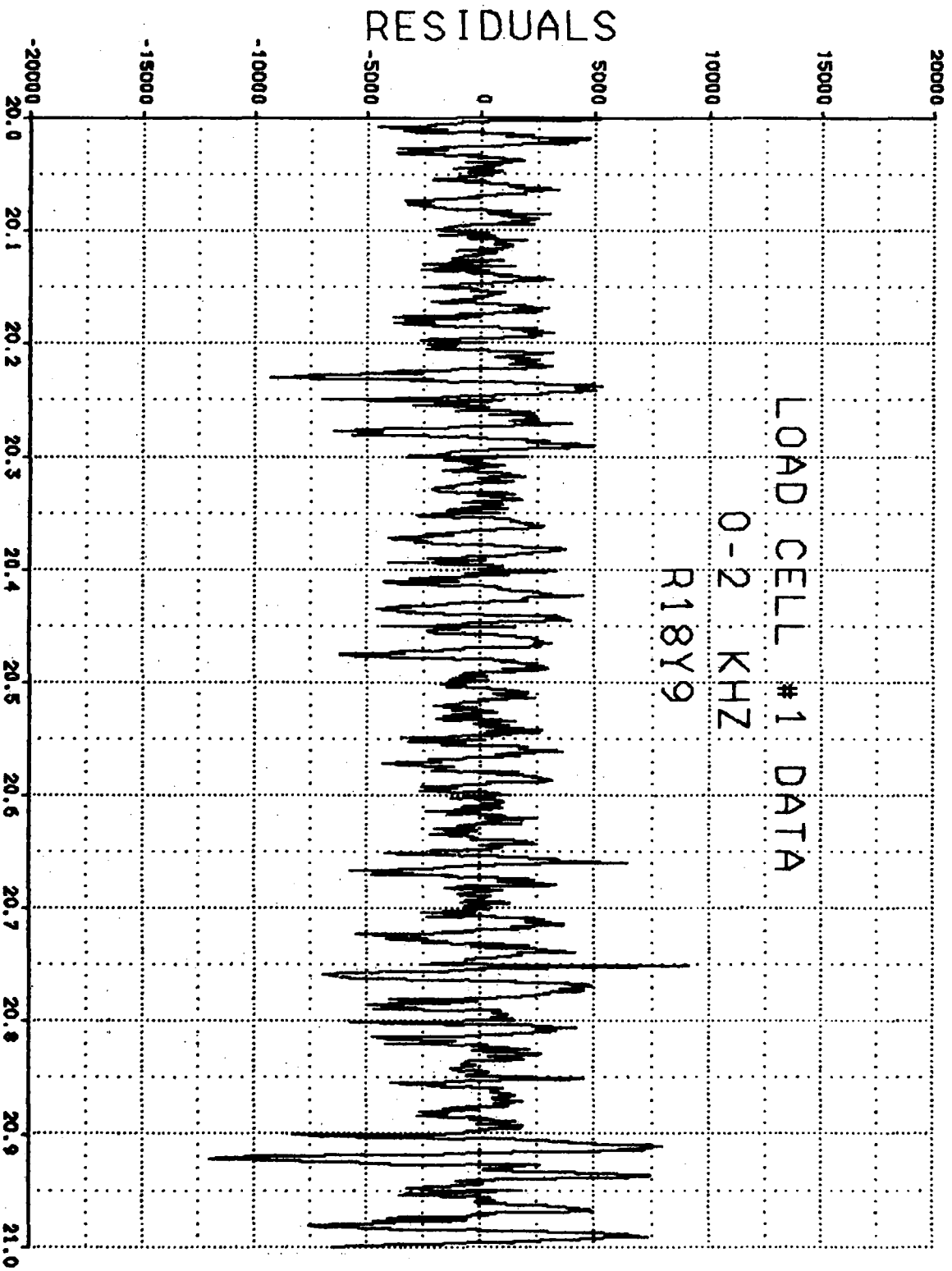
RESIDUALS
-20000
-15000
-10000
-5000
0
5000
10000
15000
20000
20.0
20.1
20.2
20.3
20.4
20.5
20.6
20.7
20.8
20.9
21.0
TIME
LOAD CELL #1 DATA
0-2 KHZ
R18Y9

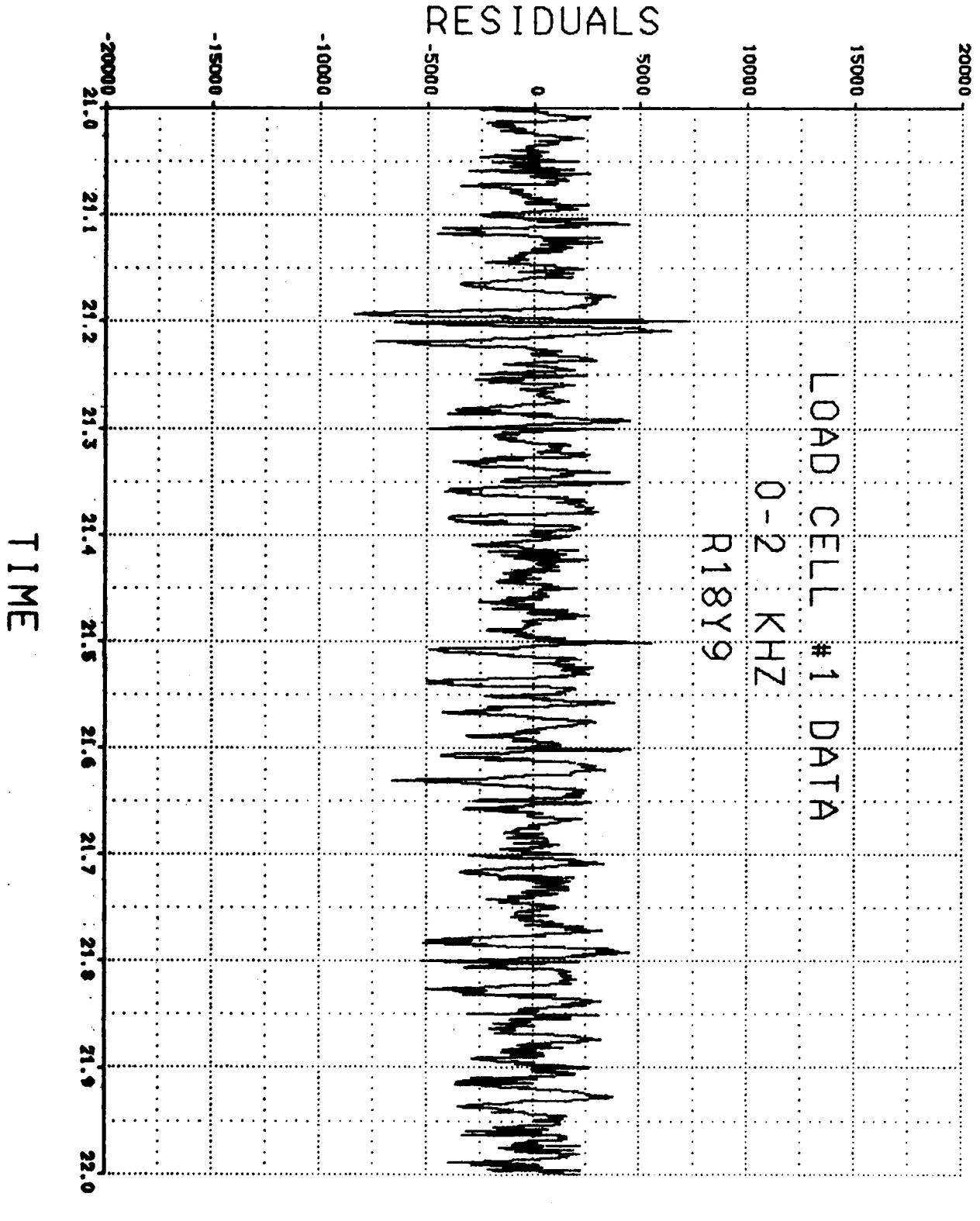
RESIDUALS
-20000
-15000
-10000
-5000
0
5000
10000
15000
20000
21.0
21.1
21.2
21.3
21.4
21.5
21.6
21.7
21.8
21.9
22.0
TIME
LOAD CELL #1 DATA
0-2 KHZ
R18Y9

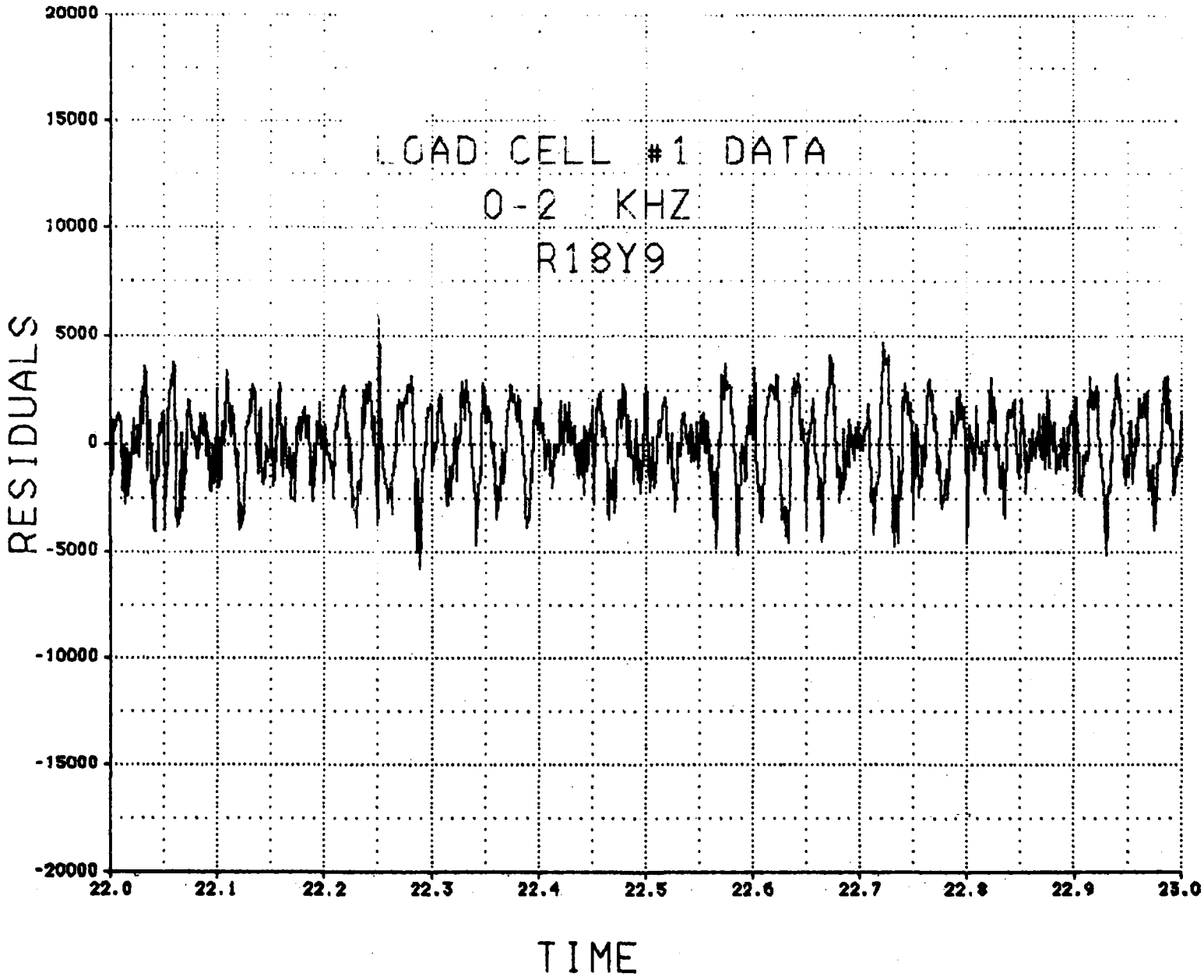
LOAD CELL #1 DATA
0-2 KHZ
R18Y9
RESIDUALS
20000
15000
10000
5000
0
-5000
-10000
-15000
-20000
22.0
22.1
22.2
22.3
22.4
22.5
22.6
22.7
22.8
22.9
23.0
TIME

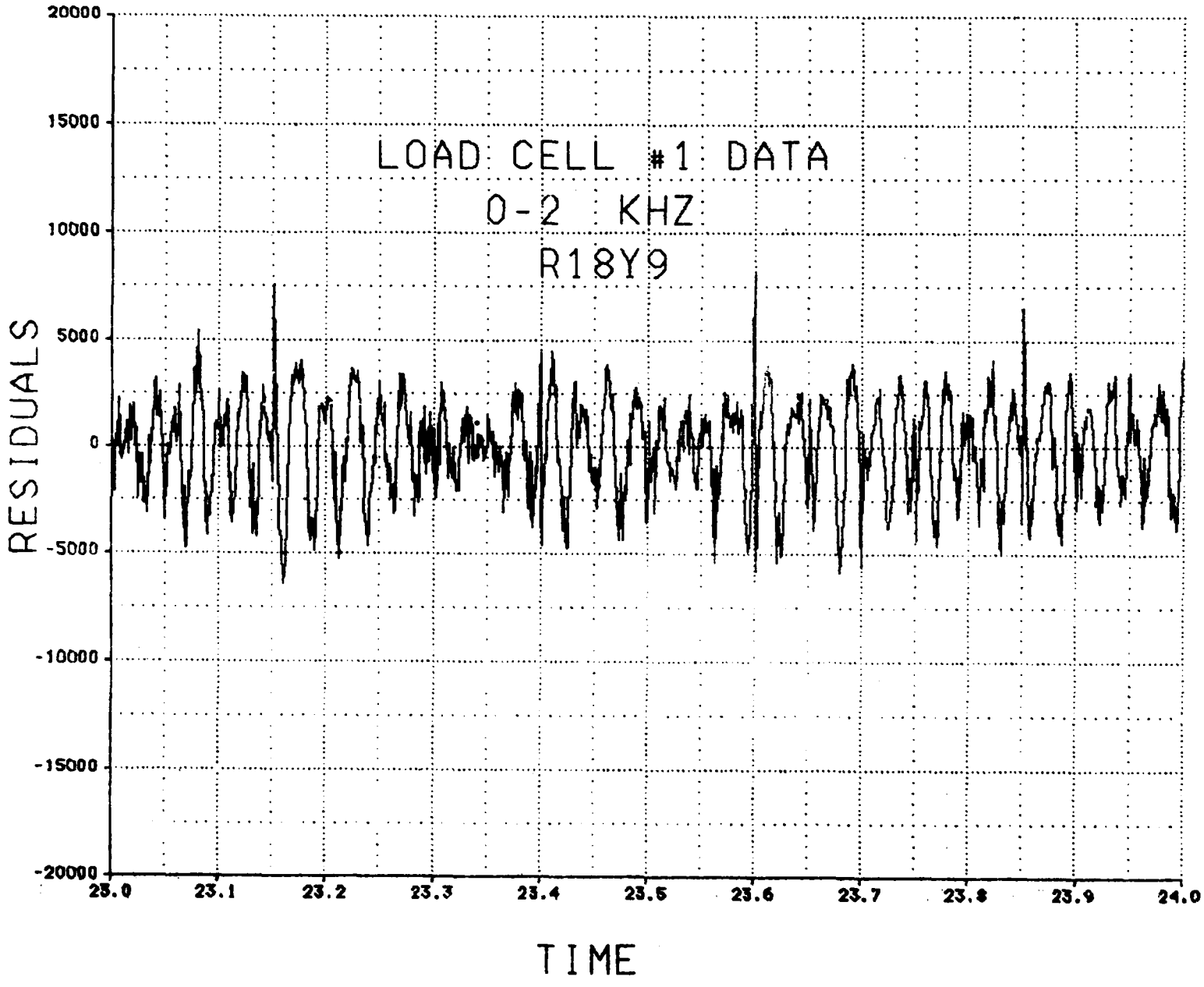
LOAD CELL #1 DATA
0-2 KHZ
R18Y9
RESIDUALS
TIME
20000
15000
10000
5000
0
-5000
-10000
-15000
-20000
23.0
23.1
23.2
23.3
23.4
23.5
23.6
23.7
23.8
23.9
24.0

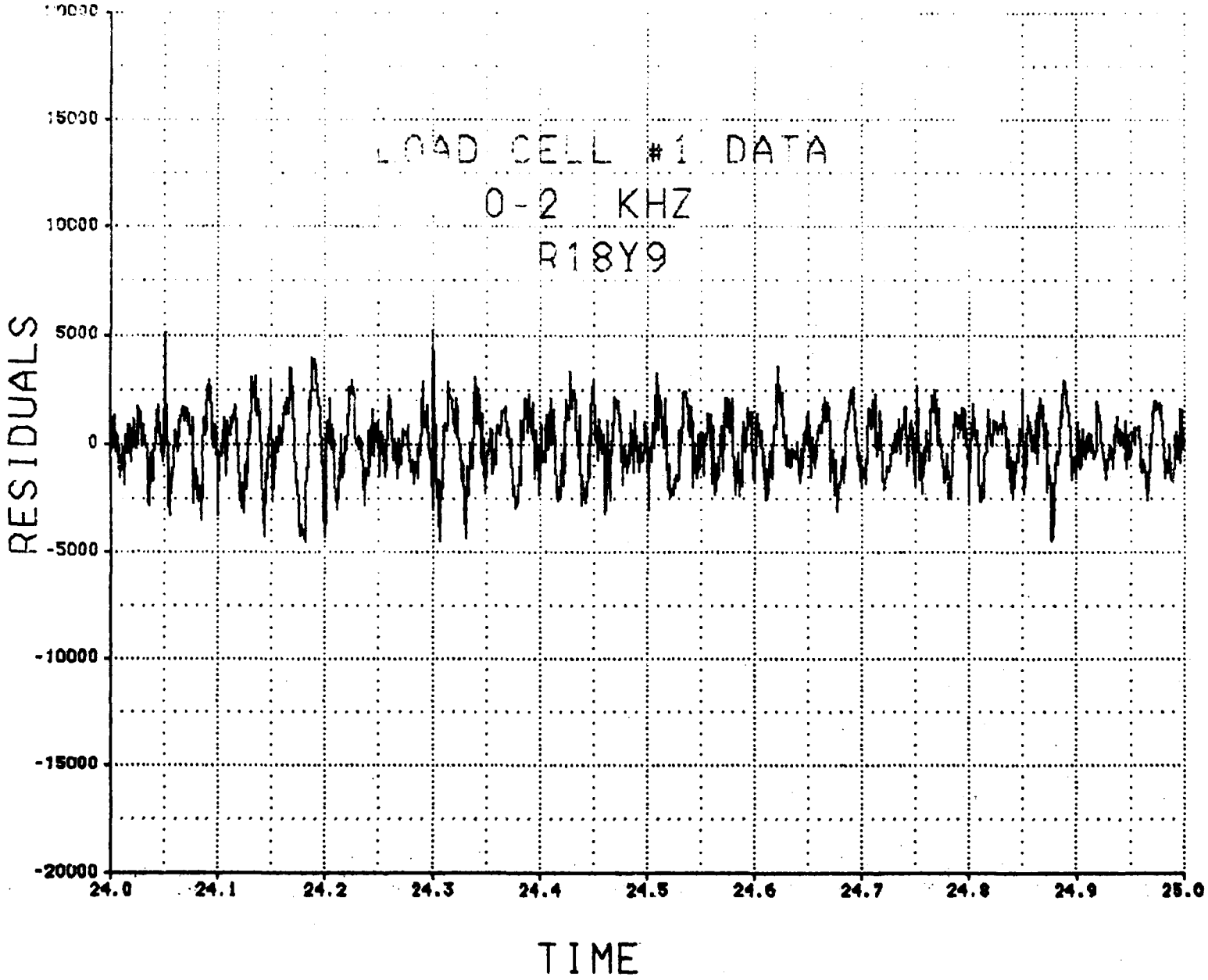
LOAD CELL #1 DATA
0-2 KHZ
R18Y9
RESIDUALS
15000
10000
5000
0
-5000
-10000
-15000
-20000
24.0
24.1
24.2
24.3
24.4
24.5
24.6
24.7
24.8
24.9
25.0
TIME

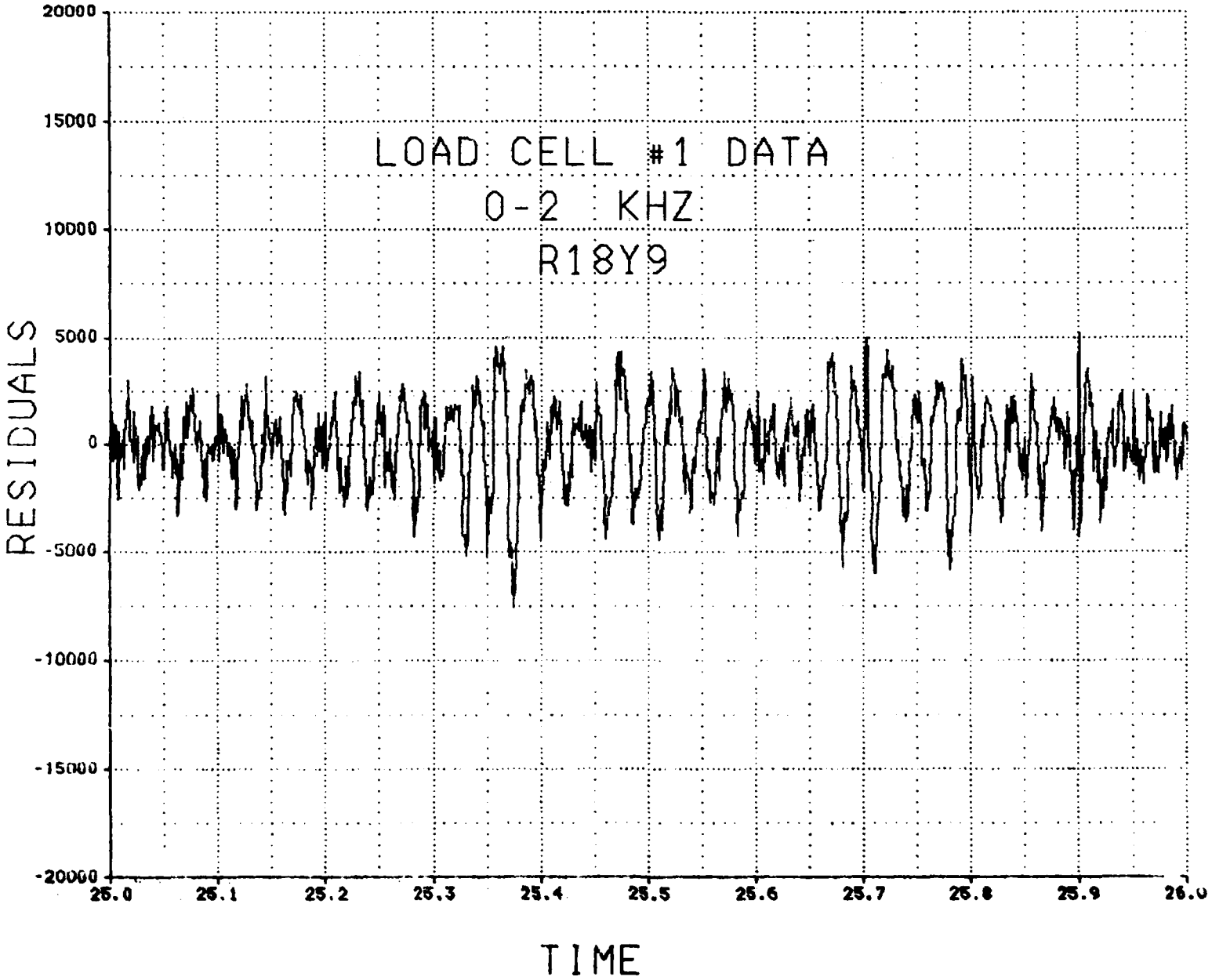
LOAD CELL #1 DATA
0-2 KHZ
R18Y9
RESIDUALS
TIME
20000
15000
10000
5000
0
-5000
-10000
-15000
-20000
25.0
25.1
25.2
25.3
25.4
25.5
25.6
25.7
25.8
25.9
26.0

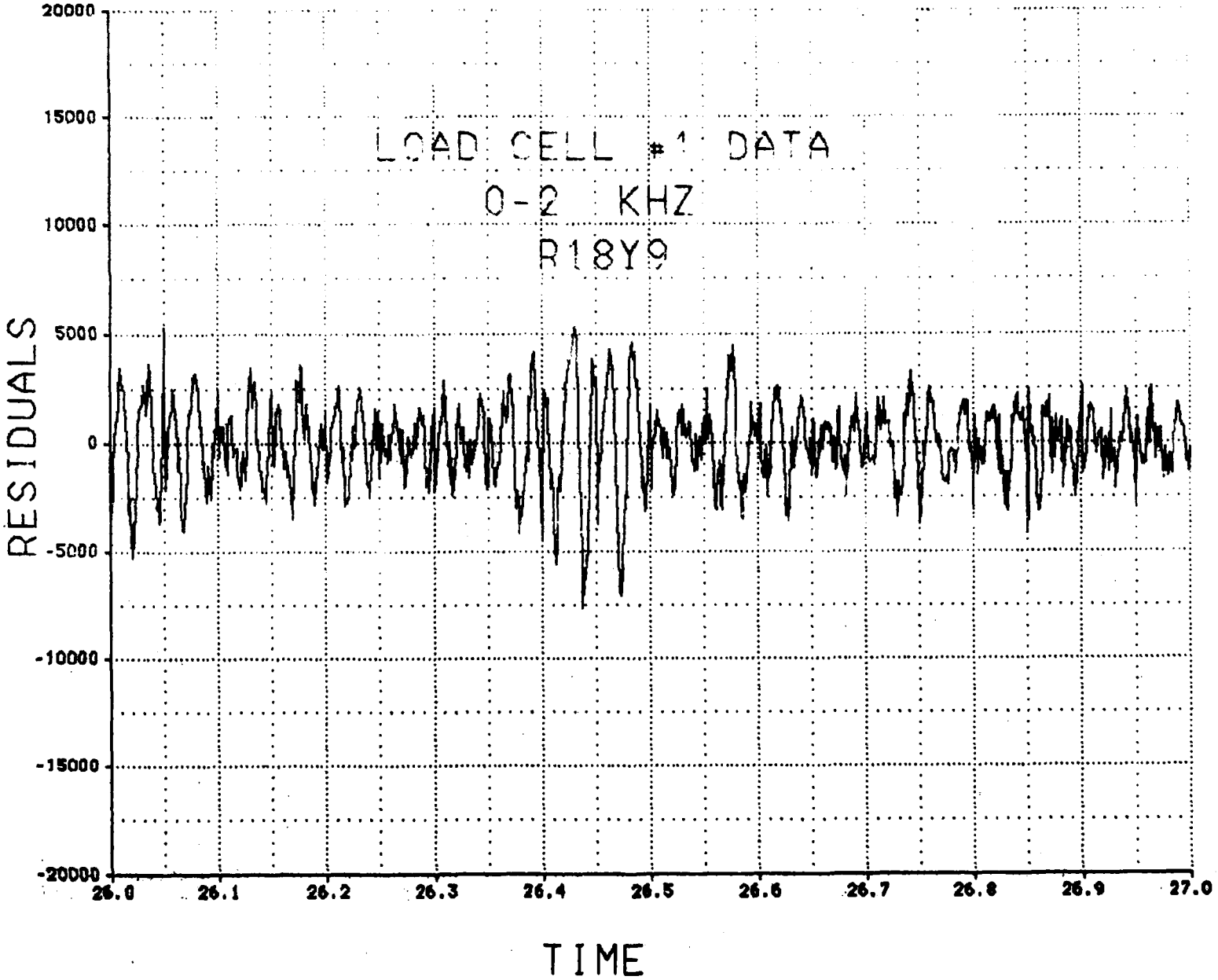
LOAD CELL #1 DATA
0-2 KHZ
R18Y9
RESIDUALS
20000
15000
10000
5000
0
-5000
-10000
-15000
-20000
26.0
26.1
26.2
26.3
26.4
26.5
26.6
26.7
26.8
26.9
27.0
TIME

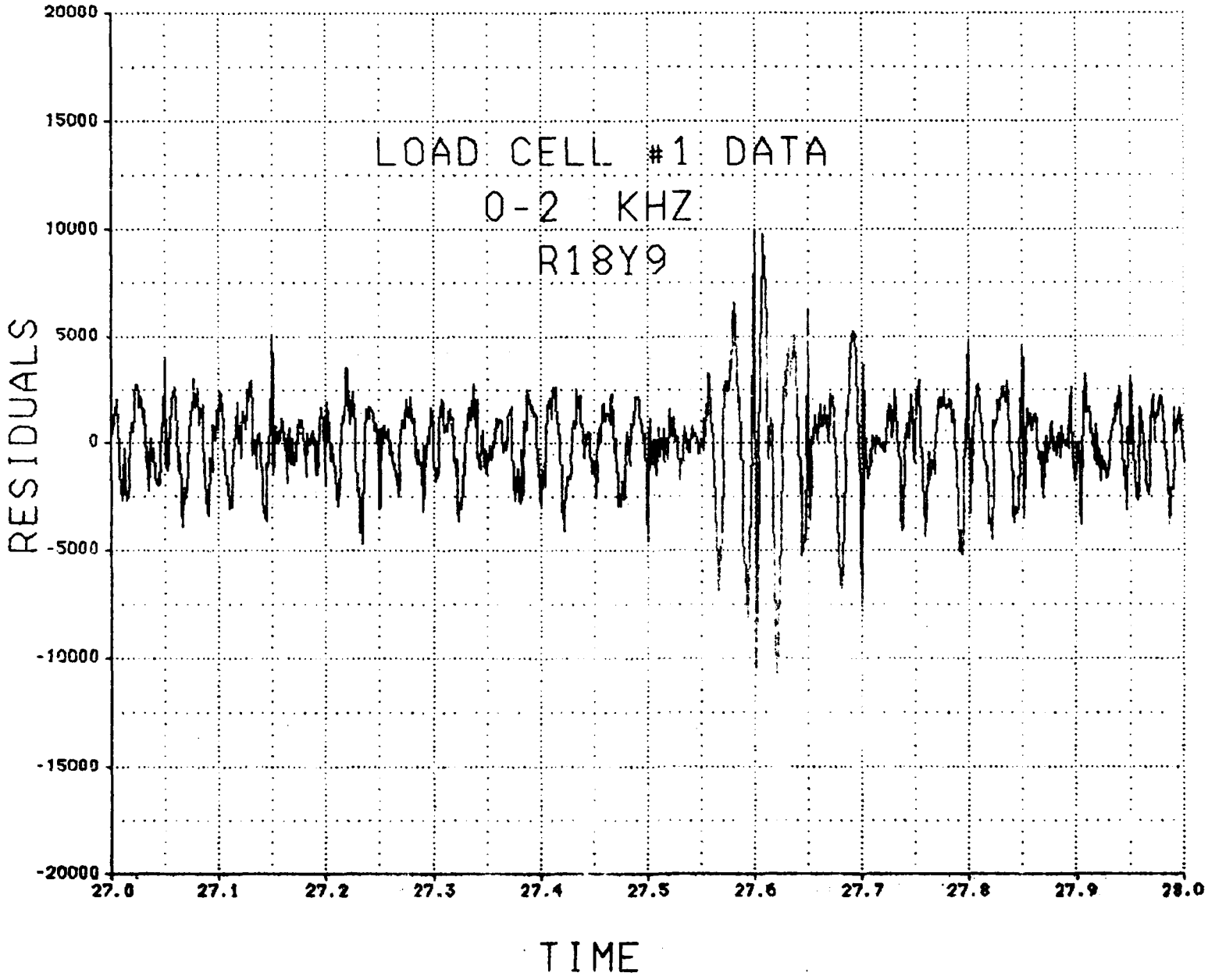
LOAD CELL #1 DATA
0-2 KHZ
R18Y9
RESIDUALS
TIME
20000
15000
10000
5000
0
-5000
-10000
-15000
-20000
27.0
27.1
27.2
27.3
27.4
27.5
27.6
27.7
27.8
27.9
28.0

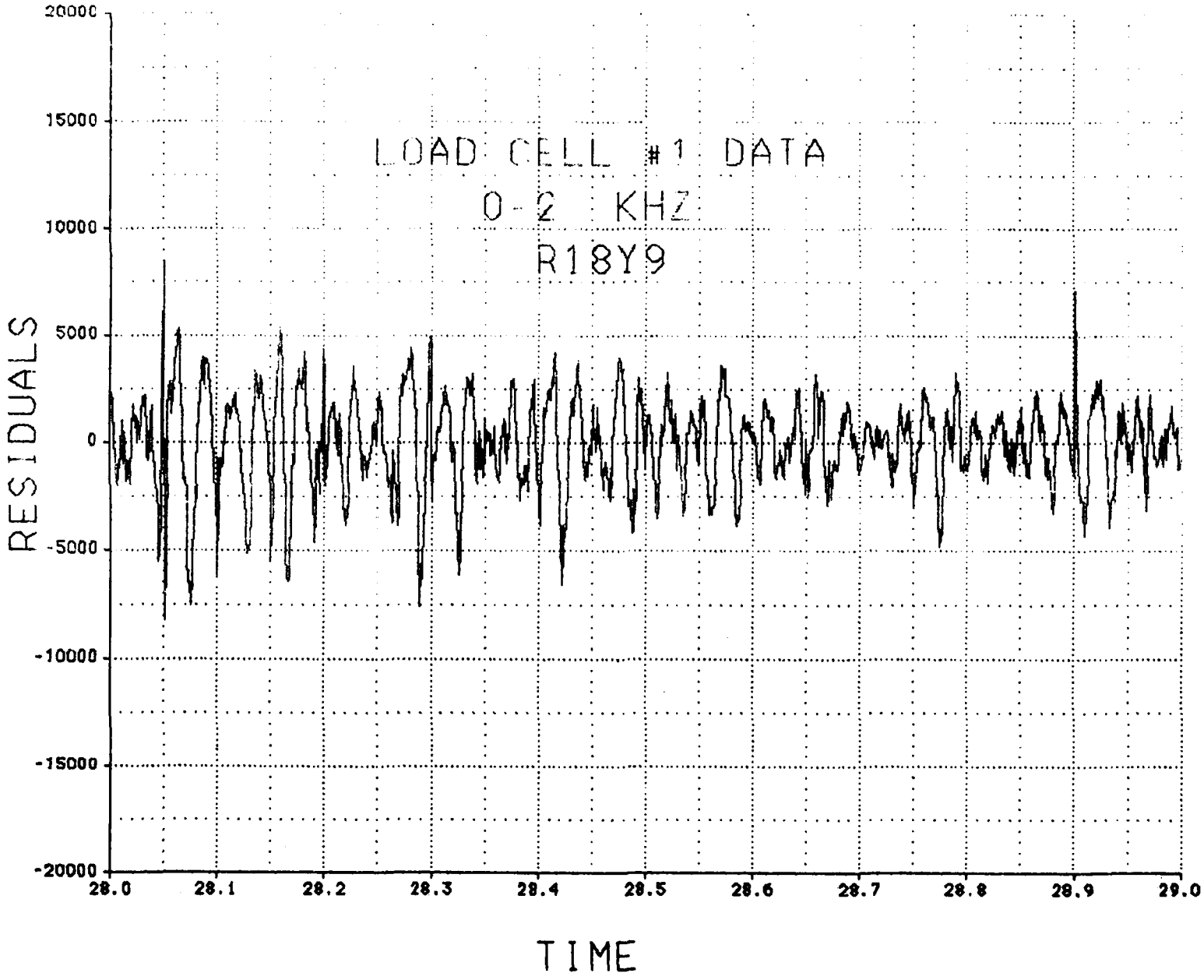
LOAD CELL #1 DATA
0-2 KHZ
R18Y9
RESIDUALS
TIME
20000
15000
10000
5000
0
-5000
-10000
-15000
-20000
28.0
28.1
28.2
28.3
28.4
28.5
28.6
28.7
28.8
28.9
29.0

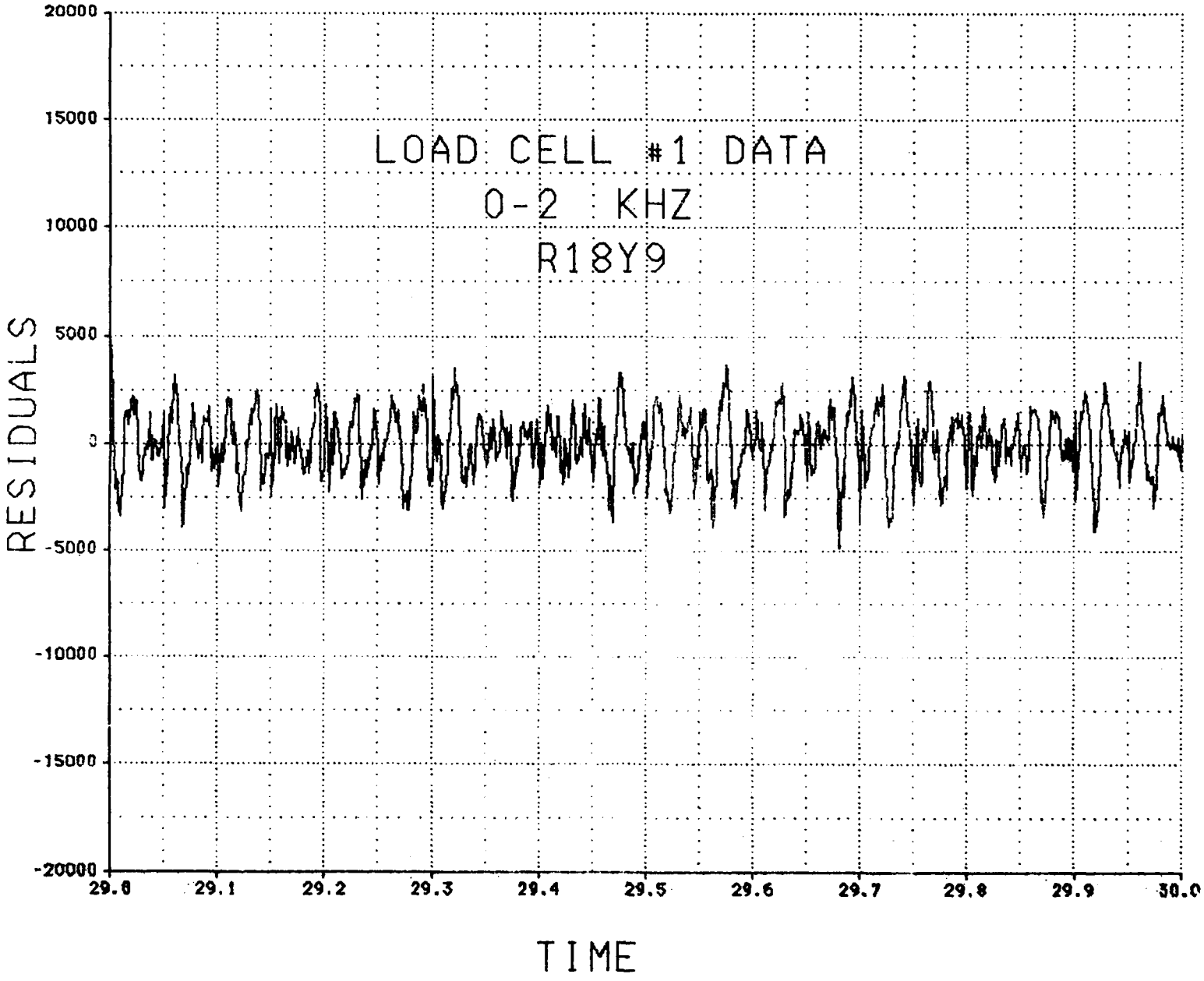
LOAD CELL #1 DATA
0-2 KHZ
R18Y9
RESIDUALS
TIME
20000
15000
10000
5000
0
-5000
-10000
-15000
-20000
29.0
29.1
29.2
29.3
29.4
29.5
29.6
29.7
29.8
29.9
30.0

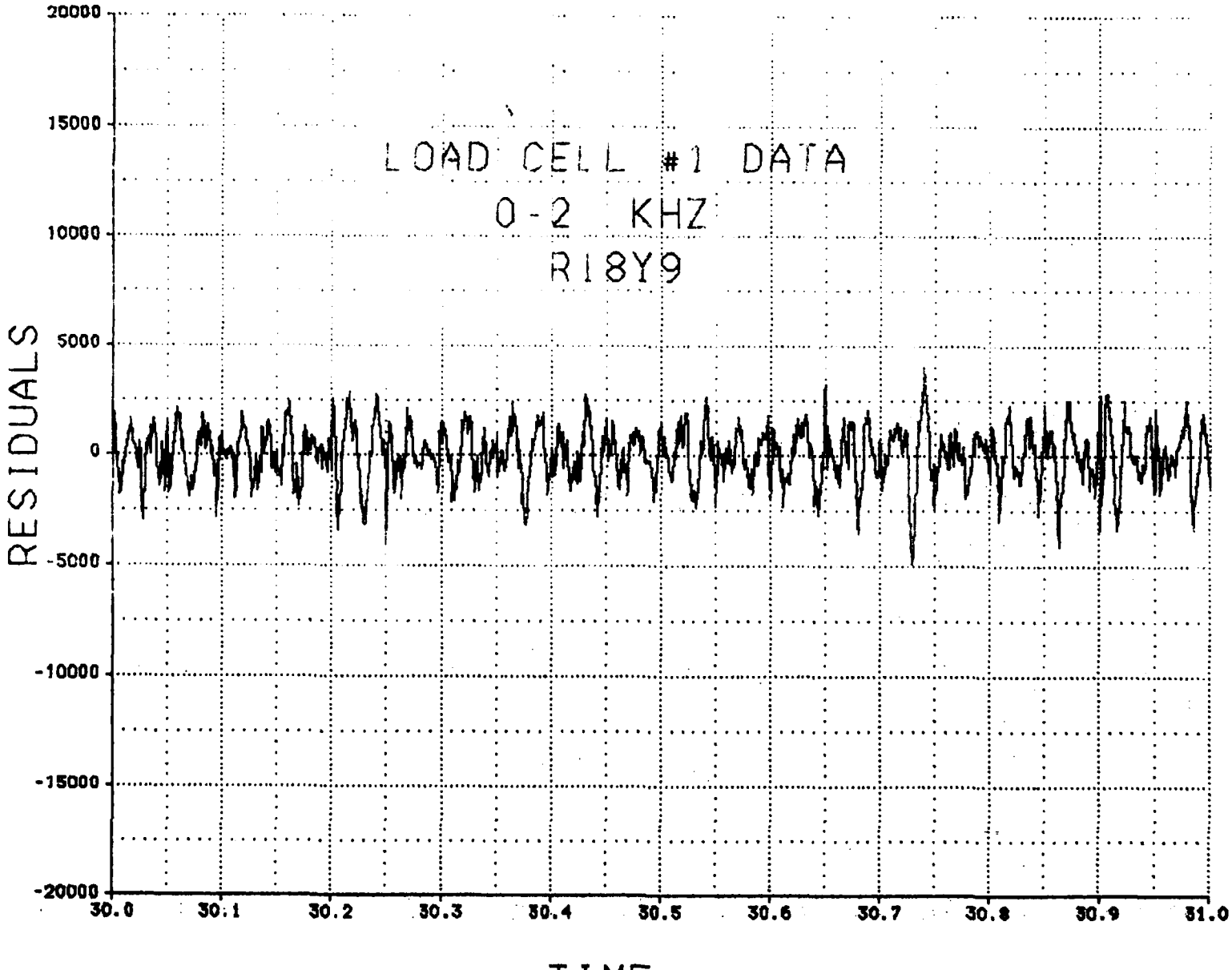
LOAD CELL #1 DATA
0-2 KHZ
R18Y9
RESIDUALS
TIME
20000
15000
10000
5000
0
-5000
-10000
-15000
-20000
30.0
30.1
30.2
30.3
30.4
30.5
30.6
30.7
30.8
30.9
31.0

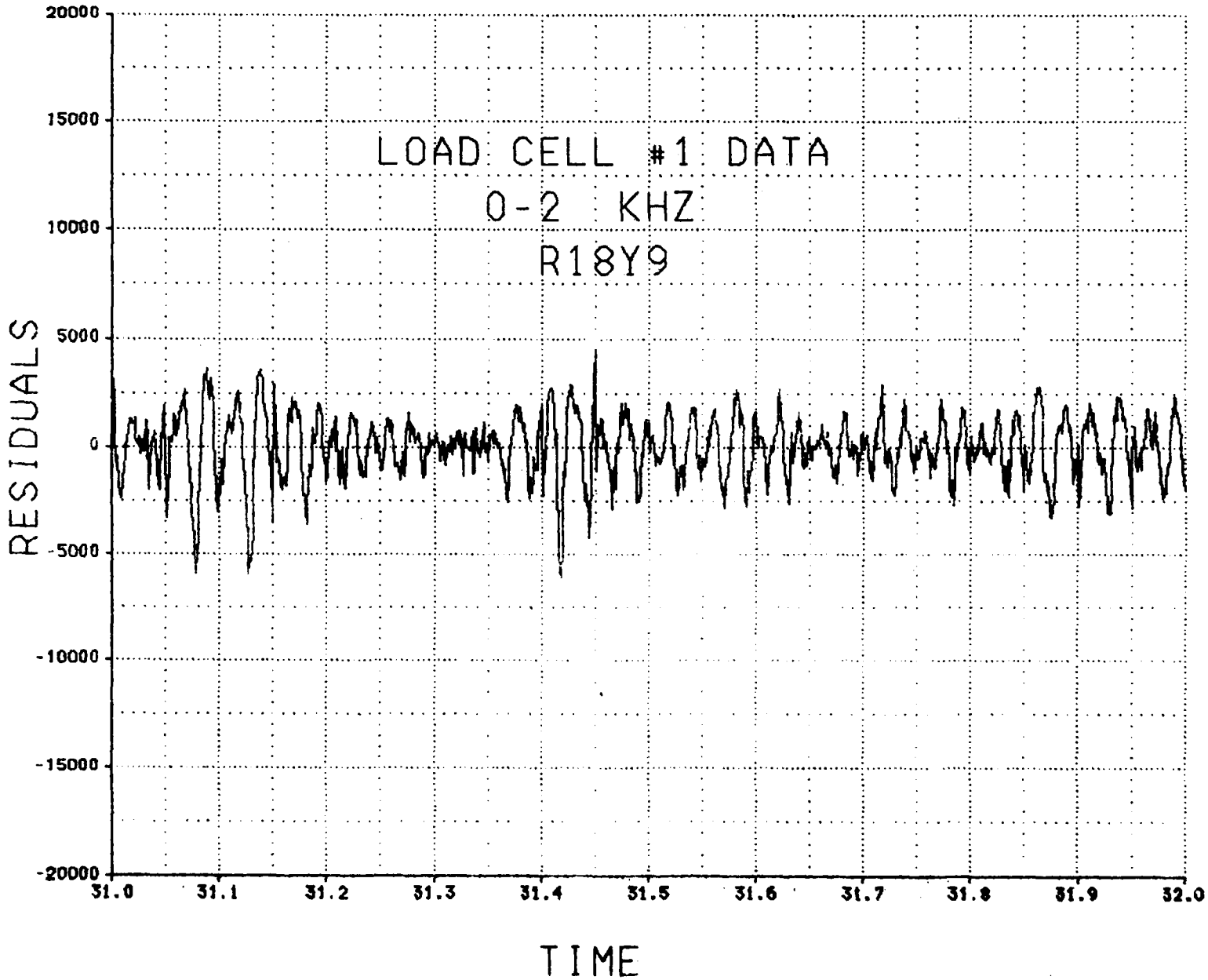
LOAD CELL #1 DATA
0-2 KHZ
R18Y9
RESIDUALS
TIME
20000
15000
10000
5000
0
-5000
-10000
-15000
-20000
31.0
31.1
31.2
31.3
31.4
31.5
31.6
31.7
31.8
31.9
32.0

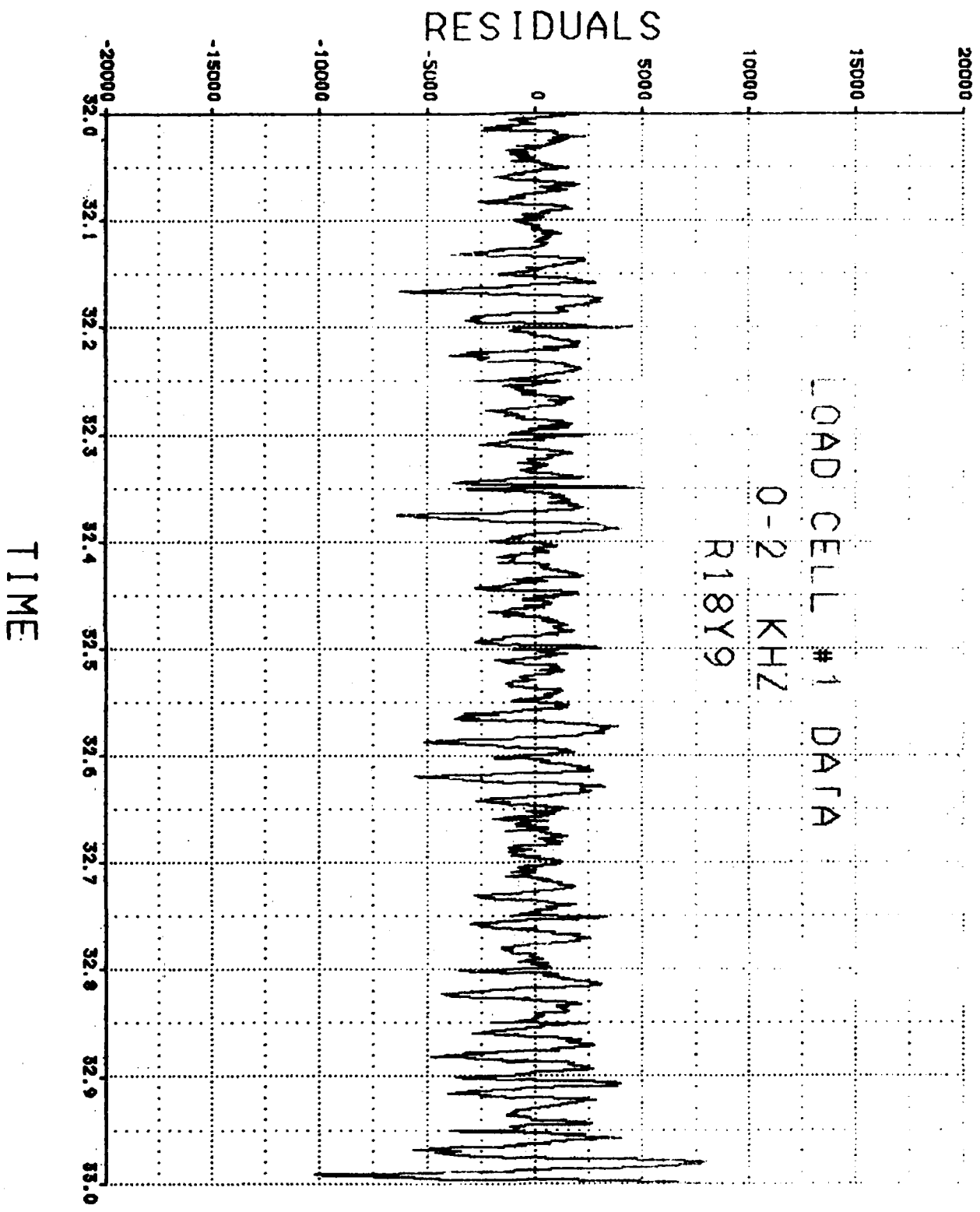
RESIDUALS
-20000
-15000
-10000
-5000
0
5000
10000
15000
20000
32.0
32.1
32.2
32.3
32.4
32.5
32.6
32.7
32.8
32.9
33.0
TIME
LOAD CELL #1 DATA
0-2 KHZ
R18Y9

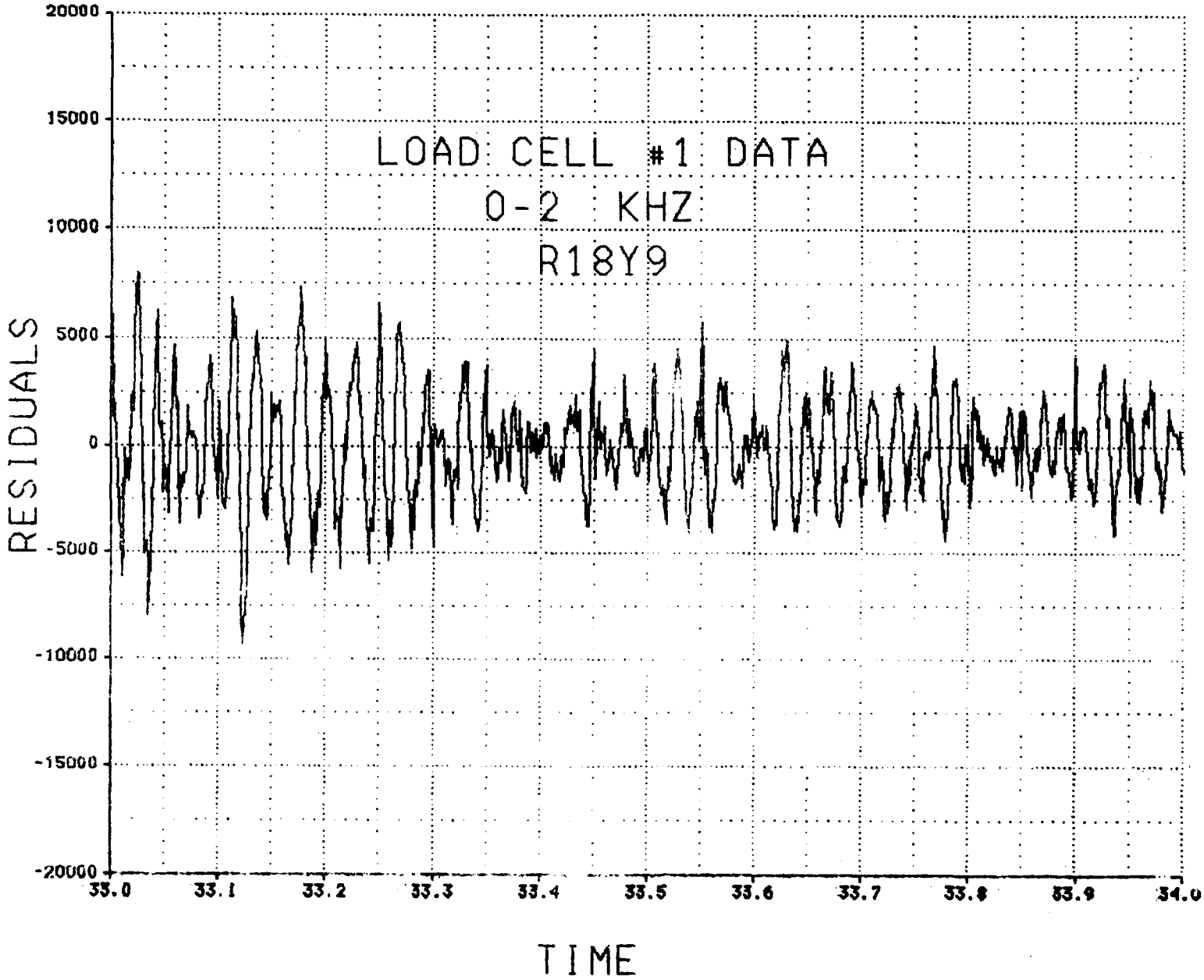
LOAD CELL #1 DATA
0-2 KHZ
R18Y9
RESIDUALS
TIME
20000
15000
10000
5000
0
-5000
-10000
-15000
-20000
33.0
33.1
33.2
33.3
33.4
33.5
33.6
33.7
33.8
33.9
34.0

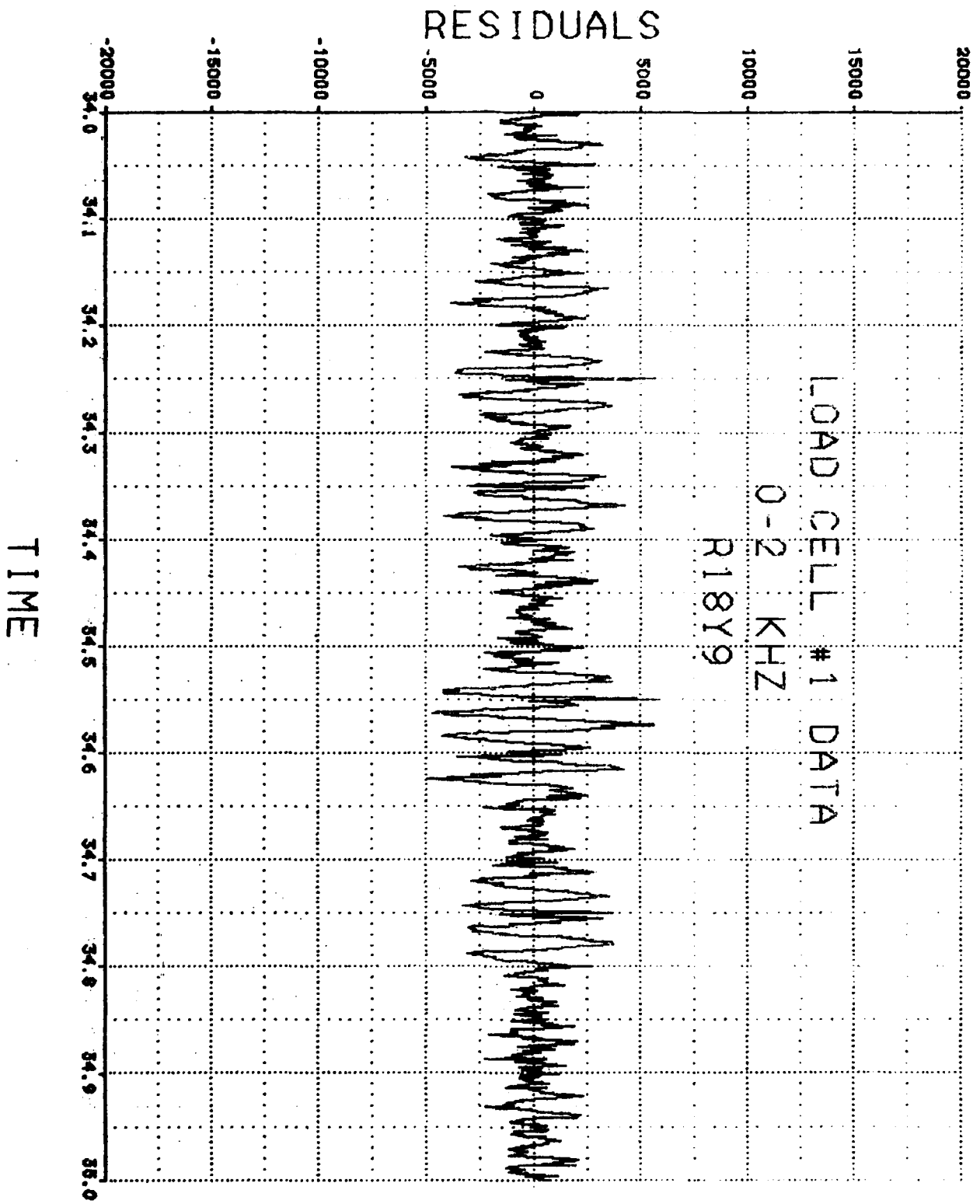
RESIDUALS
-20000
-15000
-10000
-5000
0
5000
10000
15000
20000
34.0
34.1
34.2
34.3
34.4
34.5
34.6
34.7
34.8
34.9
35.0
TIME
LOAD CELL #1 DATA
0-2 KHZ
R18Y9

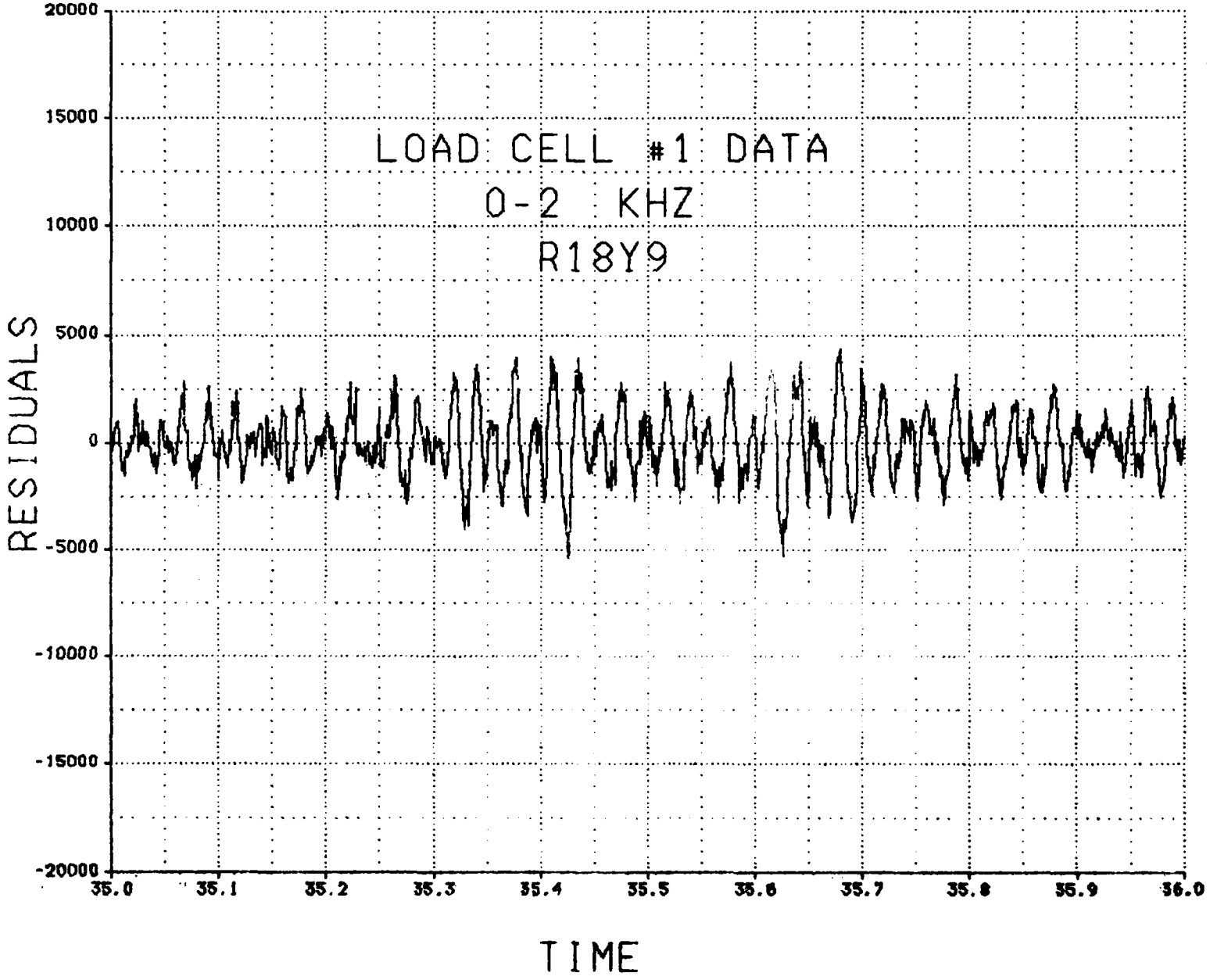
LOAD CELL #1 DATA
0-2 KHZ
R18Y9
RESIDUALS
TIME
20000
15000
10000
5000
0
-5000
-10000
-15000
-20000
35.0
35.1
35.2
35.3
35.4
35.5
35.6
35.7
35.8
35.9
36.0

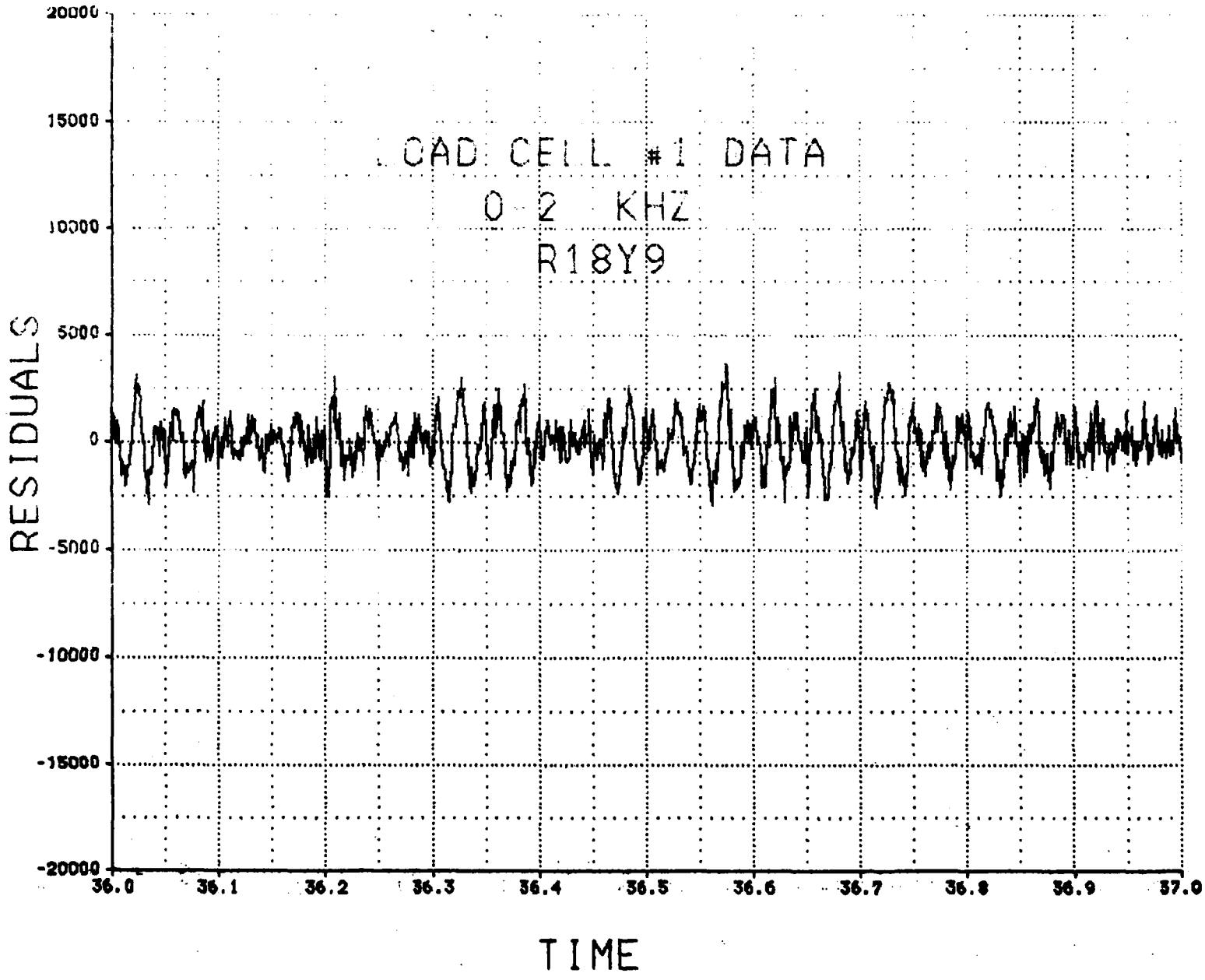
LOAD CELL #1 DATA
0.2 KHZ
R18Y9
RESIDUALS
TIME
20000
15000
10000
5000
0
-5000
-10000
-15000
-20000
36.0
36.1
36.2
36.3
36.4
36.5
36.6
36.7
36.8
36.9
37.0

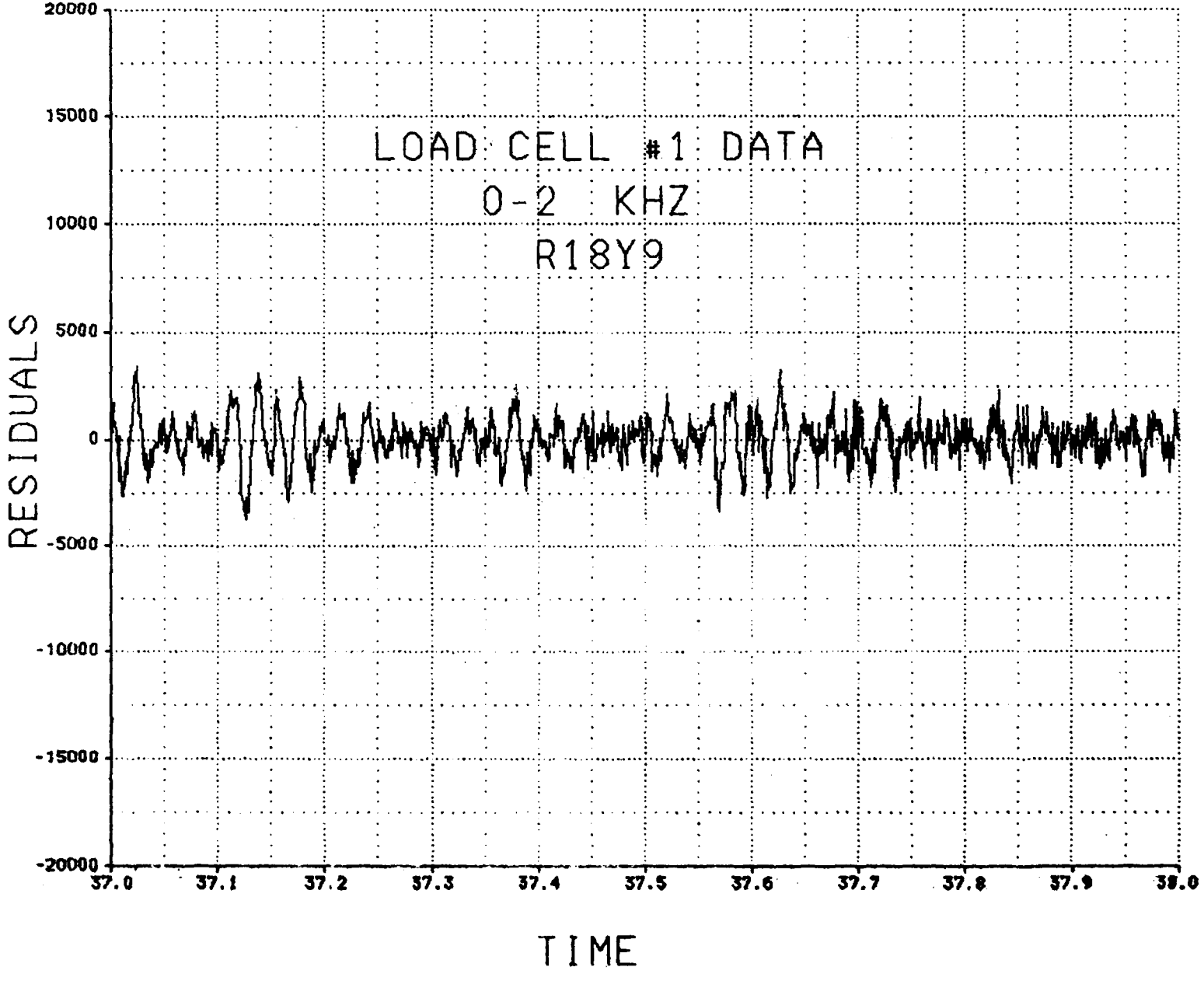
LOAD CELL #1 DATA
0-2 KHZ
R18Y9
RESIDUALS
TIME
20000
15000
10000
5000
0
-5000
-10000
-15000
-20000
37.0
37.1
37.2
37.3
37.4
37.5
37.6
37.7
37.8
37.9
38.0

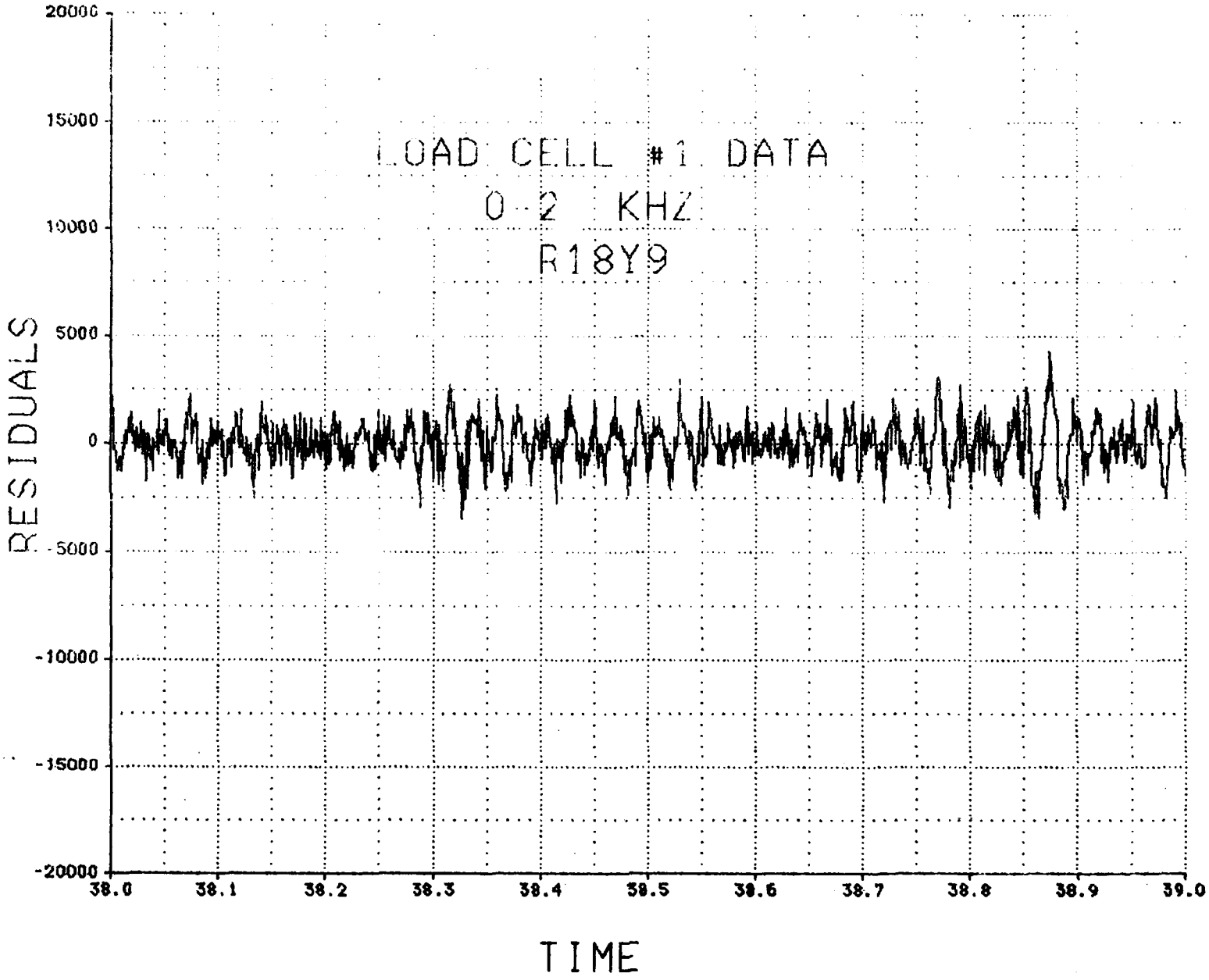
LOAD CELL #1 DATA
0-2 KHZ
R18Y9
RESIDUALS
TIME
20000
15000
10000
5000
0
-5000
-10000
-15000
-20000
38.0
38.1
38.2
38.3
38.4
38.5
38.6
38.7
38.8
38.9
39.0

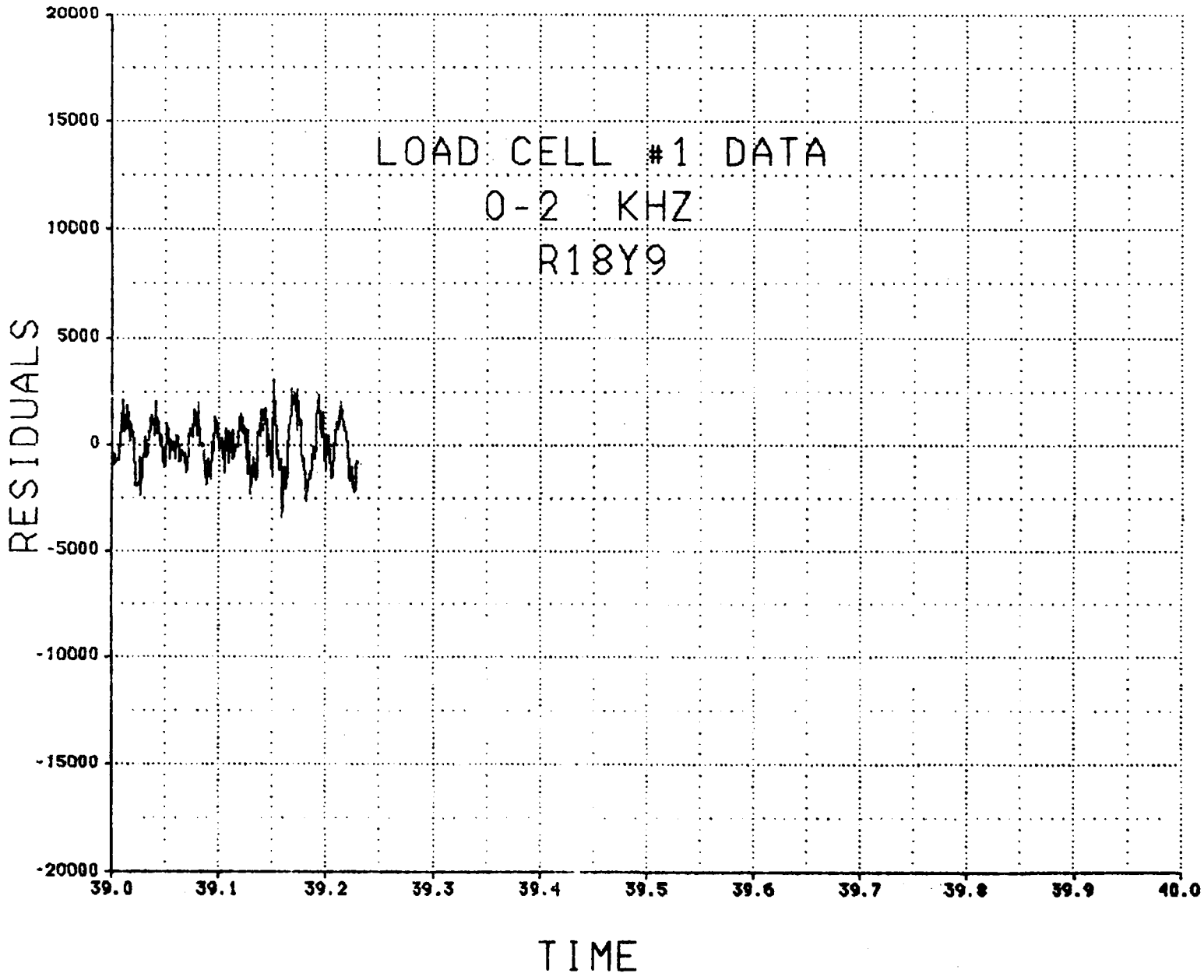
LOAD CELL #1 DATA
0-2 KHZ
R18Y9
RESIDUALS
TIME
20000
15000
10000
5000
0
-5000
-10000
-15000
-20000
39.0
39.1
39.2
39.3
39.4
39.5
39.6
39.7
39.8
39.9
40.0

DISTRIBUTION LIST

ORGANIZATION	NUMBER OF COPIES
Defense Technical Information Center Cameron Station Alexandria, VA 22314	12
3246th Test Wing Test Track Division Eglin AFB, FL 32542 (ATTN: Mr Bob Cross) ATTN: Mr Herb Brown)	2
Naval Weapons Center Track Operations, Code 6272 China Lake, CA 93555 (ATTN: Mr John Richards)	1
AFWAL/FIBRA Wright-Patterson AFB, OH 45433 (ATTN: Dr V. B. Venkayya)	1
Sandia National Laboratories Sandia Test Track (Division 1535) Albuquerque, NM 87185 (ATTN: Mr David C. Bickel)	1
Hq AD (TE) Eglin AFB, FL 32542	1
6585th Test Group Holloman AFB, NM 88330	
(GDA)	1
(TKO)	1
(TKI)	1
(TKE)	1
(PRX)	1
(TSL)	2
AUK/LSE Maxwell AFB, AL 36112	1